



HAL
open science

Optogenetics at different culture scales for beta-carotene bioproduction control in *Saccharomyces cerevisiae*

Sylvain Pouzet

► **To cite this version:**

Sylvain Pouzet. Optogenetics at different culture scales for beta-carotene bioproduction control in *Saccharomyces cerevisiae*. Biotechnology. Université Paris Cité, 2023. English. NNT : 2023UNIP7108 . tel-04562951

HAL Id: tel-04562951

<https://theses.hal.science/tel-04562951>

Submitted on 29 Apr 2024

HAL is a multi-disciplinary open access archive for the deposit and dissemination of scientific research documents, whether they are published or not. The documents may come from teaching and research institutions in France or abroad, or from public or private research centers.

L'archive ouverte pluridisciplinaire **HAL**, est destinée au dépôt et à la diffusion de documents scientifiques de niveau recherche, publiés ou non, émanant des établissements d'enseignement et de recherche français ou étrangers, des laboratoires publics ou privés.

Thèse de Doctorat – Université Paris Cité
UMR 168 - Physico-Chimie Curie, Institut Curie
UMR 7057 - Laboratoire Matière et Systèmes Complexes

**Optogenetics at different culture scales
for beta-carotene bioproduction control
in *Saccharomyces cerevisiae***

Rapporteurs :

Damien COUDREUSE - HDR CNRS
IBGC, Université de Bordeaux
Stéphanie HEUX - DR INRAE
Toulouse Biotech Institute, INSA

Examineurs :

Véronique ALBANESE - CR CNRS
Institut J. Monod, Université Paris Cité
Stéphane LEMAIRE – DR CNRS
LQCB, Sorbonne Université

Invité :

Gilles TRUAN - DR CNRS
Toulouse Biotech Institute, INSA

Directeur de thèse :

Pascal HERSEN - DR CNRS
Institut Curie, PSL, Sorbonne Université

Soutenue publiquement

le 09 Mars 2023
par **Sylvain POUZET**

École Doctorale 474

**Frontières de l'Innovation en
Recherche et Éducation (FIRE)**
(ex FdV)

Spécialité

**Génétique, omiques,
bioinformatique et biologie des
systèmes**

Resumé

Titre : Contrôle optogénétique pour la production de bêta-carotène chez *Saccharomyces cerevisiae* à différentes échelles de culture.

Résumé : Bien que les possibilités quant à la bioproduction s'élargissent, cette biotechnologie souffre encore de faibles rendements, limitant la compétitivité économique de ces procédés. Outre l'ingénierie métabolique des microorganismes, de nombreuses études visent à mieux contrôler les microorganismes pour maximiser leur potentiel de production. En effet, la production d'une molécule hétérogène déclenche souvent une charge cellulaire. Pour cela, il devient crucial de réguler activement la production et la croissance cellulaire afin de minimiser les échappements évolutifs et de mieux gérer l'allocation des ressources cellulaires. Pour cela, des outils de contrôle versatiles sont nécessaires et l'optogénétique, c'est-à-dire l'utilisation de la lumière pour contrôler des processus biologiques, apparaît comme un système idéal pour contrôler de manière réversible et dynamique le métabolisme cellulaire. Afin d'appliquer l'optogénétique à la bioproduction, des appareils de culture cellulaire pouvant illuminer les cellules sont nécessaires à chaque étape du processus de développement de nouvelles souches. Cependant, comment l'échelle de culture, les conditions de culture et les caractéristiques dépendantes à chaque appareil influencent l'activation optogénétique et son impact sur la bioproduction reste à explorer. Pour répondre à cette question, nous avons construit et implémenter une possibilité d'illumination à divers appareils de culture de laboratoire, avec un accent particulier sur l'éclairage de plaques multipuis, des tubes de culture, d'ermenmeyers, et en rendant eVOLVER, une plate-forme de culture contrôlable à haut débit, utilisable pour l'optogénétique (chapitre 1). Nous avons ensuite construit une souche de levure *Saccharomyces cerevisiae* dont la production de bêta-carotène est régulée par optogénétique, détaillée dans le chapitre 2. Pour cela, nous avons utilisé un système optogénétique basé sur EL222, un facteur de transcription activé par la lumière bleue, et la voie hétérologue du bêta-carotène. En tant que terpène, reposant sur la voie du mevalonate, un voie métabolique clé pour la production de nombreux autres composés à haute valeur ajoutée, et sa couleur orange vif, le bêta-carotène est un modèle de bioproduction idéal. Pour contrôler la production de bêta-carotène par optogénétique, l'enzyme CrtYB a été placée sous contrôle du promoteur optogénétique pC120. Ainsi, le gène ne s'exprime qu'en présence de lumière bleue et agit comme valve de contrôle de production, tandis que les autres gènes de la voie du bêta-carotène sont exprimés constitutivement. Dans le chapitre 3, pour tester les performances de cette souche à travers les échelles de culture et comprendre l'influence des paramètres de culture, nous avons procédé en 3 étapes. Premièrement, l'activation optogénétique a été caractérisée et optimisée dans chaque appareil, démontrant que l'activation dépendait fortement de la modalité d'éclairage et devait être optimisée pour être comparable entre appareils. Deuxièmement, la production, constitutive, de bêta-carotène a également été optimisée indépendamment dans chaque appareil : pour maximiser la production, le volume de culture et l'agitation s'avèrent critiques. Enfin, dans un troisième temps, la souche productrice de bêta-carotène contrôlée optogénétiquement a été validée et comparée entre appareils. Dans ce manuscrit, nous présentons et discutons le développement d'instruments optogénétique laboratoire, notamment concernant l'implémentation de l'illumination, le volume de culture, du débit expérimental et de la contrôlabilité. Nous avons montré comment rendre un système génétique de bioproduction contrôlable optogénétiquement et détaillé ses limitations. Ici, nous relierons alors des considérations techniques et des connaissances biologiques pratiques dans l'espoir d'atteindre une meilleure contrôlabilité, ouvrant la voie à des processus de bioproduction optogénétiquement contrôlés à plus grande échelle.

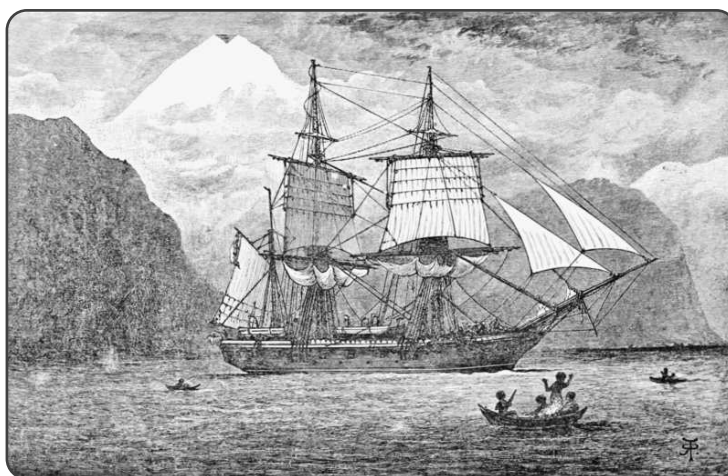
Mots-clés : Optogénétique, bioproduction, levure, *Saccharomyces cerevisiae*, bêta-carotène, biologie synthétique, ingénierie métabolique, instrumentation

Abstract

Title: Optogenetics at different culture scales for beta-carotene bioproduction control in *Saccharomyces cerevisiae*.

Abstract: As bioproduction possibilities expand, this biotechnology still suffers from low yields, making many processes not yet economically viable. Besides strain metabolic engineering, many studies aim at better controlling microorganisms to maximize their production potential. Indeed, as production often triggers cell burden, it became crucial to be able to regulate production and growth to reduce evolutionary escape and better manage cell resource allocation. For this, versatile control tools are needed and optogenetics, *i.e.*, using light to control biological processes, emerges as a convenient system to reversibly and dynamically control cell metabolism. In order to apply optogenetics to bioproduction, illumination culture devices are needed for every step of the strain development process, but it remains unclear how culture scale, culture conditions and device-dependent characteristics influence optogenetic activation and how it impacts the resulting production. To address this question, we built and adapted various lab-scale illumination culture devices, with a particular emphasis on illuminating imaging well-plates, test tubes, flasks, and adapting the eVOLVER, a high throughput highly controllable culture platform, to carry out optogenetic batch cultures (chapter 1). We then built a *Saccharomyces cerevisiae* strain in which beta-carotene production is regulated by optogenetics, detailed in chapter 2. For this, we used the EL222 optogenetic system, a single-component transcription factor that is activated by blue light, and the beta-carotene heterologous pathway. As a terpene resting on the mevalonate pathway, a key pathway for the production of many other high-value-added compounds, and its vivid orange color, beta-carotene is an ideal bioproduction model. To control beta-carotene production using optogenetic, the CrtYB enzyme of the pathway was placed under the control of the pC120 optogenetic promoter such that this gene will only be expressed in the presence of blue light, acting as a valve to control production, while other genes of the beta-carotene pathway are expressed constitutively. In chapter 3, to test how this strain's performance would translate across culture scales and what key parameters influence it, we proceeded in a 3-step manner. First, optogenetic activation was characterized and optimized in each device, demonstrating that activation was highly dependent on the illumination modality and should be optimized to be comparable between devices. Second, constitutive beta-carotene production was also independently optimized in each device: to maximize production, culture volume and stirring appeared critical. Finally, as a third step, the optogenetically-controlled beta-carotene producer strain was validated and compared across devices. In this manuscript, we present insights into the development of lab-scale optogenetic instruments, discussing light implementation, culture volume, throughput and controllability. We showed how to adapt a bioproduction genetic system to optogenetics and detailed its limitations. In definitive, we link technical considerations with practical biological insights in the hope to reach better strain controllability, setting the stage for potential larger scale optogenetically controlled bioproduction processes.

Keywords: Optogenetics, bioproduction, yeast, *Saccharomyces cerevisiae*, beta-carotene, synthetic biology, metabolic engineering, instrumentation



HMS Beagle - RT Pritchett

« Se tenir sur les épaules des géants, et voir plus loin. Voir dans l'invisible, à travers l'espace, et à travers le temps. Voyager. Voyager à travers le monde, et à travers les siècles. Imaginer, puis découvrir. Imaginer avant de découvrir. Puis voir émerger à partir de ce que l'on a distingué au loin, ce qu'il y avait d'invisible. Mais avant, longtemps avant, il y a l'émerveillement et l'étrangeté de la découverte de l'inconnu ; qui est toujours, aussi, une découverte de soi, de cette part en soi que l'on ne connaissait pas. »

Sur les épaules de Darwin. "Voyages(2)" – JC Ameisen

Pour m'avoir formé, poussé, soutenu et inspiré ; et fait grandir, humainement et scientifiquement, c'est à mes professeurs que je dédie cette thèse. Tout particulièrement à :
Mes parents, Murielle Seurot, Delphine Guillaume, Anne-Marie Bourdieu, Béatrice Meynet-Cordonnier, Christophe Gobbé, Elsa Orfeuille, Véronique Rossi, Lynn Mahaffy, Anne Plessis, et Hannes Claeys.

Acknowledgments

Je voudrais remercier tout d'abord Pascal Hersen, pour cette opportunité que tu m'as offerte pour cette thèse, pour m'avoir permis d'avancer sur ce chemin, parfois vallonné, mais toujours constructif et stimulant ! Merci pour ta patience, pour tes indications, pour la liberté que tu m'as octroyée et pour m'avoir toujours permis de travailler dans les meilleures conditions pendant ces 4 ans.

Merci Gilles Truan et Thomas Lautier pour vos suggestions et retours concernant le projet, ainsi que vos participations pour les publications. Merci Sara Castaño-Cerezo pour les expériences à Toulouse et la formation en HPLC !

Merci Jérôme Bonnet et Matthieu Coppey pour votre temps et conseils tout au long de cette thèse. Je remercie également Stéphanie Heux et Damien Coudreuse d'avoir accepté d'être rapporteurs de ma thèse, pour la lecture et leurs retours sur ce manuscrit avant la soutenance, ainsi que Stéphane Lemaire et Véronique Albanese, pour avoir accepté d'évaluer mon travail.

Merci à toute l'équipe de la Team Hersen (a.k.a. Lab 513) pour être si chouettes. Laissez-moi affirmer sans aucune retenue que je viens tous les matins au labo en sachant que je vais y retrouver des personnes fantastiques avec lesquelles je me plais, dans une ambiance sérieuse quand il le faut, mais toujours chaleureuse, et riieuse à d'autres moments ! Et ça, c'est quelque chose, je pense, qui vaut de l'or !

Céline, véritable cœur de l'équipe, merci de savoir tout ce qu'il y a à savoir au labo, merci d'être toujours disponible pour nous permettre de travailler le plus efficacement possible, merci d'organiser, et aussi d'animer, la vie de l'équipe ! Merci pour le running, pour les leçons de boxe, pour les pâtisseries diverses et pour ton optimisme, ta motivation et ta covid-resistance sans faille !

Jessie, tu es arrivée au laboratoire à un moment décisif de ma thèse, et je suis certain que celle-ci serait bien différente si tu n'avais pas été là. Merci pour ton aide si précieuse, pour tes suggestions, pour ton calme, ta détermination et ton expertise.

Matthias, on a partagé beaucoup pendant nos thèses en parallèle : merci pour ces innombrables cafés, cette fascination pour la nature, nos discussions pour tenter de mieux comprendre le monde qui nous entoure, nos débats toujours constructifs, brainstormings scientifiques, projets, intérêts nombreux et divers. On a avancé coude à coude, s'épaulant dans les moments plus difficiles et célébrant dans les meilleurs ; une belle aventure !

Merci à toute l'équipe, thank you Dimitrije for being so nicely annoying, that's why we love you so, merci Fabien pour avoir toujours réponse à mes questions, même les plus saugrenues, et pour avoir éveillé l'étincelle de levure en moi. Thank you, Alvaro, for your wit, your scientific enthusiasm, sense of rigor and benevolence. Merci Simon pour ton caractère agréable et futé, merci Lionel pour ces discussions passionnées d'histoire des sciences, et merci Pauline pour le vent de dynamisme et bonne humeur. Merci aussi Karine et Benoit pour tous ces échanges captivants.

I would also like to thank two brilliant interns I had the chance to supervise during my PhD. Guillermo, thank you for your work, pioneering the eVOLVER project, and your endless determination at the time! Vincent, thank you also for your tenacity, which was there regardless of the time of the night it was, and the hard time the microscope gave you!

Many other people I had the chance to interact with during my PhD I am very grateful: my very bests to Gabriel, Maud, Michael, Hugo, Anumita, Joel, Carolina, Kalina, and Horia!

Merci aussi aux ingénieurs travaillant dans les ateliers et plateformes, sans qui beaucoup de ce travail aurait été compromis : Oune-Saysavanh Souramasing à l'atelier du MSC, Lea Guyonnet à la cytométrie de l'hôpital, Rémy Fert de l'atelier de Curie, Arnaud Grados, William Bretts à MSC, ainsi que l'équipe BMBC à Curie pour leur aide et disponibilité. Merci aussi à toute l'administration de choc de l'unité, Fabrice et Kheira ; et merci à Brigitte Da Silva, présente à l'accueil. Elle est la première personne qu'on rencontre quand on arrive à Curie, toujours avec le sourire, qui nous fait nous sentir chez nous, nous rend content d'y rentrer chaque matin et nous conforte et motive pour démarrer la journée.

Je voudrais remercier les professeurs qui m'ont accompagné durant mon parcours, et j'ai ainsi décidé de leur dédier ma thèse. J'ai souvent voulu remercier ceux qui m'ont marqué et poussé en avant, sans vraiment savoir comment ou quand le faire. Alors, je prends cette opportunité pour le faire, car il me semble que c'est eux qui donnent ce sens de l'émerveillement et du travail, qui, je crois, vont de pair et se nourrissent l'un l'autre. Merci donc à ces profs, au sens large du terme, qui, depuis la petite enfance, puis au collège, au lycée et à la fac ont fait germer et cultivé ma passion pour le vivant, et m'ont donné les moyens pour commencer à y répondre.

Enfin, merci à mes amis, du Nord, de Haute-Savoie, de Grenoble, de Paris (un petit Gob ?) ou d'ailleurs, pour tous ces moments. Special shout out pour mes colocataires Egill, Victor et Hugo ! Merci à ma famille, loin des yeux mais toujours près du cœur, pour leur soutien inconditionnel. Et bien sûr, merci à toi Coline. Je ne sais pas encore de quoi sera faite la suite, mais j'ai hâte de la commencer avec toi !

Abbreviations

a.u.	arbitrary units (=u.a.)
ALE	Adaptive Laboratory Evolution
BC	Before Christ
bcar	beta-carotene
BF	Bright Field
c-source	Carbon-source
C13	Carbon-13
CDW	Cell Dry Weight (=DCW)
CRISPR	Clustered Regularly Interspaced Short Palindromic Repeats
CrtB	Phytoene Synthase
CrtE	Geranylgeranyl diphosphate synthase
CrtI	Phytoene Desaturase
CrtY	Lycopene Cyclase
CrtYB	CrtY and CrtB natural bifusion
CrtYBekI	CrtY, CrtB, CrtI synthetic trifusion
CSM	Complete Synthetic Medium (=SC)
DBTL	Design Build Test Learn (cycle)
DC	Direct Current
dCas9	dead Cas9
DCW	Dry Cell Weight (=CDW)
DIY	Oxygen transfer Rate
DMD	Digital Micromirror Device
DMSO	Dimethyl Sulfoxide
DNA	Deoxyribonucleic Acid
DoE	Design of Experiments
DSRS	Dynamic Sensor Response System
EL222	<i>Erythrobacter litoralis</i> 222 amino acid light responsive protein we use
FBA	Flux Balance Analysis
GAL	Galactose genes
GFP	Green Fluorescent Protein
GOI	Gene of Interest
GRAS	generally Recognized as Safe (species)
gRNA	guide RNA
HPLC	High Performance Liquid Chromatography
HR	Homologous Recombination
HSC	Hematopoietic Stem Cells
HTH	Helix turn Helix (DNA binding domain)
IDE	Integrated Development Environment
IR	Infra Red
LC-MS	Liquid Chromatography - Mass Spectrometry
LED	Light-Emitting Diode
LOV	Light Oxygen Voltage (protein domain)

LRTF	Ligand Responsive Transcription Factor
MCF	Micobial Cell Factories
MoClo	Molecular Cloning
MRTF	Metabolite responsive Transcription Factor
MVA	Mevalonate
NHEJ	Non-Homologous End Joining
OD	Optical Density
ORF	Open Reading Frame
OTR	Oxygen Transfer Rate
pC120	optogenetic promoter
PCB	Printed Circuit Board
PCR	Polymerase Chain Reaction
PP	PolyPropylene
PWM	Pulse Width Modulation
RA	Retinoic Acid
RBS	Ribosome Binding Site
RFP	Red Fluorescent Protein
RNA	Ribonucleic Acid
SC	Synthetic Complete (medium) (= CSM)
STY	Space-Time Yield
TCA	Tricyclic Acid (cycle)
u.a.	unité arbitraire (=a.u.)
UTR	Untranslated Regions (5' or 3')
UV	Ultra Violet
VP16	Viral Particle 16 (transactivational domain)
WT	Wild Type
WW1	World War I
WW2	World War II
Y2H	Yeast two hybrid
YKO	Yeast Knock Out (collection)
YPD	Yeast Extract + Peptone + D-glucose
YPE	Yeast Extract + Peptone + Ethanol
YPG	Yeast Extract + Peptone + Glycerol
YPGal	Yeast Extract + Peptone + Galactose
YTK	Yeast ToolKit (see MoClo)

Contents

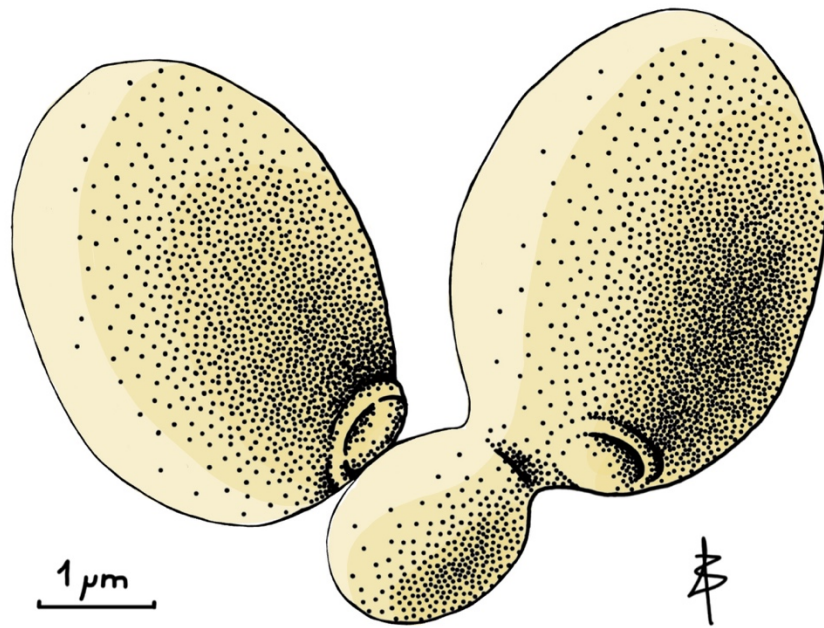
Resumé	2
Abstract	3
Acknowledgments.....	6
Abbreviations.....	8
Contents.....	10
1. Preface	16
1.1. An old friend to human civilizations.....	16
1.2. A pioneer in fundamental research.....	18
1.3. A promise for medical studies	21
1.4. A very high biotechnological potential	23
Bibliography	25
2. Introduction	28
2.1. Bioproduction.....	28
2.1.1. Microbial Cell Factories	28
2.1.2. Beta-carotene	31
2.1.3. Strain Engineering	33
2.1.4. Bioprocesses	38
2.1.5. Culture conditions.....	40
2.1.6. Industrial considerations.....	41
2.2. The cost of production.....	42
2.2.1. Burden	42
2.2.2. Metabolic burden: resources competition.....	43
2.2.3. Toxicity (stress).....	45
2.2.4. Consequences	45
2.2.5. Decoupling growth and production	46
2.3. Two-step cultivation	48
2.3.1. The growth phase.....	49
2.3.2. Inducers	49
2.4. The production phase.....	51
2.4.1. Metabolism	51
2.4.2. Growth laws.....	53

2.4.3.	Growth <i>versus</i> Production in the production phase.....	55
2.4.4.	Induction modalities	57
2.5.	Dynamic Control.....	58
2.5.1.	Control.....	59
2.5.2.	Embedded Control.....	60
2.5.3.	External control	63
2.5.4.	Control tools (Optogenetics)	64
2.5.5.	Light controlled bioproduction.....	66
2.6.	Goal of the PhD.....	66
2.6.1.	In definitive.....	67
2.6.2.	Goal of the PhD	67
2.6.3.	Content of the manuscript.....	68
	Bibliography	69
3.	The promise of optogenetics for bioproduction (review).....	77
	Abstract.....	78
3.1.	Merging optogenetic and bioproduction	78
3.1.1.	Introduction to bioproduction.....	78
3.1.2.	Optogenetics	80
3.1.3.	Adapting induction systems for optogenetics.....	80
3.2.	Control strategies.....	81
3.2.1.	Simple switch control for flux rewiring	81
3.2.2.	Dynamic switch	84
3.2.3.	Cybergenetics	85
3.3.	Scale-up instruments	86
3.3.1.	Milliliter scale.....	86
3.3.2.	Mini-bioreactor scale and feedback implementation.....	87
3.3.3.	Industrial settings and photobioreactors	87
3.4.	Discussion and conclusions	89
	Bibliography	91
4.	CHAPTER 1 – Setting up optogenetic devices	95
	Overview	95
4.1.	Microfluidics	96
4.2.	Imaging Plates (OptoBox).....	96
4.3.	Tubes Arrays (OptoTubes).....	99
4.4.	(Opto)Flasks	102
4.5.	Illuminating flat surfaces	103
4.6.	Mini bioreactors (eVOLVER).....	105

4.6.1.	eVOLVER	105
4.6.2.	Unit development	108
4.6.3.	Setup	110
4.6.4.	Software.....	111
4.6.5.	Type experiment	115
4.6.6.	Calibrations.....	117
4.6.7.	Illumination	120
4.6.8.	Other systems	122
4.7.	Lab-scale fermenters	124
4.8.	Industrial-scale bioreactors	125
4.9.	Conclusion and Perspectives.....	127
	Bibliography	128
5.	CHAPTER 2 – The making of a strain	130
5.1.	Strain construction	130
5.1.1.	Optogenetics	130
5.1.2.	Changing to mCherry	131
5.1.3.	Beta-carotene	132
5.1.4.	Opto-beta-carotene	134
5.2.	A slow producer strain	135
5.2.1.	Early observations	135
5.2.2.	Multidimensional analyses with eVOLVER	136
5.2.3.	Temperature Effects	139
5.3.	Questioning the phenotype	141
5.3.1.	Expression strength from pC120	141
5.3.2.	Questioning the trifusion design.....	143
5.3.3.	Conclusions	145
5.4.	A new functional strain	145
5.4.1.	Early checks.....	145
5.4.2.	Device and illumination.....	146
5.5.	Conclusions.....	147
	Bibliography	147
6.	CHAPTER 3 – Optogenetic control of beta-carotene bioproduction across multiple lab-scales.....	149
	Foreword.....	149
	Abstract.....	149
6.1.	Introduction	150
6.2.	Results.....	152
6.2.1.	Setting-up optogenetics in different lab-scale culture devices	152

6.2.2.	Devices and culture conditions influence optogenetic activation	154
6.2.3.	Beta-carotene production is impacted at different scales	157
6.2.4.	Optogenetic control of beta-carotene production in different devices	160
6.3.	Discussion	162
6.4.	Conclusion	164
6.5.	Materials and methods.....	165
6.5.1.	Construction of yeast strains.....	165
6.5.2.	Growth conditions	167
6.5.3.	Illumination devices	167
6.5.4.	Quantification of optogenetic activation (cytometry)	168
6.5.5.	Beta-carotene extraction and content estimation.....	169
6.5.6.	Microscopy	169
	Bibliography	170
	Supplementary information	174
7.	Conclusions	183
7.1.	Conclusions.....	183
7.1.1.	Summary.....	183
7.1.2.	Contribution.....	184
7.2.	Perspectives	185
7.2.1.	Activation strength	186
7.2.2.	Illumination onset.....	187
7.2.3.	Pulse activation.....	189
7.2.4.	Resource allocation.....	190
7.2.5.	Real-time control	191
7.3.	Discussion	191
7.3.1.	The choice of the optogenetic system.....	191
7.3.2.	The heterologous production pathway	193
7.3.3.	Controlling: production vs. growth?.....	193
7.3.4.	Auto-induction vs. external control	194
7.3.5.	Scaling-up.....	195
	Bibliography	196
8.	Appendix	198
8.1.	Résumé substantiel en français	199
8.2.	Résumé grand public.....	203
8.3.	Cybersco.py (paper)	206
8.3.1.	Introduction	206
8.3.2.	Results	207
8.3.3.	Discussion.....	212
8.3.4.	Materials and Methods	215
	Bibliography.....	216

8.4. Table of strains.....	218
8.5. Protocols	219
8.5.1. Culture media for yeast.....	220
8.5.2. MoClo for Yeast (YTK)	224
8.5.3. CRISPR for yeast.....	229
8.5.4. Yeast LiAc transformation	236
8.5.5. Beta-carotene quantification.....	239
8.5.6. Optobox	240
8.5.7. OptoTubes	245
8.5.8. eVOLVER – list of components.....	247
8.5.9. eVOLVER – installing	251



- *Saccharomyces cerevisiae* -
by Matthias Le Bec
inspired from *Science Source Prints Art Collections*

1. Preface

Saccharomyces cerevisiae, more than just a model organism

Saccharo for sugar, *myces* for mushroom and *cerevisiae* for beer: “cerveza” in Spanish or “cervoise” in French. This sugar-loving mushroom (Fig. 1) that has always been used for beer and bread making (hence its name the “baker’s yeast”), is not only important for human nutrition but has been and still is an important model organism used for fundamental research in molecular biology, works in biomedicine and is also becoming an essential biotechnological tool. In this first part, we propose a « *Petit éloge de la levure* », a little overview of the intimate relationship mankind has developed with this microorganism to get a better appreciation and understanding of its past, present, and potential future roles.

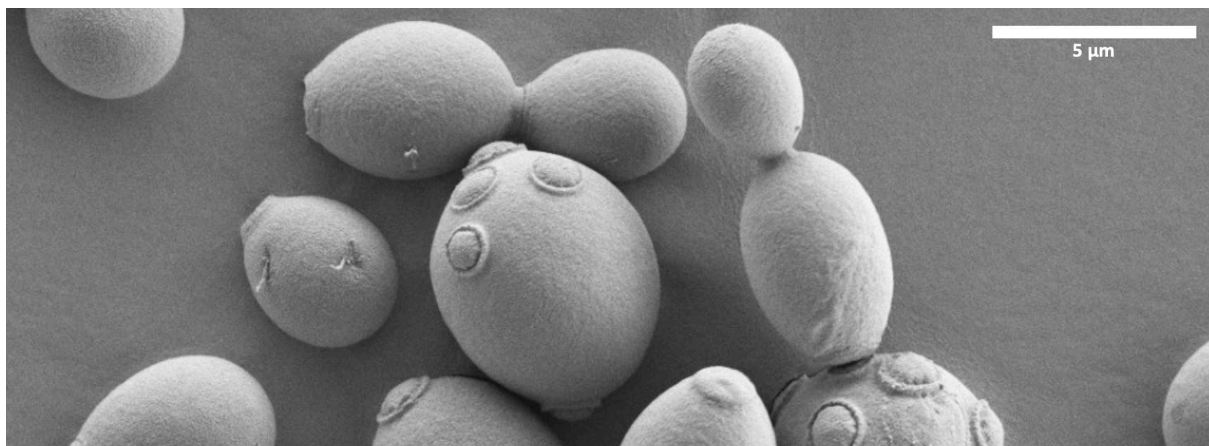


Figure 1. *Saccharomyces cerevisiae* with scanning electron microscopy (plantandmicrobiology.berkeley.edu). *S. cerevisiae* is a 5-10 μm unicellular fungi that reproduces asexually asymmetrically by budding, hence its name the “budding yeast”. Daughter cells emerge smaller than their mother cells and leave out a budding scar upon cytokinesis.

1.1. An old friend to human civilizations

Ecology. Yeasts naturally occur across the natural environment, in various ecosystems mostly thanks to their tight association with insects (social wasps, fruitflies and bees), as they reside, sporulate, germinate and mate in their guts¹. Even before domestication, *Saccharomyces cerevisiae* specifically thrived in sugary environments where it is deposited by one insect and attracts another. The first encounters between humans and *S. cerevisiae* were likely via the intermediary of fruits, and more particularly on overripe or rotten fruits, where sugar is abundant, and yeast can start to turn it to ethanol. Indeed, producing ethanol via fermentation

presents a competitive advantage to outgrow other microorganisms² and creates a detectable smell that can attract animals.

Alcoholic beverages. Once on a sweet fruit, fermentation allows the conversion of sugars (mainly sucrose – glucose linked to fructose – and fructose in fruits) into ethanol at a high metabolic rate. As hunter-gatherers, early humans picking fruits would inevitably come across fruits containing alcohol. Like other mammals, humans have the capacity to break down alcohol (ADH genes - alcohol dehydrogenases), otherwise toxic. Why humans developed such a strong taste for alcohol remains debated³. Since ethanol occurs on ripe and overripe fruits, an individual attracted to this chemical would be favored by selection as he would eat more. Besides, the associated dizziness was also argued to make individuals more prone to reproduction⁴. Whatever the reason, alcohol has occupied and still occupies a prominent position in human cultures. The earliest beer brewing is thought to date back to 10 000 BC with Sumerian and Mesopotamian civilizations, while the first actual traces date to 6 000 BC for Babylonians⁵. Today, alcoholic beverages are a multibillion dollars market across the world, and every single drop of human-produced alcohol originates from yeast fermentation: beer and wine of course, but also starting from ancient honey mead recipes to today's refined spirits (distilled fermented fruit must), and in every country across the world, with sake, palm wine, vodka, kvass, liqueurs, rum, cider, tequila, originating from various plant-based sugar sources. Different types of domesticated industrial yeasts exist today: some that are ancestral and used repeatedly, generations after generations, some coming from the flourishing yeast industry: ale and lager yeasts, and most are varieties derived from our very *Saccharomyces cerevisiae*. Here we can already start to foresee that choosing the right variety (or strain) is important for the desired beverage final result, as each strain will bring up specific flavors and aromas to the drink according to its own metabolism, which is based on its particular genetic makeup and the growing conditions (brewing compositions and recipe) specified along the brewing process.

Bread. Historically, alcoholic beverages (beer mostly) are thought to be the source of the transition from unleavened (flat) to leavened bread. It came long after wheat domestication (10 000 years ago), in Ancient Egypt (Fig. 2), that a spill of beer into cereal dough produced a serendipitous light loaf inflated with CO₂ from fermentation, while the ethanol was evaporated upon cooking. After that, it was mostly by propagating sourdough (dough starters) that leavened bread was continuously made. Fast forward to the 1800s, when bread processes were rapidly improving: at the beginning of this century, beer yeast was used to make bread without the typical sourness originating from *Lactobacillus* in the sourdoughs, and in 1846, the Vienna Process took over, *i.e.*, specifically propagating yeasts for the bread industry by skimming the foam coming from a brewing medium. From there started the rise of compressed fresh yeast, produced and sold for sole bread-making purposes. In the 1860s, Pasteur discovered the fermentation process carried out by yeast and deemed it responsible for bread's puffy nature. By fathering microbiology, Pasteur and Koch also allowed for pure strain isolation with more advanced culturing techniques. Supported by scientific advances and industrial progress, Fleischmann's Yeast Company introduces active dry yeast during WW2, with prolonged shelf life, and in 1973, Lesaffre, the current yeast world's leader, developed the instant dry yeast which requires no pre-treatment before use. For such industrial purposes, techniques to maximize biomass at very large scales have been well refined, using incremental batch and

fed-batch processes⁶ (detailed later in this introduction). It is with this flourishing industry that *Saccharomyces cerevisiae* gained its nickname of “the Baker’s Yeast”.



Figure 2. *The court bakery of Ramesses III (1217–1155 BC). "Various forms of bread, including loaves shaped like animals, are shown. From the tomb of Ramesses III in the Valley of the Kings, Twentieth Dynasty of Egypt"¹. There, 1200 BC, Egyptians were already using yeasts to inflate loaves and make bread lighter than its flat unleavened ancestor bread.*

While it is fair to state that *S. cerevisiae* has taken over the bread-making and alcoholic beverages industries, *S. cerevisiae* and other yeast species are also used for a variety of other food products, such as kombucha, kefir, chocolate, marmite, or soy sauce. For health, *S. cerevisiae* can be used as a probiotic for both humans and animals. *S. cerevisiae* improves milk quality for cows, yeast extract is a common feedstock additive, and *S. cerevisiae* var. *boulardii* is a human probiotic used for flora maintenance today, especially to counter antibiotic-associated diarrhea.

***S. cerevisiae* is positioned as one of the oldest organisms that has shaped human’s relationship with its environment, across millennia, and across civilizations. It is still central to our lives today and no day goes by, in the western civilizations at least, without us eating food or drinking beverages altered in some way by the budding yeast.**

1.2. A pioneer in fundamental research

¹ historicalcookingproject.com

Model Organism. Given its role in human affairs, it is only natural that *S. cerevisiae* quickly became an organism of interest at the scientific level. *Saccharomyces cerevisiae* is a unicellular eukaryotic fungus of about 4 μm characterized by 16 chromosomes, living as haploid or diploid, and reproducing either sexually (two mating types: α and a) or asexually (cellular division). Cells divide asymmetrically by budding (hence its other nickname “The Budding Yeast”) every 90 min in rich medium, about 30 times before dying. Upon DNA breaking, homologous recombination (HR) is largely favored over Non-Homologous End Joining (NHEJ), which considerably facilitates targeted genetic modifications compared to other organisms. It can also contain plasmids, be transformed efficiently, and be frozen for strain long-term storage. All those characteristics make *Saccharomyces cerevisiae* an organism of choice for genetic studies.

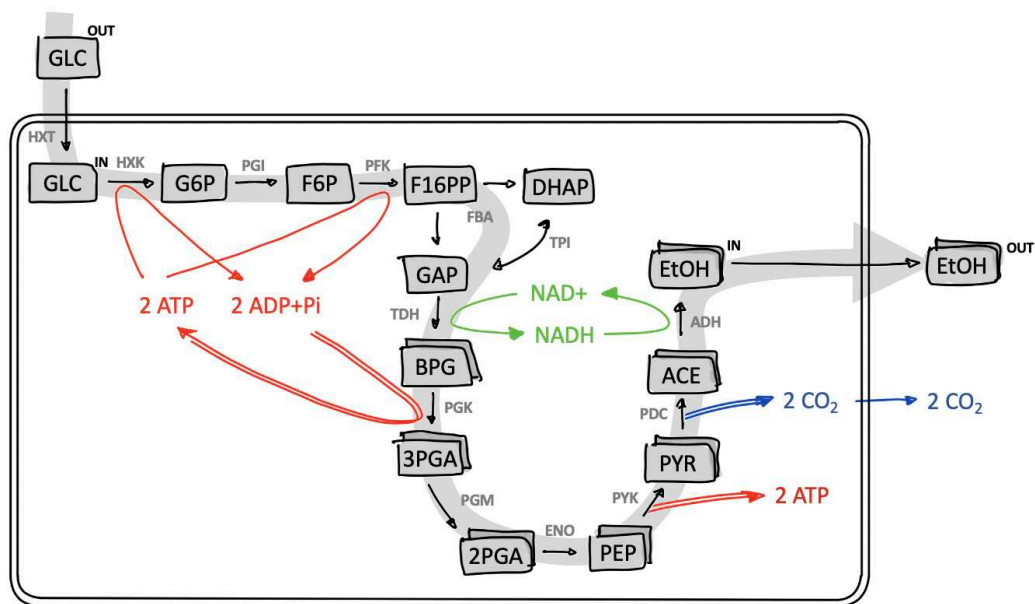


Figure 3. **Fermentation** is at the heart of *S. cerevisiae*'s role for human food and beverage uses. From 1 molecule of glucose, are produced: 2 molecules of ethanol, 2 CO_2 and 2 ATP. This mostly anaerobic process also occurs in aerobic growth conditions in *S. cerevisiae* (Crabtree effect), though less efficiently (Pasteur effect).

Discoveries. Understanding alcoholic fermentation (Fig. 3) was at the heart of early microbiology, molecular biology and biochemistry. Independent propositions that yeast was responsible for fermentation led ground for Pasteur to disprove the spontaneous generation theory (Pasteur's swan-neck flask experiments) and demonstrate that fermentation was not purely a chemical but a biological process. To bridge chemical and biological views, in 1897, Edward Büchner showed that “zymase”, a biochemical agent extracted from yeast (which could be considered today as a cell-free extract), could carry out fermentation. This opened the door for the first complete elucidation of a metabolic pathway: glycolysis, by 1940. Let's note that the very term “enzyme”, coined by Wilhelm Kühne is derived from the Greek “inside-sourdough” (“en-zymo”) or “leavened”. The nature of fermentation was also investigated early by Pasteur, showing that under anaerobic conditions, fermentation was highly efficient, whereas it was reduced in aerobic conditions (Pasteur effect, 1857). The opposite effect was

later characterized: in contrast to other yeast species, even in the presence of oxygen *S. cerevisiae* can ferment (Crabtree effect, 1929) and grow quickly, a phenomenon analogous to the effect undergone by some cancer cells (Warburg effect, 1923). In 1937, it is respiration that is elucidated via the Krebs (TCA) cycle⁷⁻⁹. Then, of major cellular processes, comes the discovery in 1970 of the cell cycle described in *S. cerevisiae* by Leland Hartwell^{10,11}. Needless to say, those discoveries had tremendous impacts on other fields of biochemistry, physiology, and medicine.

Genetics. *Saccharomyces cerevisiae* (strain S288C) was the first eukaryote to be fully sequenced, a great challenge at the time that pushed and propelled DNA sequencing technologies forward: each participating institution or country was given one chromosome to sequence, which led to the landmark paper “Life with 6000 genes” in 1996¹². Today, the challenge lies in synthesizing DNA, and similarly to the sequencing project, the Yeast Sc2.0¹³ consortium coordinates the effort to synthesize and modify yeast chromosomes (minimization, rearrangements and addition of over 4 000 lox sites disseminated across DNA) in order to build fully synthetic genomes. In the Yeast Sc3.0¹⁴ project, a minimal genome is to be found and heavy chromosomal rearrangements are planned to further test the limits of such approaches). After reading and writing, investigating gene structure and function was also carried out in yeast to a great extent with the EUROFAN I and II yeast functional analysis programs. Overall, are available the deletion collection YKO^{15,16} (find essential and conditional genes), the overexpression collection¹⁷, all single-protein tagged collection¹⁸ (that allows for protein localization and abundance assessments), mostly hosted by the EUROSCARF stock center, all that lead to better protein annotations and characterizations. It is worth noting that *S. cerevisiae* has one of the best documented and organized databases for an organism: the *Saccharomyces* Genome Database (SGD¹⁹) hosted at yeastgenome.org. As of today, despite great efforts to understand the birth²⁰ and the nature of protein functions and interactions, more work is still needed as about 30% of yeast genes remain unannotated and of unknown function.

Next Challenges in fundamental research. Yeast studies were prolific for advances in genetics, also leading to deciphering mechanisms of transcription (mediator in the early 1990s²¹) and gene regulation (GAL inducible system extensively studied) leading to the development of new biotechnological tools (Y2H techniques) to test protein-protein interactions for example. Omics technologies have been extensively used on yeast and today, a huge data collection exists, including genomics, transcriptomics, proteomics, metabolomics, fluxomics, etc., which can be looked at from a systems biology (holistic) perspective. Indeed, biology is still waiting for a transition from a descriptive to a truly comprehensive science, in which different biological processes can be mapped and linked at different cell process scales in integrated approaches²², to bring together gene regulatory networks with metabolic networks and fluxes for example. For this, representation tools²³ can help picture pathways at a larger scale, genome-scale metabolic models²⁴ can predict outputs from genetic mutations, and more mechanistic approaches, such as in resource allocation models help understand more general concepts regulating cell growth.

The huge amount of accumulated knowledge and the ease of use of *Saccharomyces cerevisiae* makes it an ideal candidate to keep on looking for fundamental principles

governing cell behavior and investigate particular aspects of cell physiology, especially those involved in medical conditions.

1.3. A promise for medical studies

Human diseases. Considered the simplest eukaryote, yeasts have many characteristics that make them much closer to our human biology than bacteria as model organisms. Mainly, their genome is contained and arranged in a nucleus, they contain mitochondria and other organelles (Fig. 4), as well as protein processing pathways through the Golgi apparatus and chaperones necessary to control protein folding. Genetically, yeasts have 20 to 30% homology with human²⁵. The extent of this conservation was shown by Paul Nurse in 1984 when he showed that the human version of CDC2 (for the cell division cycle¹⁰, CDK-1 in humans) complements yeast deletion (in *Schizosaccharomyces pombe*, a cousin of *S. cerevisiae*) despite 1.5B years of evolution²⁶! This conservation is such that using yeast is often the first step to investigate the role of a protein suspected or proven to cause a disease in human patients, to try to unravel its molecular or biochemical basis or test mutations and treatments. As an example the protein MSH2, suspected to cause hereditary nonpolyposis colorectal cancer (Lynch syndrome), was investigated in yeast where it was demonstrated to be involved in DNA mismatch repair, contributing to tumor formation^{27,28}. This consequently led to faster diagnoses and better surveillance for this disease.

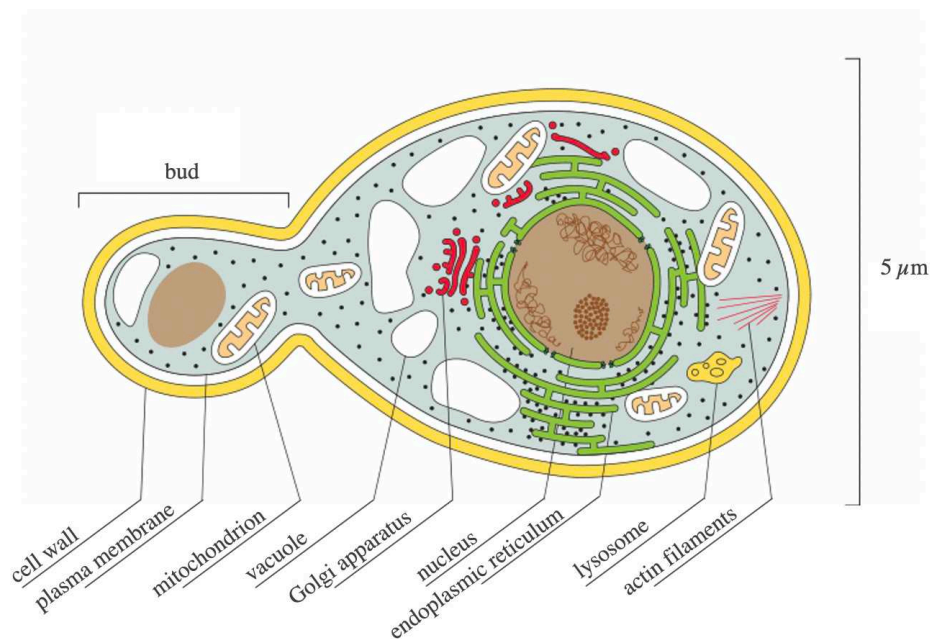


Figure 4. **Anatomy of *S. cerevisiae*.** As a eukaryote, *S. cerevisiae* has many fundamental similarities to human cells, including a nucleus, the capacity to process proteins via the endoplasmic reticulum and the Golgi apparatus, or respiration via mitochondria. Adapted from the book "Cell biology by the numbers" by Ron Milo and Rob Phillips²⁹.

Besides protein characterization, higher cell processes resulting in diseases have also been investigated in yeast. For neurodegenerative diseases, the impacts of amyloid beta aggregation and tau hyperphosphorylation on aging, oxidative stress and cell cycling were

investigated in yeast models of Alzheimer disease³⁰ as well as quality control mechanisms (chaperones and proteasome) for Parkinson's disease³¹. For genetically-based obesity, lipid management was investigated in yeast models^{32,33}, and tropical diseases have also been tackled through the expression of target enzymes from parasites (hard to cultivate) for drug screening in yeast³⁴ (from *Plasmodium* for Malaria and *Trypanosoma* for sleeping sickness).

Focus on cancer. As we have seen previously for aforementioned diseases, yeast-based approaches can be useful to uncover specific or more general cellular genetic or physiological aspects involved in a disease. Similarly, for cancer, “the emperor of all maladies”², yeast-based approaches have been extensively used. Besides the fact that cell cycle discovery in yeast was a huge breakthrough and created a framework to study cancer, yeast has also been used to better understand various specific proteins or pathways involved in specific cancer types. It is used as for drug screening and testing as well as diagnostics, and more recently for immune-related functions (see Fig. 5)³⁵.

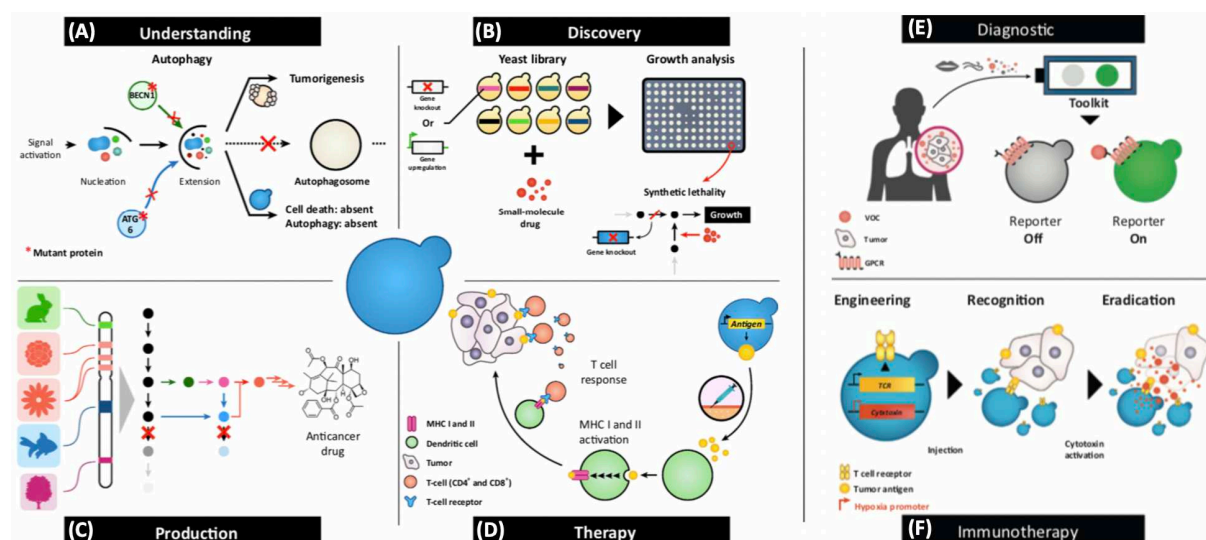


Figure 5. *Yeast contributions to cancer research* are manifold: (A) understanding the molecular bases of a cancer type thanks to protein conservation between human and yeast, (B) for anti-cancer drug testing and target discovery, (C) bioproduction of anti-cancer drugs in yeast using metabolic engineering, or (D) yeast-based vaccination using strains engineered to overexpress tumor antigen recognized and processed by the immune system. Contributions on the rise include using (E) yeast-based biosensors to detect particular set of compounds associated with cancer and (F) living medicine with yeast-based detection and delivery for tumor eradication. Adapted from Ferreira et al. 2019³⁵.

Finally, yeast can be used to bioproduce anti-cancer drugs. One important example is Paclitaxel (sold under the name Taxol®), which is originally found in low amounts in yew tree barks (*Taxus spp.*). Thanks to progress in metabolic engineering, genetic parts were identified, extracted, optimized and inserted into yeast for more sustainable production³⁶.

For medical applications, yeast can be used as a microbial cell factory to bioproduce a desired drug. This usage makes yeast a very valuable biotechnological tool, not only at

² Title of the “Biography of cancer” written by Siddhartha Mukherjee

the biomedical level, but also for a larger range of other products that could be obtained in a more sustainable way.

1.4. A very high biotechnological potential

Yeast is growing out of its role in solely fundamental research and has become a fully fleshed biotechnological tool. Using yeasts (not only *S. cerevisiae*) for bioproduction, or, as it is known in a more industrially oriented context, for biomanufacturing, is a growing trend in today's society, where a "bioeconomy" is laying its ground, thanks to advances in biomolecular technologies.

Drug manufacturing. Drugs are very high value-added compounds and are therefore the entry door for the biomanufacturing market where the still-too-high costs have to be offset. The landmark example for drug manufacturing in yeast is insulin, which is produced exclusively in microorganisms (instead of extracted from dog or cattle's pancreases), originally in *S. cerevisiae* and then in *Pichia pastoris*, the workhorse for heterologous protein production in yeast, another cousin of *S. cerevisiae* (today, a large part of insulin is actually produced in *E. coli*³⁷). Compared to bacteria, yeasts are often preferred for heterologous protein production for drugs as they can handle the production of more complex proteins, needing specific post-translational modifications for example. Produced health-related proteins range from hormones, growth factors and monoclonal antibodies, to complete vaccines (against cervical cancer - Gardasil®, for example). After proteins, a second category of biomanufactured drugs are small chemicals, and besides being discovered in the *Penicillium* fungus³⁸, antibiotics are a main product produced from yeasts. Today, more complex molecules can be produced such as artemisinin (antimalarial)³⁹, and recently scopolamine⁴⁰ (spasms/irritable bowel disease). Vitamins can also be produced in yeast, such as beta-carotene, a precursor to vitamin A, which will be of particular interest to us throughout this manuscript.

A greener world. What drives bioproduction today is the promise to manufacture chemicals and materials in a renewable non-polluting way by stepping out from the petrochemical based industries, from animal products, and from other non-environmentally friendly processes (like heavy-metal fabric dyeing). As of today, this remains ambitious, especially at scale, but companies are making it more and more real. This is the case in the cosmetics industry for example, that turns to yeast-based squalene (emollient) instead of shark oil (Amyris⁴¹) or fragrances produced in yeast (Givaudan's partnership with Ginkgo Bioworks⁴²). Bio-based dyes are of very high interest to the textile and fashion industries and yeast-based coloring molecules such as indigoidine has been already produced in microorganisms⁴³ and used to dye textile without the need for complex heavy metal additives (Colorifix⁴⁴). Finally, materials also take interest in yeast for bioproduction, some fungi are already used as an alternative for current packaging products (from their mycelium - Ecovative⁴⁵), but the stake lies particularly in finding alternatives to petrol-based plastics, finding new bioplastics with special properties or strong fibers for new biomaterials (in the US, the DARPA has invested recently in such technologies⁴⁶).

Foodtech. In the food and feed industries, yeast is already extensively leveraged for its fermenting capacity as discussed for bread and alcoholic beverages. But even more can be done with yeast using bioproduction. Its bioproduction potential is actually already exploited, and most especially because of its Generally Recognized As Safe (GRAS) status, it is an organism of choice, with eased commercial regulations, to bioproduce components that are to end up in our dinner plates. Already on the market are yeast-based milk, cream (Perfect Day⁴⁷) or cheese (New Culture⁴⁸), yeast-based proteins (chicken-like, salmon-like), and for plant-based meat to reach a bloody texture, ImpossibleFoods⁴⁹ produces soy-leghemoglobin in yeast. It is funny to think that we are not that far from the vision for yeast that Isaac Asimov has and write in the Robot series. See below.

“In the first place, by far the largest crop we deal with (and the percentage is growing) is yeast. We have upward of two thousand strains of yeast in production and new strains are added monthly. The basic food-chemicals of the various yeasts [...] is mostly sugar mixtures derived from the hydrolysis of cellulose, but, in addition, there are various food factors which must be added [...]. The beefsteak you thought you ate today was yeast. The frozen fruit confection you had for dessert was iced yeast. We have filtered yeast juice with the taste, appearance, and all the food value of milk. It is flavor, more than anything else, you see, that makes yeast feeding popular and for the sake of flavor we have developed artificial, domesticated strains [...]. Remains the complicating factor of popular fads with passing time; and of the possibility of the development of new strains with the new requirements and new popularity.”

Excerpt from "I, Robot" (The evitable conflict) by Isaac Asimov - 1950

A technological lock. As of today, bioproduction technology holds many promises, through the use of yeast and other microorganisms. Those could impact major industrial sectors, notably the food, materials, consumer products and health sectors. Investors and already there, and policy incentives are coming⁵⁰. However, it is the yields and scalability of the bioproduction processes that are the main obstacles to making bioproduction a really efficient biotechnology with the great impact it can have on our society. For this, more research is needed to unlock the huge potential that can be provided by microbes, and yeast has already proved to stand in one of the best positions to help achieve this goal.

Bibliography

1. Liti G. The fascinating and secret wild life of the budding yeast *S. cerevisiae*. *Elife*. 2015;4:1-9. doi:10.7554/eLife.05835
2. Jouhten P, Ponomarova O, Gonzalez R, Patil KR. *Saccharomyces cerevisiae* metabolism in ecological context. *FEMS Yeast Res*. 2016;16(7):1-8. doi:10.1093/femsyr/fow080
3. Carrigan MA, Uryasev O, Frye CB, et al. Hominids adapted to metabolize ethanol long before human-directed fermentation. *Proc Natl Acad Sci U S A*. 2015;112(2):458-463. doi:10.1073/pnas.1404167111
4. Money NP. *The Rise of Yeast.*; 2018.
5. McGovern P, Jalabadze M, Batiuk S, et al. Early Neolithic wine of Georgia in the South Caucasus. *Proc Natl Acad Sci U S A*. 2017;114(48):E10309-E10318. doi:10.1073/pnas.1714728114
6. Gomez-Pastor R, Perez-Torrado R, Garre E, Matall E. Recent Advances in Yeast Biomass Production. *Biomass - Detect Prod Usage*. Published online 2011. doi:10.5772/19458
7. Krebs HA, Johnson WA. Metabolism of ketonic acids in animal tissues. *Biochem J*. 1937;31(4):645-660. doi:10.1042/bj0310645
8. Krebs HA, Johnson WA. The role of citric acid in intermediate metabolism in animal tissues. *FEBS Lett*. 1980;117(August):K2-K10. doi:10.1016/0014-5793(80)80564-3
9. Barnett JA. A history of research on yeasts 6: The main respiratory pathway. *Yeast*. 2003;20(12):1015-1044. doi:10.1002/yea.1021
10. Hartwell LH, Culotti J, Reid B. Genetic Control of the Cell-Division Cycle in Yeast, I. Detection of Mutants. *Proc Natl Acad Sci*. 1970;66(2):352-359. doi:10.1073/pnas.66.2.352
11. Orlando DA, Lin CY, Bernard A, et al. Global control of cell-cycle transcription by coupled CDK and network oscillators. *Nature*. 2008;453(7197):944-947. doi:10.1038/nature06955
12. Goffeau A, Barrell BG, Bussey H, et al. Life with 6000 Genes conveniently among the different interna- Old Questions and New Answers The genome . At the beginning of the se- of its more complex relatives in the eukary- *Saccharomyces cerevisiae* has been completely sequenced *Schizosaccharomyces pombe* indicate. *Science (80-)*. 1996;274(October):546-567.
13. Pretorius IS, Boeke JD. Yeast 2.0-connecting the dots in the construction of the world's first functional synthetic eukaryotic genome. *FEMS Yeast Res*. 2018;18(4):1-15. doi:10.1093/femsyr/foy032
14. Dai J, Boeke JD, Luo Z, Jiang S, Cai Y. Sc3.0: revamping and minimizing the yeast genome. *Genome Biol*. 2020;21(1):205. doi:10.1186/s13059-020-02130-z
15. Giaever G, Chu AM, Ni L, et al. Functional profiling of the *Saccharomyces cerevisiae* genome. *Nature*. 2002;418(6896):387-391. doi:10.1038/nature00935
16. Giaever G, Nislow C. The yeast deletion collection: A decade of functional genomics. *Genetics*. 2014;197(2):451-465. doi:10.1534/genetics.114.161620
17. Sopko R, Papp B, Oliver SG, Andrews BJ. Phenotypic activation to discover biological pathways and kinase substrates. *Cell Cycle*. 2006;5(13):1397-1402. doi:10.4161/cc.5.13.2922
18. Huh W, Falvo J V, Gerke LC, et al. Global analysis of protein localization in budding yeast. *Nature*. 2003;425(6959):686-691. doi:10.1038/nature02026
19. Cherry JM, Hong EL, Amundsen C, et al. *Saccharomyces* Genome Database: The genomics resource of budding yeast. *Nucleic Acids Res*. 2012;40(D1):700-705.

- doi:10.1093/nar/gkr1029
20. Carvunis AR, Rolland T, Wapinski I, et al. Proto-genes and de novo gene birth. *Nature*. 2012;487(7407):370-374. doi:10.1038/nature11184
 21. Biddick R, Young ET. Yeast Mediator and its role in transcriptional regulation. *Comptes Rendus - Biol*. 2005;328(9):773-782. doi:10.1016/j.crv.2005.03.004
 22. Dutkowski J, Kramer M, Surma MA, et al. A gene ontology inferred from molecular networks. *Nat Biotechnol*. 2013;31(1):38-45. doi:10.1038/nbt.2463
 23. Caspeta L, Kerkhoven EJ, Martinez A, Nielsen J. The yeastGemMap: A process diagram to assist yeast systems-metabolic studies. *Biotechnol Bioeng*. 2021;118(12):4800-4814. doi:10.1002/bit.27943
 24. Lopes H, Rocha I. Genome-scale modeling of yeast: chronology, applications and critical perspectives. *FEMS Yeast Res*. 2017;17(5):1-14. doi:10.1093/femsyr/fox050
 25. Liu W, Li L, Ye H, et al. From *Saccharomyces cerevisiae* to human: The important gene co-expression modules. *Biomed reports*. 2017;7(2):153-158. doi:10.3892/br.2017.941
 26. Lee MG, Nurse P. Complementation used to clone a human homologue of the fission yeast cell cycle control gene *cdc2*. *Nature*. 1987;327(6117):31-35. doi:10.1038/327031a0
 27. Strand M, Prolla TA, Liskay RM, Petes TD. Destabilization of tracts of simple repetitive DNA in yeast by mutations affecting DNA mismatch repair. *Nature*. 1993;365(6443):274-276. doi:10.1038/365274a0
 28. Fishel R, Lescoe MK, Rao MR, et al. The human mutator gene homolog MSH2 and its association with hereditary nonpolyposis colon cancer. *Cell*. 1993;75(5):1027-1038. doi:10.1016/0092-8674(93)90546-3
 29. Milo R, Phillips R. *Cell Biology by the Numbers*. Garland Science; 2015. doi:10.1201/9780429258770
 30. McDonald J, Dhakal S, Macreadie I. Yeast contributions to Alzheimer's Disease. *J Hum Clin Genet*. 2020;2(2):1-19. doi:10.29245/2690-0009/2020/2.1114
 31. Menezes R, Tenreiro S, Macedo D, Santos CN, Outeiro TF. From the baker to the bedside: Yeast models of parkinson's disease. *Microb Cell*. 2015;2(8):262-279. doi:10.15698/mic2015.08.219
 32. Kohlwein SD. Obese and anorexic yeasts: Experimental models to understand the metabolic syndrome and lipotoxicity. *Biochim Biophys Acta - Mol Cell Biol Lipids*. 2010;1801(3):222-229. doi:10.1016/j.bbalip.2009.12.016
 33. Al-Anzi B, Arpp P, Gerges S, Ormerod C, Olsman N, Zinn K. Experimental and Computational Analysis of a Large Protein Network That Controls Fat Storage Reveals the Design Principles of a Signaling Network. Tucker-Kellogg G, ed. *PLOS Comput Biol*. 2015;11(5):e1004264. doi:10.1371/journal.pcbi.1004264
 34. Bilsland E, Sparkes A, Williams K, et al. Yeast-based automated high-throughput screens to identify anti-parasitic lead compounds. *Open Biol*. 2013;3(2):120158. doi:10.1098/rsob.120158
 35. Ferreira R, Limeta A, Nielsen J. Tackling Cancer with Yeast-Based Technologies. *Trends Biotechnol*. 2019;37(6):592-603. doi:10.1016/j.tibtech.2018.11.013
 36. Nowrouzi B, Li RA, Walls LE, et al. Enhanced production of taxadiene in *Saccharomyces cerevisiae*. *Microb Cell Fact*. 2020;19(1):1-12. doi:10.1186/s12934-020-01458-2
 37. Huang M, Bao J, Nielsen J. Biopharmaceutical protein production by *Saccharomyces cerevisiae*: current state and future prospects. *Pharm Bioprocess*. 2014;2(2):167-182. doi:10.4155/pbp.14.8
 38. Fleming A. On the Antibacterial Action of Cultures of a *Penicillium*, with Special Reference to their Use in the Isolation of *B. influenzae*. *Br J Exp Pathol*.

- 1929;10(3):226-236.
39. Paddon CJ, Westfall PJ, Pitera DJ, et al. High-level semi-synthetic production of the potent antimalarial artemisinin. *Nature*. 2013;496(7446):528-532. doi:10.1038/nature12051
 40. Srinivasan P, Smolke CD. Biosynthesis of medicinal tropane alkaloids in yeast. *Nature*. 2020;585(7826):614-619. doi:10.1038/s41586-020-2650-9
 41. Amyris. Amyris, Make good. No compromise. <https://amyris.com/ingredients>
 42. Ginkgo Bioworks. Producing Rare, Natural Ingredients with Givaudan. Published 2021. <https://www.ginkgobioworks.com/2021/08/30/givaudan/>
 43. Banerjee D, Eng T, Lau AK, et al. Genome-scale metabolic rewiring improves titers rates and yields of the non-native product indigoidine at scale. *Nat Commun*. 2020;11(1). doi:10.1038/s41467-020-19171-4
 44. Colorifix. Colorifix, We bring color to your life. <https://colorifix.com>
 45. Ecovative. Ecovative, Mycelium technology. <https://www.ecovative.com>
 46. Defense Advanced Research Programs Agency (DARPA). DARPA Successfully Transitions Synthetic Biomanufacturing Technologies to Support National Security Objectives. Published 2021. <https://www.darpa.mil/news-events/2021-12-08>
 47. Perfect Day. Perfect Day: Sustainable Animal-Free Dairy & Protein. <https://perfectday.com/process/>
 48. New Culture. New Culture, Cow Cheese without the cow. <https://www.newculture.com>
 49. Impossible Foods. Impossible Foods: Meat made from plants. <https://impossiblefoods.com>
 50. US Government. Joe Biden Administration. Executive Order on Advancing Biotechnology and Biomanufacturing Innovation for a Sustainable, Safe, and Secure American Bioeconomy. <https://www.whitehouse.gov/briefing-room/presidential-actions/2022/09/12/executive-order-on-advancing-biotechnology-and-biomanufacturing-innovation-for-a-sustainable-safe-and-secure-american-bioeconomy/>

2. Introduction

2.1. Bioproduction

Bioproduction is defined as the use of biological systems to produce biomolecules of commercial importance. Among those biological systems are yeast and bacteria, molds, mammalian, insect and plant cells^{1,2}, and more recently, mini-cells and cell-free systems, all allowing for bioproduction. Here, we will focus on the use of microorganisms, mainly yeasts and bacteria, used for bioproduction, sometimes referred to “biomanufacturing” via “precision fermentation”. Since those microorganisms are easy to handle, comparatively inexpensive to cultivate, robust, divide at a quicker rate, can renew indefinitely and reach high cell densities, they have been extensively used as “microbial cell factories”.

2.1.1. Microbial Cell Factories

Synthetic Biology attempts to turn biology into an engineering discipline, using a bottom-up approach, with a “Build to understand” mindset (Richard Feynman’s quote³). Instead of trying to reverse engineer biological systems (as in fundamental research), forward engineering is used to build new things upon what is known, using basic engineering principles, mainly, standardization of parts, modularity and automation. Advances in synthetic biology have essentially relied on two pillars. On the one hand, it relied on understanding that gene expression and therefore cell behavior is governed by tightly regulated molecular networks. The works of Jacob and Monod⁴ set the stage to understand the grammar of gene expression and to identify independent genetic parts that could be combined to build higher function and control cell behavior. On the other hand, the rise in DNA reading, editing and writing technologies allowed for continuously increased throughput, leading today to even more automation in the lab, illustrated by the recent multiplication of Biofoundries around the world. The hopes with synthetic biology are high, for health (new and smart drugs), environment (bioremediation, sensing), materials (bioplastics, textiles), agriculture (farming input producing microorganisms), food (synthetic meat, animal-free), and other sectors (data-storage, biocomputing). And in many of those advances, lies the need for efficient bioproduction. Approaching biology like any other engineering discipline is still very challenging as biological systems remain noisy and lack predictability and stability as they are always subjected to their inherent stochasticity and to natural selection. Engineering biological systems therefore remains sometimes more similar to tinkering, where modifications are made and tested step by step in a Design – Build – Test – Learn (DBTL) cycle, which is a standard procedure today to improve strains and consequently, improve production yields (detailed later).

Historic. Using microorganisms to turn one substrate into a desired product was used since ancient times. While those processes, mostly fermentation, were spontaneous and unavoidable at times, humans learned to tame those processes to make alcoholic beverages, bread, dairy products and other fermented food on purpose without understanding the origin of the transformation. Only after the works of Pasteur and Koch in the late 1800s, microbiology

was born. The paternity of industrial bioproduction often goes to Chaim Weizmann, who was the first to identify single strains to ferment in large-scale anaerobic liquid fermenters. In his quest to initially produce synthetic rubber, he discovered *Clostridia acetylbutylicum* (a gram-positive bacteria) that could ferment glucose into acetone and butanol. In the end, acetone was used to make cordite gunpowder for WW1 and butanol, the by-product, for paints and resins⁵. Similarly, Pfizer developed methods to produce citric acid from sugar, which is still the main source today, using *Aspergillus niger* (mold). Amino-acids, vitamins and other solvents were also produced during this period, which consisted mainly in primary metabolites, *i.e.*, required for cell growth and produced during the exponential growth phase. In 1929, Alexander Fleming published the discovery of the first antibiotic from the fungus *Penicillium*⁶, a secondary metabolite, produced mainly after the exponential growth phase. After that, great efforts were made to find other antibiotics in other microorganisms and to refine bioproduction processes to maximize antibiotic production⁷. After the discovery of the structure of the DNA⁸, the genetic code and the nature of proteins, recombinant DNA technologies⁹ allowed for the production of heterologous proteins in microorganisms and led to the production of, among others, insulin and growth hormone, while there were previously extracted from animals, as well as other drugs. In addition, industrial enzymes for research (Taq, restriction enzymes), food (amylases, lipases), textile (cellulases), and cleaning (proteases) industries became a booming market. Then came the advent of complex metabolic engineering for the production of specific chemicals via the combination of expressed heterologous enzymes recapitulating a production pathway (often that does not occur naturally).

Native products / Recombinant proteins / Heterologous pathways. We saw that there are different products bioproduced using microorganisms. Chronologically, (1.) endogenous (native) metabolites, (2.) heterologous (recombinant) proteins, and (3.) heterologous chemicals from synthetic pathways (which could also be considered metabolites). In terms of metabolism, endogenous metabolites rely on the host's metabolism and historically, the host was actually chosen for its natural production capacities. On the other hand, heterologous proteins and chemicals produced have to be grafted to the host's metabolism via various promoters (gene regulation) and at chosen metabolic entry points (endogenous precursor pool).

To improve production yields, the engineering stakes and approaches vary for each of the 3 product categories (although they also overlap to some extent). For example, while recombinant proteins production engineering focuses mostly on protein processing and trafficking bottlenecks, heterologous pathway expression will focus more on improving the pathway itself, and its relationship with the host's metabolism, as well as other approaches also useful to improve natural compound production (particularly well-reviewed in Davy *et al.* 2017¹⁰). **In this manuscript, we will focus mainly at the level of chemical production via the genomic integration of a heterologous pathway. Our example will be the beta-carotene production in *Saccharomyces cerevisiae*.**

Chassis are organisms or strains that are repeatedly used as background or framework for bioproduction (Fig. 6). Some chassis organisms are used because of their natural capacity to produce certain metabolites (*Yarrowia lipolytica* for lipids) or precursors, or some, like *S. cerevisiae* and *E. coli* for the amount of knowledge and tools already available, and their

regulatory status (such as “Generally Recognized As Safe” – GRAS, facilitating market placing). They are selected also based on their natural physiological capacities (*Pichia pastoris* yeast for secretion and glycosylation, *Pseudomonas putida* bacteria for its industrial robustness), or other qualities (*Vibrio natrigens*: 10 min doubling time!). And finally, some are selected based on what they can use as feedstock: light for cyanobacteria and microalgae, or methanol for *Pichia pastoris*. Besides their natural capabilities, organisms are optimized, and new strains can be used as new chassis, for instance, a *S. cerevisiae* strain using xylose as feedstock, an *E. coli* strain that produces a lot of a precursor needed for the production of various heterologous metabolites or a certain category, which can therefore be repeatedly used for the production of various compounds. The choice of the chassis strain is very important for industrial purposes where the sole objective is to maximize production yields. In the lab, and in our case, our chassis is the specific genetic background for *S. cerevisiae* CEN.PK2-1C, as we favor *S. cerevisiae* for the largest amount of knowledge and data accessible in the literature and available biotechnological tools, and this background for its higher tolerance to industrial conditions¹¹.

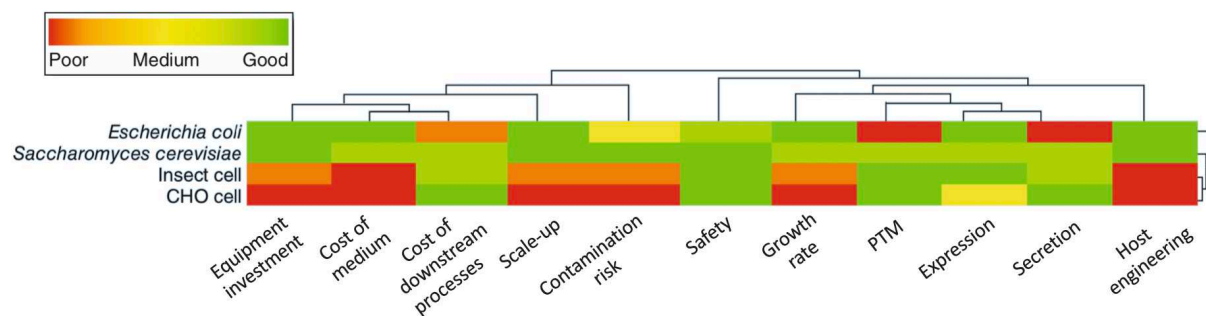


Figure 6. **Different cell types can be used for bioproduction**, each with different advantages and drawbacks given various evaluation criteria. We will focus mostly on bacteria (*E. coli*) and yeast (*S. cerevisiae*) which gather most qualities needed for efficient bioproduction of certain proteins and various chemicals, although insect and Chinese hamster ovary (CHO) cell (the standard mammalian cell model) are used for the production of more complex proteins like antibodies, which may favor protein quality (folding and PTMs) over quantity. PTM stands for Post-Translational Modifications. Diagram adapted from Huang et al. 2014¹².

Biomanufacturing has been in use for more than a century. Besides naturally produced metabolites (most important of them perhaps being antibiotics), we now know how to make microorganisms produce chemicals they never could before, or even new-to-nature compounds that have use for various industries. This possibility could revolutionize our use of biological systems, and lead toward what some call the 4th industrial revolution resulting in a “bio-based economy”. Bioproduction works, but not well enough for production of all new bioproduction-based chemicals to be economically competitive with current production methods (*status quo*). Some are already competitive however, this is the case for very high value-added molecules and proteins (mainly drugs) but more commodity chemicals (e.g., bioplastics) remain at the proof-of-concept stage. More and more synthetic biology companies emerge and appear to subsist (such as Ginkgo Bioworks, Conagen, and Amyris), but it becomes clear today that to improve and expand bioproduction’s scope of applications, yields must be increased. We could go as far as to suggest that this technological lock needs a breakthrough similar to that of James

Watt's steam engine in the 1770s: while some steam engines existed before, it is the increase in yield provided by Watt (and coworkers) that allowed the steam engine to be applied to many economic sectors and then further democratized and world widely diffused. Thus, increases in production lower costs, and the savings can be passed on to the clients, given that the product comes with a reduced price compared to its *status quo* version^{13,14}.

Stakes. To make bioproduction economically competitive, increasing overall yields is central. For that, one can:

1. Increase the number of producing cells (biomass yield – gCDW/L)
2. Increase the production per cell (content – g/gCDW)
3. Increase the efficiency of downstream processing (purification strategies).

We will focus mainly at the level of the content, and first see how one can improve content once the chassis has been selected and actually produces a small quantity of a chemical of interest. In the following sections of this 1st part of the introduction, we explore how those objectives are approached via strain engineering, bioprocessing and culture conditions, and what their limitations are. **To illustrate those strategies, in this thesis we use the study case of beta-carotene production.**

2.1.2. Beta-carotene

Beta-carotene is a terpene of the carotenoid family (Fig. 7). It is a compound known for its characteristic yellow/orange color, typically found in plants as a secondary metabolite, mostly to protect photosystems from photodamage¹⁵. It is our main source of vitamin A (retinol) as it is its precursor and is therefore important for our human diet¹⁶. Its antioxidant (health) and photochemical (coloring agent) properties make this carotenoid a valuable molecule in a wide range of industries: in cosmetics (sun protection), health (antioxidant and dietary supplement as provitamin A), feed (increases eggs yolk and salmon aspects) and food (mostly used as coloring agent in beverages and others)¹⁷.

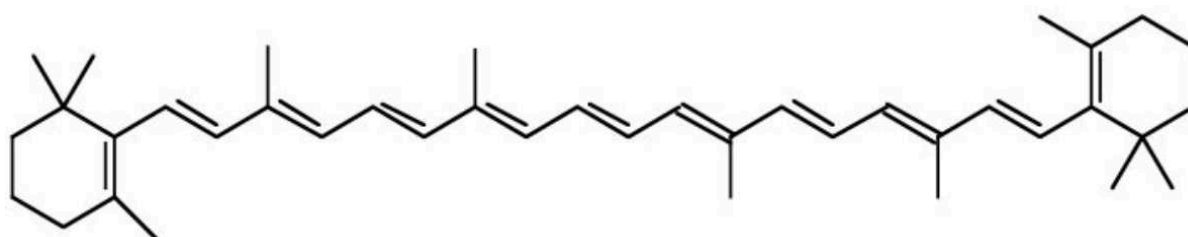


Figure 7. **Beta-carotene** is a tetraterpene (C40), in the carotenoid family. Its photo oxidant and color properties grant a vibrant yellow-orange color to cells or objects that carry it, making it a convenient proxy for genetic expression and proof-of-concept studies.

Production methods. As of today, major sources of beta-carotene remain chemical synthesis: starting from petrochemical sources of isobutene and formaldehyde, citral is obtained. It reacts with acetone to obtain beta-ionone, which is then condensed via enol-ether

or Wittig reactions¹⁸ to obtain beta-carotene. In second, come natural sources: extraction from plants (carrots, oil of palm fruit, and sweet potato) and extraction from naturally producing microorganisms. Beta-carotene is naturally produced by the microalgae *Dunaliella spp.*¹⁹ and even *Spirulina*¹⁷, or molds like *Blakeslea trispora*, the yeasts *Rhodotorula spp.*²⁰, and notably *Xanthophyllomyces dendrorhous* (a.k.a. *Phaffia rhodozyma*), which will be the source species for our genetic construction in the following chapters. It is also produced by some bacteria like *Deinococcus radiurans*, and beta-carotene has also been successfully produced in *E. coli*²¹. Many studies have demonstrated the production of beta-carotene in *S. cerevisiae*, but, to the best of our knowledge, it remains at the lab scale. *Dunaliella salina* (beta-carotene produced as a reaction to intense sunlight and stress for protection) and *Blakeslea trispora* (beta-carotene as precursors of sexual pheromones) are the ones used at the industrial scales¹⁷. At the lab scale, *Yarrowia lipolytica* is gaining popularity, and it has proven itself for beta-carotene production at high levels thanks to its high endogenous propensity to accumulate lipids²². In *S. cerevisiae*, beta-carotene localizes mostly in lipid droplets²³.

Pathway. Beta-carotene is relying on the isoprenoid/mevalonate (MVA) metabolic pathway. In most organisms, first, acetyl-CoA is channeled towards mevalonate production, and then to IPP and DMAPP production, precursors to many other high value-added molecules²⁴. In *S. cerevisiae*, IPP and DMAPP condensation produces geranyl-pyrophosphate (GPP) and the addition of a second IPP molecule gives farnesyl-pyrophosphate and FPP (Fig. 8). FPP can be converted to either farnesol (FOH) via DPP1p; two FPP molecules can condensate to form squalene via ERG9p (pathway for ergosterol and other sterols synthesis, essential for the cell membranes); or, via the addition of another IPP molecule to GGPP, the precursor of the beta-carotene pathway. For beta-carotene production, the heterologous pathway used in this PhD is grafted to *S. cerevisiae*'s metabolism via GGPP. Using the CrtYB bi-functional enzyme, GGPP can be converted to phytoene (uncolored). Using CrtI, phytoene is converted to lycopene (red pigment), and in subsequent reactions using CrtYB yet again, Lycopene is converted to beta-carotene. CrtYB and CrtI both originating from *Xanthophyllomyces dendrorhous*. In our design, two additional genes are inserted: the tHMG1 and CrtE enzymes, which act as boosters to produce more of the GGPP precursor. This design is based on Rabeharindranto *et al.* 2018²⁵, itself originating from Verwaal *et al.* 2007²⁶ (more details in other chapters).

Fundamental research. We have seen that beta-carotene originates from the isoprenoid pathway. This is the case also for other compounds of economic importance such as artemisinin (an anti-malarial drug)²⁷, Taxol® (Paclitaxel - anti-cancer)²⁸, celastrol (anti-obesity)²⁹, but also other molecules involved in fragrances like limonene and menthol. Therefore, any new improvements in bioproduction found using beta-carotene can benefit all compounds based on this pathway. Moreover, the production of a colorful compound that can be detected with the naked eye makes beta-carotene a particularly convenient product for various bioengineering studies. Thus, beta-carotene is often used as a proxy or output for various proofs of concept and genetic systems such as signal processing engineering³⁰, development of sensors in yeast³¹, promoter engineering³², or testing the efficacy of new genetic systems³³ (like in our case).

second, because metabolic imbalance can result in the accumulation of unwanted potentially toxic intermediate chemical species. For this, investigating fluxes inside the pathway can be relevant, mostly via HPLC, to detect various chemical species²⁵. To improve the flux within the pathway, the amount of enzyme or the activities can be optimized. Enzymatic concentrations can be tuned mostly via the used promoters, ribosome binding site (RBS – Kozak sequence in yeast), and more rarely terminators and 5' and/or 3' untranslated regions. For example, it was shown that having all carotenogenic enzymes under equally strong constitutive promoters was *not* necessarily the best way to maximize production³⁷, and by controlling enzymes' transcription differentially, a sweet spot can be determined that maximizes production³⁰. Tuning enzymatic activities can be another way to balance the pathway. Different combinations of orthologs, which may have different affinity and/or activity can be tested: for example, *Staphylococcus aureus*' tHMG1 was found to be more efficient than *S. cerevisiae*'s³⁸. In our case, we simply used CrtYB, CrtI and CrtE from *Xanthophyllomyces dendrorhous* and HMG1 catalytic site as extra copies from *S. cerevisiae*. Also, protein engineering (via rational design or evolution) can lead to increased yields³⁸. We can also note that the locus of insertion in the genome can impact the expression of the enzymes (context dependency) and that the location of the pathway's genes respective to the others may also influence production (organization as operons is often favored). Another way to improve pathway efficiency is compartmentalization, which brings enzymes together in the same organelle, in the same cluster³⁹, or even going to the extent of fusing enzymes together (which was shown to work for beta-carotene production by fusing CrtYB and CrtI^{25,40}). All those techniques are used to create more proximities between enzymes and create localized nanofactories inside the cell, which will accelerate enzymatic reactions⁴¹. For example, localizing the whole astaxanthin (a derivative of beta-carotene) pathway in either single compartments (lipid body, endoplasmic reticulum or peroxisome independently) resulted in increased production in *Yarrowia lipolytica*⁴⁰.

Pathway-scale flux engineering. Taking a step back, after having focused on the pathway regardless of the cellular context, we can look at how to improve the pathway by taking into account where it has been grafted in the cell's metabolism and see if immediate bottlenecks can be identified. Those are questions of mostly identifying obvious bottlenecks (directly related to the pathway) in the carbon flux towards production to identify and improve precursor supply and product accumulation. Bottleneck and limiting steps can be identified using Flux Balance Analysis or Metabolic Flux Analyses (C13). By quantifying specific metabolites, in the context of bioproduction, it was shown that the step for the conversion of HMG-coA to mevalonate was limiting such that tHMG (the catalytic unit of the yeast HMG1 enzyme) was isolated and overexpressed to increase flux through the mevalonate pathway²⁶. Similarly, CrtE, an enzyme we use for beta-carotene production, backs up the endogenous BTS1 enzyme for the conversion of FPP to GGPP, the key precursor to the heterologous beta-carotene pathway. Conversely, to increase the flux towards the pathway of interest, one can also shut down or reduce the carbon flux feeding to other competing pathways. In our design, the DPP1 enzyme was deleted to increase FPP flux towards GGPP instead of FOH²⁵. Similarly, the ERG9 enzyme, which has its reaction also branching from FPP, could be deleted but proved essential for the lipid biosynthesis pathway. In other beta-carotene production designs, the

expression of this enzyme is reduced to facilitate the flux even more²³. Although increasing copy number can often seem like a good strategy to increase production at this stage to increase fluxes or solve bottlenecks, there is a balance to be found between expression and production⁴². For instance, Lopez *et al.* 2020⁴³ found that increasing precursor supply was more important than increasing copy number to produce beta-carotene. Increasing the input flux is important but managing the output flux can be equally crucial. The accumulation of the final product can be a problem, and increasing accumulation capacities can be one strategy, or evacuating the final product can help maintain production. For example, in Bu *et al.* 2022²³, the beta-carotene storage capacity of *S. cerevisiae* was increased by engineering lipid droplets associated genes, and beta-carotene secretion has also shown to be possible and beneficial using ABC transporters in yeast⁴⁴ and in *E. coli*⁴⁵.

Cell-scale flux engineering. Until now, our reference point was our heterologous pathway. However, the limitations of bioproduction can come from many sources, sometimes less intuitive, at the larger cell scale and may involve other biological processes. With a bird's eye view of cell metabolism, it can be interesting to approach cell processes as independent modules, like it was proposed in some studies^{21,46} by differentiating improvement that can be done at the scale of the central carbon metabolism (Glycolysis, TCA), pentose phosphate pathway, cofactor metabolism (ATP, NADPH), MVA pathway and the beta-carotene pathway. For example, beta-carotene production has often been linked to the cell concentration in NADPH and oxidative stress, and it was shown that improving NADPH supply resulted in improved yields both in *E. coli*⁴⁷ and *S. cerevisiae*^{48,49}. It is important to consider the interplays between metabolic fluxes and cofactors levels or fluxes⁵⁰ in order to keep metabolic pools at a steady level, and prevent limitations, especially regarding metabolites considered as "currencies" (or "energy molecules"), such as NAD(P)H, ATP, GTP, or glutamate. Understanding interplays between heterologous pathways and cell's endogenous modules can also lead to novel strategies: while the endogenous yeast lipid metabolism can be considered a competitor to beta-carotene production⁵¹, experiments have shown that actually increasing *S. cerevisiae* lipid metabolism leads to higher carotenoid yields⁵²⁻⁵⁴.

Global engineering. Until now, strategies to improve production remained relatively close to rational design. On the opposite, methods based on evolution produce genetic and metabolic changes that are sometimes hard to identify and that can impact the cell at any physiological level. They include mainly Adaptive Laboratory Evolution (ALE) a.k.a. directed evolution, where a strain is often subjected to chemical mutagens, generation after generation, or where genetic libraries are tested (rounds of error-prone PCRs) as well as other techniques⁵⁵. The main challenge with ALE is the selective pressure and the selection process. The selective pressure can be in terms of growth rate (often the case for tolerance engineering, for toxic compounds, where a drop in fitness is observed upon bioproduction), or in terms of increased stress that will favor the production of the product of interest. However, one must always make sure that the product interest is produced in increasing quantities since knocking out the production pathway is often the best way to restore the strain fitness. There are today great efforts to develop biosensors that detect specific chemicals, to perform biosensor-assisted evolution. The biosensor can then trigger the production of either a Fluorescent Protein (FP – then screening and selection using droplet-based microfluidics techniques or cytometry) or an

essential gene, leading to increased growth (biosensor-based growth coupling). Efforts to identify the relevant mutations (using omics and systems biology approach) can then lead to new targets for strain engineering using rational design. For beta-carotene production, given its anti-oxidant properties, oxidative stress (hydrogen peroxide shocks) was used as selection pressure for the evolution of improved production in *S. cerevisiae*: Reyes *et al.* 2014⁵³ found genes involved in lipid biosynthesis and the MVA pathway increased, as well as genes involved in stress regulation differentially expressed and some involved in cellular respiration downregulated, ultimately leading to improved beta-carotene production.

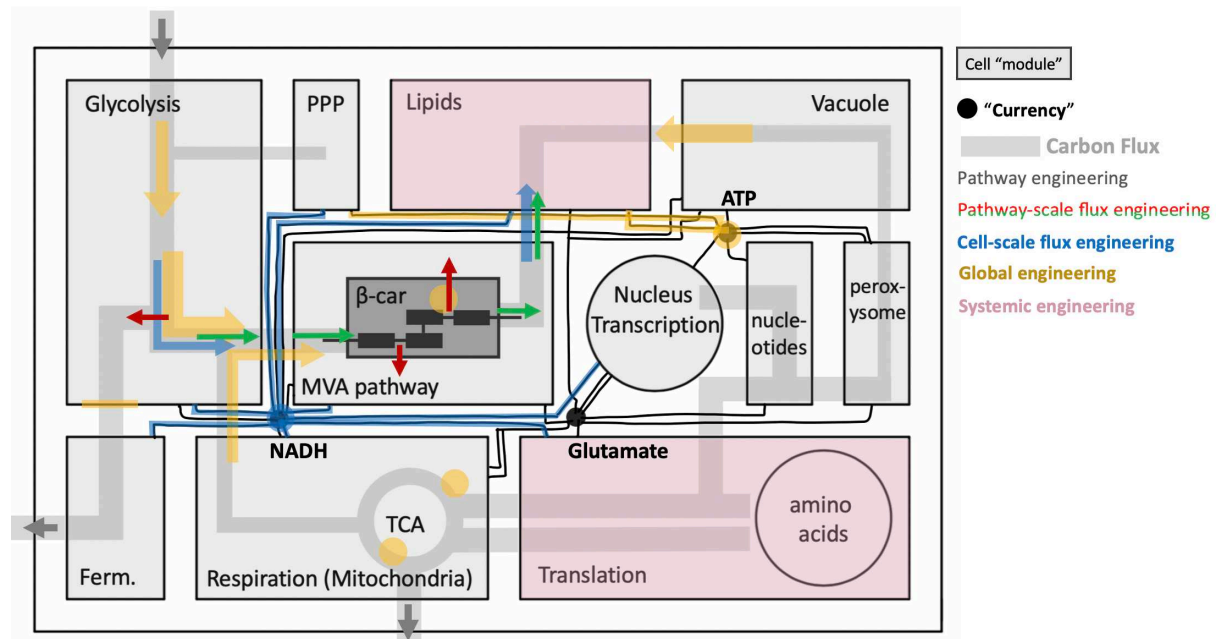


Figure 9. **Metabolic engineering by scales.** In this cell diagram (with different cell modules depicted), we propose a by-scale outlook of strain engineering approaches. First, the heterologous pathway can be optimized on its own, by tuning relative and absolute enzymes levels and activities (dark grey and black – at the center of the diagram). Then, other metabolic pathways feeding in or out from the heterologous pathway can be improved: debottlenecking, increasing fluxes (green arrows) and preventing competing reactions (red arrows) to generally improve carbon flux channeling to the heterologous pathway. Still relying on rational design, cell scale flux engineering (blue) addresses larger scale limitations (like increasing the pool of NADH, a “cell currency”) or further increase flux redirection “from further away” to the heterologous pathway. Global engineering (in yellow), often by adaptive lab evolution (ALE – non-rational design) can impact sometimes unidentified or unexpected parts of metabolism leading to higher production. “Systemic engineering” (in pink, encompassing entire cell modules) focuses more on chassis development methods, where a whole cell process can be improved to favor, for example, a more sustained translation, or the lipid management in the cell, which has been shown to improve beta-carotene production.

Systemic engineering. Lastly, another way to improve bioproduction, in general, is to improve some of the cell’s processes, *a priori*, regardless of the chemical to be produced. This is done more in a chassis-development strategy. For instance, we have seen that increasing the lipid metabolism can be advantageous for beta-carotene production, as it can also be the case for many products, and thus it can be interesting to get *S. cerevisiae*’s lipid metabolism more similar to that of the oleaginous yeast *Yarrowia lipolytica*’s⁵⁶. Other system-level strategies can include increasing global translation capacities (by overexpressing translation initiation factors in *P. pastoris*⁵⁷, or increasing tRNA level in the widely-used *E. coli* BL21-derived Rosetta strain), or the Unfolded Protein Response (UPR) in yeast. Other approaches include

genome minimization (via the Sc3.0 project⁵⁸), aiming at removing genes that are not immediately useful. For example, in *S. cerevisiae*, GPD1p is a constitutively expressed inactivated (phosphorylated) enzyme, important for osmotic stress detection and quick response; but under controlled laboratory growth conditions, its use can be argued, and its expression cost probably spared.

Recent techs. At each scale of the engineering process, molecular biology techniques are more and more intertwined with more bioinformatic and computational methods. Indeed, metabolic engineering is actually more and more guided by omics data and models. Different types of models are mainly used to analyze quantitative data in a comprehensive manner, predict and suggest changes to improve strain performance: mainly 1. genome-scale / constraint-based (static) metabolic models, 2. Dynamic/kinetic models, and 3. hybrid, resource allocation, or machine learning-based models that try to bridge the two first types⁵⁹. Many examples exist already⁶⁰: in our context, an alternative of the MVA pathway (more efficient and less costly) was optimized and inserted in *S. cerevisiae* using genomics and metabolomics (LC-MS and C13 fluxomics) approaches⁶¹, which could prove useful for the production of metabolites downstream of the pathway, such as beta-carotene.

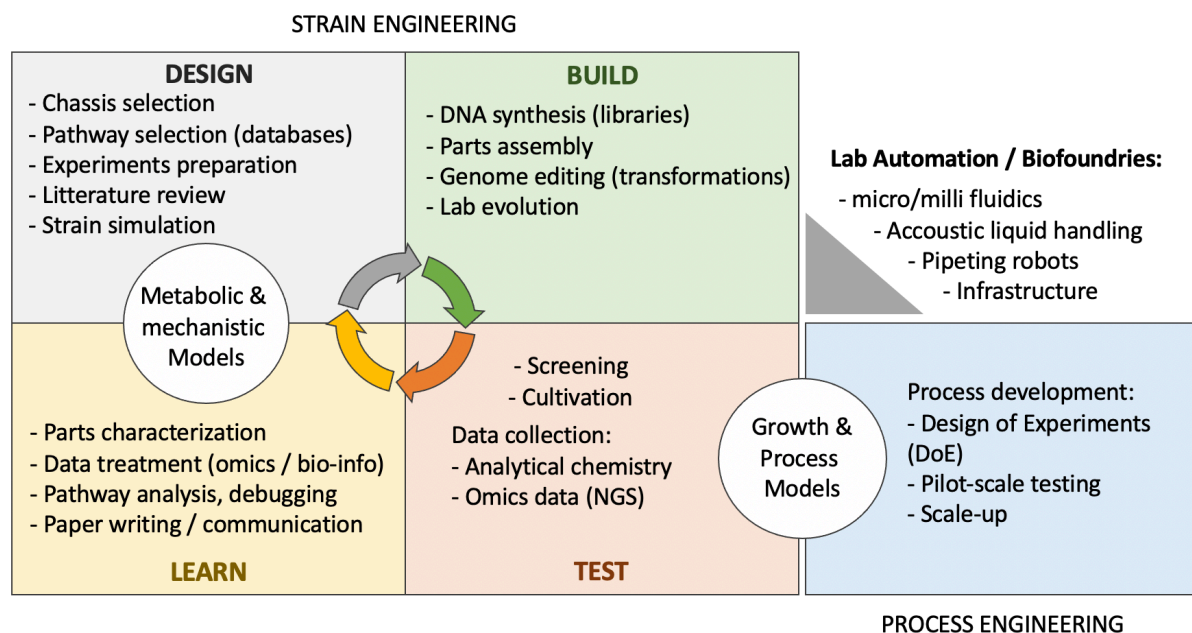


Figure 10. **The DBTL cycle** (Design Build Test Learn) is an iterative process used for strain development (metabolic engineering). Each incremental modification steps are first **Designed** and prepared *in silico*, using molecular biology software and enzymes databases and cell models. Based on those, strain construction (**Build**) begins, by hand, or more and more using lab automation systems. After the **Build** step, the **Testing** process is needed to screen and test the various resulting strains. Quantifications are carried out to best assess strains' production performance (HPLC, GC-MS, etc.) and to find further improvement targets (NGS techniques). Those data are analyzed and feed predictive algorithms and cell models (**Learn**) for further improvements. The **Test** step can also lean into process development where candidate strains are tested in larger-scale experiments of more complex growth processes.

DBTL cycle. To maximize production yields, the producing strains are iteratively modified, tested, screened, selected and further upgraded and improved. Of course, the engineering scales we detailed above are not mutually exclusive, quite the contrary. As each modification can be incremental, each modification acts as a checkpoint to deciding how to pursue it. The classification we proposed is just an arbitrary view to better think the whole metabolic engineering possibilities. During the strain development process, it is always necessary to jump from one engineering scale to another many times as one new modification may impact previous ones. This whole iterative process is referred to as the Design-Built-Test-Learn cycle and is the framework most metabolic engineering efforts rely on today⁶² (Fig. 10).

Strain engineering is not the only parameter to take into consideration to maximize yields. As an example, Lopez *et al.* 2019⁶³ showed that depending on the genetic architecture of the beta-carotene production, the scalability of two different producer strains was different: rationally engineered *versus* evolved beta-carotene producer strains tested for 72h in shake flasks *versus* in fed-batch 1L bioreactors obtained opposite scalability performances: in flasks, the evolved strain produces 3 times as much as the rationally engineered strain, and this is the opposite in fed-batch. It is often the case that content, yield and titer vary with different culture processes and growth conditions. **Consequently, despite best efforts made to increase production, one strain's performance will inevitably vary across culture processes and growth conditions.**

2.1.4. Bioprocesses

Cells can be cultivated following 3 main categories: in batch, continuous or fed-batch ways. Those are also referred to as “bioprocesses” or “cultivation strategies” (Fig. 12).

Batch is the standard culture method used in the lab at various scales. It consists in inoculating a strain to a defined (or not) culture medium and letting it grow in a closed system. This way, a finite quantity of resources is available. As cells grow, nutrients will be depleted, limitations in various compounds will occur such that the cell metabolism changes over time. Most of the time, in the lab, *Saccharomyces cerevisiae* is cultivated in the rich medium YPD (Yeast Extract, Peptone and Dextrose – Glucose 2%) aerobically. The classical growth profile obtained is presented in Fig. 11. It starts with the lag phase, allowing the cell to adapt to its new environment. Then comes the exponential phase, where *S. cerevisiae* cells typically have a 90 min doubling time, such that cell count doubles every hour and a half. There, fermentation takes place: glucose is consumed and fermented to ethanol and CO₂. Upon glucose depletion, the “diauxic shift” occurs, and cell metabolism shifts to respiration. Cell growth slows down as cells respire ethanol to CO₂. Once the ethanol and other compounds (acetate, glycerol from overflow metabolism) consumed, a limitation in carbon source occurs and cells enter the stationary phase leading to quiescence, followed by death. In lab culture conditions, it is mostly a carbon-source limitation that stops the growth, while other resources, like nitrogen, phosphate and sodium resources are considered in excess (as well as metallic ions or vitamins). Owing to the high growth rate of cells fermenting in rich medium, batch is preferred as a first step for

rapid biomass accumulation, despite of the low energy yield of fermentation compared to respiration.

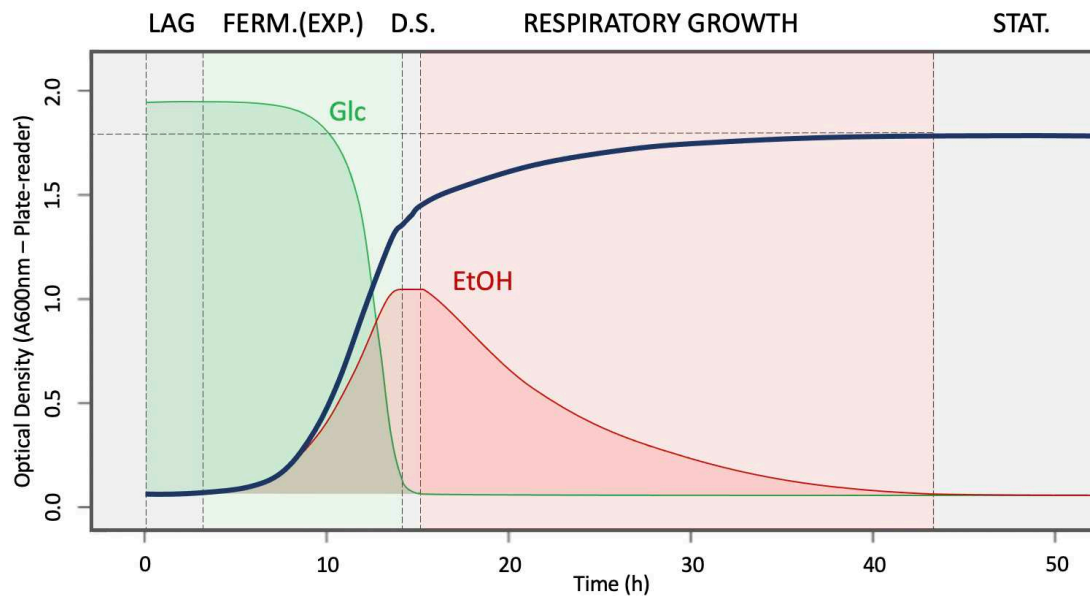


Figure 11. *S. cerevisiae* typical growth profile in batch on glucose. After the lag phase, cells ferment glucose at a high rate, producing ethanol and CO_2 . Upon glucose depletion, the diauxic shift occurs, and cell metabolism shifts to respiration where ethanol is turned into CO_2 . After ethanol depletion, cells enter the stationary phase. Blue line: cell density (data from plate-reader). Green and red lines: glucose and ethanol consumption profiles (by hand).

Fed-batch can be considered a semi-continuous process. During fed-batch, a certain quantity of (often) a limiting nutrient is fed into the culture medium in order to put the cell in a desired metabolic state. It is often used after batch phases to increase the total biomass of the culture in a medium by adding the carbon source (limiting factor) proportionally to the cell density. For example, by keeping glucose at low (controlled) levels, the respiratory metabolism can be maintained in yeast, in order to limit overflow metabolism, with a smaller amount of glucose, to slowly further increase biomass yield.

Continuous culture consists in perfusing culture medium continuously, with an inflow rate equal to the outflow rate such that the cell quantity remains constant in the culture volume (chemostat). This way, cells are kept in a constant environment, and in a stable metabolic state. This method is great as it allows for the removal of a secreted product, especially if the accumulation can become toxic to cells. There are variants of continuous bioprocesses: sometimes called “perfusion”, with or without cell retention, and with or without removal of the secreted product from the medium. But keeping cells for long in a continuous culture can raise strain stability issues, mainly, evolutionary escapes, as well as increasing contamination risks.

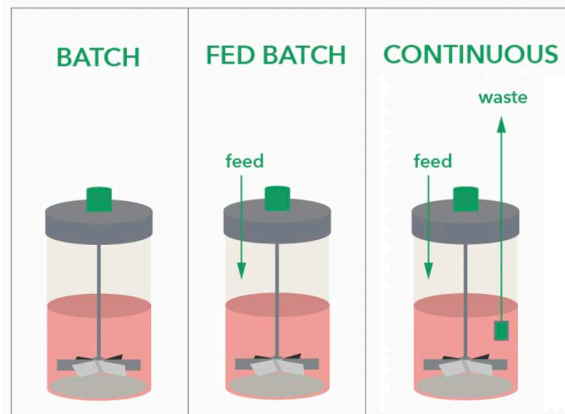


Figure 12. **Cultivation techniques (bioprocesses).** Batch consists in a finite amount of nutrients in the process: an initial solution is created and cells will grow with no external input or output, resulting in non-constant growth dynamics. In fed-batch, nutrients are gradually fed in, such that the culture volume slowly increases, and limitations in nutrients and metabolism can be better controlled. In continuous culture, medium is regularly fed in and taken out to maintain a constant volume and metabolic cell state. Adapted from pharsol.com.

In the following sections and chapters of this manuscript, we will mostly focus on batch cultures and discuss fed-batch contributions.

2.1.5. Culture conditions

After strain engineering and bioprocesses, **the culture conditions can directly impact the performance of the strain:** culture parameters, which often change with culture scale and bioprocess (temperature and pH, etc.), but also medium composition (nutrients), which can be either an initial choice or will also change with culture scale.

Medium composition is crucial for a successful bioprocess, as it will directly impact cell metabolism, and thus, bioproduction. Indeed, “significant yield improvement can be reached through the choice of an adequate culture medium”⁶⁴. Nutrients needed are mainly: a carbon-source (often carbohydrates, sometimes alcohols, even fatty acids⁶⁵, or even utilization of a mixture of carbon-sources), a nitrogen source (from peptone in the lab – mostly peptides, or NH_4 in industrial conditions, tryptone, casamino acids), a phosphate source, vitamins (biotin, thiamine, folic acid...), and trace minerals (Mg, Zn). For bioproduction, two strategies can be used: develop a strain to perform best in a certain environment, and/or tune the medium to maximize production from the strain. Those strategies are not mutually exclusive, but, often, in lab settings, YPD is the reference point, and in industrial settings, a feedstock is chosen, and the strain will be developed to best produce from it. For example, the most widely used feedstock in the industry is molasse (a by-product from the sugarcane industry) as C-source, but some companies work with chassis that feed on ligno-cellulosic materials (Amyris), or glycerol, which is interesting as it is a bioproduct/waste of the biodiesel industry.

The composition of the medium, through metabolism, will ultimately impact bioproduction in terms of growth rate and production content and thus titer. For beta-carotene production, for example, adding oil in the medium increases bioproduction, as it increases beta-carotene secretion in the medium⁶⁶. Adding acetate in the medium also improves yields, as it

helps replenish NADH pools⁴⁹. Finally, beta-carotene production on xylose (respired c-source) was shown to be more efficient than on glucose, even without the use of tHMG to increase carbon-flux to the MVA pathway⁶⁷, most likely as a respirative metabolism naturally favors that pathway.

Culture parameters include mostly pH, dissolved gas concentrations, mainly oxygen (O₂), carbon dioxide (CO₂) and temperature. The stake is often O₂ levels that have to be controlled via Oxygen Transfer Rate (OTR) that depends on the culture device and culture volume (and therefore **culture scale**): stirring and bubbling can both improve the OTR and are a key element in bioreactor design. Controlling temperature can also prove more complex in large volumes. All this leads to culture conditions that may differ from lab-scale cultures. Given a strain and a medium composition, the best culture parameters can be determined using Design-of-experiment (DoE) approaches. Beta-carotene production has actually been reported to be sensitive to aeration and temperature⁶⁸, and we witnessed it in our very hands (see [chapters 2 and 3](#)), with increased content with lower temperature, and poor production with low aeration.

2.1.6. Industrial considerations

Two notes to finish on this part. To maximize production, one needs a well-engineered strain, a functional process, an appropriate medium composition and optimized culture parameters. From there lies the question of **economic feasibility**. Indeed, this is not a trivial question since lab-made producer strains often fail to be performant at industrial scales or the amount of the chemical produced does not offset production and purification costs, or are not competitive enough relative to the *status quo*.

The culture scale, for industrial production can be an obstacle in terms of economic feasibility. When strains are developed in the lab, in terms of metabolic engineering or with specific chemicals used to control cell behavior (*e.g.*, inducers), some costs that are considered negligible at the small scale become a true obstacle at the large scale: small chemicals in specific media at the small scale can represent a non-negligible cost at large scale. Besides, while culture medium is well defined at the lab-scale, favoring reproducibility, media derived from molasses at the large scale lack consistency and can impair reproducibility and therefore yields and costs. Moreover, large scale cultures offer different growth conditions for strains developed and selected for small scale performances, such that the transfer from lab-scale finely tuned strain to larger scale can fail. Some propose then to actually “start with the end in mind”⁶⁹ and test as soon as possible a strain at the large scale. Finally, adding anti-foaming, changing the medium, and varying culture conditions will ultimately impact strain performance.

For industrial considerations, the **Space-Time yield (STY)** has to be maximized: it is the amount of compound synthesized per volume per day (g/L/day). Its maximization can guide the bioprocess design, such that a long medium-scale fed-batch can perhaps be more advantageous than many small-scale batches. Indeed, the STY will depend on the strain production kinetics given the medium composition cost and the process. It is really after all, a

measure of production economic feasibility. This metric encompasses the utilization time of bioreactors (occupancy) relative to the final production as well as other diverse costs like the cost of the bioreactor sterilization in terms of money and time (needed to cool the bioreactor down after sterilization).

Finally, **Downstream processing** has to be optimized such that the downstream yield (amount of product that is successfully purified) is maximized. It represents a non-negligible cost for production and strongly impacts the economic feasibility: improving those technologies is key to reducing general bioproduction costs, besides just improving yields (which is what we focus on in the lab). The involved technologies are dependent on the compound to be purified, but they often rely on centrifugation, separation, cell rupture, filtration steps and purification steps. Briefly, beta-carotene can be extracted from yeast at the lab scale by breaking cells (bead-beater) in a hydrophobic solvent (acetone, hexane, dodecane, DMSO). Breaking cells can also be done using saponification, which will more easily separate the cell's lipids, where the beta-carotene lies. The solvent used for extraction will be important as it can also determine if the beta-carotene extracted can be considered food-grade.

To conclude this part on bioproduction, synthetic biology advances allowed for the development of biomolecular technologies and more sophisticated genetic designs. To increase yields, strain engineering is often considered the first necessary step and is what labs mostly focus on today. But cultivation techniques (bioprocesses), as well as medium composition and culture conditions can also strongly impact strain performance.

2.2. The cost of production

Strain metabolic engineering comes as a very powerful method to produce heterologous compounds in microbes. Regardless of the production performances of the strain, a default in fitness is often observed when cultivating the strain, *i.e.*, a producer strain often presents a lower growth rate compared to its non-producer ancestor. This means that there is an inherent cost to the production, which the cell has to face. This drop in fitness can lead to evolutionary escapes (strain instability) and production batch variability. Thus, we need to understand the nature of this cost, and its origin.

We ask: How does a strain behave when asked to produce a heterologous compound? What are the consequences of the presence of a heterologous pathway in the strain? Where does this cost originate from? And what are the consequences of this cost?

2.2.1. Burden

Burden can be defined as “the cost of production”. A cost in terms of resources, and more often seen as a cost in terms of fitness.

Theoretical definition. From an optimality point of view, we consider that microorganisms are best adapted to their environment. Consequently, the growth rate of the

microorganism (and therefore its fitness) is maximized in a wild-type strain. This way, any change made will ultimately give rise to a cost. In terms of fitness, since the production of a protein that does not benefit the cell will draw on at least transcription and translation resources, there is necessarily a cost. Besides, if a cell is producing a new non-necessary chemical, some of its resources (carbon atoms for example) will go to the production of this molecule and not to biomass formation. This conceptual framework states that there cannot *not* be a production burden. Burden has been defined along these lines as the “proportion of the resources of a host cell – either energy molecules (*e.g.*, NAD(P)H and ATP) or carbon building blocks – that are used to construct and operate engineered pathways”⁷⁰, and “metabolic burden: the amount of resources (raw material and energy) that is withdrawn from the host’s metabolism for maintenance and expression of the foreign DNA”⁷¹. It is also referred to as “metabolic load”⁷² or “resource burden”⁷³.

Experimental definition. Sometimes, this burden however is negligible or cannot be detected even though the strain produces a certain heterologous compound. Experimentally, the question therefore becomes: “can we actually measure the cost?”, which should result in a drop in growth rate, *i.e.*, a drop in fitness, and/or a lower biomass at the end of the batch process (since some of the resources were not allocated to biomass production). Experimentally, this can be hard to measure: for example, a 1% fitness drop due to GFP strong expression is expected using a strong TDH3 (aka GPD or GAPDH) constitutive promoter⁷⁴ but is hardly detectable using a plate-reader used to obtain growth curves. In some papers, the burden is actually defined by this very decrease in fitness: “unnatural load, consuming cellular resources and leading to decreased growth rates that can predispose synthetic constructs to evolutionary instability and unexpectedly alter their behavior”⁷⁵. However, a drop in fitness caused by heterologous expression and/or product formation is not necessarily only due to the consumption of cellular resources. Rather, the expression and production can lead to metabolic imbalances, and/or hinder certain cellular processes, resulting in toxicity and stress; this, in turn, causing a lower growth rate.

Burden, as employed across papers, often mixes those two (very compatible) potential effects (metabolic burden and toxicity), which can be very difficult to characterize and disentangle experimentally. We detail those two effects in the two following sections, as well as methods to reduce or alleviate it.

2.2.2. Metabolic burden: resources competition

Draw on cell resources. The first way that bioproduction induces burden is by mere consumption of cell resources, sometimes termed “competition” (with endogenous processes) for cellular resources. In this regard, just adding DNA to the genome leads to higher replicative (maintenance) costs, in terms of nucleotides. Although the duplication maintenance of an additional average gene (1.4 kb in yeast⁷⁶) compared to the whole yeast genome (12 Mb) can generally be considered negligible, it is not necessarily the case for other cell processes such as transcription, translation and effects on metabolic fluxes.

Transcription is often considered negligible when it comes to burden. The transcription cost depends on the copy number and/or the number of genes inserted. But it depends also on the promoter used. Kafri *et al.* 2016⁷⁴ showed that transcription can be a limiting factor in low phosphate growth conditions (as to why remains elusive). Hence, a burden originating from transcription can be identified in some conditions. To reduce this burden, it can be interesting to tune RNA half-life instead of transcription strength (mostly defined by its 5' and 3' UTRs): a medium expression and increased half-life can theoretically lead to similar protein levels. Another transcription-related burden can occur when the same promoter is used many times, such that it will recruit a non-negligible part of transcription factors pool normally used for other endogenous genes. Thus, other genes' expression will be reduced. Varying promoters or creating new synthetic promoters⁷⁷ may solve this to some extent.

Translation is one of the most studied causes of burden and gave rise to resource allocation models described later. Ribosomes are at the heart of the auto-replicative nature of cells and drive the positive feedback implying that more ribosomes result in a higher growth rate. Ribosomal proteins are the most abundant proteins in cells and the distribution of ribosomes and their quantity and availability in the cell define growth rate. Thus, heterologous protein production, recruiting ribosomes, will easily impact growth rate as its mRNAs recruit ribosomes. It can consequently create a shortage in ribosome availability, leading to a lower growth positive feedback (reduced **translation initiation**). This has been reported especially in poor medium growth (SC) or in respiratory metabolism (glycerol + ethanol) where ribosome content is reduced⁷⁴. On the other hand, **translation elongation** can be the limiting factor in certain conditions and induce a drop in growth rate. It is the case in low nitrogen conditions for example, where a shortage in amino acids is responsible for a lower growth rate, when the translation demand increases because of heterologous expression. Besides, tRNA availability can also be challenged by heterologous expression, leading to ribosome stalling and sequestration of the mRNA molecule. Especially, increased demand for rare tRNAs because of non-codon-optimized sequences. Tuning ribosome binding sites can also help reduce burden. Ceroni *et al.* 2015⁷⁵ proposed reduced-burden designs, showing that the best designs (lowest burden) are the ones that maintain the most ribosomes free; stating, for example, that a “high-copy, weak-RBS construct would be more efficient than a medium-copy, strong-RBS construct with similar output levels”.

Metabolite fluxes. Heterologous metabolic pathways are grafted to the cell's metabolism, where they, at least at the first step, draw in a metabolite to convert it to the product of interest. Therefore, they inevitably pull on a cell's metabolite pools and consume these resources. Despite fluxes being generally dynamically regulated in cells via different sensing systems coupled with gene regulatory networks, heterologous production can create shortages or lower the fluxes towards other cell processes, resulting in impaired growth.

Co-Factors. “Energetics” of the cell rest upon some key metabolites, sometimes called “currencies” (mentioned earlier). They are special kinds of metabolites, important to many various cell processes and reactions. Thus, currencies shortages can limit a broad range of cellular processes, causing a burden. For instance, a high demand in GTP due to increased translation (amino-acid polymerization) could also impact transcription and protein folding⁷⁴.

Enzymatic reactions of a heterologous metabolic pathway requiring ATP or NADH for their enzymes can also draw significantly on those pools. Engineering strategies to increase or replenish those pools efficiently can be useful, and for this, metabolic rewiring or other heterologous enzymes expression can be of interest⁷⁸.

2.2.3. Toxicity (stress)

Second, **apart from simply drawing resources from the cell, protein expression and production of unnatural products can impair cell processes**. This could, in general, be referred to as “toxicity”, and result in cellular stress. Although the use of the notion of “toxicity” could be argued because it is used in many situations (often as soon as there is a fitness decrease), we focus on processes that impact growth *not* simply by resource competition.

Product and protein accumulation is the first obvious effect of production. A protein expressed under the strong pTDH3 promoter in *S. cerevisiae* can represent already 2% of the proteome⁷⁴, and different proteins can have different expression limits, up till it causes a burden⁷⁹. Protein production can overload the quality (chaperones) and/or the degradation machineries (proteasome), because of misfolded proteins accumulation, notably in the Endoplasmic Reticulum (ER) when on the way to be secreted⁸⁰. Others can overload the capacities of localization processes (mitochondrial⁷⁹ or nuclear⁸¹ transport for example). The accumulation of the final heterologous chemical produced can also hinder cell processes (product toxicity). This is particularly expected for example when producing toxic compounds (*e.g.*, antibiotics). To alleviate that, secretion can be engineered. Efforts have actually been carried out to improve beta-carotene secretion, using ABC transporters, in *S. cerevisiae*⁴⁴, resulting in increased production yields.

Intermediate toxicity. By-products and even the final product can impact metabolism (intermediate toxicity). This toxicity is often an agonist phenomenon, where the newly formed product or intermediate will interfere with native biochemical reactions. For example, an intermediate product can be an ATP analog, which may inhibit ATP-related function by interaction with certain proteins involved in respiration in the mitochondria⁸². To alleviate this toxicity, pathway engineering can be used to better channel the substrates and toxic products and reduce the half-life of the toxic intermediate species, using larger-scale methods such as tolerance engineering driven by laboratory evolution.

2.2.4. Consequences

Design Strategy. When faced with fitness loss caused by the expression of heterologous proteins leading to the production of heterologous compounds, understanding the precise nature of the growth defect can be difficult. However, defining the origin of the defect is necessary in order to solve it when possible. It can be even more difficult as different effects from different origins can combine and be hard to disentangle. Therefore, it is important to proceed step by step with the DBTL cycle, *i.e.*, optimize iteratively to avoid confounding

factors that make solving a burden impossible. Indeed, in terms of design, there can be relatively low-producing strains with high burden, but also a higher-producing strain with a comparatively reduced burden. In the end, we want a high producer that has a mild burden, and this burden must be related to resource consumption, mostly translational resources, as it is inevitable, and therefore is the “healthiest” burden, while others could be solved or compensated for. We can go as far as to argue that having a highly producing strain that has no burden means that the strain could produce even more!

Evolutionary escape is a direct consequence of the production cost, and a major issue for bioproduction processes. Indeed, a high producer with a relatively low growth rate will be unfavored by natural selection compared to a strain with a higher growth rate *i.e.*, literally, a higher fitness. When the production of a heterologous compound is causing burden, impairing production itself via a single mutation (strain instability) can result in an increased fitness and consequently be selected for. Then, this faster-growing clone can take over a large part of the cell population, quickly consume resources and completely disturb the production process, seriously impacting the reproducibility and the robustness of the processes. The longer the cultures and the higher the burden, the more likely it is to trigger evolutionary escapes. To reduce the risk, different genetic strategies are available to increase a strain’s genetic stability and different synthetic addiction methods⁸³, where the product is often detected by a biosensor, in turn allowing for growth (by controlling the expression of an essential gene), reducing potential escapes^{84,85}.

Other effects. Burden is also an issue because slow growth rates can equate to overall slower bioprocesses (therefore lower the space-time yield). Indeed, for production yields to be high, one needs a high number of cells producing a high amount of targeted product (detailed in the next section). Besides, a slow growth can be the result of all cells growing more slowly, and/or a portion of cells regularly dying along the process. When cells die, they may lyse in the medium, thereby changing the medium composition and create foam that will complicate the process (hence the use of anti-foaming agents).

Burden is a problem for many reasons, and solving it using metabolic engineering techniques can prove tricky. Another possibility is to focus on the bioprocess: until now, we mostly considered cells in rich environments striving to grow and produce at the same time (genes controlled by constitutive promoters), but, in practice, for heterologous compound production, most bioprocesses rely on decoupling the growth from the production, using inducible genetic systems.

2.2.5. Decoupling growth and production

The possibility to, first, accumulate biomass at high speed, and second, produce no matter the growth rate is an attractive solution not only to cope with evolutionary escapes, but for general process efficiency. As a matter of fact, this way to proceed can easily follow the classical batch process (Fig. 13-Top) where cell number increases rapidly in the exponential phase, and then more slowly after the diauxic shift. Production in an environment where growth

is inherently slower could reduce the selective pressure pushing for evolutionary escape and have other advantages for bioproduction (discussed below).

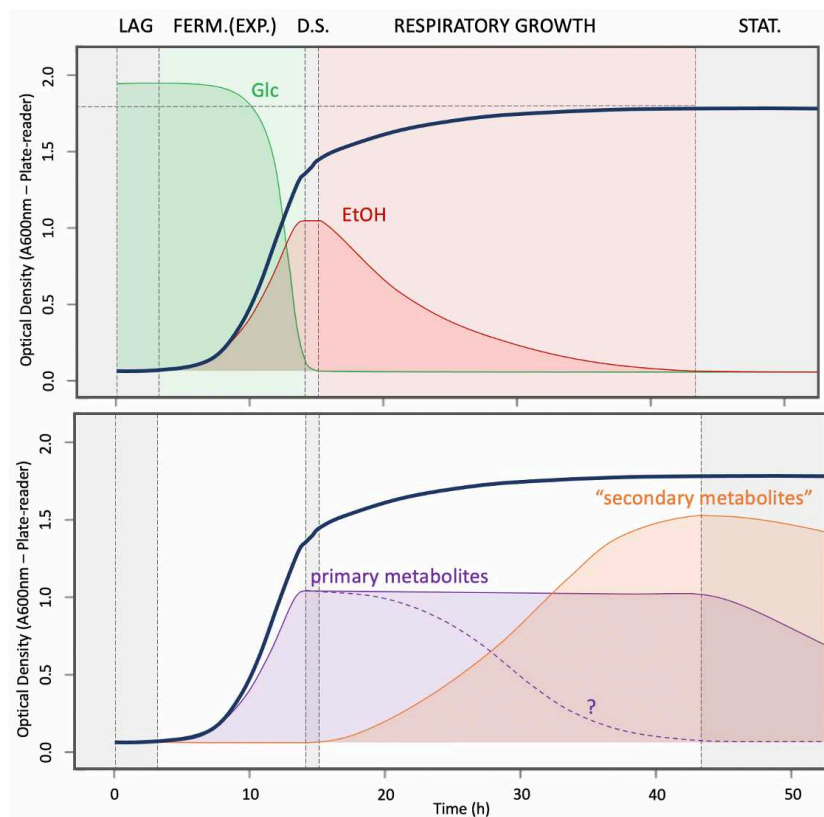


Figure 13. **Batch growth and production dynamics.** During the exponential phase, biomass builds up quickly by fermenting glucose into ethanol. After the diauxic shift, ethanol is slowly respired before entering the stationary phase (top). During the exponential phase, primary metabolites are produced at a high rate, i.e., metabolites essential to growth (central metabolism). After the diauxic shift, cells grow at a slower pace, and in some natural producers, secondary metabolites are produced (from secondary metabolism), which are generally involved in survival or reproduction. This view of batch dynamics can be taken advantage of, for modern bioprocesses where growth and production can be decoupled to reduce the effects of burden.

Historically, the first big bioproduction processes were for acetone, citric acid, or antibiotic production. It was then found that compound production and accumulation occurred mainly after the exponential growth phase when cells appeared not to grow any more (or only grew slowly). In a rich medium, cells would grow exponentially, and when a nutrient limitation is reached, most often a c-source limitation (in *S. cerevisiae* batches, this being glucose), cells will slow their growth, metabolism will change, and the product will be produced. In natural producers, it is produced at this moment because the cell is “programmed” to produce it to survive in this natural environment where it can’t just outcompete other microorganisms by growing anymore. A few years back, batch cultures and metabolism were conceptualized around primary metabolism (core metabolic pathways), and secondary metabolism (secondary metabolic pathways) (Fig. 13-Bottom). While primary metabolites are necessary for rapid growth, secondary metabolites are mostly produced in anticipation of slow growth and for survival. Those terms are mostly used for natural producers of antibiotics, as well as to discuss

the production of some molecules in plants (natural insect repellents or attractants like caffeine, nicotine, fragrances...). In *S. cerevisiae*, the use of this terminology is arguable, but it can help us better understand the different phases during growth in batch.

While different bioprocesses exist, all will require a first biomass accumulation phase, which will be most efficient as no production burdens the cell, followed by a production phase. Thus, we propose here to focus on this method, referred to as “two-step cultivation”, where growth and production are decoupled, and understand its stakes and limitations.

2.3. Two-step cultivation

The **two-step cultivation** is the base for most bioprocesses today, the process being batch, fed-batch, or intermediaries/combinations of the two, it can generally be considered a two-step cultivation with (i.) biomass accumulation followed by a switch to (ii.) production (Fig. 14). The switch from the growth to the production phase, although it can occur in different ways, remains mostly based on C-source limitation. Nonetheless, it can also be controlled in other ways, which we will discuss later. Those two phases make up the final titer:

$$\text{Titer (g/L)} = \text{Biomass yield (gCDW/L)} \cdot \text{Cell Content (g/gCDW)}$$

Therefore, both the biomass formed during the growth phase and the product formed during the post-diauxic (production) phase could be individually increased to maximize the titer. However, in practice, growth and production rely on each other, such that the switch must be finely tuned. Note that we will consider here the simplest case where the batch starts off with glucose and the product accumulates inside cells (no secretion); like this is the case for beta-carotene production in this manuscript.

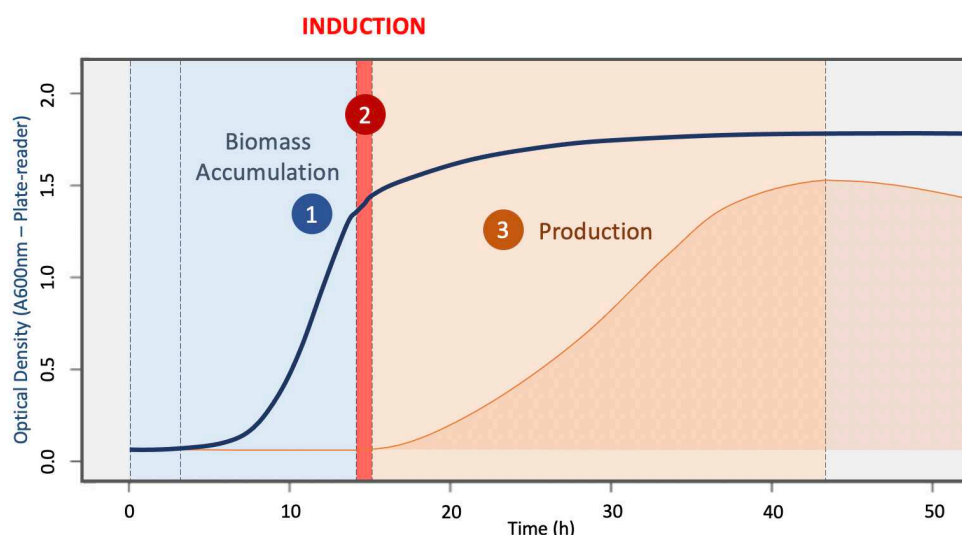


Figure 14. **Decoupling growth and production with a two-step bioproduction cultivation strategy.** Here, in batch, the exponential phase represents the biomass accumulation, i.e., the **growth phase** where no bioproduction occurs, such that there is no or minimal burden. An induction is carried out, thereby activating the production of the heterologous compound during the slow growth phase (post diauxic shift): this is the **production phase**. This way, despite burden being present during this phase, bioproduction doesn't conflict with biomass accumulation and lower evolutionary escape rates are to be expected during the production phase.

2.3.1. The growth phase

The growth phase aims at building up the highest biomass as quickly as possible so that all this mass can transition to production and multiply yields. This is important in terms of space-time yield (economic feasibility) and also follows the natural behavior of yeasts in batch starting with glucose or molasses. Methods have been developed to increase cell densities such that the culture medium containing cells reaches a paste-like texture.

In practice, to maximize biomass, different processing steps are used⁸⁶. First, successive batches cultures are carried out: after inoculation and growth in shake flask, the culture is transferred in increasing sizes of batch bioreactors, where fermentation of sucrose (most often, from molasses) takes place. Sometimes, contrary to what we stated before, growth on ethanol can be included in the growth phase, and induction of production occurs therefore afterward. From then on, successive fed-batch can be performed: there, sugars are regularly fed, at a rate proportional to the cell density such that it is respired. This way, one glucose yields more biomass, and without increasing the volume too much, cell density increases a lot.

Induction timing. One may want to limit growth to some extent and remain mindful of the nutrient composition of the medium at the end of the growth phase. Indeed, nutrient depletions may limit the efficiency of the production phase and impact the final production titer. Standard protocols do exist and often also recapitulate what we described just before: batch, fed-batch, and only then transition and induction for production⁸⁷. Also, as mentioned earlier, the amount of accumulated biomass (pre-induction biomass level) will impact the bioproduction yields^{64,88}, such that the absolute maximization of biomass is not necessarily the best solution. Besides, from a practical point of view, biomass concentration exceeding 100 gDCW/L can cause issues regarding cooling, OTR and separation (for downstream processing)⁶⁴.

All in all, induction timing is important, and it may depend on technical considerations, on the targeted product and on the medium composition. Many papers have shown that the switch timing can indeed significantly impact production^{89,90}. When the timing is chosen, induction is carried out. For this, various genetic systems are available with different characteristics.

2.3.2. Inducers

The rise of inducible systems. Decoupling growth from production, instead of producing constitutively with a burden, requires genetic systems that will be silent during the growth phase and activated on demand, after biomass accumulation is completed. For this, inducible systems are what we are looking for to control a biological process, *i.e.*, bioproduction.

Auto-induction. Historically, this shift occurred naturally at the end of the growth phase, upon carbon depletion in the medium, triggering a shift from primary to secondary metabolism. It is therefore based on a metabolic switch, and promoters responding to this change can be

used to control bioproduction induction. In *S. cerevisiae* and other yeasts, many promoters responding to glucose depletion can be used. GAL promoters (mostly pGAL1-10) are one of the first ones used (not only as they respond to galactose as inducer) but especially since after glucose depletion, the glucose-repression mechanism is alleviated and other genes, typically GAL genes are suddenly un-repressed. Other genes that also respond to this environmental change are available: for example, high-affinity glucose transporters that are overexpressed upon glucose depletion⁹¹. Other promoters responding to specific other nutrient depletion can be used: pMET25 is triggered by methionine depletion⁹², and pPHO5 upon phosphate starvation⁹³. What is sought after are tightly regulated promoters that control genes strongly upregulated after environmental change. Upon this moment, growth slows down, and production is unleashed. Also, quorum sensing systems can be used to control induction given the cell density. All the above examples are auto-inducible systems that do not require external inducers: it can be convenient as no external input is needed, but this can also be an issue as fine tuning will be difficult, and changes in medium which impact metabolism might make the system hardly predictable.

Carbon-sources as inducers. Various inducer types exist. On various yeast species, inducible promoters by c-source are one well-represented class: induction via galactose, lactose, ethanol, methanol, fatty acids, xylose, or starch⁹⁴. One very well-known inducer for *S. cerevisiae* is galactose, which activates GAL genes (GAL1-10,3,7). It is one of the first and best-characterized induction systems and has been used for various biotechnological tools (synthetic transcription factors, two-hybrid systems), with pGAL1-10 as the classical inducible promoter for bioproduction studies. Galactose is however rather expensive at the large scale. Besides, galactose is metabolized by the cell, so that concentrations have to be adjusted constantly and allows for cell growth. In *P. pastoris*, a yeast relative to *S. cerevisiae*, favorite for bioproduction, methanol is the preferred inducer: the whole bioproduction industry relying on *P. pastoris*, which is a methylotrophic yeast, uses methanol induction. During methanol induction, the pAOX1 promoter is strongly and tightly activated. The AOX1 gene codes for the alcohol oxidase that turns methanol (CH₃OH) and O₂ into formaldehyde (CH₂O) and hydrogen peroxide (H₂O₂). Methanol is convenient because it is a cheap and abundant⁹⁵ but its otherwise toxic and flammable properties are a major drawback. Similar to galactose, methanol can be metabolized, which can be a problem. Some *P. pastoris* strains (MutS) were developed so that methanol behaved mostly only as an inducer. In *E. coli*, we will mention arabinose (pBAD) and especially IPTG (analog of lactose – activating pLac) which are widely used as chemical inducers.

Other chemical inducers. In *S. cerevisiae*, methionine is well known for repressing pMET3, and copper (II) ion regulates pCUP1 and pCTR3. Exogenous chemicals can also be used, like tetracycline antibiotic regulating Tet-off systems. Many synthetic systems exist today to use different molecules as inducers, especially as more sensors are developed for microorganisms⁹⁶. The question remains regarding the price at industrial scales.

More inducers. Inducers actually rely on transcription factors that respond to signals and will then transcribe genes of interest. While we have talked here about chemical inducers, other types of inducers are available: temperature can be used as an inducer, with low

temperature impacting metabolism and therefore growth, and high temperature can trigger the Heat Shock Response (HSR), where a few targeted genes (HS proteins – often chaperones) are upregulated. pH can be considered an inducer too, with pH-responsive promoters⁹⁷, and redox-responsive inducers⁹⁸. Another inducer we will talk about later is light, which can be used to activate light-inducible transcription factors.

In two-step cultivation, the growth phase is carried out until the switch to the production phase. The switch is decided given medium composition, cell metabolism and physical constraints, and controlled using various induction systems. Then, the production phase starts as the genes responsible for heterologous production are expressed.

2.4. The production phase

The production phase aims at turning each cell accumulated during the growth phase into an efficient microbial cell factory and maximizing each cell's production, *i.e.*, *maximizing* its content (amount of produced molecule per cell – g/gCDW). The production phase is characterized by a generally slow-growth in an environment where some nutrients are limiting. With production ongoing, cells may also face burden.

We will ask here how the production phase is characterized in terms of metabolic state, why low growth can be considered better for bioproduction, and discuss the relationships between growth and production.

2.4.1. Metabolism

Metabolism is one of the first parameters that will influence the efficiency of the production. Indeed, post-diauxic growth in *S. cerevisiae* relies mostly on respiration instead of fermentation. The carbon source has changed, or, in other cases, a nutrient has become limiting. Cells therefore enter and remain for some time in a different metabolic state compared to that of exponential growth phase. This metabolic state can then be more permissive to some cellular processes and favor metabolic endogenous pathways directly or indirectly influencing the production of the heterologous compound.

For example, we mentioned the glucose repression mechanisms earlier: in high glucose concentrations, the regulator MIG1p represses many genes. But upon glucose depletion from the medium, this repression is alleviated, and other genes can be expressed. Especially, genes involved in respiration are expressed, and this metabolic shift orchestrated via gene regulatory networks allows the cell to enter a metabolic state where certain fluxes are favored. Typically, in a respiratory metabolism, this results in an increased Acetyl-coA pool, and this can favor beta-carotene as its metabolic pathway stems (in part) from this metabolite.

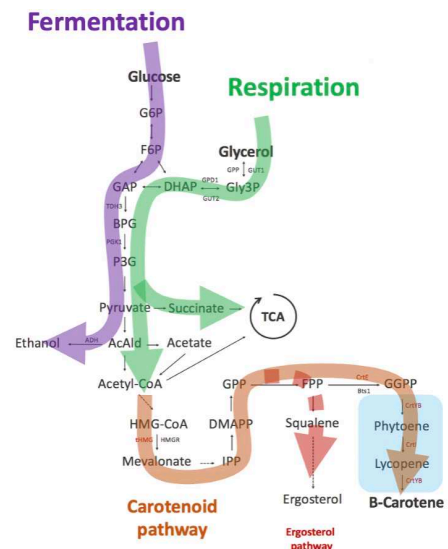
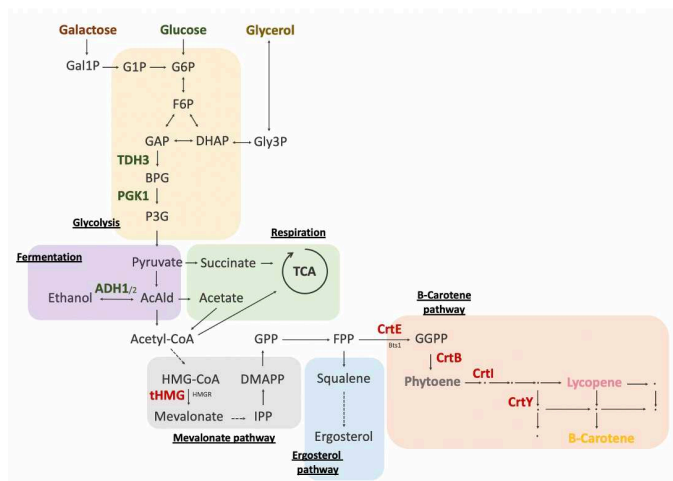


Figure 15. *Metabolic map, and flux* given metabolic state, for beta-carotene production in *S. cerevisiae*. Different complementary metabolic pathways exist in the cell. Depending on the growth environment, metabolism is adjusted, and certain pathways are favored over others, resulting in more or less resources channeled for the bioproduction of a targeted molecule. For beta-carotene production, as a respirative metabolism increases the acetyl-coA pool. From this metabolic entry point, more carbon can be channeled to the MVA pathway, resulting in higher levels of beta-carotene produced. In contrast, with a fermentive metabolism, the carbon flux is mostly channeled to the formation of ethanol.

Burden might also change with metabolism, or itself cause metabolic changes. If the cell is stressed, the Unfolded Protein response (UPR) or the Heat-Shock Response (HSR) can be triggered and impact cell functions, and thus, production.

Sidenote on constitutive promoters. It is interesting how *inducible* promoters are opposed to *constitutive* promoters. Those “constitutive” promoters encompass, after all, at least 3 promoter types: “true” constitutive promoters (related to translation notably, like pTEF1-2, but still subjected to general metabolism), glucose-inducible promoters (such as those to hexose transporters like pHXTs, that actually depends on the glucose concentrations), as well as, and mostly, glycolytic (glycolysis-related) promoters (often highly expressed with various c-sources, like pTDH3/pGAPDH, pPGK1, pFBA1, pTPI1, pADH1 but not ethanol or lipids c-sources for example). “Constitutive” is often used as a synonym for “strongly activated in non-limiting standard glucose conditions”, which neglects the reality of the everchanging metabolism based on gene regulatory networks and controlled expression of enzymes. When with those limitations in mind, it is, however vague, a convenient term that facilitates communication.

All in all, certain metabolic states are better than others for the production of certain compounds. For example, for beta-carotene production, Sun *et al.* 2020⁶⁷ showed that growth on xylose (respiratory metabolism) improved production, and that the effect of the tHMG booster gene was irrelevant in xylose growth and production. **Understanding better the relationship between the heterologous pathway and the cell metabolism (metabolite pools involved, potential toxicity and burden) will help fight burden, and understand and anticipate how growth environment impacts production.**

Besides metabolism, other more mechanistic approaches to growth rate can help explain why production can be favored at lower growth rates.

2.4.2. Growth laws

A slow growth, besides a somewhat more permissive metabolism that could favor bioproduction, has been shown to be advantageous to bioproduction as more cell resources can be allocated to production and less to cell processes involved in growth, *i.e.*, ribosome synthesis. At the heart of those approaches lies the self-replicating nature of biological systems.

Resource Allocation models are a class of models that are not metabolism centered and focus on resource competition. Be they coarse-grain (set of precise reactions) or mechanistic (general reactions categories)⁹⁹, they attempt to describe those dynamics. They generally encompass different general cell functions, mostly nutrient import and processing, protein production, and at their heart, ribosome production (Fig. 16). Ribosomes, as self-replicating machines, are necessary for their own production as well as for the production of other proteins. Papers using such models focus on describing protein fractions inside the cells. They mainly show that the higher the growth rate, the higher the ribosomal fraction and the lower the other proteins' fractions. One of the landmark papers that launched this idea is Scott *et al.* 2014¹⁰⁰ where ribosome content was shown to explain growth laws given a trade-off between, nutrient availability and translation capacity.

Applied to bioproduction issues, such models can capture the relationships and limits between the induction of a heterologous circuit and the host growth capacity and suggest strategies for production control, and show that there is an intermediary induction sweet spot¹⁰¹. Indeed, a too-high induction can cause a shortage in so-called 'free' ribosomes, needed for various cell processes. If all ribosomes are used for heterologous compound protein and compound production, then burden takes over, growth plummets and production cannot continue¹⁰².

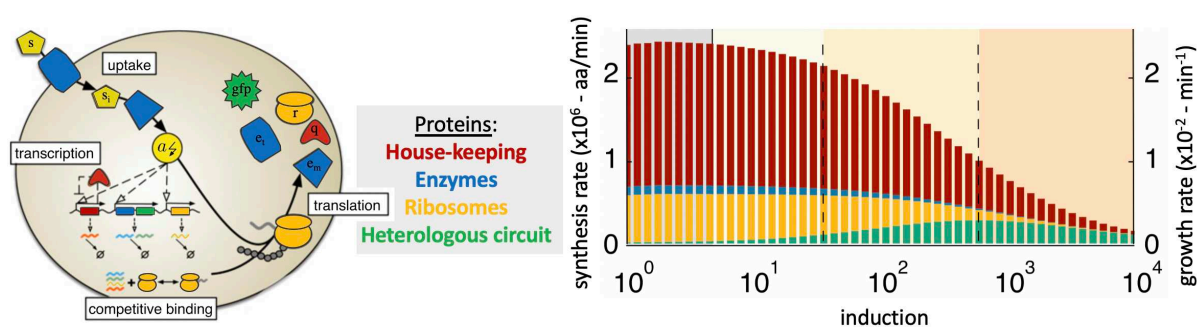


Figure 16. **Resource Allocation model** (adapted) from Weisse *et al.* 2015¹⁰¹. In this model, house-keeping proteins (red), enzymes (import and metabolic - blue), ribosomes (yellow) and a heterologous circuit (green) are simulated in a cell resource allocation model. In brief, energy is imported and processed by transport and metabolic enzymes. This energy is then used for transcription and translation of the different produced mRNAs. Different mRNAs have different ribosome binding sites, resulting in different protein fractions inside the cells. The more a heterologous system is induced (the more mRNA produced), the more the resources in the cells will be reallocated, impacting growth, and finally production. We see that a sweet spot of induction can be found.

Those models are very insightful, and can also simulate cell populations, as well as some culture processes to some extent¹⁰¹. Those concepts have also been confronted with experimental data¹⁰³ but they remain to be used to explain for example how the use of a constitutive promoter for bioproduction positively correlates to growth, which is not what is necessarily seen with RA models. Other processes may play out, and one is metabolism, discussed earlier. Indeed, metabolism-based and mechanistic models are yet difficult to combine. **Those resource allocation models give valuable explanations regarding how, with a low growth, more resources are allocated to production instead of growth (ribosome production).**

Dilution and accumulation dynamics are another aspect of the impact of low growth, and another way to conceptualize the impact of low growth, not on production *per se*, but on the accumulation of the synthesized product in cells. Typically, for cells that produce a protein regardless of their growth rate, the accumulation of this protein (or the result of the enzymatic reaction carried out by this protein), so the per-cell quantity will be solely dependent on the growth rate (Fig. 17). This way, a slow growing cell will not dilute too much what it produces with its daughter cells. In practice, a lot of production with slow-growing cells can cause issues in terms of protein concentrations and cell volume¹⁰⁴ and this view does not consider proteome homeostasis and regulation. However, it is a convenient framework to conceptualize and try to anticipate the dynamics of the accumulation of a formed product in growing cells.

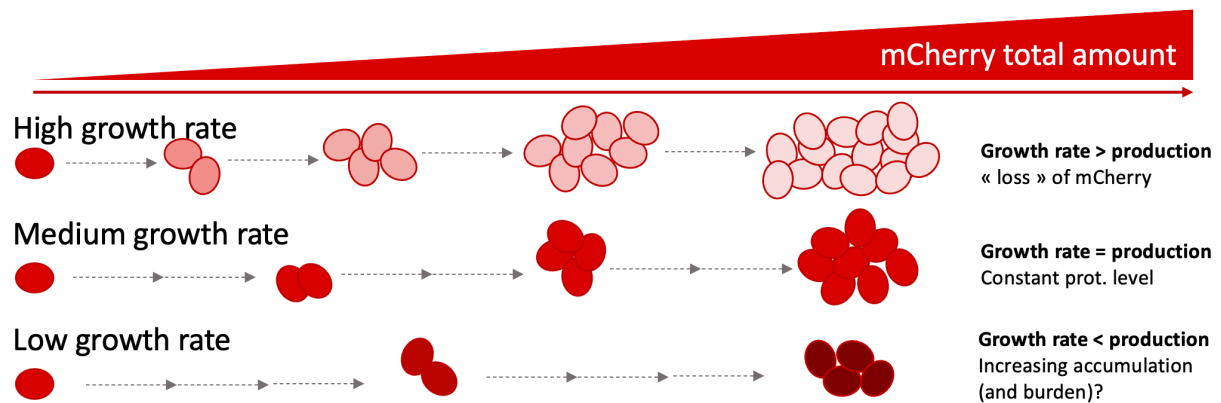


Figure 17. **Dilution and accumulation** of the produced proteins (mCherry as example here – red fluorescent protein) or heterologous molecules in cells can depend on the growth rate. At high growth rate (top), the produced mCherry proteins are quickly diluted between dividing cells, leading to low per-cell protein levels. At low growth rate (bottom), mCherry production is less subjected to dilution triggered by cell division, resulting in higher accumulation and concentrations in cells. A third case is displayed, where protein production rate and cell division are balanced (middle), resulting in a constant protein level in cells in time.

A lower growth rate in the post-diauxic phase can potentially lead to higher cell contents (and production yields) because the cell's metabolic state might be more permissive to biosynthetic pathways associated with the targeted product, because a lower growth rate means fewer resource allocated to ribosome formation and more to other cell processes such as bioproduction and it leads to less dilution amongst cells and

higher product accumulation. Therefore, the arguments to produce in lower growth rate are often both metabolic and mechanistic.

We could go as far as to suggest that the cells should not be growing in order to only produce. We can then ask to what extent one needs or can, actually reduce growth.

2.4.3. Growth *versus* Production in the production phase

In theory, the ideal way to produce after the growth phase would be to totally stop cells from growing and have them only produce for as long as they can. For this, they would need to remain metabolically active and use all resources they import to turn them into the targeted product. In yeast, quiescence could be suggested as such a state, but the metabolism in this state is very slow, with translation mostly inhibited¹⁰⁵, and thus it is not a suitable metabolic state for production. Therefore, to try to reach a state of metabolic activity coupled with maximal production, growth, however low, is needed.

“The challenge is to engineer a system where we get **enough growth** to have a productive microbial ‘chemical factory’ but not so much that we can’t **channel enough of the sugars into a pathway** to make large quantities of our target molecules.”

Kristala J. Prather (MIT), EMBO Synthetic Biology Practical Course, 2018

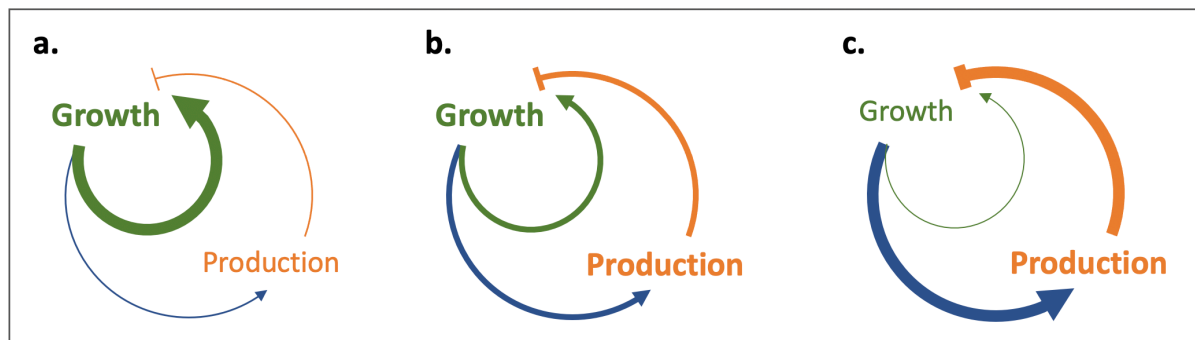


Figure 18. **Production relies on growth.** When most cell resources are allocated to growth, production is neglected (a.); however, if too many resources are allocated to production (c.), it will impact growth, which will in turn impact production. Therefore, a balance between growth and production has to be found such that production can be sustained by a constant growth.

Production needs growth because it allows keeping cells in an active metabolic state where they import resources and turn them into energy and building blocks needed for bioproduction. But especially, energy and building blocks (amino acids, nucleotides...) are also needed for cell maintenance, *i.e.*, to produce and renew structural proteins, and compensate for burden that can be caused by the expression of the heterologous pathways. In this view, growth maintains the cell healthy and provides resources for both growth and production. This creates a rather simple dynamic between growth and production: production relies on growth, but also

inhibits it (Fig. 18). What this relationship and feedback tell us is that there is a balance to be found between growth and production to maximize the production: a trade-off to be settled.

And **in practice**, there is indeed a balance between growth and production that can be observed. But it will also depend on the way the production is genetically controlled. Looser *et al.* 2015⁸⁷ reported this in *P. pastoris*: to tune this trade-off, either/both growth and/or production can be controlled. In classical bioproduction methods in *P. pastoris*, growth and production can be both controlled together with the use of methanol (c-source for growth and inducer for bioproduction) or separately with specific mutant strains (mutS), and in *E. coli*, bioproduction can be controlled with IPTG while the c-source can be controlled in fed-batch to regulate growth. Looser *et al.* 2015⁸⁷ report that a growth rate sweet spot can be found with inducible production in *P. pastoris*, in order to maximize the strain productivity (Fig. 19). However, with strains where production is under the control of the endogenous strong constitutive pTDH3 promoter (GAP), production tends to be proportional to growth (although this relationship is not always linear). This shows that this relation is not as straightforward as the models we presented earlier, and production can be positively or negatively growth-related, indifferent to growth⁹⁴, or bell-shape related⁸⁷. It remains today a cumbersome task, though necessary, to test various growth rates to maximize production, and using growth and production models could considerably simplify those tasks.

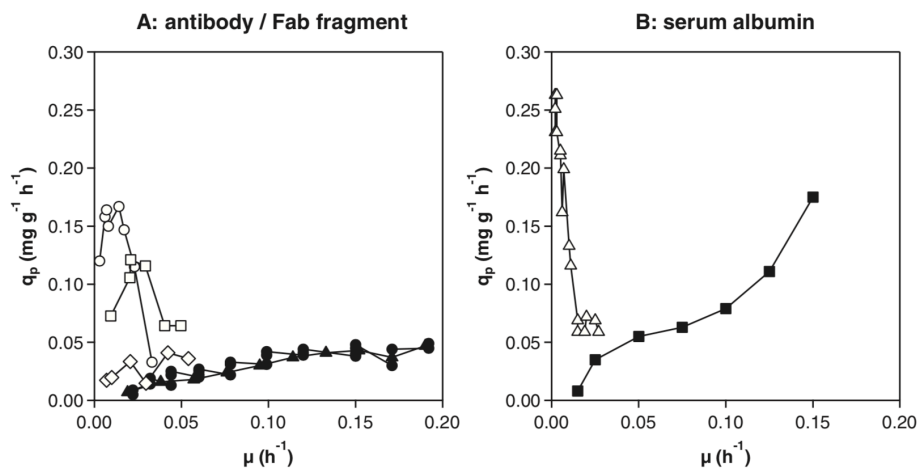


Figure 19. **Productivity given growth rate** for two recombinant proteins. White points ($\square\Delta$) represent inducible systems. Productivity follows a bell shape, where a best growth rate can be defined for high productivity. Before this optima, lower productivities can be interpreted as lacking growth to sustain production, and beyond this point, can be interpreted as resources starting to be allocated more to growth than production. Black points ($\bullet\blacksquare$) represent constitutive expression systems: productivity appears correlated to growth, though lower than inducible systems. Different curves originate from different papers – adapter from Looser *et al.* 2015⁸⁷.

In definitive, growth is always needed for bioproduction, and a slow growth is better for inducible systems as more resources can be allocated to production, but not so much that production will jeopardize growth.

We have seen that the relationship between growth and production is complex and has to be fine-tuned, during the production phase of the two-step cultivation process, in order to maximize cell content, to obtain the highest production yields. For this, inducers used to control (mostly) production have to be handled with great care, and different induction modalities could lead to higher yields.

2.4.4. Induction modalities

Simple induction switch. Given metabolism, growth laws, and the growth vs. production trade-off, we understand that a simple switch, where, after the growth phase, bioproduction is fully unleashed, regardless of the cell's state may result in cells producing for some time (productive time), but then face strong burden and stop growing and. To address this issue, different induction modalities are possible.

Induction strength. Since a maximal induction can cause too much burden, one first solution would be to induce production at an intermediate level for it to generate less burden and for production to last longer. Using intermediate concentrations of inducer can be one way to modulate the induction. However, not all promoters have a good **dynamic range** (fold between lowest and highest activity). Besides, some may have a digital behavior (all or nothing) or be hard to control. As a solution, in order to use them at intermediate levels, one might want to process with activation pulses.

Induction pattern. Besides controlling the heterologous pathway, pulses can also be used to control growth, via a fed-batch feeding by pulses⁸⁷. More advanced induction patterns are found in Hoffmann & Rinas 2004⁷¹ where they discuss gradual inductions instead of pulse addition that could help reduce burden. However, this once again depends on the properties of the induction system. Indeed, not all induction systems have good **response dynamics** (time between on and off states), and especially, some don't allow for reversibility, or with very slow dynamics, such that control is actually difficult. Besides, tuning and finding the best way to induce is actually difficult: it is cumbersome and time-consuming to determine what pulse frequency is the best and may require a lot of trial and error.

To try to counter this problem, more and more papers discuss the advent of “smarter” approaches that would actually rely on the state of the cell to guide the induction decision, and best cope with burden to maximize bioproduction. This raises a lot of questions, regarding what systems to use to detect burden, how to read this information, and what to do once received. Those questions take us close to actual control (in the “control engineering” sense), where production induction is controlled based on a certain cue, *i.e.*, dynamic control.

2.5. Dynamic Control

Defining dynamic control is not a particularly easy task. It is sometimes used simply to address control of dynamical systems, which include biological systems. Some people talk about dynamic control just when the switch from growth to production is internal, because it responds dynamically to certain cellular and/or environmental cues^{106,107}. Others talk about dynamic control when there is a control that varies in time and this is what we're going to use here: we refer to dynamic control as opposed to a simple step control. In our very case, this is mostly turning a system on, or off, or at an intermediary level, depending, or not, on certain cues, multiple times, during the production phase. With dynamic control, we expect to go beyond "simple" two-step cultivation strategies.

Static and Dynamic metabolic engineering represent two different paradigms to control heterologous pathways. Previously, we have mentioned metabolic engineering methods that make a strain produce constitutively but with a cost in terms of mostly growth, impairing biomass accumulation. Decoupling growth and production with inducible systems allows to shift this issue to the production phase only, as well as benefiting from a lower growth metabolic and mechanistic properties. The genetic changes made so far are called "static" since everything is determined and tuned *a priori* with no direct change possible during the process, nor reversibility. Those static systems are unable to adjust to the cell's metabolism and sense and act upon stress caused by burden. As explained before, the hope is that, by reversibly inducing production, stress and burden can be mitigated. This can be considered as a process engineering method (instead of metabolic engineering), or a so-called *dynamic* metabolic engineering method. We will see that this control can be made internally, in the cell, or externally (induction by the user). This dichotomy of static *versus* dynamic engineering was first proposed by Holt *et al.* 2010¹⁰⁶ with the goal to engineer pathways that responds to changing environments or to changing internal composition. Since then, dynamic metabolic engineering has been a commonly used term^{108–110}.

In bioreactors, the notion of control is also omnipresent. At the large scale, everything is controlled, in the strictest sense, as in "maintained constant". Temperature, pH, dissolved gases (oxygen most importantly), and sometimes other characteristics of the medium are maintained at an optimal value, given real-time measures. For example, for fed-batch cultures, the amount of nutrients fed in the batch is often proportional to the cell density. So "control" is definitely *not* an unfamiliar term to the bioproduction field. In the following sections, we will talk about the control of the microorganisms themselves, and not only maintaining important growth variables constant, which is a necessary prerequisite, but is also beyond the scope of our interest.

Today, most production techniques actually go beyond the two-stage fermentation we presented earlier. More complex induction patterns have existed for a long time already and were shown to be beneficial, such as in 1990 when Hortacsu *et al.*¹¹¹ showed that a slow decrease in temperature (for a temperature-controlled induction) was beneficial for production yields and also investigated induction cycles.

We discussed briefly different induction modalities to optimize bioproduction. We started to ask: what to control? How to control it? and based on what signals?

2.5.1. Control

Control Theory. Control, in its wide sense, is using various tools to change the behavior of a given complex system. The basic example of control is to maintain a changing variable (output of a system) at a given setpoint. For this, if the way the variable changes in time is well described and known, adjustments can be programmed in advance without looking at the variable: this is **open-loop** control. However, if the variable inconsistently varies in time (such as in noisy biological systems), the solution is to measure the variable regularly and adjust it in real-time: this is **feedback-control**, where a feedback-loop is set up (Fig. 20). For this, one needs a sensor (to report the output value), and a controller (a way to adjust the input given the deviation from the target setpoint). This kind of exercise is what we want to do with cells to control production or growth. In the following sections, we tackle bioproduction techniques in the context of control theory, and distinguish first embedded control from external control, and open from closed (feedback)-loop controls.

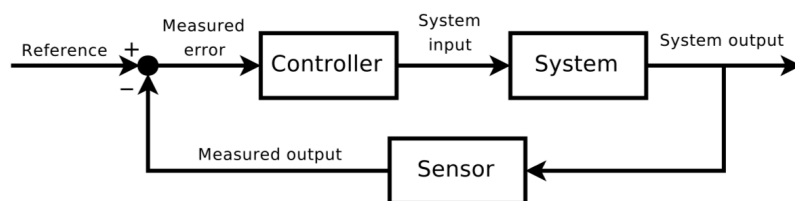


Figure 20. **Feedback-control.** In control theory, for feedback control, the output of the system is measured with a sensor and confronted to the reference point. The controller can rely on various control methods and based on the error; it proposes an input for the system to correct the trajectory.

Controlling growth and seeing how production follows. Controlling growth is what is usually done with constitutively producing strains. This can be achieved using a limiting C-source, N-source or P-source, most of the time. It can also be achieved by using antibiotics (expensive to scale up), or by controlling essential genes, such as an auxotrophy, or even a gene of the glycolysis pathway¹¹². This most often consists in maintaining a value constant (increase in cell density), regardless of the immediate cell's state.

Controlling both growth and production. As explained before, using methanol in *P. pastoris*, both growth and production are controlled, such that, when finding the right growth rate and/or production, it is hard to actually understand or predict what is limiting and why a certain concentration is better than another. Using galactose as an inducer in *S. cerevisiae* yields the same kind of “problem”: it is used as a carbon-source and as an inducer. In those examples, growth and production are controlled together, but we will see with other systems they can be both controlled (using dual/binary system¹¹²), so that they behave antagonistically during the production phase.

Controlling production is usually what is done in most lab studies. This is the case with MutS mutants of *P. pastoris*, where methanol controls mostly production while growth remains low but present. Using IPTG in *E. coli* also allows to control only production. Controlling only production is interesting because this corresponds to actually controlling directly the burden put on cells. I would go as far to suggest that controlling production will eventually result in more predictability for the system: growth rate control interferes with metabolism and cell physiology at many levels, while the results of the production can be investigated and anticipated to some extent. In terms of easiness, controlling production can also appear easier than controlling growth since production is, after all, a less complex mechanism than growth *per se* (although growth can also be controlled with one single essential gene).

In definitive, they are different practical ways to precisely control microorganisms during the production phase. But to perform actual feedback-control, one must rely on a signal from the cell and act upon it. The whole control mechanism can be carried out directly inside the cell (embedded control) or carried out externally, using models and user-activated control (external control).

2.5.2. Embedded Control

Cells use feedback-control mechanisms all the time. Although glucose homeostasis is the landmark example used to illustrate feedback control in biological systems, there are countless constant regulations that occurs in a single cell, which can be identified as feedback control systems. Cells can be seen as engineered systems, where regulations have been fine-tuned by evolution. The extreme view is to say that every protein is continuously regulated by metabolites, proteins, cell physiology and also regulates others, sometimes directly, most of the time, indirectly, such that even metabolites must be considered as regulators for or from transcription factors¹¹³. There, cells are seen as highly dynamic systems, or just simply put, as living systems. Cells (microorganisms) are constantly integrating signals from the environment, and from their internal compositions, to best adjust their metabolism in order to, most of the time grow at an optimal rate, and other times, change their physiology to survive^{113,114}.

Internal Open-loop control. We have seen that auto-inducible use endogenous cell circuits to activate, mostly, the production. Although it can be considered dynamic control to an extent, it is a simple switch to production, and no further regulation is encoded. Such switch could however be exploited. For instance, if switched on by a depletion in carbon source, an intermittent fed-batch strategy could be used to turn production on and off¹¹⁵ (to some extent, this could however be considered external control). Another strategy is to use different auto-inducible systems to regulate the entry into the production phase to try to mitigate the burden: in order to control beta-carotene production in *S. cerevisiae*, Xie *et al.* 2015¹¹⁵ used the pHXT1 high glucose concentration responsive promoter to control ERG9 (entry to a competing, but essential pathway), and the pGAL promoter, induced at low glucose concentrations to control the beta-carotene pathway. With this system, 3 different fermentation phases could be obtained, and yields increased - they call this a “sequential control” strategy. This system is an open-loop, since no internal feedback is involved, and is non-reversible in simple batch cultures.

Harnessing natural systems. One of the easiest ways to perform feedback control is actually to use endogenous systems. The landmark paper in this field was Farmer *et al.* 2000¹¹⁶ where the authors demonstrated and coined the term “metabolic control engineering”. In this paper, lycopene (precursor to beta-carotene) is produced in *E. coli*. With a control theory approach, they define what is needed to engineer a controller for a heterologous pathway: “(1) a signaling molecule to reflect the relevant metabolic state, (2) a sensor to monitor this signal, (3) a controller to process the sensory input, (4) a “control valve” (*i.e.*, a promoter) to modulate gene expression, and (5) the rate-limiting steps of the pathway that are to be modulated”¹¹⁶. They decided to monitor acetylphosphate levels, which reflect the cellular glycolytic flux, using parts of the *E. coli*’s Ntr regulon, where NRI (*glnG*), acts as a sensor and regulator via the *glnAp2* promoter (Fig. 21A). With this promoter they controlled a key endogenous enzyme leading carbon flux to lycopene production, and a gluconeogenic enzyme (its overexpression severely impacts growth). With this elegant embedded feedback-control strategy, they produced 150mg/L lycopene compared to a lower 10mg/L with a strong IPTG inducible promoter. We see here that they balanced production based on available pools, but also took advantage of the overflow metabolism. Others have also suggested balancing product toxicity with cell secretion (which also triggers a certain burden), one burden mitigating another¹¹⁷.

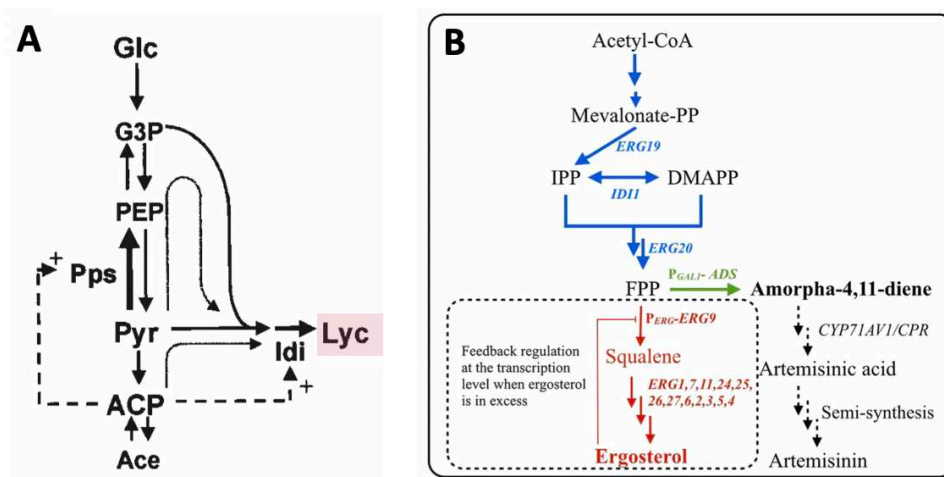


Figure 21. **Embedded feedback-control** in the MVA pathway for production of lycopene in *E. coli* (A) and artemisinic acid in *S. cerevisiae* (B). In Farmer *et al.* 2000¹¹⁶ (A), the pyruvate quantity channeled for lycopene production, is controlled dynamically via a promoter responding to the Acetyl phosphate (ACP – a precursor to acetate – Ace) concentration, an indicator of glucose availability, controlling the *Idi* enzyme. In Yuan *et al.* 2015¹¹⁸ (B), *ERG9* is controlled by *pERG1*, a promoter identified to respond to ergosterol concentrations. Ergosterol being an essential component for cell growth, only when in excess it will allow for redirection of the carbon flux to artemisinic acid production, with this design.

Another example is in Yuan *et al.* 2015¹¹⁸ where, to maximize the production of amorpha-4,11-diene, they feedback-control the FPP node (also an important node of the mevalonate pathway for beta-carotene production) (Fig. 21B). The authors identified *pERG1* as repressed by ergosterol. By putting *ERG9* (an enzyme that converts FPP to squalene) under *pERG1*, the FPP flux towards squalene and then ergosterol is reduced dynamically, and not interrupted, such that the FPP flux towards amorpha-4,11-diene is maintained and does not impact the cell negatively, resulting in a 5-fold increase in production¹¹⁸. Here, we see that

those approaches do work, and that dynamically regulating production can improve yields compared to their counterpart “static” inducible systems.

Dynamic Sensor Response Systems (DSRS). As explained earlier, 5 components of the control system are needed. It can be however challenging to find the right components and to tune them so that they work seamlessly together. For example, Dahl *et al.* 2013¹¹⁹, after having shown that FPP could actually be toxic to the cell, sought to find sensors and responders to FPP. They carried out a whole-genome transcriptional analysis using *E. coli* cells overproducing or not FPP, to find, for instance, that the PhoPQ regulon (known to respond to Mg^{2+} concentrations) was a good candidate. To find a good (bio)sensor, Zhang *et al.* 2012¹²⁰ used a known ligand-responsive transcription factor, and engineered the cognate promoter to obtain a better dynamic range. Besides, they wanted to differentially regulate two components of the pathway, and investigated combinations of promoters, like in Liu *et al.* 2018¹²¹ where they compared different feedback architectures. All this shows that this approach is not straightforward. Dahl *et al.* 2013¹¹⁹ coined the term “Dynamic Sensor Response Systems” (DSRS) to refer to those systems, the most convenient being Metabolite (or Ligand) Responsive Transcription Factors (MRTF or LRTF¹⁰⁸). It is sometimes simpler to actually use systems coming from other organisms, like in David *et al.* 2016¹²² where a Manoyl-coA sensor from *E. coli* was used to dynamically regulate the production of 3-hydroxypropionic acid in *S. cerevisiae*. The challenge is more and more to find the appropriate biosensors for specific metabolites. Let’s note also that those DSRS can also be used for Adaptive Laboratory Evolution (ALE) in static metabolic engineering, termed “Biosensor assisted evolution”¹²³ where the DSRS can control the expression of an essential gene, giving an evolutionary advantage to the highest producers.

Burden-driven designs. All those sensors presented earlier are actually specific to certain chemicals. But more generalizable approaches can be pursued. For example, beyond the PhoPQ regulon to respond to FPP levels, Dahl *et al.* 2013¹¹⁹ found that some general stress response promoters could also be good candidates to inform on the FPP level and use them for feedback control. Indeed, more general, more portable systems are desirable to be used, irrespective of the burden type. This can be advantageous because it would alleviate the need to each time find the appropriate DSRS, but a more general system can also make it less efficient than a precise one, with less control over what actually happens and less responsive than a precise DSRS. Even more versatile, more adaptable systems have been developed^{124,125}, where burden induces the expression from the *htpg1* promoter (originally controlling a molecular chaperone chosen for its best response dynamics to burden), which controls the expression of specific gRNA(s) (Fig. 22). Upon burden, the gRNAs are expressed and bind to a constitutively expressed dCas9 to repress targeted genes. This construction makes this system universal (for engineering in *E. coli*), especially scalable (set of gRNAs possible), with quick dynamics (no translation needed here, no delay).

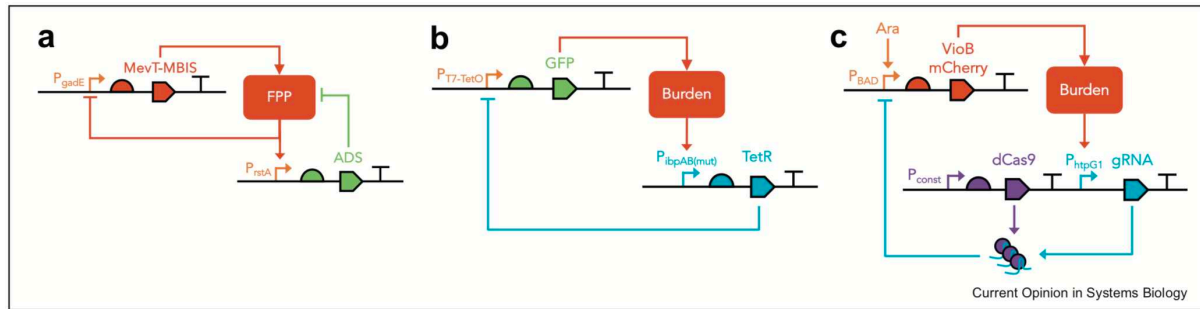


Figure 22. **Dynamic regulation design to prevent excessive burden.** (a.) FPP-specific regulation using a repressor controlled via a FPP-responsive promoter. (b.) A more general burden-responsive promoter is used to repress GFP production dynamically. (c.) CRISPRi-based systems are available, facilitating engineering, potentially with arrays of guides able to target many genes at the same time. This system is also based on a more general burden-responsive promoter controlling the expression of gRNAs. Figure from Boo *et al* 2019¹²⁵.

Limitations. Those systems are proof that dynamic control is a key to better production using microorganisms. Those host-aware approaches are necessary and possible. Internal control is very powerful, but is still subjected to trial and error, and once the system working, it is often not investigated how the system actually behaves during the production phase. Hence, such systems don't necessarily give biological information or meaningful insights into the cell's behavior: there are only a few models that actually describe how such systems works. Besides, it is very dynamic, but completely independent and no human input is really possible. There is in definitive no way to correct the system, should it run amok for some reason. There is no way for the user to have an input and actually try to push beyond what the cell naturally does, to investigate an unnatural behavior, that could lead to other ways to improve bioproduction in the end. **To facilitate user input, external dynamic control could really be advantageous and provide other types of insights into biological systems.**

2.5.3. External control

Multiple inductions. Already in Martin & Demain¹²⁶, in 1980, the authors discuss how "continuously or intermittently" adding source can be used to extend the productive time for (endogenous) antibiotic production in fed-batch culture. Carbon-source feeding can be seen as a parameter to control production or/and control growth as we have seen. One needs to find the good timing and concentrations, then the cycle can be set constantly, with no additional control. Researchers did not wait for sophisticated inducers to be widely available in microorganisms to try to do multiple production inductions or more complex induction patterns in production processes. As mentioned already, in 1990 Hortacsu *et al.*¹¹¹ tried sequential activation (temperature controlled) and fit a model to predict the best induction pattern. Once determined *a priori*, the induction profile is kept consistently and can be repeated. This is open-loop control: a control profile is set, checked, and can be reused, blindly. No feedback comes from the broth during the process. Similarly, Aucoin *et al.* 2006¹²⁷ showed that multiple inductions (also temperature controlled, and only 2 inductions) can improve GFP production in batch.

Dissociating **growth or production**, strictly, during the production phase is also an interesting strategy. There, production occurs with an (almost completely) interrupted growth

or growth without any production. This was done with optogenetics in Zhao *et al.* 2018¹¹², where illumination allows for growth with PDC1 expression (a glycolytic enzyme), and dark inhibits PDC1 but activates isobutanol production in *S. cerevisiae*. With such a strategy, the authors found that cycling regularly between the two states was necessary to maintain production (by replenishing NAD⁺ levels). After a full illumination 48h growth period, they found that intermittent illumination, every 10h for 30min at 15 sec on + 65 sec off, was the best conditions to maximize isobutanol production, which went over 11 days of culture.

More complex induction patterns, nonrepetitive, have been also used, mostly with a sequential control of the production. This is the case in Xie *et al.* 2015¹¹⁵, where beta-carotene production in *S. cerevisiae* is controlled sequentially thanks to the use of two inducible systems, resulting in three fermentation phases based on glucose concentrations. With fed-batch, they can control the glucose concentration in the medium and therefore act upon the induction. They concluded that their fed-batch strategy progressively induced the production, rather than a strong full-on switch. Using optogenetics, Zhao *et al.* 2020⁹⁰ propose different induction modalities to start the production after the growth phase: a weak early induction followed by a strong induction, which is shown to improve yields.

This shows here once again that multiple inductions is a working strategy. Those reversible inductions can be carried out in open-loop, but defining the appropriate timing and intensity can be difficult. All those methods aim for a better control of cell metabolism, more dynamic and more reversible. Many inducible systems exist, which combine various qualities and drawbacks. Recently, optogenetic systems used in microorganisms arises as a very attractive control system.

2.5.4. Control tools (Optogenetics)

The ideal inducer. For inductions, most of the time, chemical inducers are used. We mentioned earlier metabolizable inducers (sugars for example), which will be consumed more or less quickly by the cells, and non-metabolizable inducers (IPTG, aTc), which will remain in the medium. The first therefore has relatively slow reversibility, while the second is reversible only upon cumbersome medium change. Poor reversibility, thus, poor control. Also, both types of inducers take time to spread in the medium, which can lead to cell induction heterogeneity, especially in very large volumes. How to finely control then? To best control a genetic system, we need an inducer that is highly controllable (responds very fast to the user (or computer)-decision) and is quickly reversible (versatility); both when it reaches the cell, and when the cell biologically responds to the signal (when the biological effect starts to appear). It must have a good dynamic activation range (to obtain intermediate induction levels) and activate cells homogeneously (limited cell-to-cell noise – phenotypic heterogeneity). Ideally, it should also not interfere with- nor be dependent on- the cell's metabolism (orthogonal), thus not creating any burden. Besides, technically, it should behave consistently (in time, and across batches – process robustness), its behavior be predictable (well characterized), and eventually, be as cheap as possible. Using light as an inducer via optogenetic systems combines many of those qualities and this is what we will focus on.

Optogenetics. Light is highly controllable (in intensity, reversibility, in space and time) by the user via electronic systems, is fast to reach its target, and, depending on the intensity and wavelength, non-invasive and harmless. Optogenetics have historically been used in the neurosciences field to depolarize neurons on demand (light-gated ion channels), and soon optogenetic systems with other functions emerged, making it useful for controlling other physiological processes in other systems, including in microorganisms. In brief, a conformational change triggered by light can allow a user to control protein interaction (homodimerization for EL222¹²⁸, or oligomerization), which can lead to protein activation, relocalization or anchoring, and thus control higher cell processes such as transcription (in our case), translation, and other protein-associated function. For bioproduction, it is most often a regulation of transcription that is sought after, but enzymes clustering was also demonstrated³⁹.

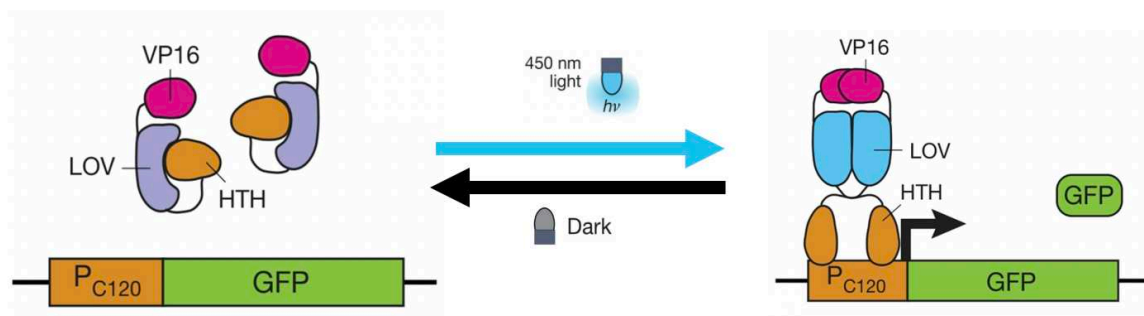


Figure 23. *The EL222 optogenetic system adapted from Zhao et al. 2018¹¹². The EL222 light-activated transcription factor is composed of a VP16 (viral particle) transactivational domain, a LOV (Light Oxygen Voltage) photosensitive domain, and a caged HTH (Helix turn helix) DNA binding domain. Upon Blue illumination, a change of conformation uncages the HTH domain, the protein dimerizes and the HTH domain can bind to its cognate sequence on the pC120 promoter. There, interacting with the RNA polymerase via its VP16 domain, the transcription of downstream genes is favored.*

The EL222 optogenetic system. Many optogenetics systems exist, relying on different components coming from plants or bacteria, responding to different wavelengths (see optobase.org¹²⁹ and my review after this introduction). The lab chose to focus on the EL222 optogenetic system adapted from Jose Avalos Lab¹¹² (Fig. 23). The EL222 blue light-responsive transcription factor has true practicality since it is a single-component optogenetic system and does not rely on any exogenous cofactor (which is the case for some plant-based optogenetic systems). The protein is NLS-VP16-EL222 (Nuclear Localization Signal; VP16 (Viral Particle) as trans-activational domain – interacts with the RNA polymerase). The EL222 domain (222 amino acids coming from *Erythrobacter litoralis*) is composed of a light-responsive LOV (Light Oxygen Voltage sensor) domain, and an HTH (Helix Turn Helix) effector DNA-binding domain. The protein interacts with a flavin mononucleotide (FMN) cofactor (chromophore), naturally present in all microorganisms. Upon blue light illumination, the FMN binds covalently to the cystein75¹³⁰ of the LOV domain (photochemical protein adduct), triggering a change in conformation. This will allow for protein dimerization and especially for uncaging and stabilizing of the DNA-binding domain, which will target the protein to the pC120 promoter, where the VP16 transactivational domain will favor transcription of the downstream gene, by interacting with the RNA polymerase. In the OPTO-

EXP system¹¹², the gene under optogenetic control is simply placed under the pC120 promoter, such that light activates gene expression. Since then, other systems based on EL222 have been developed, like the OPTO-AMP, where pC120-GAL4 acts as an amplifier to express genes under pGAL promoters⁹⁰ and obtain a stronger gene expression upon illumination.

Optogenetics comes up as a versatile tool to control biological systems and will enable finer control of biological processes with the hope to improve production yields. Nevertheless, as an emerging technology, some aspects of its use remain to be investigated.

2.5.5. Light controlled bioproduction

Designing **optogenetic systems for bioproduction** or, more generally, for inducible systems in microorganisms has favored an approach that actually hybrids optogenetics and commonly used inducible genetic circuits. This way, the genetic circuits involved are already characterized, and optogenetic systems become “portable”, such that any producer strain can theoretically be made optogenetic with one single transformation. This resulted in optogenetic systems relying on the GAL system in *S. cerevisiae* (galactose)¹¹², or the lac operon (IPTG)¹³¹, the pBAD system (arabinose)¹³² and the T7 RNA polymerase in *E. coli*⁸⁹.

To know more about those systems, we invite you to read the review we published in 2020 “**The Promise of Optogenetics for Bioproduction: Dynamic Control Strategies and Scale-Up Instruments**”¹³³, placed after this introduction, where more examples of optogenetic use for bioproduction are also detailed.

Scalability. Up until now, optogenetics used for bioproduction has mostly been demonstrated at the lab scale, using various intermediate-scale devices and also in bioreactors of up to 5L, to the best of our knowledge. Labs have different culture systems, for different usages, different culture volumes and bioprocesses. As mentioned before, scalability can be an issue along the strain development process, such that a strain performing better than others at a certain scale and in a specific cultivating process can often end up outperformed by another, should the scale and process vary. This scalability issue is known for classical bioproduction studies⁶⁹, and is very hard to anticipate. Using optogenetics, another complexity layer is added to the biological system. **Genetically, the light-based control system can have its own constraints. Technically, the optogenetic system’s controllability and activity will also depend on the light input in the culture system, which may vary at different culture scales. There is therefore a real need to better understand the interplays and constraints that arise as optogenetics is used to control biological systems in the context of bioproduction.**

This is what we propose to address in this manuscript.

2.6. Goal of the PhD

2.6.1. In definitive

In this general introduction, we situated optogenetics in the context of bioproduction.

We first introduced bioproduction and established that to make this biotechnology more widely available, increases in production yields are necessary. For this, strain engineering is one first cornerstones. We discussed metabolic engineering techniques, illustrated by examples improving beta-carotene production in different organisms, which is the heterologous chemical we will focus on in this work. Importantly, after strain engineering, we highlighted the significance of the cultivation process used. As the production of a heterologous compound can trigger burden in cells, decoupling growth and production arose as a solution to counter evolutionary escapes and maximize production at low growth rates. Consequently, in a two-step cultivation process, inducible systems become indispensable to control this burden and allow first biomass accumulation, followed by a production phase induced by various types of inducers. Production in the production phase can be subjected to many factors, including cell metabolism, growth laws and resource allocation, and dilution and accumulation dynamics. Based on this, we saw that the relationship between growth and production is a fine one, and that maximizing bioproduction in the production phase requires fine control of the growth and/or the production. For this, applying control principles to biological systems is an attractive solution. Embedded control systems are available to better manage resource allocation during the production phase, but without any user input, which makes those systems hard to tune and understand. **Externally dynamically controlling producer strains is a promising technique, but has been hampered by poorly controllable inducers, limiting the flexibility of the possible induction patterns. To address this issue, optogenetics appears as the ideal tool to best control biological systems and be applied for bioproduction purposes.**

In the review positioned after this general introduction, you will find a more detailed view of the application of optogenetics to bioproduction: current uses, and future prospects. More optogenetics systems are detailed, and a particular emphasis is put on adapting current induction systems to optogenetics. Various studies are reviewed and classified given the type of control that is performed, which complements what we detailed in this general introduction. Finally, some optogenetic cultivation devices are presented and discussed.

With those two reviews, I hope to convince you of the relevance of optogenetics for bioproduction and show you how it is already applied, with various genetic tools available as well as illumination devices.

Now, we need a concrete, practical understanding of using optogenetics for bioproduction: understanding the challenges regarding strain development, in terms of metabolic engineering, control, and instrumentation.

2.6.2. Goal of the PhD

During my PhD, we asked:

How to scale up optogenetics?

- How to work in the lab with optogenetics? How adaptable are lab devices? How to adapt optogenetics at different scales?
- What is the impact of those different scales on activation? What parameters influence optogenetic activation at scales? How does optogenetic control compare at those different scales? How does scale influence the control we can have over the cells?

How to apply optogenetics for bioproduction?

- How to best handle the strain development process to apply optogenetics to bioproduction? What are the biological and technical constraints?
- How does scale influence bioproduction controlled by optogenetics? What most significant parameters influence strain performance? What are the challenges and limitations in terms of scalability?

2.6.3. Content of the manuscript

To answer those questions, this manuscript is organized into 3 chapters:

In **Chapter 1**, I present and discuss various lab devices that allow for optogenetics at different culture scales: what use each has, what parameters can be controlled and what advantages and limitations they possess. I will put a particular emphasis on 4 illumination devices that I built during my PhD: the OptoBox, the OptoTubes, the OptoFlasks, and especially the eVOLVER device, which I adapted for optogenetics, allowing for high throughput easily controllable automated cultures.

In **Chapter 2** are presented the genetic constructions for the development of a light-inducible beta-carotene producer strain, based on the EL222 optogenetic system. Two strains are detailed. A first strain was made, which had unexpected production dynamics. This strain was characterized and then optimized to finally obtain an optogenetic beta-carotene producer strain with characteristics allowing for simple production and control experiments.

Following the development of 4 illumination devices and the beta-carotene optogenetic strain, we investigate the impact of those devices on the optogenetic activation, beta-carotene production, and finally on optogenetic control of beta-carotene production. This **chapter 3** will have a “paper manuscript” format, which has been submitted and is currently under revision.

Finally, in the **last chapter**, I will summarize and discuss the obtained results and propose future directions and open questions.

Bibliography

1. Demain AL, Vaishnav P. Production of recombinant proteins by microbes and higher organisms. *Biotechnol Adv.* 2009;27(3):297-306. doi:10.1016/j.biotechadv.2009.01.008
2. Tripathi NK, Shrivastava A. Recent Developments in Bioprocessing of Recombinant Proteins: Expression Hosts and Process Development. *Front Bioeng Biotechnol.* 2019;7(December). doi:10.3389/fbioe.2019.00420
3. Way M. "What I cannot create, I do not understand." *J Cell Sci.* 2017;130(18):2941-2942. doi:10.1242/jcs.209791
4. Jacob F, Monod J. Genetic regulatory mechanisms in the synthesis of proteins. *J Mol Biol.* 1961;3(3):318-356. doi:10.1016/S0022-2836(61)80072-7
5. *Economic Microbiology: Primary Products of Metabolism.* Elsevier; 1978. doi:10.1016/B978-0-12-596552-1.X5001-3
6. Fleming A. On the Antibacterial Action of Cultures of a Penicillium, with Special Reference to their Use in the Isolation of B. influenzae. *Br J Exp Pathol.* 1929;10(3):226-236.
7. Zhang YHP, Sun J, Ma Y. Biomanufacturing: history and perspective. *J Ind Microbiol Biotechnol.* 2017;44(4-5):773-784. doi:10.1007/s10295-016-1863-2
8. WATSON JD, CRICK FHC. Molecular Structure of Nucleic Acids: A Structure for Deoxyribose Nucleic Acid. *Nature.* 1953;171(4356):737-738. doi:10.1038/171737a0
9. Cohen SN, Chang ACY, Boyer HW, Helling RB. Construction of Biologically Functional Bacterial Plasmids In Vitro. *Proc Natl Acad Sci.* 1973;70(11):3240-3244. doi:10.1073/pnas.70.11.3240
10. Davy AM, Kildegaard HF, Andersen MR. Cell Factory Engineering. *Cell Syst.* 2017;4(3):262-275. doi:10.1016/j.cels.2017.02.010
11. Nijkamp JF, van den Broek M, Datema E, et al. De novo sequencing, assembly and analysis of the genome of the laboratory strain *Saccharomyces cerevisiae* CEN.PK113-7D, a model for modern industrial biotechnology. *Microb Cell Fact.* Published online 2012. doi:10.1186/1475-2859-11-36
12. Huang M, Bao J, Nielsen J. Biopharmaceutical protein production by *Saccharomyces cerevisiae* : current state and future prospects . *Pharm Bioprocess.* 2014;2(2):167-182. doi:10.4155/pbp.14.8
13. The Economist, Keasling JD. The cost of cosmetics: How gene editing could reduce the cost of cosmetics. <https://youtu.be/XR5FOS0d8E0>
14. Langer E, Rader R. Biopharmaceutical Manufacturing: Historical and Future Trends in Titrers, Yields, and Efficiency in Commercial-Scale Bioprocessing. *Bioprocess J.* 2015;13(4):47-54. doi:10.12665/j134.langer
15. Telfer A, De Las Rivas J, Barber J. β -Carotene within the isolated Photosystem II reaction centre: photooxidation and irreversible bleaching of this chromophore by oxidised P680. *BBA - Bioenerg.* 1991;1060(1):106-114. doi:10.1016/S0005-2728(05)80125-2
16. Barros MP, Rodrigo MJ, Zacarias L. Dietary Carotenoid Roles in Redox Homeostasis and Human Health. *J Agric Food Chem.* 2018;66(23):5733-5740. doi:10.1021/acs.jafc.8b00866
17. Bogacz-Radomska L, Harasym J. β -Carotene-properties and production methods. *Food Qual Saf.* 2018;2(2):69-74. doi:10.1093/fqsafe/fyy004
18. Ribeiro BD, Barreto DW, Coelho MAZ. Technological Aspects of β -Carotene Production. *Food Bioprocess Technol.* 2011;4(5):693-701. doi:10.1007/s11947-011-0545-3

19. Kleinegris DMM, van Es MA, Janssen M, Brandenburg WA, Wijffels RH. Carotenoid fluorescence in *Dunaliella salina*. *J Appl Phycol*. 2010;22(5):645-649. doi:10.1007/s10811-010-9505-y
20. Malisorn C, Suntornsuk W. Optimization of β -carotene production by *Rhodotorula glutinis* DM28 in fermented radish brine. *Bioresour Technol*. 2008;99(7):2281-2287. doi:10.1016/j.biortech.2007.05.019
21. Zhao J, Li Q, Sun T, et al. Engineering central metabolic modules of *Escherichia coli* for improving β -carotene production. *Metab Eng*. 2013;17:42-50. doi:10.1016/j.ymben.2013.02.002
22. Larroude M, Celinska E, Back A, Thomas S, Nicaud JM, Ledesma-Amaro R. A synthetic biology approach to transform *Yarrowia lipolytica* into a competitive biotechnological producer of β -carotene. *Biotechnol Bioeng*. 2018;115(2):464-472. doi:10.1002/bit.26473
23. Bu X, Lin JY, Duan CQ, Koffas MAG, Yan GL. Dual regulation of lipid droplet-triacylglycerol metabolism and ERG9 expression for improved β -carotene production in *Saccharomyces cerevisiae*. *Microb Cell Fact*. 2022;21(1):1-13. doi:10.1186/s12934-021-01723-y
24. Clomburg JM, Qian S, Tan Z, Cheong S, Gonzalez R. The isoprenoid alcohol pathway, a synthetic route for isoprenoid biosynthesis. *Proc Natl Acad Sci U S A*. 2019;116(26):12810-12815. doi:10.1073/pnas.1821004116
25. Rabeharindranto H, Castaño-Cerezo S, Lautier T, et al. Enzyme-fusion strategies for redirecting and improving carotenoid synthesis in *S. cerevisiae*. *Metab Eng Commun*. 2019;8(December 2018):1-11. doi:10.1016/j.mec.2019.e00086
26. Verwaal R, Wang J, Meijnen JP, et al. High-level production of beta-carotene in *Saccharomyces cerevisiae* by successive transformation with carotenogenic genes from *Xanthophyllomyces dendrorhous*. *Appl Environ Microbiol*. 2007;73(13):4342-4350. doi:10.1128/AEM.02759-06
27. Paddon CJ, Westfall PJ, Pitera DJ, et al. High-level semi-synthetic production of the potent antimalarial artemisinin. *Nature*. 2013;496(7446):528-532. doi:10.1038/nature12051
28. Nowrouzi B, Li RA, Walls LE, et al. Enhanced production of taxadiene in *Saccharomyces cerevisiae*. *Microb Cell Fact*. 2020;19(1):1-12. doi:10.1186/s12934-020-01458-2
29. Hansen NL, Miettinen K, Zhao Y, et al. Integrating pathway elucidation with yeast engineering to produce polypunonic acid the precursor of the anti-obesity agent celastrol. *Microb Cell Fact*. 2020;19(1):1-17. doi:10.1186/s12934-020-1284-9
30. Benzinger D, Ovinnikov S, Khammash M. Synthetic gene networks recapitulate dynamic signal decoding and differential gene expression. *Cell Syst*. 2022;13(5):353-364.e6. doi:10.1016/j.cels.2022.02.004
31. Shaw WM, Yamauchi H, Mead J, et al. Engineering a Model Cell for Rational Tuning of GPCR Signaling. *Cell*. 2019;177(3):782-796.e27. doi:10.1016/j.cell.2019.02.023
32. Liu R, Liu L, Li X, Liu D, Yuan Y. Engineering yeast artificial core promoter with designated base motifs. *Microb Cell Fact*. 2020;19(1):1-9. doi:10.1186/s12934-020-01305-4
33. Duplus-Bottin H, Spichty M, Triqueneaux G, et al. A single-chain and fast-responding light-inducible cre recombinase as a novel optogenetic switch. *Elife*. 2021;10:1-52. doi:10.7554/eLife.61268
34. Hadadi N, Hatzimanikatis V. Design of computational retrobiosynthesis tools for the design of de novo synthetic pathways. *Curr Opin Chem Biol*. 2015;28:99-104. doi:10.1016/j.cbpa.2015.06.025

35. Delépine B, Duigou T, Carbonell P, Faulon JL. RetroPath2.0: A retrosynthesis workflow for metabolic engineers. *Metab Eng.* 2018;45(December 2017):158-170. doi:10.1016/j.ymben.2017.12.002
36. Fisher AK, Freedman BG, Bevan DR, Senger RS. A review of metabolic and enzymatic engineering strategies for designing and optimizing performance of microbial cell factories. *Comput Struct Biotechnol J.* 2014;11(18):91-99. doi:10.1016/j.csbj.2014.08.010
37. Durmusoglu D, Al'Abri IS, Collins SP, et al. In Situ Biomanufacturing of Small Molecules in the Mammalian Gut by Probiotic *Saccharomyces boulardii*. *ACS Synth Biol.* 2021;10(5):1039-1052. doi:10.1021/acssynbio.0c00562
38. Li Q, Sun Z, Li J, Zhang Y. Enhancing beta-carotene production in *Saccharomyces cerevisiae* by metabolic engineering. *FEMS Microbiol Lett.* 2013;345(2):94-101. doi:10.1111/1574-6968.12187
39. Zhao EM, Suek N, Wilson MZ, et al. Light-based control of metabolic flux through assembly of synthetic organelles. *Nat Chem Biol.* 2019;15(6):589-597. doi:10.1038/s41589-019-0284-8
40. Ma Y, Li J, Huang S, Stephanopoulos G. Targeting pathway expression to subcellular organelles improves astaxanthin synthesis in *Yarrowia lipolytica*. *Metab Eng.* 2021;68:152-161. doi:10.1016/j.ymben.2021.10.004
41. Montañó López J, Duran L, Avalos JL. Physiological limitations and opportunities in microbial metabolic engineering. *Nat Rev Microbiol.* 2021;0123456789. doi:10.1038/s41579-021-00600-0
42. Aw R, Polizzi KM. Can too many copies spoil the broth? *Microb Cell Fact.* 2013;12(1):128. doi:10.1186/1475-2859-12-128
43. López J, Bustos D, Camilo C, Arenas N, Saa PA, Agosin E. Engineering *Saccharomyces cerevisiae* for the Overproduction of β -Ionone and Its Precursor β -Carotene. *Front Bioeng Biotechnol.* 2020;8(September):1-13. doi:10.3389/fbioe.2020.578793
44. Bu X, Lin JY, Cheng J, et al. Engineering endogenous ABC transporter with improving ATP supply and membrane flexibility enhances the secretion of β -carotene in *Saccharomyces cerevisiae*. *Biotechnol Biofuels.* 2020;13(1):1-14. doi:10.1186/s13068-020-01809-6
45. Doshi R, Nguyen T, Chang G. Transporter-mediated biofuel secretion. *Proc Natl Acad Sci U S A.* 2013;110(19):7642-7647. doi:10.1073/pnas.1301358110
46. Li C, Swofford CA, Sinskey AJ. Modular engineering for microbial production of carotenoids. *Metab Eng Commun.* 2020;10(October 2019):e00118. doi:10.1016/j.mec.2019.e00118
47. Wu Y, Yan P, Li Y, et al. Enhancing β -Carotene Production in *Escherichia coli* by Perturbing Central Carbon Metabolism and Improving the NADPH Supply. *Front Bioeng Biotechnol.* 2020;8(June):1-13. doi:10.3389/fbioe.2020.00585
48. Zhao X, Shi F, Zhan W. Overexpression of ZWF1 and POS5 improves carotenoid biosynthesis in recombinant *Saccharomyces cerevisiae*. *Lett Appl Microbiol.* 2015;61(4):354-360. doi:10.1111/lam.12463
49. Bu X, Sun L, Shang F, Yan G. Comparative metabolomics profiling of engineered *Saccharomyces cerevisiae* lead to a strategy that improving β -carotene production by acetate supplementation. *PLoS One.* 2017;12(11):1-21. doi:10.1371/journal.pone.0188385
50. Gao H, Tuyishime P, Zhang X, Yang T, Xu M, Rao Z. Engineering of microbial cells for L-valine production: challenges and opportunities. *Microb Cell Fact.* 2021;20(1):1-16. doi:10.1186/s12934-021-01665-5
51. Zhao Y, Zhang Y, Nielsen J, Liu Z. Production of β -carotene in *Saccharomyces*

- cerevisiae through altering yeast lipid metabolism. *Biotechnol Bioeng.* 2021;118(5):2043-2052. doi:10.1002/bit.27717
52. Ma T, Shi B, Ye Z, et al. Lipid engineering combined with systematic metabolic engineering of *Saccharomyces cerevisiae* for high-yield production of lycopene. *Metab Eng.* 2019;52(July 2018):134-142. doi:10.1016/j.ymben.2018.11.009
 53. Reyes LH, Gomez JM, Kao KC. Improving carotenoids production in yeast via adaptive laboratory evolution. *Metab Eng.* 2014;21:26-33. doi:10.1016/j.ymben.2013.11.002
 54. Olson ML, Johnson J, Carswell WF, Reyes LH, Senger RS, Kao KC. Characterization of an evolved carotenoids hyper-producer of *Saccharomyces cerevisiae* through bioreactor parameter optimization and Raman spectroscopy. *J Ind Microbiol Biotechnol.* 2016;43(10):1355-1363. doi:10.1007/s10295-016-1808-9
 55. Menegon YA, Gross J, Jacobus AP. How adaptive laboratory evolution can boost yeast tolerance to lignocellulosic hydrolyses. *Curr Genet.* 2022;68(3-4):319-342. doi:10.1007/s00294-022-01237-z
 56. Jiang W, Li C, Li Y, Peng H. Metabolic Engineering Strategies for Improved Lipid Production and Cellular Physiological Responses in Yeast *Saccharomyces cerevisiae*. *J Fungi.* 2022;8(5). doi:10.3390/jof8050427
 57. Staudacher J, Rebnegger C, Dohnal T, Landes N, Mattanovich D, Gasser B. Going beyond the limit: Increasing global translation activity leads to increased productivity of recombinant secreted proteins in *Pichia pastoris*. *Metab Eng.* 2022;70(October 2021):181-195. doi:10.1016/j.ymben.2022.01.010
 58. Dai J, Boeke JD, Luo Z, Jiang S, Cai Y. Sc3.0: revamping and minimizing the yeast genome. *Genome Biol.* 2020;21(1):205. doi:10.1186/s13059-020-02130-z
 59. Gudmundsson S, Nogales J. Recent advances in model-assisted metabolic engineering. *Curr Opin Syst Biol.* 2021;28:100392. doi:10.1016/j.coisb.2021.100392
 60. Ramzi AB, Baharum SN, Bunawan H, Scrutton NS. Streamlining Natural Products Biomanufacturing With Omics and Machine Learning Driven Microbial Engineering. *Front Bioeng Biotechnol.* 2020;8(December):1-10. doi:10.3389/fbioe.2020.608918
 61. Kirby J, Dietzel KL, Wichmann G, et al. Engineering a functional 1-deoxy-D-xylulose 5-phosphate (DXP) pathway in *Saccharomyces cerevisiae*. *Metab Eng.* 2016;38(510):494-503. doi:10.1016/j.ymben.2016.10.017
 62. Nielsen J, Keasling JD. Engineering Cellular Metabolism. *Cell.* 2016;164(6):1185-1197. doi:10.1016/j.cell.2016.02.004
 63. López J, Cataldo VF, Peña M, et al. Build your bioprocess on a solid strain- β -carotene production in recombinant *saccharomyces cerevisiae*. *Front Bioeng Biotechnol.* 2019;7(JUL):1-9. doi:10.3389/fbioe.2019.00171
 64. Vandermies M, Fickers P. Bioreactor-scale strategies for the production of recombinant protein in the yeast *yarrowia lipolytica*. *Microorganisms.* 2019;7(2). doi:10.3390/microorganisms7020040
 65. Fathi Z, Tramontin LRR, Ebrahimipour G, Borodina I, Darvishi F. Metabolic engineering of *Saccharomyces cerevisiae* for production of β -carotene from hydrophobic substrates. *FEMS Yeast Res.* 2021;21(1):1-11. doi:10.1093/femsyr/foaa068
 66. Verwaal R, Jiang Y, Wang J, et al. Heterologous carotenoid production in *Saccharomyces cerevisiae* induces the pleiotropic drug resistance stress response. *Yeast.* 2010;27(12):983-998. doi:10.1002/yea.1807
 67. Sun L, Atkinson CA, Lee YG, Jin YS. High-level β -carotene production from xylose by engineered *Saccharomyces cerevisiae* without overexpression of a truncated HMG1 (tHMG1). *Biotechnol Bioeng.* 2020;117(11):3522-3532. doi:10.1002/bit.27508
 68. Mata-Gómez LC, Montañez JC, Méndez-Zavala A, Aguilar CN. Biotechnological

- production of carotenoids by yeasts: An overview. *Microb Cell Fact*. 2014;13(1):1-11. doi:10.1186/1475-2859-13-12
69. Crater JS, Lievens JC. Scale-up of industrial microbial processes. *FEMS Microbiol Lett*. 2018;365(13):1-5. doi:10.1093/femsle/fny138
 70. Wu G, Yan Q, Jones JA, Tang YJ, Fong SS, Koffas MAG. Metabolic Burden: Cornerstones in Synthetic Biology and Metabolic Engineering Applications. *Trends Biotechnol*. 2016;34(8):652-664. doi:10.1016/j.tibtech.2016.02.010
 71. Hoffmann F, Rinas U. Stress induced by recombinant protein production in *Escherichia coli*. *Adv Biochem Eng Biotechnol*. 2004;89:73-92. doi:10.1007/b93994
 72. Glick BR. Metabolic load and heterologous gene expression. *Biotechnol Adv*. 1995;13(2):247-261. doi:10.1016/0734-9750(95)00004-A
 73. Frei T, Cella F, Tedeschi F, et al. Characterization and mitigation of gene expression burden in mammalian cells. *Nat Commun*. 2020;11(1):1-14. doi:10.1038/s41467-020-18392-x
 74. Kafri M, Metzler-Raz E, Jona G, Barkai N. The Cost of Protein Production. *Cell Rep*. 2016;14(1):22-31. doi:10.1016/j.celrep.2015.12.015
 75. Ceroni F, Algar R, Stan GB, Ellis T. Quantifying cellular capacity identifies gene expression designs with reduced burden. *Nat Methods*. 2015;12(5):415-418. doi:10.1038/nmeth.3339
 76. Milo R, Jorgensen P, Moran U, Weber G, Springer M. BioNumbers The database of key numbers in molecular and cell biology. *Nucleic Acids Res*. 2009;38(SUPPL.1):750-753. doi:10.1093/nar/gkp889
 77. Kotopka BJ, Smolke CD. Model-driven generation of artificial yeast promoters. *Nat Commun*. 2020;11(1):1-13. doi:10.1038/s41467-020-15977-4
 78. Kim J-E, Jang I-S, Sung BH, Kim SC, Lee JY. Rerouting of NADPH synthetic pathways for increased protopanaxadiol production in *Saccharomyces cerevisiae*. *Sci Rep*. 2018;8(1):15820. doi:10.1038/s41598-018-34210-3
 79. Eguchi Y, Makanae K, Hasunuma T, Ishibashi Y, Kito K, Moriya H. Estimating the protein burden limit of yeast cells by measuring the expression limits of glycolytic proteins. *Elife*. 2018;7:1-23. doi:10.7554/eLife.34595
 80. Kim H, Yoo SJ, Kang HA. Yeast synthetic biology for the production of recombinant therapeutic proteins. *FEMS Yeast Res*. 2015;15(1). doi:10.1111/1567-1364.12195
 81. Kintaka R, Makanae K, Moriya H. Cellular growth defects triggered by an overload of protein localization processes. *Sci Rep*. 2016;6(August):1-11. doi:10.1038/srep31774
 82. Zhu ZT, Du MM, Gao B, et al. Metabolic compartmentalization in yeast mitochondria: Burden and solution for squalene overproduction. *Metab Eng*. 2021;68(October):232-245. doi:10.1016/j.ymben.2021.10.011
 83. Rugbjerg P, Olsson L. The future of self-selecting and stable fermentations. *J Ind Microbiol Biotechnol*. 2020;47(11):993-1004. doi:10.1007/s10295-020-02325-0
 84. Lee S-W, Rugbjerg P, Sommer MOA. Exploring Selective Pressure Trade-Offs for Synthetic Addiction to Extend Metabolite Productive Lifetimes in Yeast. *ACS Synth Biol*. Published online 2021. doi:10.1021/acssynbio.1c00240
 85. Rugbjerg P, Sarup-Lytzen K, Nagy M, Sommer MOA. Synthetic addiction extends the productive life time of engineered *Escherichia coli* populations. *Proc Natl Acad Sci U S A*. 2018;115(10):2347-2352. doi:10.1073/pnas.1718622115
 86. Gomez-Pastor R, Perez-Torrado R, Garre E, Matall E. Recent Advances in Yeast Biomass Production. *Biomass - Detect Prod Usage*. Published online 2011. doi:10.5772/19458
 87. Looser V, Bruhlmann B, Bumbak F, et al. Cultivation strategies to enhance productivity of *Pichia pastoris*: A review. *Biotechnol Adv*. 2014;33(6):1177-1193.

- doi:10.1016/j.biotechadv.2015.05.008
88. Gasmi N, Ayed A, Ammar BBH, Zrigui R, Nicaud JM, Kallel H. Development of a cultivation process for the enhancement of human interferon alpha 2b production in the oleaginous yeast, *Yarrowia lipolytica*. *Microb Cell Fact*. 2011;10:1-11. doi:10.1186/1475-2859-10-90
 89. Raghavan AR, Salim K, Yadav VG. Optogenetic Control of Heterologous Metabolism in *E. coli*. *ACS Synth Biol*. 2020;9(9):2291-2300. doi:10.1021/acssynbio.9b00454
 90. Zhao EM, Lalwani MA, Chen J-M, Orillac P, Toettcher JE, Avalos JL. Optogenetic Amplification Circuits for Light-Induced Metabolic Control. *ACS Synth Biol*. 2021;10(5):1143-1154. doi:10.1021/acssynbio.0c00642
 91. Prielhofer R, Maurer M, Klein J, et al. Induction without methanol: Novel regulated promoters enable high-level expression in *Pichia pastoris*. *Microb Cell Fact*. 2013;12(1):1-10. doi:10.1186/1475-2859-12-5
 92. Solow SP, Sengbusch J, Laird MW. Heterologous protein production from the inducible MET25 promoter in *Saccharomyces cerevisiae*. *Biotechnol Prog*. 2005;21(2):617-620. doi:10.1021/bp049916q
 93. Korber P, Barbaric S. The yeast PHO5 promoter: From single locus to systems biology of a paradigm for gene regulation through chromatin. *Nucleic Acids Res*. 2014;42(17):10888-10902. doi:10.1093/nar/gku784
 94. Mattanovich D, Branduardi P, Dato L, Gasser B, Sauer M, Porro D. Recombinant protein production in yeasts. In: *Methods in Molecular Biology*. Vol 824. ; 2012:329-358. doi:10.1007/978-1-61779-433-9_17
 95. Olah GA. Beyond Oil and Gas: The Methanol Economy. *Angew Chemie Int Ed*. 2005;44(18):2636-2639. doi:10.1002/anie.200462121
 96. Martin-Yken H. Yeast-Based Biosensors: Current Applications and New Developments. *Biosensors*. 2020;10(5):51. doi:10.3390/bios10050051
 97. Lalwani M, Zhao E, Biotechnology JA-C opinion in, 2018 U. Current and future modalities of dynamic control in metabolic engineering. *Elsevier*. Accessed July 9, 2020. <https://www.sciencedirect.com/science/article/pii/S0958166917302653>
 98. Min BE, Hwang HG, Lim HG, Jung GY. Optimization of industrial microorganisms: recent advances in synthetic dynamic regulators. *J Ind Microbiol Biotechnol*. 2017;44(1):89-98. doi:10.1007/s10295-016-1867-y
 99. Santos-Navarro FN, Boada Y, Vignoni A, Picó J. Gene Expression Space Shapes the Bioprocess Trade-Offs among Titer, Yield and Productivity. *Appl Sci*. 2021;11(13):5859. doi:10.3390/app11135859
 100. Scott M, Klumpp S, Mateescu EM, Hwa T. Emergence of robust growth laws from optimal regulation of ribosome synthesis. *Mol Syst Biol*. 2014;10(8):747. doi:10.15252/msb.20145379
 101. Weiße AY, Oyarzún DA, Danos V, Swain PS. Mechanistic links between cellular trade-offs, gene expression, and growth. *Proc Natl Acad Sci U S A*. 2015;112(9):E1038-E1047. doi:10.1073/pnas.1416533112
 102. Nikolados EM, Weiße AY, Ceroni F, Oyarzún DA. Growth Defects and Loss-of-Function in Synthetic Gene Circuits. *ACS Synth Biol*. 2019;8(6):1231-1240. doi:10.1021/acssynbio.8b00531
 103. MetzI-Raz E, Kafri M, Yaakov G, Soifer I, Gurvich Y, Barkai N. Principles of cellular resource allocation revealed by condition-dependent proteome profiling. *bioRxiv*. Published online 2017:1-21. doi:10.1101/124370
 104. Knapp BD, Odermatt P, Rojas ER, et al. Decoupling of Rates of Protein Synthesis from Cell Expansion Leads to Supergrowth. *Cell Syst*. 2019;9(5):434-445.e6. doi:10.1016/j.cels.2019.10.001

105. Sun S, Gresham D. Cellular quiescence in budding yeast. *Yeast*. 2021;38(1):12-29. doi:10.1002/yea.3545
106. Holtz WJ, Keasling JD. Engineering Static and Dynamic Control of Synthetic Pathways. *Cell*. 2010;140(1):19-23. doi:10.1016/j.cell.2009.12.029
107. Lalwani MA, Zhao EM, Avalos JL. Current and future modalities of dynamic control in metabolic engineering. *Curr Opin Biotechnol*. 2018;52:56-65. doi:10.1016/j.copbio.2018.02.007
108. Cress BF, Trantas EA, Ververidis F, Linhardt RJ, Koffas MAG. Sensitive cells: Enabling tools for static and dynamic control of microbial metabolic pathways. *Curr Opin Biotechnol*. 2015;36:205-214. doi:10.1016/j.copbio.2015.09.007
109. Liu D, Mannan AA, Han Y, Oyarzún DA, Zhang F. Dynamic metabolic control: towards precision engineering of metabolism. *J Ind Microbiol Biotechnol*. 2018;45(7):535-543. doi:10.1007/s10295-018-2013-9
110. Zhou S, Yuan SF, Nair PH, Alper HS, Deng Y, Zhou J. Development of a growth coupled and multi-layered dynamic regulation network balancing malonyl-CoA node to enhance (2S)-naringenin biosynthesis in *Escherichia coli*. *Metab Eng*. 2021;67(May):41-52. doi:10.1016/j.ymben.2021.05.007
111. Hortacsu A, Ryu DDY. Optimal Temperature Control Policy for a Two-Stage Recombinant Fermentation Process. *Biotechnol Prog*. 1990;6(6):403-407. doi:10.1021/bp00006a001
112. Zhao EM, Zhang Y, Mehl J, et al. Optogenetic regulation of engineered cellular metabolism for microbial chemical production. *Nature*. 2018;555(7698):683-687. doi:10.1038/nature26141
113. Ledezma-Tejeida D, Schastnaya E, Sauer U. Metabolism as a signal generator in bacteria. *Curr Opin Syst Biol*. 2021;28:100404. doi:10.1016/j.coisb.2021.100404
114. Khammash MH. Cybergenetics: Theory and Applications of Genetic Control Systems. *Proc IEEE*. 2022;110(5):631-658. doi:10.1109/jproc.2022.3170599
115. Xie W, Ye L, Lv X, Xu H, Yu H. Sequential control of biosynthetic pathways for balanced utilization of metabolic intermediates in *Saccharomyces cerevisiae*. *Metab Eng*. 2015;28:8-18. doi:10.1016/j.ymben.2014.11.007
116. Farmer WR, Liao JC. Improving lycopene production in *Escherichia coli* by engineering metabolic control. *Nat Biotechnol*. 2000;18(5):533-537. doi:10.1038/75398
117. Dunlop MJ, Keasling JD, Mukhopadhyay A. A model for improving microbial biofuel production using a synthetic feedback loop. *Syst Synth Biol*. 2010;4(2):95-104. doi:10.1007/s11693-010-9052-5
118. Yuan J, Ching CB. Dynamic control of ERG9 expression for improved amorpha-4,11-diene production in *Saccharomyces cerevisiae*. *Microb Cell Fact*. 2015;14(1). doi:10.1186/s12934-015-0220-x
119. Dahl RH, Zhang F, Alonso-Gutierrez J, et al. Engineering dynamic pathway regulation using stress-response promoters. *Nat Biotechnol*. 2013;31(11):1039-1046. doi:10.1038/nbt.2689
120. Zhang F, Carothers JM, Keasling JD. Design of a dynamic sensor-regulator system for production of chemicals and fuels derived from fatty acids. *Nat Biotechnol*. 2012;30(4):354-359. doi:10.1038/nbt.2149
121. Liu D, Zhang F. Metabolic Feedback Circuits Provide Rapid Control of Metabolite Dynamics. *ACS Synth Biol*. 2018;7(2):347-356. doi:10.1021/acssynbio.7b00342
122. David F, Nielsen J, Siewers V. Flux Control at the Malonyl-CoA Node through Hierarchical Dynamic Pathway Regulation in *Saccharomyces cerevisiae*. *ACS Synth Biol*. 2016;5(3):224-233. doi:10.1021/acssynbio.5b00161
123. Shen YP, Pan Y, Niu FX, Liao YL, Huang M, Liu JZ. Biosensor-assisted evolution for



- high-level production of 4-hydroxyphenylacetic acid in *Escherichia coli*. *Metab Eng.* 2022;70(September 2021):1-11. doi:10.1016/j.ymben.2021.12.008
124. Ceroni F, Boo A, Furini S, et al. Burden-driven feedback control of gene expression. *Nat Methods.* 2018;15(5):387-393. doi:10.1038/nmeth.4635
 125. Boo A, Ellis T, Stan GB. Host-aware synthetic biology. *Curr Opin Syst Biol.* 2019;14:66-72. doi:10.1016/j.coisb.2019.03.001
 126. Martin JF, Demain AL. Control of antibiotic biosynthesis. *Microbiol Rev.* 1980;44(2):230-251. doi:10.1128/membr.44.2.230-251.1980
 127. Aucoin MG, McMurray-Beaulieu V, Poulin F, et al. Identifying conditions for inducible protein production in *E. coli*: Combining a fed-batch and multiple induction approach. *Microb Cell Fact.* 2006;5(1):27. doi:10.1186/1475-2859-5-27
 128. Motta-Mena LB, Reade A, Mallory MJ, et al. An optogenetic gene expression system with rapid activation and deactivation kinetics. *Nat Chem Biol.* 2014;10(3):196-202. doi:10.1038/nchembio.1430
 129. Kolar K, Knobloch C, Stork H, Žnidarič M, Weber W. OptoBase: A Web Platform for Molecular Optogenetics. *ACS Synth Biol.* 2018;7(7):1825-1828. doi:10.1021/acssynbio.8b00120
 130. Nash AI, McNulty R, Shillito ME, et al. Structural basis of photosensitivity in a bacterial light-oxygen-voltage/ helix-turn-helix (LOV-HTH) DNA-binding protein. *Proc Natl Acad Sci U S A.* 2011;108(23):9449-9454. doi:10.1073/pnas.1100262108
 131. Lalwani MA, Ip SS, Carrasco-López C, et al. Optogenetic control of the lac operon for bacterial chemical and protein production. *Nat Chem Biol.* Published online 2020. doi:10.1038/s41589-020-0639-1
 132. Romano E, Baumschlager A, Akmeriç EB, et al. An inducible AraC that responds to blue light instead of arabinose. *bioRxiv.* Published online July 14, 2020:2020.07.14.202911. doi:10.1101/2020.07.14.202911
 133. Pouzet S, Banderas A, Bec M Le, Lautier T, Truan G, Hersen P. The promise of optogenetics for bioproduction: Dynamic control strategies and scale-up instruments. *Bioengineering.* 2020;7(4):1-17. doi:10.3390/bioengineering7040151

3. The promise of optogenetics for bioproduction (review)

After the general introduction that contextualized the use of optogenetics for bioproduction, we propose here the review I wrote and published regarding the actual use of optogenetic for bioproduction and challenges to come.

Review

The Promise of Optogenetics for Bioproduction: Dynamic Control Strategies and Scale-Up Instruments

Sylvain Pouzet ^{1,2,3,*}, Alvaro Banderas ^{1,2,3}, Matthias Le Bec ^{1,2,3} , Thomas Lautier ^{4,5}, Gilles Truan ⁴  and Pascal Hersen ^{1,2,3,*}

¹ Laboratoire Physico Chimie Curie, Institut Curie, PSL Research University, CNRS UMR168, 26 rue d'Ulm, 75005 Paris, France; alvaro.banderas@curie.fr (A.B.); matthias.lebec@curie.fr (M.L.B.)

² Sorbonne Université, 75005 Paris, France

³ Laboratoire MSC, UMR7057, Université Paris Diderot-CNRS, 75013 Paris, France

⁴ Toulouse Biotechnology Institute, Université de Toulouse, CNRS, INRAE, INSA, 31400 Toulouse, France; thomas.lautier@insa-toulouse.fr (T.L.); gilles.truan@insa-toulouse.fr (G.T.)

⁵ Singapore Institute of Food and Biotechnology Innovation, Agency for Science Technology and Research, Singapore 138673, Singapore

* Correspondence: sylvain.pouzet@curie.fr (S.P.); pascal.hersen@curie.fr (P.H.)

Received: 13 October 2020; Accepted: 19 November 2020; Published: 24 November 2020



Abstract: Progress in metabolic engineering and synthetic and systems biology has made bioproduction an increasingly attractive and competitive strategy for synthesizing biomolecules, recombinant proteins and biofuels from renewable feedstocks. Yet, due to poor productivity, it remains difficult to make a bioproduction process economically viable at large scale. Achieving dynamic control of cellular processes could lead to even better yields by balancing the two characteristic phases of bioproduction, namely, growth *versus* production, which lie at the heart of a trade-off that substantially impacts productivity. The versatility and controllability offered by light will be a key element in attaining the level of control desired. The popularity of light-mediated control is increasing, with an expanding repertoire of optogenetic systems for novel applications, and many optogenetic devices have been designed to test optogenetic strains at various culture scales for bioproduction objectives. In this review, we aim to highlight the most important advances in this direction. We discuss how optogenetics is currently applied to control metabolism in the context of bioproduction, describe the optogenetic instruments and devices used at the laboratory scale for strain development, and explore how current industrial-scale bioproduction processes could be adapted for optogenetics or could benefit from existing photobioreactor designs. We then draw attention to the steps that must be undertaken to further optimize the control of biological systems in order to take full advantage of the potential offered by microbial factories.

Keywords: bioproduction; biomanufacturing; optogenetics; cybergenetics; dynamic regulation; bioprocess; biotechnology; photobioreactors

1. Merging Optogenetics and Bioproduction

1.1. Introduction to Bioproduction

Human societies have employed bioproduction since the ancient Egyptians first fermented grapes to produce ethanol for wine. Since then, bioproduction has been employed to address numerous global issues, such as the production of acetone using *Clostridium acetobutylicum* by Chaim Weizmann during World War One, the discovery of penicillin by Alexander Fleming in 1928 and the production of insulin by conventional *Saccharomyces cerevisiae* in the early 1980s [1]. Biomanufactured products have become

ubiquitous components of our daily lives, including therapeutics (antibiotics, hormones [2], vaccines [3]), enzymes (stabilizers and cocktails [4]) and chemicals (amino acids, dyes [5], biodiesel [6]). The rise of systems biology (*omics* tools and databases, bioinformatics, metabolic engineering) and synthetic biology (cloning, metabolic and protein engineering, CRISPR, DNA synthesis) has expanded the possibilities for bioengineering, and sophisticated pathways have been successfully implemented into various cellular chassis; for example, the production of artemisinin [7], cannabinoids [8], and tropane alkaloids such as scopolamine [9]. Similarly to chemistry in the 19th century, biology is now shifting from a descriptive field to a constructive field, and bioproduction holds the potential to play a significant role by enabling the biomanufacturing of affordable medicines, and the sustainable production of high value-added chemicals and biofuels from renewable feedstock.

Despite these advances, biomanufacturing a new product remains challenging in many ways. Advances in systems and synthetic biology, as well as automation using high-throughput robotics, have reduced the time required to successfully produce a molecule or enzyme using a specific chassis. Nonetheless, achieving an economically viable and market-competitive production process using such whole-cell applications can be tricky, due to difficulties with scaling-up, the long duration of process development and the expensive, specific downstream processing steps. Therefore, extensive efforts have been made to optimize bioprocesses for existing engineered strains. The accumulation of the maximal number of producing cells is the first step towards maximizing production yield. However, the production of a molecule of interest will consume cellular resources and may generate toxic intermediaries or by-products. Thus, production often creates a stress or a burden that impairs cells' ability to grow. Such burden can give rise to microbial heterogeneity and evolutionary escape, and lead to poor yields. Two-phase fermentation strategies are frequently implemented in bioreactors to minimize this burden. In the first phase, growth is favored; the production system is "silent" and cells actively divide without producing any heterologous component, allowing biomass to accumulate. In the second phase, production is "unleashed", for example by inducing the expression of the recombinant enzyme or activating a synthetic pathway that leads to the production of the molecule of interest. During this second phase, the total content of metabolic precursors is divided between the cells' endogenous needs and the synthetic pathway. Thus, the decoupling of growth from production—often irreversibly—has become standard in bioproduction, and this strategy is employed at every production scale. The switch from growth to the production phase can be mediated by various inducible promoters that respond to specific cues; for example, a triggered change in temperature [10] or pH [11], or the presence of a specific molecule such as IPTG (in *E. coli*), galactose (in *S. cerevisiae*) or methanol (in *Pichia pastoris*), or other changes in the environment (nutrient depletion, high cell density). Strong, non-reversible inductions are frequently employed; however, more comprehensive and subtle induction patterns are now increasingly preferred. In this context, the use of light as an inducer has attracted interest, given its ability to be finely tuned in space, time and intensity.

Optogenetics, i.e., using light to control cellular processes, is a versatile tool to induce production in industrial microorganisms. Light is a straight-forward output for computer control systems, as it is tunable down to the millisecond scale, reversible, and offers a range of different and compatible signals of various wavelengths. Moreover, light is more easily delivered and removed from bioreactors compared to the extensive media changes that would be required for chemical inducers, it is considered to be rather non-invasive to cells, and it is cheaper than chemical inducers. Only a small number of studies have applied this emerging strategy to bioproduction. However, researchers increasingly acknowledge optogenetics as a promising tool to achieve fine (and even real-time) control of complex biological systems. In this review, we aim to highlight recent advances and explore the limitations of merging optogenetics with bioproduction in the context of simple and more sophisticated bioproduction control strategies. We also discuss recent optogenetic instruments that will help to develop, characterize and control newly built strains, and the potential issues and opportunities that may be encountered during the scale-up of light-controlled bioproduction processes to the industrial scale.

1.2. Optogenetics

Light is widely used by biological systems, not only as an energy source, but also as a signal to which they respond in a variety of ways. Bacteria can express different types of photoreceptors to regulate, for example, the synthesis of protective pigments. Bacterial photoreceptors (opsins, LOV domains—blue light; CcaS/CcaR—red and green light) and plant cryptochromes (CRY2-CIB1—blue light), phytochromes (Phy-PIF—red/far-red light), or UV response systems (UVR8-COP1—UV light), form the basis of most optogenetic systems developed to date [12]. Although optogenetics was first used in neurosciences to excite or inhibit specific neurons via light-gated ion channels [13], the technique has recently been extended to other mammalian cell types to study developmental timing and coordination [14], regulatory cascades' responses to dynamic signals [15], and cellular biophysical processes [16]. With respect to microbial systems, numerous optogenetic systems have been developed and used to investigate the protein control of biofilm formation, metabolic flux control (reviewed in [17]) and dynamic regulation of gene expression to dissect pathway dynamics [18]. In non-neural studies, light is used to control protein interactions, which can give rise to various molecular functions (dimerization, relocalization, anchoring, phosphorylation/activation, oligomerization). In the context of bioproduction, it is the transcriptional control resulting from such optogenetic interactions that is mostly employed.

Some optogenetic systems are particularly efficient and versatile. In the pDusk system [19], the histidine kinase YF1 phosphorylates the transcription factor FixJ in the dark, which activates transcription from the *FixK2* promoter. This process is reversed by blue light stimulation. In contrast, to achieve induction upon blue light stimulation, the pDawn system [19] (Figure 1a) was built by adding another regulation step: by placing the lambda phage repressor cI under the control of the *FixK2* promoter, the repressor cI is repressed by light, which enables the activation of the target promoter *pR*. In the PhyB-PIF system [20], the PhyB and PIF proteins dimerize upon red light stimulation (Figure 1b) and dissociate when exposed to far red light. The two photosensitive domains PhyB and PIF are usually fused separately to effector protein domains, typically a DNA-binding domain and a trans-activation domain, to regulate transcription. This interaction requires the presence of the cofactor phycocyanobilin (PCB), which is naturally present in plants, but must be externally added or engineered in microbial systems. In the single-component EL222 system [21] (Figure 1c,f), the engineered EL222 protein (composed of a caged DNA-binding domain, LOV domain and VP16 transactivation domain) homodimerizes upon blue light stimulation, which promotes DNA binding and transcription from the C120 promoter. When the CcaS/CcaR system is stimulated by green light [22] (Figure 1d) in the presence of the cofactor PCB, membrane-bound CcaS phosphorylates the transcription factor CcaR, which activates transcription from the *Cpcg2* promoter. This process is reversed by red light, which therefore prevents transcription. Finally, similar to the PhyB-PIF system, the Cry2 and Cib1 proteins of the CRY2-CIB1 system [23] dimerize upon blue light stimulation (which is reversed in the dark) due to the interaction between photons and the (naturally present) protein cofactor flavin adenine dinucleotide (FAD). Cry2 has also been engineered to self-multimerize upon light stimulation [24], as illustrated in Figure 1e. For more details on these and other optogenetic systems, we recommend consulting optobase.org [25].

1.3. Adapting Induction Systems for Optogenetics

In an effort to adapt current genetic induction systems for bioproduction, several systems have been designed to facilitate the transition of existing industrial organisms from chemical to optogenetic induction without the need for full reconstruction or redesign.

Optogenetic regulation has been achieved in *E. coli* by combining optogenetics with classical IPTG, arabinose or T7 regulation systems. IPTG, the gold standard inducer in *E. coli*, binds the LacI repressor and thus induces the expression of genes containing a *lac* operator in their promoter by preventing LacI from shielding DNA from RNA polymerase. Lalwani et al. [26] (Figure 1a) placed *LacI* under the control of the pDawn system, so that blue light induces *LacI* expression and therefore represses

the genes of interest. In contrast, the absence of light represses *LacI* expression and therefore activates the various IPTG-inducible promoters. This system was optimized to reduce leakiness, and although the expression dynamics are slower than those of IPTG induction systems (2 h delay), the final induction levels are higher and production exceeds that of the IPTG induction systems. Thus, the pDawn system is a successful alternative to IPTG induction, and has already been tested and applied to bioproduction and scaled-up to 2 L [26]. The pDusk and pDawn systems also highlight the possibility of activating or repressing a system by illumination or darkness, depending on how the optogenetic system is connected to the bioproduction system. Similarly, Romano et al. [27] substituted arabinose with light to control the BAD promoter by switching the endogenous dimerization domain of the AraC transcription factor with the VVD blue light optogenetic domains, which dimerize upon blue light stimulation. Thus, this system is compatible with pBAD-based vectors or strains, which are frequently used in smaller-scale studies. Finally, expression control using the T7 promoter is another standard in *E. coli* and is also used in *S. cerevisiae*. Raghavan et al. [28] used a split version of the T7 RNA polymerase (T7RNAP), with each part of split-T7RNAP fused to the N- or C-terminus domain of an intein, and also to either the Phy or PIF component of *Arabidopsis thaliana* phytochrome (see Figure 1b). The red light illumination of the PCB cofactor triggers the Phy-PIF interaction, which allows the intein domains to interact; trans-splicing occurs to deliver a functional T7RNAP that promotes the expression of genes under the control of the T7 promoter. Raghavan et al. successfully used this system to control the production of lycopene in *E. coli*. However, this system relies on the PCB cofactor and is not reversible, since T7RNAP is stabilized once trans-spliced. A similar strategy was used to increase the controllability and simplicity of T7RNAP. Baumschlager et al. [29] created a split version of T7RNAP that heterodimerizes upon blue light illumination due to the presence of engineered VVD domains fused to each T7RNAP termini (“Magnet” domains [30]), to create an Opto-T7RNAP system that exhibits rapid, reversible dynamics. Another version, paT7P-1, was developed by Han et al. [31].

Zhao et al. [32] connected the well-studied galactose regulation system used in the yeast *Saccharomyces cerevisiae* to the EL222 optogenetic system (Figure 1c). The authors first built the simple OPTO-EXP system, in which the protein EL222 induces the transcription of genes controlled by the C120 promoter (more subtle versions of this promoter have since been made and evaluated [33]). Then, to reverse the system and achieve activation in the dark (OPTO-INVRT), Zhao et al. placed *GAL80* under the control of the C120 promoter. In the presence of the (non-naturally) constitutively expressed GAL4 transcription factor, genes under the control of the GAL promoter are expressed in the dark. Upon blue light illumination, GAL80 is expressed and inhibits the activity of GAL4, therefore repressing genes under the control of the GAL promoter. Using both the OPTO-EXP and OPTO-INVRT systems, genes can be actively induced or repressed in a mutually exclusive way given the presence or absence of light, making this bidirectional system particularly versatile. Zhao et al. used this system to achieve dynamic control of isobutanol production up to the 2 L scale at high cell density.

It is worth noting that optogenetic systems have also been implemented in non-conventional microorganisms, such as *Pseudomonas putida* [34], and other chassis already used in industry, such as *Bacillus subtilis* [35]. The widely used yeast *Pichia pastoris* has not, to date, been adapted to optogenetic control, but we expect this to be achieved within a few years. Moreover, widely used synthetic biology systems have also been adapted for optogenetics: photo-inducible CRE recombinases [36] and photosensitive degrons [37] could be used to complement the current optogenetic systems used for bioproduction.

2. Control Strategies

2.1. Simple Switch for Flux Rewiring

Flux control lies at the heart of bioproduction strategies. To prevent production from impairing the accumulation of biomass, production is inhibited and induced after a growth phase; only then is metabolic flux redirected towards the product of interest. Chemicals or auto-induction systems

have been extensively used to achieve flux control, and optogenetics has the potential to perform at least as well as other methods of induction, while also improving controllability. Using the CcaS/CcaR optogenetic system, Senoo et al. [38] (Figure 1d) and Tandar et al. [39] controlled the expression of the *tpiA* and *pgi* genes, respectively, two important genes that channel metabolite flux towards glycolysis in *E. coli*. Both studies demonstrated enrichment in their respective competing pathways, as expected. To obtain more insight into induction timing, Raghavan et al. [28] used the PhyB-PIF system (Figure 1b) and Lalwani et al. [26] used FixJ (Figure 1a) to explore light induction at different optical densities during growth. Raghavan et al. found that the illumination pulse was most efficient during the late exponential phase of growth, and Lalwani et al. found that constant illumination at an OD of about 1 was optimal. Thus, similarly to chemical inducers, the timing of illumination must be considered in the context of the growth state; the optimal timing may essentially depend on the induction time delay of the optogenetic system, as well as the amount of burden that the cells will experience.

Compartmentalization is another strategy that can be controlled using optogenetics to redirect flux towards a specific metabolite, by using higher-order structures that bring enzymes close to each other to create reversible metabolons inside the cell. Thus, intermediate metabolites are channeled to the next enzymes in the pathway, located in close proximity, which increases the final product yield. Zhao et al. [40] built two systems for this purpose: OptoClusters (Figure 1e) is based on the engineered Cry2olig domain [24], which oligomerizes upon blue light stimulation, fused to the intrinsically disordered region (IDR) FUSN to create a phase-separated synthetic organelle. On the other hand, the PixELLS system (based on PixE/PixD from *Synechocystis* sp. fused to FUSN) loses its phase-separated structure upon blue light stimulation. These two systems form or dissociate droplets within seconds upon light stimulation. After optimization, Zhao et al. demonstrated flux redirection control using the VioC and VioE enzymes fused to the optogenetic components to control deoxyviolacein formation (Figure 1e).

Although light can be used as a simple switch-like inducer, it is its reversibility and high-controllability that makes it a singular tool facilitating the fine-tuning of cell-processes in a dynamic way.

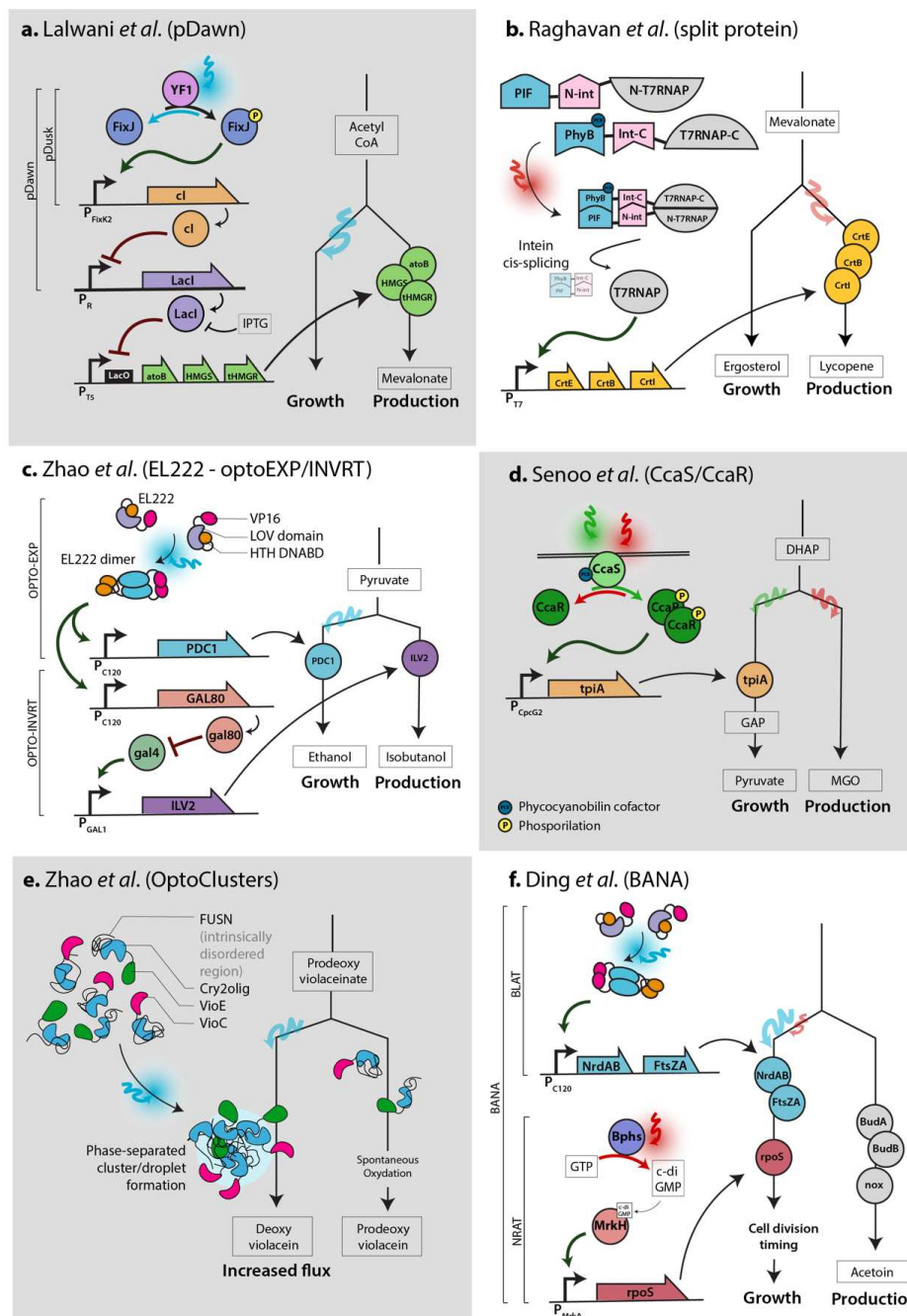


Figure 1. Different optogenetic systems can be used to achieve flux control in various ways. Sketch of circuits adapted from each paper. (a) Lalwani et al. [26] controlled mevalonate production using the pDawn system. (b) Raghavan et al. [28] used a light-responsive split T7 RNA polymerase (T7RNAP) to control lycopene production. (c) Zhao et al. [32] used EL222—composed of the VP16 trans-activation domain, light-voltage photosensitive domain (LOV) and helix-turn-helix DNA-binding domain (HTH DNABD)—to dynamically regulate isobutanol production. Blue light stimulation activates gene expression in the OPTO-EXP system, and gene expression in the optoINVRT system is activated in the dark via the GAL regulatory pathway (GAL4 is constitutively expressed in this system). (d) Senoo et al. [38] used the CcaS/CcaR system to regulate glycolysis flux. (e) Zhao et al. [40] developed a light-induced phase-separated cluster formation. Sequential enzymatic reactions are favored in this conformation. (f) Ding et al. [41] used the EL222 and Bphs systems to regulate division timing in *E. coli* to restore the growth rate and improve acetoin production.

2.2. Dynamic Switch

Many recent papers mention the possibility of using optogenetic systems to achieve dynamic control over bioproduction. During the production phase, cells may still undergo some growth (or simply maintenance) and experience a burden. However, this trade-off between growth and production can be more closely controlled (Figure 2). This idea was confirmed by studies that used stress-related promoters to modulate the induction of bioproduction systems [42] and lead to increased production. This “host aware” [43] or “burden-driven” strategy shows that dynamic control must be considered, based on the cellular state of the producing cell, in order to improve yields.

Given the ease with which such strategies can be implemented using optogenetics, dynamic control is starting to appear in bioproduction studies. For instance, Lalwani et al. [26] tested the ability of illumination duty cycles to control protein expression levels over a period of about 17 min. They managed to recapitulate a full range of induction strengths (similarly to [33]), which can be very difficult to obtain using chemical inducers (such as IPTG) that induce high expression levels regardless of their concentration, i.e., in a more switch-like manner. Controllability is significant, since strong and sudden induction is not necessarily the best strategy to maximize yield. Indeed, an overload of toxic intermediates and overexpression of a recombinant protein may impair folding and create stress [44], and therefore directly limit production.

Dynamic induction could enable repeated and reversible switching between the growth and production phases, which would let cells produce, then “recover” from production, and then produce again later. Current chemical induction systems may allow such dynamic control to an extent, but auto-induced systems (based on nutrient limitation or cell density) are frequently irreversible. Indeed, using chemical inducers such as IPTG would require complex media changes, and inducers such as galactose or methanol are metabolized by the cells, and thus hard to control. Temperature-sensitive promoters could act as reversible systems, but provide low reactivity. In addition, temperature changes involve hard-to-handle bioprocesses and certain temperatures will not necessarily fit the thermal optima of the enzymes required for endogenous and synthetic pathways. Using optogenetics to control the production of isobutanol in *S. cerevisiae*, Zhao et al. [32] applied bidirectional control using the OPTO-EXP and OPTO-INVRT systems to express *PDC1* (essential for fermentation and growth) only upon light stimulation, and express isobutanol-related genes in the dark. This way, using light, they not only favored the channeling of metabolic flux towards production, but also blocked the competing route; instead of just opening a single valve, they opened one and closed another to specifically control growth and production. Using this system as a simple switch, Zhao et al. realized that the cells were unable to consume all of the glucose in the medium by the end of the production phase, probably due to metabolic arrest related to NAD^+ depletion. However, using periodic 30 min light pulses to activate *PDC1* every 10 h, the NAD^+ pool could be restored; this method tripled the amount of isobutanol produced. Most importantly, the authors demonstrated that dynamically controlling growth and production—not simply just separating them—has substantial potential in improving yield (Figure 2b).

In light of these advances, the next logical step is to best adjust the induction pattern based on the cell's state or content of specific metabolite pools, and automatize this dynamic control in real-time. Such control could be achieved using a cybergenetics approach.

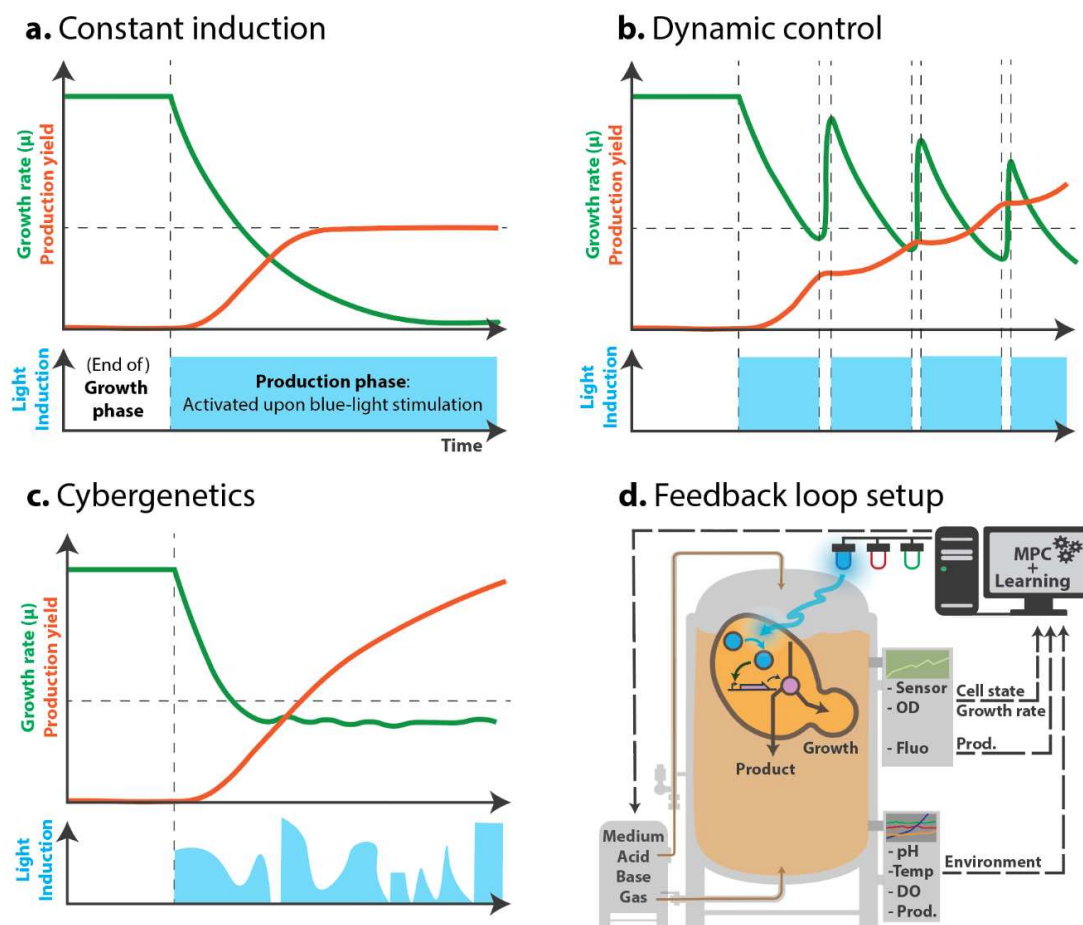


Figure 2. Sketch of different putative light-induction patterns to balance growth and production. (a–c). Green curve: growth rate; orange curve: production yield. In blue: light induction pattern that activates bioproduction. (a). With a constant and irreversible induction, production yield increases and plateaus as growth plummets and stalls due to bioproduction-induced stress. (b). Dynamic control of induction: alternating growth and production phases allows cells to “recover” from the production phase and resume growth, before starting to produce again. This strategy was successfully implemented in Zhao et al. [32]. (c). Cybergenetic control would allow for balancing, in real-time, growth and production, by inducing production given the cell’s state. In this sketch, keeping cell growth at a certain rate could ensure a low stress level that would result in a sustained productivity. (d). To implement the feedback loop, besides regular bioproduction parameters control (medium composition, pH, temperature, etc.), the optogenetic actuator (induction upon blue light in this example) is regulated given an output from the system (a cue from the environment, a measure of the growth, or cell fluorescence indicating production level, stress or metabolite pool status) that is interpreted by an algorithm (Model predictive control - MPC) to predict and act upon the behavior of the cell and balance the bioproduction process.

2.3. Cybergenetics

Cybergenetics seeks to combine control engineering with synthetic biology as a mean to control biological processes in real-time from outside the cell. Cybergenetics requires three elements: an actuator (for example, an optogenetic system), a biosensor (a reporter of the metabolic state, via a fluorescent protein level or growth rate) and a computer algorithm to control the actuator (via light) based on the biosensor output (subtly reviewed by Carrasco-Lopez et al. [45]). While simple dynamic induction is considered open-loop control (Figure 2b), cybergenetics aims to close this loop to achieve automation via real-time feedback loop control (Figure 2c,d). Such closed-loop control is especially important when experiments yield poor reproducibility, as closed-loop control can adapt and stabilize noisy systems.

Cells naturally use internal control mechanisms to adapt to changes in their environment, cope with fluctuations in internal metabolite pools and respond to stress. In the context of bioproduction, this natural ability has already been exploited to balance growth and production. Taking advantage of the innate regulatory networks of *E. coli*, Ceroni et al. [42] used the stress-responsive pHtpG1 promoter to control the expression of a guide RNA to repress—via a constitutively expressed dead Cas9—the expression of a heterologous gene used to produce the fusion protein VioB-mCherry. Using this “burden-responsive biomolecular feedback controller”, they managed to improve production using a continuous production strategy, but did not compare the results to the two-phase strategy. Such a host-aware approach has not yet been implemented using optogenetics, though this step appears feasible and promising. Another strategy to monitor burden in the cell employs metabolite-responsive transcription factors (MRTFs; see [46]) to report the level of a key metabolite pool required for the production of the final product, or the final product itself, to prevent stress.

Automated control of protein expression levels is also of particular interest. Indeed, as mentioned before, excessive expression can decrease production. Given the potential changes in the environment and cell density, closed-loop control is required to maintain constant per-cell expression throughout the production phase. Using fluorescent proteins as biosensors, such real-time control was demonstrated using chemicals as inducers [47–49] and using optogenetics with the Phy-PIF [50] and CcaS/CcaR systems [51].

In addition to controlling the intracellular concentration of a protein, Miliias-Argeitis et al. [51] showed that the growth rate of *E. coli* could be regulated via optogenetics using the CcaS/CcaR system to control the *metE* gene, which is responsible for the last step of methionine biosynthesis. Controlling the growth rate in bioproduction is important, since productivity can be either proportional or inversely proportional to growth, or only be optimal at a certain growth rate [52]. In this context, by tuning the intensity and time of both blue and near-IR illumination, Ding et al. [41] finely controlled the division timing of *E. coli* by connecting their custom optogenetic systems to control the expression of the ribonucleotide reductases *NrdAB* or *NrdA* and division proteins *ftsZA* or *Sula*, which influence dNTP biosynthesis and cell division (Figure 1f). This system enhanced the yields of acetoin and poly(lactate-co-3-hydroxybutyrate) by shortening and prolonging cell division, respectively (which restored a reduced growth rate in both cases), in two different strains, up to the 5 L scale. Although closed-loop feedback control was not employed, this method demonstrates the potential of growth control for bioproduction and the possibility of combining several optogenetic systems responding to different wavelengths. Both aspects could very well be applied in the context of cybergenetics (Figure 2d).

3. Scale-Up Instruments

3.1. Milliliter Scale

Optogenetic experiments with microbial cultures require dedicated equipment to screen for and characterize strains, and to initiate the scale-up work. This is why, at present, most labs either develop new devices in-house or adapt previously published systems, mostly in a highly flexible Do-It-Yourself (DIY) spirit. Therefore, basic knowledge of electronics, a 3D printer, a laser cutter and some device programming, i.e., the presence of a typical fablab, are usually required. The resulting device should be robust, not too expensive, and rather simple to build and calibrate.

The Light-Plate Apparatus devised by Gerhardt et al. [53] (Figure 3a) was one of the first platforms able to accommodate 24-well plates and apply two wavelengths per well. It only requires printed circuit boards (PCB) that can be easily ordered from specialized companies, some LEDs, LED sockets, 3D-printed parts for assembly, a soldering iron, a chip burner and a few screws. With this system, once the illumination power of the LEDs has been calibrated, the programming is very simple thanks to the graphical user interface (GUI) provided and experiments can be designed fairly quickly, enabling various illumination intensities and patterns to be independently delivered to any well, providing a good

throughput of strain testing. Similar systems have been reported for microwell plates (up to 96-wells or more) [27,54] or larger volumes (up to 10 mL [55,56]). These types of systems are great for small-scale experiments, such as strain characterization and screening various illumination patterns or media compositions. However, reading an output (a fluorescence level, a growth rate, etc.) from each well can be hard to automate and labor-intensive, especially if time-course profiles have to be achieved manually. For this type of study, and at such scale, plate-readers may be of value, particularly if the plate-reader can illuminate various wells independently while simultaneously measuring fluorescence or the optical density. Such sophistication is already available in state-of-the-art plate-readers. Yet, such instruments remain much more expensive and harder to handle than DIY devices.

3.2. Mini-Bioreactor Scale and Feedback Implementation

Once a producing optogenetic strain has passed screening and milliliter small scale characterization, it can be time to monitor its growth and production dynamics at larger scale and test illumination patterns accordingly. DIY mini-bioreactor systems have recently been developed by different labs to enable such real-time measurements and, most importantly, contain illumination setups. These systems include the eVOLVER [57] (Figure 3b) and Chi.Bio [58] systems, both of which work with at least 30 mL culture volumes, are customizable, and allow fluidic inputs and illumination at various wavelengths, as well as optical density measurements, and stirring and temperature control. Both devices are open-source projects, freely providing all details regarding the construction steps and components used. Both of the authors also offer commercial versions of their devices with appropriate GUIs for designing experiments and extracting output data. Usually, a set of these small bioreactors (typically 16 mini-bioreactors) are used to screen various media compositions, illumination patterns, temperatures, stirring speeds, etc. Moreover, compared to previously discussed well plates-based optogenetic instruments, eVOLVER and Chi.Bio enable the manipulation of larger culture volumes, an important intermediate step towards scaling-up to industrial conditions. Therefore, these systems combine the advantages of a small, versatile screening tool, while actually more closely mimicking larger-scale settings in terms of control and monitoring. Note, however, that pH and dissolved oxygen levels are two important factors that are not considered in those devices—although they could be implemented in the future. The embedded optogenetic hardware (mainly LEDs) can be easily tuned, and Chi.Bio especially allows for the measurement of at least two fluorescence outputs thanks to its seven-color LED and small spectrophotometer. To better control the production given the cell's state, the devices' measurement capacities will come to be crucial if fluorescent biosensors are to be used to establish automatized real-time control.

Since these devices are quite small and emit relatively powerful light, there are only a few concerns related to poor light penetration or distribution in the medium. However, it will be crucial to address this issue when scaling-up to industrial settings. Although the small size of those instruments comes as an advantage in the lab, variations in growth and production caused by the effects of larger culture volumes cannot be assessed using these devices, such that they will not replace pilot-scale testing. Nonetheless, they will be essential to start balancing growth and production and fine tune computer control models.

3.3. Industrial Settings and Photobioreactors

Even in the absence of optogenetics, scaling-up to the industrial scale (from 10 to 10,000 L) represents a challenge for any potential industrial strain. At such scales, the raw materials used for fermentation will change given the costs and quantities of chemicals required to piece together the culture medium. Moreover, mixing and oxygenation become more demanding due to the energy needed to move dense culture volumes; the inoculum volume may become critical, and pressure and shear stress may be unevenly distributed. All of these changes might impact the performance of the strain at the larger scale [59], which may prompt researchers to another round of refinement of the initial strain design. One of the main concerns regarding optogenetics at larger scales is

the penetration of light in the medium. Indeed, high-density cell cultures can become very opaque, which would prevent light from reaching a maximum number of cells (light-shading effect), or make it hard to sufficiently activate the biological process (due to dilution of the signal). Simply adding light panels around a standard bioreactor (Figure 3(c1,c4)) can overcome these issues at relatively small scales (2 to 250 L), but poses serious issues for scaling-up. Indeed, the low surface to volume ratio of larger bioreactors is a crucial factor that must be considered in the context of light exposure [60].

Light penetration is a crucial issue for the cultivation of micro-algae and cyanobacteria. As these organisms are also a valuable chassis for bioproduction (mostly for biofuels), this issue has actually been addressed in various ways, along with how to deal with pH, dissolved oxygen (DO), temperature and mixing. Different types of photobioreactors are commercially available and used to produce various biomasses or specific compounds [60]. Closed-type algal photobioreactors, such as airlift or bubble columns (Figure 3(c4)), stacked tubular (Figure 3(c3)), flat-plate and multilayered photobioreactors [61], are illuminated from the outside. These designs aim to increase the surface area of the culture in contact with, mostly, ambient light or custom light sources, and counteract the shading effect caused by high culture density or large volumes. In bioproduction, yeast cultures can result in an extremely dense, very opaque, paste-like textured medium, so that the number of cells is maximized to reach higher titers. The compatibility of algal photobioreactors with such high-density yeast cultures remains to be tested; and although light penetration is the main advantage of such photobioreactors, large-scale algal photobioreactors may not be adaptable to heavy and dense cultures (harder to pump, harder to cool down, less diffusion in the medium). Besides, algal photobioreactors often rely on continuous cultures, which generates a significant risk of evolutionary escape in burdened yeast cultures. We suggest that lower-density yeast cultures may potentially benefit light penetration and controllability. Owing to a refined dynamic control strategy, the reduction in the final biomass could be compensated for by increased production per cell; the trade-off between these aspects will need to be balanced.

Another solution to the light penetration issue could be the use of “inverted” optogenetic systems, where genes for the production phase are activated in the dark, when light becomes scarce, i.e., when a certain cell density is reached [26]; however, this would hardly allow for dynamic control.

Finally, it may be possible to redesign or tune existing large-scale bioreactors. Most standard large-scale bioreactors are made of metal, which limits the use of light; however, internal illumination may overcome this issue (Figure 3(c2)). Internal illumination is usually achieved using optical fibers or light wells that reach inside the culture medium and transmit light collected outside into the bioreactor, or by using fluorescent lamps. LEDs are increasingly being used, as they offer the advantages of being able control the exact wavelength used in the medium [60] and even possibly deliver several wavelengths to control combinations of multiple optogenetic systems. However, such modifications may also conflict with other aspects of the bioreactor, such as the stirring mechanism (Figure 3(c2)). As an alternative to modifying the original design, one could also take advantage of existing plug devices—such as probes or external loops—which may be used to easily implement optogenetic control into existing bioreactors. For instance, during the synthesis of organic chemicals, photochemical reactors sometimes use external illumination chambers (flat panels or coils around a light source; see Figure 3(c5,c6)). Illumination chambers could enable the regulation of the optogenetic system based on the regulated flow of cells across the illuminated chamber, therefore tuning the amount of light received per cell per time. Such an approach may minimize the redesign of the bioreactors and thus may be a more feasible and economically advantageous first step to combine optogenetics and bioproduction at a large scale.

Finally, it is worth noting that modeling light distribution given bioreactor design [62], together with the optogenetic system, metabolic pathways and the bioprocess, will be key to optimizing bioproduction [63,64].

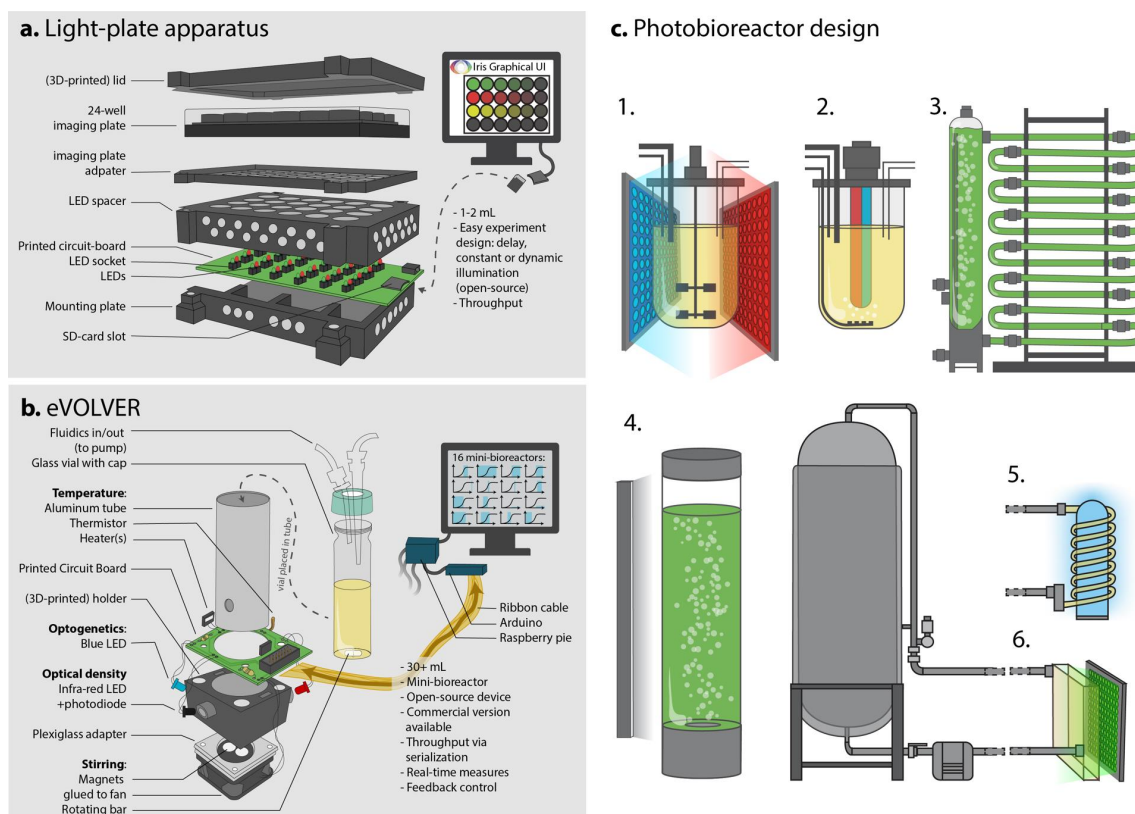


Figure 3. Instrumentation for optogenetic control and scale-up of bioproduction. (a). The light-plate apparatus [53] allows screening and simple experiments using small culture volumes in imaging plates and easily-programmable well-independent experiments. (b). The eVOLVER system [57] used as mini-bioreactors allows larger scale (30 mL) cultures and dynamic real-time control, as well as culture and illumination conditions screening thanks to its 16-unit array. (c). Bioreactor design to improve light penetration is crucial to successfully implement optogenetics as an induction method at the industrial scale. (1). Externally illuminated 10 L fermenter-type bioreactor using LED panels. Such systems offer the best control over every process parameter. (2). Internally illuminated 10 L bioreactor, which would allow better light penetration in a dense culture medium. Note the subsequent change in the gas-exchange strategy. (3). Stacked tubular photobioreactor, typically used for algal culture, increases the surface to volume ratio of large culture volumes to maximize light exposure. Up to thousands of liters of cultures can be handled, but temperature may be difficult to control and O₂ and CO₂ levels may fluctuate [61]. (4). Standard 250 L bubble column algal photobioreactor (illumination pane on the left) is considered an intermediate volume for algal cultivation. It is easy and cheap to set up and can be scaled-up, but has a relatively low surface to volume ratio. (6). Connection of an illumination chamber to a 1000 L bioreactor could allow illumination of flowing cells and reduce the need for large fermenter-type bioreactor redesign. Similarly, in (5), a loop passing out of the fermenter coils around a light source to enhance exposure to light.

4. Discussion and Conclusions

As metabolic engineering increasingly relies on the fine tuning of intricate endogenous and synthetic pathways, light is becoming the inducer of choice for bioproduction—as evidenced by the fact that many standard induction systems have already been connected to optogenetic systems. Light can be used to regulate metabolic valves in a similar manner to existing inducers used in bioproduction: by unleashing bioproduction after a growth phase. However, light can also be used to control cellular growth itself by regulating endogenous essential genes, or even used to actively and dynamically balance both bioproduction and growth using bidirectional optogenetic systems. Optogenetics enables increasingly simpler and more precise dynamic control over these processes,

and holds the promise of maximizing yields from industrial organisms engineered for complex pathways that frequently require multilevel regulation. The automation of this dynamic control via a cybergenetics approach seems the natural next step: under industrial conditions, every aspect of the culture is rigorously monitored and controlled, including temperature, pressure, pH, medium composition, dissolved oxygen and optical density. In addition to controlling these external cellular cues, cybergenetics aims to control the intricate internal behavior of cells based on a designated output (Figure 2d). This output can be the level of the final product detected using a biosensor, the cellular concentration of an enzyme or component of the pathway, or the burden that production represents—which can be detected using metabolite pool biosensors, stress-related promoters or directly monitoring the growth rate. Cybergenetic control could be achieved using various optogenetic systems, i.e., actuators, and biosensors that currently exist (with many others in development) [65]. The last element needed for cybergenetics is an appropriate control algorithm that takes into account and predicts the behavior of the cell, as well as how the culture density affects the diffusion of light—to better control the bioproduction *versus* growth trade-off. Various algorithms have been tested for the control of rather simple behaviors, such as the expression level of a fluorescent protein, and some of these already use optogenetic systems. Building models to represent burden will require extensive experimental fitting, and this may be facilitated by implementing machine learning strategies that can train from concrete experimental data [66]. Such models can easily be tested on smaller scales in the lab before being adapted to large culture volumes.

Many optogenetic devices have been developed in recent years to tackle every step of strain development; the real challenge now is to prove that optogenetics can truly be used in the context of bioproduction at the industrial scale in an economically sustainable manner. Thanks to their generally well-developed graphical user interfaces, small-scale devices that allow illumination of imaging plates will be convenient for the throughput testing of various media compositions, genetic designs and, most importantly, light illumination intensities or basic illumination patterns. Mini-bioreactors will enable the testing of larger volumes and fluidics inputs and outputs. They offer the capacity to control temperature and stirring and, crucially, to monitor growth and production in real-time—as well as implement feedback loop control based on such outputs. Mini-bioreactors that enable the use of optogenetics without critical light penetration issues will allow users to start to tune the dynamic control of the strain to optimize bioproduction. However, due to the opacity of high-density yeast cultures, light penetration becomes one major issue when shifting dynamic control from the small scale to the industrial scale. Although light panels or internal illumination strategies may be suitable solutions for bioreactors up to about 250 L, larger scale bioreactors will require further modeling, redesign or tuning, though existing algal photobioreactors or photochemistry may provide inspiration.

The use of light as an inducer can facilitate real-time dynamic control strategies. The first applications of light to bioproduction—as well as the optogenetic instruments presented here—show that although challenges remain to be solved, the application of optogenetics to bioproduction holds the promise of maximizing yields in bioproduction; promise that can be expected to be fulfilled in the years to come.

Author Contributions: Writing—original draft preparation, S.P., A.B., M.L.B., T.L., G.T. and P.H.; writing—review and editing, S.P., P.H. All authors have read and agreed to the published version of the manuscript.

Funding: This research was funded by the European research council grant ERC-SmartCells (724813), the H2020 FET-OPEN grant COSYBIO (766840) and from the grants ANR-16-CE12-0025-01, ANR-11-LABX-0038 and ANR-10-IDEX-0001-02 of the French national research agency (ANR).

Conflicts of Interest: The authors have no conflict of interest to declare.

References

1. Pham, J.V.; Yilma, M.A.; Feliz, A.; Majid, M.T.; Maffetone, N.; Walker, J.R.; Kim, E.; Cho, H.J.; Reynolds, J.M.; Song, M.C.; et al. A review of the microbial production of bioactive natural products and biologics. *Front. Microbiol.* **2019**, *10*, 1–27. [[CrossRef](#)]
2. Germann, S.M.; Baallal Jacobsen, S.A.; Schneider, K.; Harrison, S.J.; Jensen, N.B.; Chen, X.; Stahlhut, S.G.; Borodina, I.; Luo, H.; Zhu, J.; et al. Glucose-based microbial production of the hormone melatonin in yeast *Saccharomyces cerevisiae*. *Biotechnol. J.* **2016**, *11*, 717–724. [[CrossRef](#)] [[PubMed](#)]
3. Gerngross, T.U. Advances in the production of human therapeutic proteins in yeasts and filamentous fungi. *Nat. Biotechnol.* **2004**, *22*, 1409–1414. [[CrossRef](#)] [[PubMed](#)]
4. van Dijk, J.M.; Hecker, M. *Bacillus subtilis*: From soil bacterium to super-secreting cell factory. *Microb. Cell Fact.* **2013**, *12*, 3. [[CrossRef](#)] [[PubMed](#)]
5. Grewal, P.S.; Modavi, C.; Russ, Z.N.; Harris, N.C.; Dueber, J.E. Bioproduction of a betalain color palette in *Saccharomyces cerevisiae*. *Metab. Eng.* **2018**, *45*, 180–188. [[CrossRef](#)] [[PubMed](#)]
6. Buijs, N.A.; Siewers, V.; Nielsen, J. Advanced biofuel production by the yeast *saccharomyces cerevisiae*. *Curr. Opin. Chem. Biol.* **2013**, *17*, 480–488. [[CrossRef](#)]
7. Paddon, C.J.; Westfall, P.J.; Pitera, D.J.; Benjamin, K.; Fisher, K.; McPhee, D.; Leavell, M.D.; Tai, A.; Main, A.; Eng, D.; et al. High-level semi-synthetic production of the potent antimalarial artemisinin. *Nature* **2013**, *496*, 528–532. [[CrossRef](#)]
8. Luo, X.; Reiter, M.A.; d’Espaux, L.; Wong, J.; Denby, C.M.; Lechner, A.; Zhang, Y.; Grzybowski, A.T.; Harth, S.; Lin, W.; et al. Complete biosynthesis of cannabinoids and their unnatural analogues in yeast. *Nature* **2019**, *567*, 123–126. [[CrossRef](#)]
9. Srinivasan, P.; Smolke, C.D. Biosynthesis of medicinal tropane alkaloids in yeast. *Nature* **2020**, *585*, 614–619. [[CrossRef](#)]
10. Menart, V.; Jevševar, S.; Vilar, M.; Trobiš, A.; Pavko, A. Constitutive versus thermoinducible expression of heterologous proteins in *Escherichia coli* based on strong PR,PL promoters from phage lambda. *Biotechnol. Bioeng.* **2003**, *83*, 181–190. [[CrossRef](#)]
11. Chou, C.-H.; Aristidou, A.A.; Meng, S.-Y.; Bennett, G.N.; San, K.-Y. Characterization of a pH-inducible promoter system for high-level expression of recombinant proteins in *Escherichia coli*. *Biotechnol. Bioeng.* **1995**, *47*, 186–192. [[CrossRef](#)] [[PubMed](#)]
12. Pudasaini, A.; El-Arab, K.K.; Zoltowski, B.D. LOV-based optogenetic devices: Light-driven modules to impart photoregulated control of cellular signaling. *Front. Mol. Biosci.* **2015**, *2*, 1–15. [[CrossRef](#)] [[PubMed](#)]
13. Yizhar, O.; Fenno, L.E.; Davidson, T.J.; Mogri, M.; Deisseroth, K. Optogenetics in Neural Systems. *Neuron* **2011**, *71*, 9–34. [[CrossRef](#)] [[PubMed](#)]
14. Izquierdo, E.; Quinkler, T.; De Renzis, S. Guided morphogenesis through optogenetic activation of Rho signalling during early *Drosophila* embryogenesis. *Nat. Commun.* **2018**, *9*, 1–13. [[CrossRef](#)] [[PubMed](#)]
15. Johnson, H.E.; Toettcher, J.E. Signaling Dynamics Control Cell Fate in the Early *Drosophila* Embryo. *Dev. Cell* **2019**, *48*, 361–370. [[CrossRef](#)]
16. Valon, L.; Etoc, F.; Remorino, A.; Di Pietro, F.; Morin, X.; Dahan, M.; Coppey, M. Predictive Spatiotemporal Manipulation of Signaling Perturbations Using Optogenetics. *Biophys. J.* **2015**, *109*, 1785–1797. [[CrossRef](#)]
17. Liu, Z.; Zhang, J.; Jin, J.; Geng, Z.; Qi, Q.; Liang, Q. Programming bacteria with light-sensors and applications in synthetic biology. *Front. Microbiol.* **2018**, *9*, 2692. [[CrossRef](#)]
18. Harrigan, P.; Madhani, H.D.; El-Samad, H. Real-Time Genetic Compensation Defines the Dynamic Demands of Feedback Control. *Cell* **2018**, *175*, 877–886. [[CrossRef](#)]
19. Ohlendorf, R.; Vidavski, R.R.; Eldar, A.; Moffat, K.; Möglich, A. From dusk till dawn: One-plasmid systems for light-regulated gene expression. *J. Mol. Biol.* **2012**, *416*, 534–542. [[CrossRef](#)]
20. Shimizu-Sato, S.; Huq, E.; Tepperman, J.M.; Quail, P.H. A light-switchable gene promoter system. *Nat. Biotechnol.* **2002**, *20*, 1041–1044. [[CrossRef](#)]
21. Motta-Mena, L.B.; Reade, A.; Mallory, M.J.; Glantz, S.; Weiner, O.D.; Lynch, K.W.; Gardner, K.H. An optogenetic gene expression system with rapid activation and deactivation kinetics. *Nat. Chem. Biol.* **2014**, *10*, 196–202. [[CrossRef](#)] [[PubMed](#)]

22. Tabor, J.J.; Levskaya, A.; Voigt, C.A. Multichromatic control of gene expression in *Escherichia coli*. *J. Mol. Biol.* **2011**, *405*, 315–324. [[CrossRef](#)] [[PubMed](#)]
23. Kennedy, M.J.; Hughes, R.M.; Peteya, L.A.; Schwartz, J.W.; Ehlers, M.D.; Tucker, C.L. Rapid blue-light-mediated induction of protein interactions in living cells. *Nat. Methods* **2010**, *7*, 973–975. [[CrossRef](#)] [[PubMed](#)]
24. Taslimi, A.; Vrana, J.D.; Chen, D.; Borinskaya, S.; Mayer, B.J.; Kennedy, M.J.; Tucker, C.L. An optimized optogenetic clustering tool for probing protein interaction and function. *Nat. Commun.* **2014**, *5*, 1–9. [[CrossRef](#)]
25. Kolar, K.; Knobloch, C.; Stork, H.; Žnidarič, M.; Weber, W. OptoBase: A Web Platform for Molecular Optogenetics. *ACS Synth. Biol.* **2018**, *7*, 1825–1828. [[CrossRef](#)]
26. Lalwani, M.A.; Ip, S.S.; Carrasco-López, C.; Day, C.; Zhao, E.M.; Kawabe, H.; Avalos, J.L. Optogenetic control of the lac operon for bacterial chemical and protein production. *Nat. Chem. Biol.* **2020**, 1–9. [[CrossRef](#)]
27. Romano, E.; Baumschlager, A.; Akmeriç, E.B.; Palanisamy, N.; Houmani, M.; Schmidt, G.; Öztürk, M.A.; Ernst, L.; Khammash, M.; Di Ventura, B. An inducible AraC that responds to blue light instead of arabinose. *bioRxiv* **2020**. [[CrossRef](#)]
28. Raghavan, A.R.; Salim, K.; Yadav, V.G. Optogenetic control of heterologous metabolism in *E. coli*. *ACS Synth. Biol.* **2020**, *9*, 2291–2300. [[CrossRef](#)]
29. Baumschlager, A.; Aoki, S.K.; Khammash, M. Dynamic Blue Light-Inducible T7 RNA Polymerases (Opto-T7RNAPs) for Precise Spatiotemporal Gene Expression Control. *ACS Synth. Biol.* **2017**, *6*, 2157–2167. [[CrossRef](#)]
30. Kawano, F.; Suzuki, H.; Furuya, A.; Sato, M. Engineered pairs of distinct photoswitches for optogenetic control of cellular proteins. *Nat. Commun.* **2015**, *6*, 1–8. [[CrossRef](#)]
31. Han, T.; Chen, Q.; Liu, H. Engineered Photoactivatable Genetic Switches Based on the Bacterium Phage T7 RNA Polymerase. *ACS Synth. Biol.* **2017**, *6*, 357–366. [[CrossRef](#)] [[PubMed](#)]
32. Zhao, E.M.; Zhang, Y.; Mehl, J.; Park, H.; Lalwani, M.A.; Toettcher, J.E.; Avalos, J.L. Optogenetic regulation of engineered cellular metabolism for microbial chemical production. *Nature* **2018**, *555*, 683–687. [[CrossRef](#)] [[PubMed](#)]
33. Benzinger, D.; Khammash, M. Pulsatile inputs achieve tunable attenuation of gene expression variability and graded multi-gene regulation. *Nat. Commun.* **2018**, *9*, 1–10. [[CrossRef](#)] [[PubMed](#)]
34. Hueso-Gil, A.; Nyerges, Á.; Pál, C.; Calles, B.; De Lorenzo, V. Multiple-Site Diversification of Regulatory Sequences Enables Interspecies Operability of Genetic Devices. *ACS Synth. Biol.* **2020**, *9*, 104–114. [[CrossRef](#)] [[PubMed](#)]
35. Castillo-Hair, S.M.; Baerman, E.A.; Fujita, M.; Igoshin, O.A.; Tabor, J.J. Optogenetic control of *Bacillus subtilis* gene expression. *Nat. Commun.* **2019**, *10*, 1–11. [[CrossRef](#)] [[PubMed](#)]
36. Duplus-Bottin, H.; Spichty, M.; Triqueneaux, G.; Place, C.; Mangeot, P.E.; Ohlmann, T.; Vittoz, F.; Yvert, G. A monogenic and fast-responding Light-Inducible Cre recombinase as a novel optogenetic switch. *bioRxiv* **2020**. [[CrossRef](#)]
37. Hasenjäger, S.; Trauth, J.; Hepp, S.; Goenrich, J.; Essen, L.-O.; Taxis, C. Optogenetic Downregulation of Protein Levels with an Ultrasensitive Switch. *ACS Synth. Biol.* **2019**, *8*, 1026–1036. [[CrossRef](#)]
38. Senoo, S.; Tandar, S.T.; Kitamura, S.; Toya, Y.; Shimizu, H. Light-inducible flux control of triosephosphate isomerase on glycolysis in *Escherichia coli*. *Biotechnol. Bioeng.* **2019**, *116*, 3292–3300. [[CrossRef](#)]
39. Tandar, S.T.; Senoo, S.; Toya, Y.; Shimizu, H. Optogenetic switch for controlling the central metabolic flux of *Escherichia coli*. *Metab. Eng.* **2019**, *55*, 68–75. [[CrossRef](#)]
40. Zhao, E.M.; Suek, N.; Wilson, M.Z.; Dine, E.; Pannucci, N.L.; Gitai, Z.; Avalos, J.L.; Toettcher, J.E. Light-based control of metabolic flux through assembly of synthetic organelles. *Nat. Chem. Biol.* **2019**, *15*, 589–597. [[CrossRef](#)]
41. Ding, Q.; Ma, D.; Liu, G.Q.; Li, Y.; Guo, L.; Gao, C.; Hu, G.; Ye, C.; Liu, J.; Liu, L.; et al. Light-powered *Escherichia coli* cell division for chemical production. *Nat. Commun.* **2020**, *11*, 1–14. [[CrossRef](#)] [[PubMed](#)]
42. Ceroni, F.; Boo, A.; Furini, S.; Gorochoowski, T.E.; Borkowski, O.; Ladak, Y.N.; Awan, A.R.; Gilbert, C.; Stan, G.B.; Ellis, T. Burden-driven feedback control of gene expression. *Nat. Methods* **2018**, *15*, 387–393. [[CrossRef](#)] [[PubMed](#)]

43. Boo, A.; Ellis, T.; Stan, G.B. Host-aware synthetic biology. *Curr. Opin. Syst. Biol.* **2019**, *14*, 66–72. [[CrossRef](#)]
44. Gasser, B.; Saloheimo, M.; Rinas, U.; Dragosits, M.; Rodríguez-Carmona, E.; Baumann, K.; Giuliani, M.; Parrilli, E.; Branduardi, P.; Lang, C.; et al. Protein folding and conformational stress in microbial cells producing recombinant proteins: A host comparative overview. *Microb. Cell Fact.* **2008**, *7*, 11. [[CrossRef](#)] [[PubMed](#)]
45. Carrasco-López, C.; García-Echauri, S.A.; Kichuk, T.; Avalos, J.L. Optogenetics and biosensors set the stage for metabolic cybergenetics. *Curr. Opin. Biotechnol.* **2020**, *65*, 296–309. [[CrossRef](#)] [[PubMed](#)]
46. Xu, P. Production of chemicals using dynamic control of metabolic fluxes. *Curr. Opin. Biotechnol.* **2018**, *53*, 12–19. [[CrossRef](#)] [[PubMed](#)]
47. Fiore, G.; Perrino, G.; Di Bernardo, M.; Di Bernardo, D. In Vivo Real-Time Control of Gene Expression: A Comparative Analysis of Feedback Control Strategies in Yeast. *ACS Synth. Biol.* **2016**, *5*, 154–162. [[CrossRef](#)]
48. Lugagne, J.B.; Sosa Carrillo, S.; Kirch, M.; Köhler, A.; Batt, G.; Hersen, P. Balancing a genetic toggle switch by real-time feedback control and periodic forcing. *Nat. Commun.* **2017**, *8*, 1671. [[CrossRef](#)]
49. Uhlenendorf, J.; Miermont, A.; Delaveau, T.; Charvin, G.; Fages, F.; Bottani, S.; Batta, G.; Hersen, P. Long-term model predictive control of gene expression at the population and single-cell levels. *Proc. Natl. Acad. Sci. USA* **2012**, *109*, 14271–14276. [[CrossRef](#)]
50. Miliás-Argeitis, A.; Summers, S.; Stewart-Ornstein, J.; Zuleta, I.; Pincus, D.; El-Samad, H.; Khammash, M.; Lygeros, J. In silico feedback for in vivo regulation of a gene expression circuit. *Nat. Biotechnol.* **2011**, *29*, 1114–1116. [[CrossRef](#)]
51. Miliás-Argeitis, A.; Rullan, M.; Aoki, S.K.; Buchmann, P.; Khammash, M. Automated optogenetic feedback control for precise and robust regulation of gene expression and cell growth. *Nat. Commun.* **2016**, *7*, 1–11. [[CrossRef](#)]
52. Looser, V.; Bruhlmann, B.; Bumbak, F.; Stenger, C.; Costa, M.; Camattari, A.; Fotiadis, D.; Kovar, K. Cultivation strategies to enhance productivity of *Pichia pastoris*: A review. *Biotechnol. Adv.* **2014**, *33*, 1177–1193. [[CrossRef](#)] [[PubMed](#)]
53. Gerhardt, K.P.; Olson, E.J.; Castillo-Hair, S.M.; Hartsough, L.A.; Landry, B.P.; Ekness, F.; Yokoo, R.; Gomez, E.J.; Ramakrishnan, P.; Suh, J.; et al. An open-hardware platform for optogenetics and photobiology. *Sci. Rep.* **2016**, *6*, 1–13. [[CrossRef](#)] [[PubMed](#)]
54. Bugaj, L.J.; Lim, W.A. High-throughput multicolor optogenetics in microwell plates. *Nat. Protoc.* **2019**, *14*, 2205–2228. [[CrossRef](#)] [[PubMed](#)]
55. Wang, H.; Yang, Y.T. Mini Photobioreactors for in Vivo Real-Time Characterization and Evolutionary Tuning of Bacterial Optogenetic Circuit. *ACS Synth. Biol.* **2017**, *6*, 1793–1796. [[CrossRef](#)] [[PubMed](#)]
56. Olson, E.J.; Hartsough, L.A.; Landry, B.P.; Shroff, R.; Tabor, J.J. Characterizing bacterial gene circuit dynamics with optically programmed gene expression signals. *Nat. Methods* **2014**, *11*, 449–455. [[CrossRef](#)]
57. Wong, B.G.; Mancuso, C.P.; Kiriakov, S.; Bashor, C.J.; Khalil, A.S. Precise, automated control of conditions for high-throughput growth of yeast and bacteria with eVOLVER. *Nat. Publ. Gr.* **2018**, *36*, 614–623. [[CrossRef](#)]
58. Steel, H.; Habgood, R.; Kelly, C.; Papachristodoulou, A. In situ characterisation and manipulation of biological systems with Chi.Bio. *PLoS Biol.* **2020**, 1–12. [[CrossRef](#)]
59. Crater, J.S.; Lievens, J.C. Scale-up of industrial microbial processes. *FEMS Microbiol. Lett.* **2018**, *365*, 1–5. [[CrossRef](#)]
60. Chang, J.-S.; Show, P.-L.; Ling, T.-C.; Chen, C.-Y.; Ho, S.-H.; Tan, C.-H.; Nagarajan, D.; Phong, W.-N. Photobioreactors. In *Current Developments in Biotechnology and Bioengineering: Bioprocesses, Bioreactors and Controls*; Elsevier: Amsterdam, The Netherlands, 2017; pp. 313–352.
61. Płaczek, M.; Patyna, A.; Witzak, S. Technical evaluation of photobioreactors for microalgae cultivation. In Proceedings of the E3S Web of Conferences, Szczyrk, Poland, 25–27 October 2017; Volume 19.
62. Gernigon, V.; Chekroun, M.A.; Cockx, A.; Guiraud, P.; Morchain, J. How Mixing and Light Heterogeneity Impact the Overall Growth Rate in Photobioreactors. *Chem. Eng. Technol.* **2019**, *42*, 1663–1669. [[CrossRef](#)]
63. Xu, L.; Weathers, P.J.; Xiong, X.R.; Liu, C.Z. Microalgal bioreactors: Challenges and opportunities. *Eng. Life Sci.* **2009**, *9*, 178–189. [[CrossRef](#)]
64. Posten, C. Design principles of photo-bioreactors for cultivation of microalgae. *Eng. Life Sci.* **2009**, *9*, 165–177. [[CrossRef](#)]

65. Rogers, J.K.; Church, G.M. Genetically encoded sensors enable real-time observation of metabolite production. *Proc. Natl. Acad. Sci. USA* **2016**, *113*, 2388–2393. [[CrossRef](#)] [[PubMed](#)]
66. Zhang, J.; Petersen, S.D.; Radivojevic, T.; Ramirez, A.; Pérez-Manríquez, A.; Abeliuk, E.; Sánchez, B.J.; Costello, Z.; Chen, Y.; Fero, M.J.; et al. Combining mechanistic and machine learning models for predictive engineering and optimization of tryptophan metabolism. *Nat. Commun.* **2020**, *11*, 4880. [[CrossRef](#)]

Publisher’s Note: MDPI stays neutral with regard to jurisdictional claims in published maps and institutional affiliations.



© 2020 by the authors. Licensee MDPI, Basel, Switzerland. This article is an open access article distributed under the terms and conditions of the Creative Commons Attribution (CC BY) license (<http://creativecommons.org/licenses/by/4.0/>).

4. CHAPTER 1 – Setting up optogenetic devices

In this first chapter, we will discuss the use of optogenetic devices for various culture scales, for different uses, with a particular emphasis on those I adapted from the literature and built during my PhD. This chapter expands on the diverse types of optogenetic devices presented in the review placed just before this chapter¹.

Overview

Optogenetics can be used for a wide range of biological studies. It can be for the characterization of the optogenetics system itself, characterization of a strain, screening of different strains, or different illumination conditions, as well as simply illuminating larger volumes for the actual bioproduction process. All those steps require specific tools.

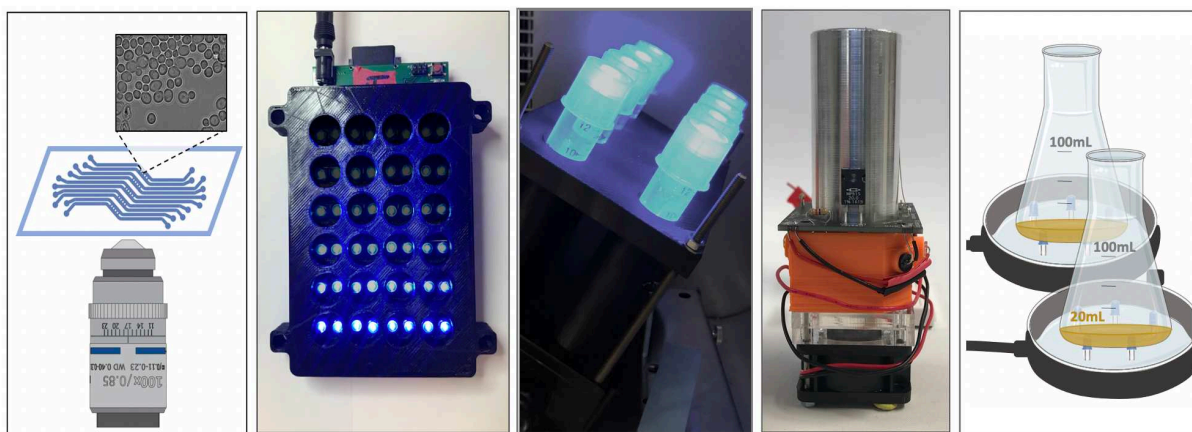


Figure 24. **Optogenetic devices** developed and used during my PhD. From left to right: using microfluidics to investigate single behavior; the OptoBox to cultivate small culture volumes and screen for illumination conditions; the OptoTubes, for overnight cultures and other simple tests; the eVOLVER, automated culture platform with higher illumination control, and real-time feedback; and the OptoFlasks, for larger culture volume in flasks, classical container for bioproduction studies. Each device has its own culture characteristics, illumination modalities, and specific uses.

In the context of bioproduction, different devices allow for different usages, and starting from the beginning at different scales is important for bioproduction process development. Microfluidics can be used to characterize an optogenetic system as well as production dynamics at the single-cell level. Strain development often requires the need for screening for optimal strain behavior, such that small-scale arrays are required. Besides, screening for appropriate illumination conditions requires the possibility of testing many conditions at the same time and arrays of culture devices are convenient, at the small scale in illuminating imaging plates or simple culture tubes. Then, larger culture volumes (flasks) are needed to obtain high biomasses for actual product quantification using HPLC analyses for example. From then, arrays of small bioreactors are needed to begin to start scaling-up the bioproduction process and start anticipating scaling issues, some of which can be specific to optogenetics. And finally, large-scale processes require specific equipment to be able to bring light at the heart of massive bioreactors. In definitive, it is important to test strains at different scales to get as close as possible to industrial settings while keeping flexibility in prototyping culture conditions and strain development.

In the following parts of this chapter, we will address different types of equipment and optogenetic devices that were adapted from other papers, developed in the lab (Fig. 24), and are mentioned in diverse papers to give an overview of the possibilities and tools put together during my PhD. We will address what usage can be made from each device, how it is built, how it works, as well as its advantages and drawbacks. This represents a major output of my PhD: joining the world of synthetic biology to the world of instrumentation for optogenetically controlled bioproduction.

4.1. Microfluidics

Microscopy and microfluidics experiments allow for powerful single-cell analyses. Those analyses can give information regarding the dynamics of the activation of the optogenetic system, the physiology of the cells (check for burden, size, aspect), and also production dynamics given activation as well as ideas on how to manage resource allocation trade-offs, by measuring also growth rate. Besides, with a single-cell approach, it can give clues about population dynamics, *i.e.*, cell activation heterogeneity or potential evolutionary escapes.

Control approaches have recently benefited a lot from microfluidics. In Rullan *et al.* 2018², a whole control platform was developed with optogenetic strains to study transcriptional dynamics as well as control cell expression in real-time to reduce cell-to-cell heterogeneity (noise, or expression stochasticity). In our lab also, the cybersco.py setup³ was developed for diverse application, especially “smart microscopy”, including the use of optogenetic control (see appendix 8.3). Those approaches are usually hybridized with mechanistic cell models that allow for predicting cell trajectories as well as the illumination intensity or pattern required.

The setup required to carry out optogenetics using a microscope is basic and every epifluorescence microscope can theoretically perform optogenetics. Simply, the blue LED of the lamp (often the one used for GFP image acquisition) is used to activate the optogenetic system. Illumination is usually very short because the LED intensity is very high with microscope lamps. Illumination can also be used to target specific cells in the field of view (after image segmentation) in order to specifically control them and make spatial studies, studying population dynamics and nutrient diffusion. Although quite accessible for us in the lab, I found that not all microfluidics setups allow for perfect characterization: in our case, population movements in the chip made quantifications more challenging than expected, and we decided not to investigate more with microfluidics, and use larger-scales illumination equipment.

4.2. Imaging Plates (OptoBox)

Imaging plates (or well plates) are standard lab equipment: they consist of arrays of wells that can contain low volumes of various solutions and biological material. They are mostly used for the throughput they allow for: one sample can be spread in 4, 16, 24, 96 (or even more) wells, while each receives a unique treatment. To adapt such culture devices for optogenetics, stands containing controllable LEDs have been developed. **Using imaging plate**

illuminating devices (Fig. 25) is particularly convenient for screening strains and screening illumination conditions. With such low volumes, cultures are easy to set up and imaging plates are well-suited to interact with various types of lab robots (Opentron, Tecan, etc.).

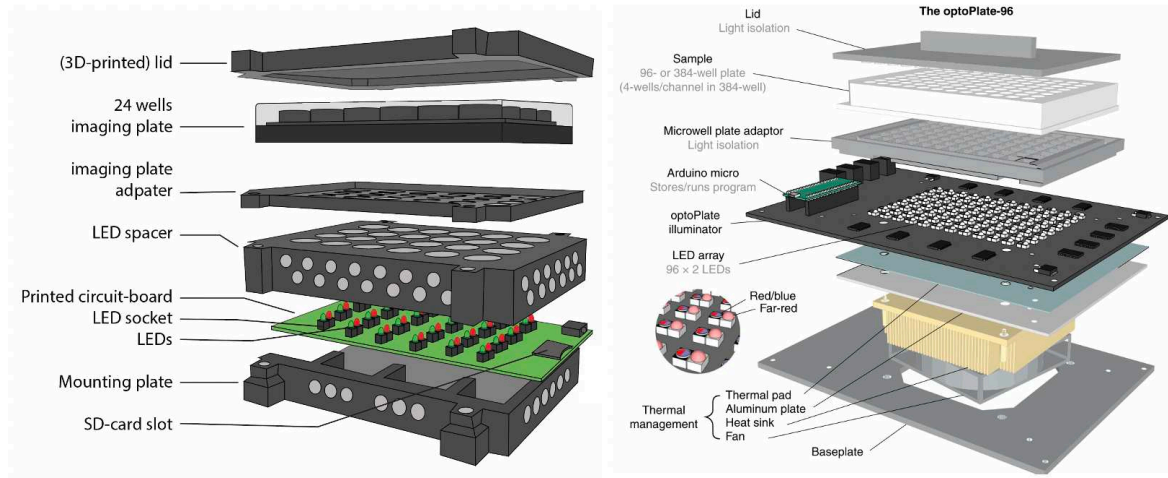


Figure 25. **Imaging plate illuminating devices.** (Left): the OptoBox⁴ we use in the Lab (24 well plates), is a DIY device, where every part can be easily 3D printed, the printed circuit board ordered, and LEDs chosen and adjusted. All parts are held together via screws and placed in a shaking incubator. (Right): Another more recent design for 96 well plates⁵, also claiming to be DIY, with a heat sink at the base.

Do-it-Yourself (DIY) methods have been promoted in many papers, as a way to build such illumination devices, and some companies are starting to offer commercial versions of illumination devices (Fig. 28). In brief, those devices are often composed of a holder, an array of LEDs connected to a programmable controller (an Arduino for example), and adapter for the imaging plate to fit in, and a lid. Heat dissipation has to be thought out in the design and using opaque imaging plates is important to prevent light from leaking from one well to another.

The OptoBox (Fig. 25-Left, 26) was the first optogenetic device developed in the lab. From the original paper⁴, the printed circuit boards (PCB) were ordered with LED sockets and blue LEDs. LED sockets are soldered by hand and LEDs are slid in (sockets allow for easily replacing or changing LEDs in each well). There are two LEDs per well: this is convenient, to use various optogenetic systems at the same time, or to control some optogenetic systems that are activated or deactivated by two different wavelengths. The 3D-printable parts were slightly rescaled, so they fit with our 3D printer, and once printed, all parts were assembled (Fig. 26). The PCB circuit needs to be “burnt” to be functional and LEDs were calibrated so that they all emit the same light intensity for a same input value from the software (Protocol 8.9.6). For this, we used a power meter, and each LED is independently tested. A calibration file is then generated, included in the SD card, and used for every subsequent experiment.

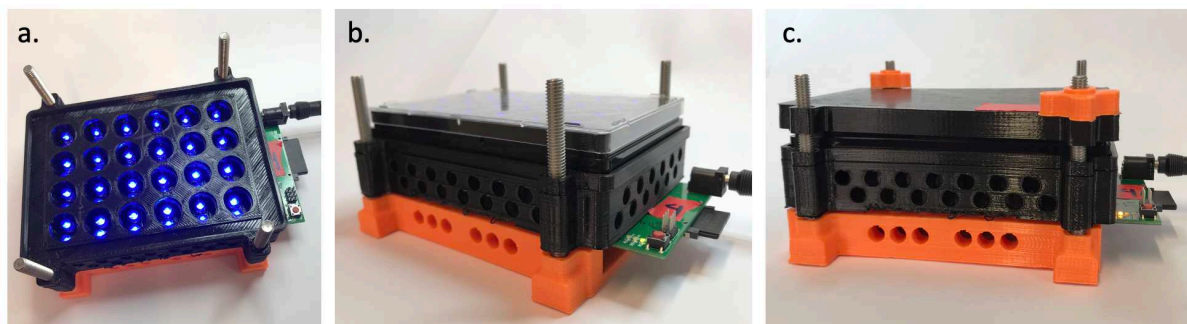


Figure 26. **The OptoBox**, built in our lab, adapted from Gerhardt et al. 2016⁴. (a.) Empty OptoBox, with the holder, printed circuit board attached to the led spacer (all blue LEDs turned on) and the plate adaptor onto which the opaque 24-well plate is fit (b.). (c.) A lid is placed on top of the imaging plate and held tight with a bolt screwed to the long screws. A program is loaded directly on the SD card plugged into the PCB (b.). Once all set, the box is placed and secured in a shaking incubator, where it can be plugged to 5V and the experiment starts. See also (Protocol 8.9.6).

Controllability is a big stake in developing such devices: for this, they not only need to be highly controllable *per se* (any type of illumination pattern and intensity in time), but also be user friendly, and adaptable to many different types of optogenetic systems (requiring different wavelengths). Therefore, the development of the software to control each LED in an independent manner is crucial. With the OptoBox, for example, the “Iris” online software was developed to independently or dependently program the two LEDs of each well with illumination patterns across the array (varying intensity per well for example) or illumination patterns in time: linear increase or decrease, switches, regular pulses, and more complex patterns. From this software, the program can be downloaded and copied onto the SD card that is then plugged into the device to carry out the program.

Plate-readers are another promising tool to work at this culture scale. The aforementioned systems do not read any output, such that they have to be used with other instruments, like cytometers or microscopes, to measure desired outputs (a fluorescent protein, or to detect a specific phenotype) at the end of the illumination time. Although the financial investment required for a plate-reader is non-negligible compared to imaging-plate illuminating devices, the possibility to activate optogenetically cells in a plate-reader is very attractive for the real-time outputs it can yield in terms of growth or fluorescence level. It makes this approach almost closer to what one can do using microfluidics, with high controllability regarding the light input, and extensive output monitoring. Two possibilities exist today. One is to repurpose a module of the TECAN plate-reader to illuminate samples: using the injection tube (controlled via Arduinos) which is linked to different LEDs via an optical fiber⁶ (Fig. 27-Left). Another more recent method is to build on the optoPlate-96 mentioned earlier (Fig. 25-Right) and add an “optoReader” module⁷ (Fig. 27-Right). This device allows for optical density and fluorescence measurements, besides being able to illuminate with up to 3 wavelengths.

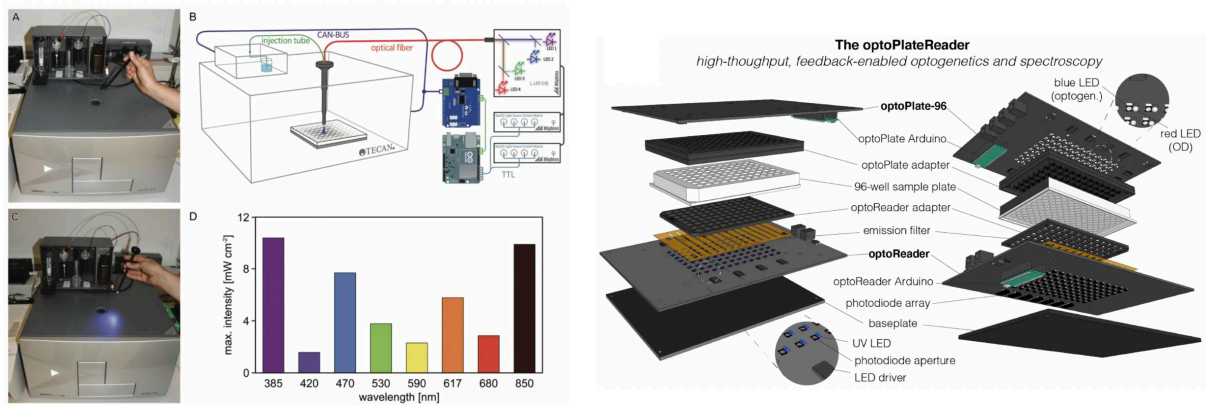


Figure 27. Using **plate-readers** for optogenetic studies is very attractive for both the control of the illumination input and the fluorescent and growth output that can be read in real-time. **Left:** Repurposing the injection module of a TECAN plate-reader⁶ to illuminate wells independently. For this, an optical fiber was inserted in the liquid injector. **Right:** building on the Opto-Plate-96⁵, the optoReader module allows for real-time measures of optical density and fluorescence.

Commercial versions of imaging-plate illuminating devices do exist (Fig. 28). Some have been used in recent papers⁸ but their use remains scarce. So far in the microbial optogenetics field, which is after all, still a relatively new field, it seems that labs still prefer to develop their own devices and software. Some companies offer similar devices, few with user-friendly software allowing for complex rather independent illumination sequences (Cetoni LED array). Some companies spun out of labs after strong publications to commercialize optogenetic devices (like eVOLVER from Wong *et al.* 2018⁹ who founded fynchbio – see section 4.7). Labs are still leaders in producing devices that match their precise needs. Companies usually “happen” or catch up afterward.



Figure 28. Available **commercial versions** of imaging-plate illuminating devices. Most have general purpose controller, resulting in all LEDs behaving the same, while some come with sophisticated software enabling complex and well-specific illumination patterns.

4.3. Tubes Arrays (OptoTubes)

Simple cultures tubes can be arranged in arrays and used for microbial cultures, usually handling 2-5mL cultures. They are often used for overnight precultures for other types of experiments. Sometimes, a culture needs to be kept in light, if an essential gene is under optogenetic control for example. Besides simple cultures, this scale can also be used to characterize optogenetic systems and investigate the dynamics of gene circuits¹⁰.

Illumination is often carried out from the bottom of the tubes. The design consists in LED arrays, where LEDs are regularly positioned at the bottom of a holder that can accommodate the culture tubes. One or multiple LEDs can be placed for either multiple optogenetic systems or some with reversible dynamics like in Olson *et al.* 2014¹⁰ (Fig. 29) where the CcaS/CcaR optogenetic system is activated in green light and deactivated in red light while the Cph8/OmpR system is deactivated also with red light but active in the dark. The LED array can then be controlled using a controller such as an Arduino. As LEDs intensities may vary between Arduino pins and between LEDs, a calibration can be required.

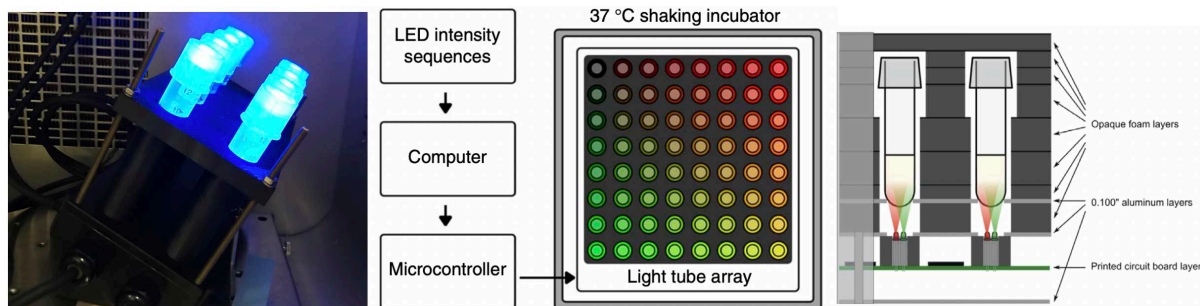


Figure 29. **OptoTubes** built in our lab (left), is a device similar in principle to the imaging-plate illuminating systems, encompassing a LEDs-carrying stand and a holder to place the tubes to be illuminated. **Middle-right: Light Tube Array**¹⁰ allowing for even more throughput. While we mostly used our OptoTubes to illuminate simple cultures or prepare them for experiments, some larger-scale designs allow for high-throughput studies, but also require more sophisticated control systems.

Assembly of the device is easy: soldering, 3D printing and assembling are core simple skills. In our lab, I built a system with 8 LEDs for an 8-tube holder (Fig. 30). With few samples and very simple illumination patterns (continuous illuminating at maximal intensity most often), LEDs are directly connected to an Arduino, where one single pin controls one single LED, each controlled by coding the Arduino in C++. If the required number of illuminated tubes increases and with for more complex experimental design, a real interface might be needed, and a software developed. As we will see later on, programmable interfaces such as Node-Red are great to deal with Arduino automation. Besides, the Arduino pin number might be insufficient, given that not all pins can support intermediate illumination values (PWM, see next paragraph), hence the use of an Arduino Due in our OptoTubes design.

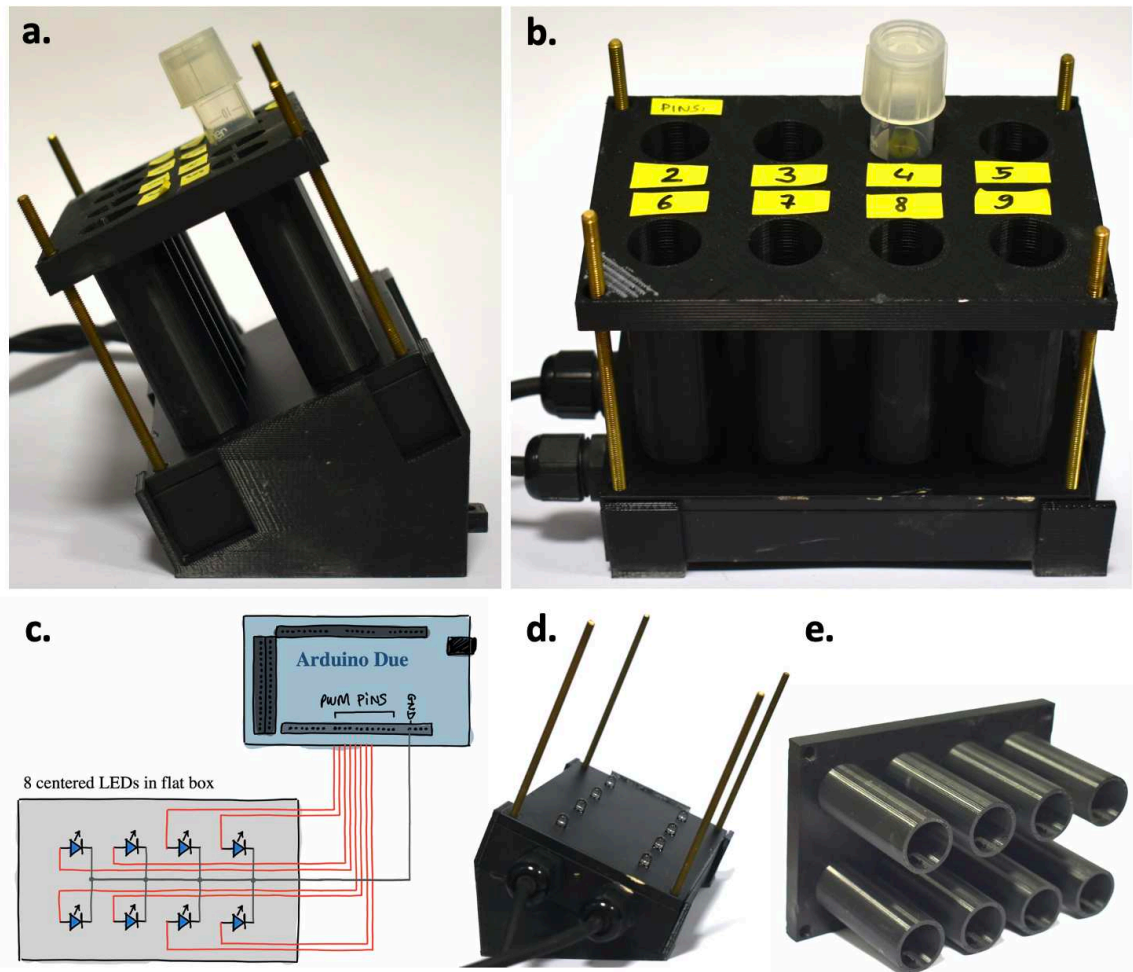


Figure 30. *The OptoTubes developed in the Lab. (a.) Side view, (b.) front view. (c.) Electronic connections required to control 8 LEDs with intermediate intensities. Here, each LED can be independently controlled by the Arduino onto which a code has been uploaded for a specific experiment. (d.) stand and flat box containing the LEDs on top of which the 3D-printed tube holder (e.) is placed.*

Sidenote on the Arduino. Arduinos are simple controllers that allow neophytes to easily control small electronic equipment. It is an open-source project and company that sells different Arduino boards (the most widely known is the Arduino UNO) that all function on the same basis. With a rudimentary knowledge of C++, the board can be programmed with the Arduino IDE installed on a computer, to control various pins of the Arduino. Once this is done, the board can then function independently from the computer and run the code. Pins can have many usages but, most basically, D2 to D13 digital pins are used to send a signal and control something, and A0 to A5 analog pins are used to receive and measure a signal (Fig. 31). Among digital pins used to send signals, a few sustain PWM (pulse width modulation). With this, an analog signal can be approximated, making it possible to send signals that are not only ON or OFF, but carry intermediate levels. This is especially important to control a LED for illumination at intermediate intensities.

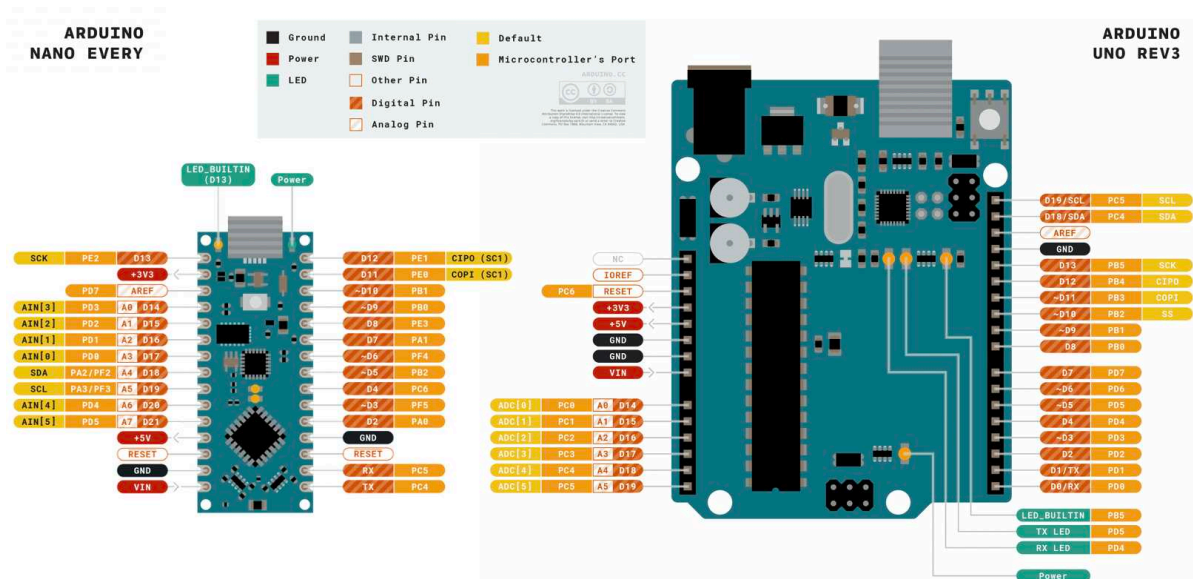


Figure 31. *Arduino Nano* (left) has 4 PWM pins, allowing to control 4 LEDs with intermediate intensities. *Arduino Uno* (right) has 6 PWM pins. Pinouts are represented - from docs.arduino.cc. PWM Pins are marked with (~): those pins are key to allow intermediate intensities, instead of simple digital pins allowing only to control the ON or OFF state of a LED. *Arduino* libraries exist however to adapt to some extent PWM to any simple digital pin (e.g., *SoftPWM Library*).

4.4. (Opto)Flasks

Shake flasks (Erlenmeyer flasks) are a standard tool to carry out a culture in a relatively large volume, with good oxygenation, and to obtain a sufficient amount of biomass to perform extractions or analyses of chemical production. As we sought to do just that, we devised ways to illuminate flasks. One of the first ways we thought to do that was by surrounding the flask with a LED strip (Fig. 32-Left) but quickly set this idea aside as it is inconvenient to stick and unstick the LED strip in ways that might vary from time to times and might create reproducibility issues (intensities could be controlled via the input voltage though). Instead, I designed an illuminating stand (sometimes referred to as “OptoPetri”) made of LEDs soldered in a circular pattern (in a petri dish) with different numbers of LEDs to vary the illumination intensity (Fig. 32-Right). LEDs were soldered in series of 4, in order to obtain the appropriate power of 20mA per LED, which is recommended in the LED specs, and is comparable to the illumination of LEDs connected directly to an Arduino pin. Although increasing the resistance with many LEDs is an arguable design from the electronics point of view, it is anyway commonly accepted for a small number of LEDs in series.

How to illuminate the culture is important, and in our design, special care was taken to illuminate the culture medium while being shaken. Indeed, when the flask is in a shaking incubator, the medium segregates to the edges of the flask and flows there in a circular pattern. Therefore, the LEDs were positioned according to this circular pattern, to face the region where the medium will actually flow *during* the culture process, in the shaking incubator, and not when the flask is still. It is an important notion, rarely discussed, such that, for example in the OptoBox, which is also placed in a shaking incubator, it might have been interesting to position the LEDs on the sides of the well instead of in the middle (although it could also be negligible given the size of the well compared to that of the LED).

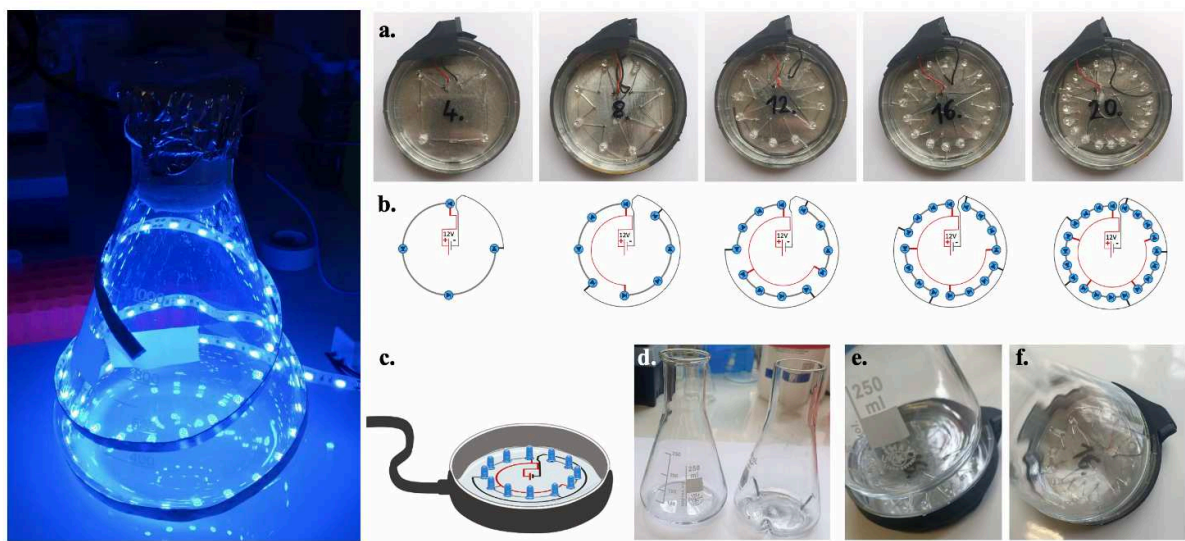


Figure 32. *OptoFlasks designs. Left: the design where a LED strip was placed around the flask was dropped mostly for its lack of versatility and reproducibility. Right: actual designs used for the later study. LEDs are arranged in a petri dish (a.) in series of 4 (b.) to make various illuminating stands on top of which flasks can be positioned. (e-f.). With various numbers of LEDs in different stands, the amount of light sent into 50mL cultures can be tested and adjusted.*

With **our current design**, LEDs are connected to a 12V input, and are simply turned on as the plug is connected to the DC power supply socket. Therefore, no complex illumination patterns can be carried out there, but of course using an Arduino, relays and/or transistors, this system could be adapted for more complex experiments. A redesign that includes another controller can also be imagined. The advantage of this system is its versatility and simplicity: once the flask is inoculated, it simply has to be positioned on the illumination stand, placed and taped in a larger metallic holder in the incubator and connected to the 12V power supply.

4.5. Illuminating flat surfaces

We take a short detour to discuss another way to illuminate cells, which focuses not on typical microbial liquid cultures. Those devices focus on illuminating 2D surfaces that can contain microorganisms that may respond to light, such as mammalian cells growing in (flat rectangular) culture flasks, like some researchers do in our unit.

Simple systems were designed in order to accommodate the illumination of large surfaces. In the following setup I made (Fig. 33), a LED strip was arranged and glued in order to illuminate a square surface under which cell plates will be positioned. To control the illumination timing, the current circulating from the minus end of the LED strip power supply cable is controlled by the Arduino via a MOSFET transistor. This way, the current is allowed to flow only when the signal coming from the Arduino is ON. With this, an illumination of 200ms every minute can be carried out for example. Similarly, by connecting the transistor to a PWM pin, intermediate light intensities can be reached. To control other culture parameters, this electronic setup can easily be placed into an incubator.

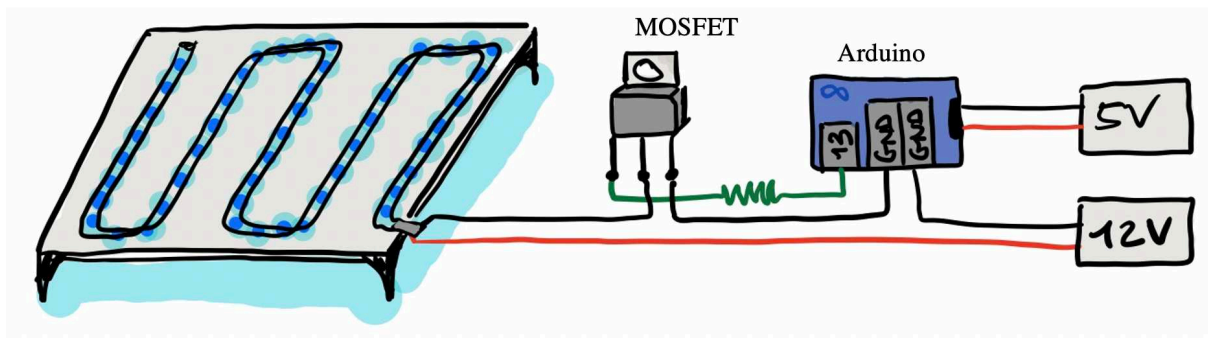


Figure 33. **Flat-surface illumination** design for Mathieu and Lorena for optogenetic mammalian cell control. Here, a LED strip is laid out onto a flat elevated surface. The LED strip 12V power supply is controlled via a mosfet transistor by an Arduino bearing the user-defined code for the desired illumination pattern. With this simple system, flat surfaces like petri dishes or mammalian cell culture vessels can be illuminated regularly with a high illumination temporal control.

Video-projectors are another convenient way to illuminate flat surfaces in an even more precise and dynamic fashion. It is not the first time that optogenetic systems and devices have been developed¹¹ as proof of concept, and controlling cells on a flat surface using optogenetics is especially convenient to study spatial dynamics issues. For example, in our team, Matthias Le Bec studied how the invertase, the enzyme that breaks down sucrose into glucose and fructose can be optogenetically controlled and how this control can impact the production of glucose which spread as a gradient in the agar medium, impacting cell growth dynamics in a 2D surface. Such an approach is used to ask questions about cooperativity and division of labor in microbial communities.

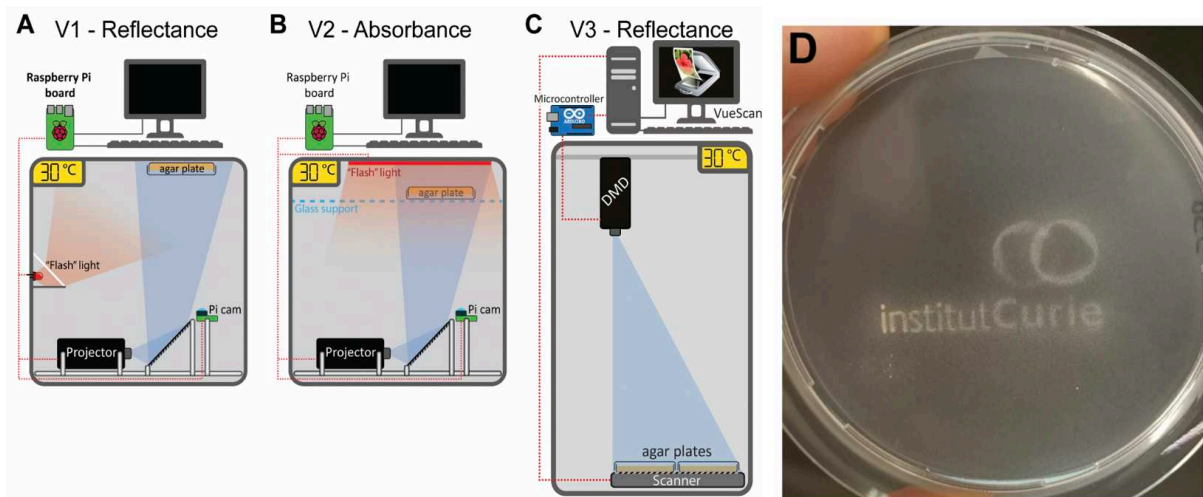


Figure 34. The **OptoCube** is an illumination device allowing for high temporal and especially high spatial illumination control. A blue light projector is used to display a light pattern on a flat surface (e.g., a petri-dish). In this device, besides illumination, a picture at regular intervals allows the user to follow the changes appearing on the illuminated surface. This can be achieved in different ways (a-c.). Here, cell proliferation is controlled by blue light. With the appropriate light pattern, the logo of the Institut Curie was drawn on cells laid on an agar plate. Courtesy from Matthias Le Bec, from his PhD manuscript.

In the **OptoCube** device that was developed by Matthias (Fig. 34), to activate a portion of the surface, a projector (or a Digital Micromirror Device - DMD) is used to send blue light patterns on agar plates in an incubator. To image the progression of cell growth over time on agar plates, a “Bright Field” image needs to be acquired regularly. This can be done using a camera and a light source (usually red, in order not to activate the optogenetic system). As the camera and light did not yield homogenous data in space, they were replaced by a scanner in the last version of the device (Fig. 34C). The illumination patterns can be tuned up to the 0.1mm resolution as well as to the second time resolution. Both illumination and scanning are controlled and synchronized via a custom-made python script, where the DMD is controlled via an Arduino in a similar fashion that is exposed just above.

4.6. Mini bioreactors (eVOLVER)

Arrays of small bioreactors are used in scaling-up studies, to bring a process to the industrial scale. With this, a researcher starts to handle a culture device where cells behave closer to how they would at the large scale. Therefore, one can start to vary growth conditions and culture parameters to see how they affect the production of a compound, or the viability or stability of a strain for example. This way, those arrays can be used for screening various conditions. Usually, they are very expensive tools and are not devices that any lab can afford to have (given the price), can use (sometimes cumbersome processes), or want to use (given their specific purpose). Hence, several DIY systems have been proposed to bring cheaper, easier and more adaptable small bioreactors arrays into labs. In my PhD, I set up and improved the eVOLVER system, first proposed by Wong *et al.* 2018⁹. I describe below the system and my contributions.

4.6.1. eVOLVER

The eVOLVER system from Wong *et al.* 2018⁹ is an automated cell culture platform, where various parameters of the cultures can be monitored and controlled. Its DIY and open-source qualities make this platform highly modular and accessible to anyone with basic knowledge of electronics and a bit of coding. What is put forward in such a system is the automation of the culture, the monitoring and control of parameters, as well as the throughput that can be obtained with an array of small culture devices. Those qualities make this tool very valuable to tackle various biological questions.

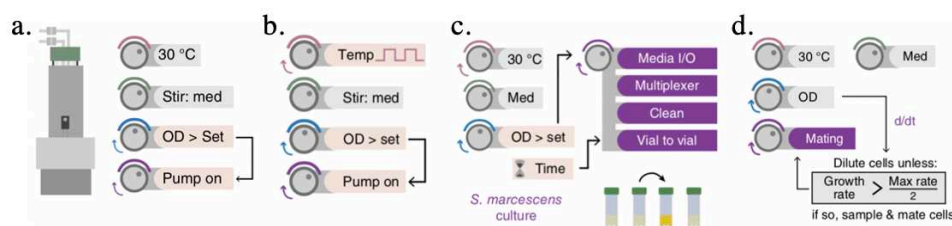


Figure 35. *eVOLVER* type experiments proposed in the original publication⁹, relying mostly on the fluidics module of the *eVOLVER* which we didn't implement to solely focus on the optogenetics. (a.) keeping the OD constant; (b.) keeping the OD constant with fluctuating culture temperature; (c.) conditional medium change and dilutions; (d.) real-time growth rate measure and conditional automated mating.

Experiments. In the original paper, the authors use the eVOLVER platform first to carry out long-term laboratory evolution of strains in different growth conditions, hence its name, the “eVOLVER”. This is allowed via OD detection controlling the fluidics inputs and outputs given varying growth rates in time in a single culture and across cultures (Fig. 35). On the same line, complex fluidics manipulations are demonstrated via the use of a millifluidic multiplexing module as a way to mix media and feed various continuous cultures dynamically. We see here that those experiments rely heavily on the fluidics system. In our case, we saw this tool more as a bioreactor, to carry out mostly batch cultures, hence we did not implement all the fluidics part, but we adapted the system for culture handling optogenetic control.

The original setup is composed of 4 parts (Fig. 36):

1. The 4x4 array of small bioreactors, is composed of so-called “smart sleeves”. They are called “sleeves” because a culture vial can be inserted in each of them. Each of the 16 sleeves harbors electronics components to monitor and/or control the Optical Density (OD), temperature and stirring rate. The inserted culture vial contains a stirring magnet, for stirring, and the necessary tubing for dilutions or feeding if necessary.
2. The integrated electronic module is made of a multiplexer motherboard that connects all the sleeves to boards dedicated to each available function on the sleeves. Those boards communicate to 4 Arduinos, which in turn communicate with a Raspberry Pi via an RS485 board and shield. The Raspberry Pi communicates with a lab computer where the python script is programmed and run.
3. The fluidics module, controlled via another set of electronics hardware, allows for complex millifluidics manipulation via a fluidics network containing integrated pneumatic valves controlled by solenoids.
4. The software allows for experiment coding, running, results visualization and sharing.

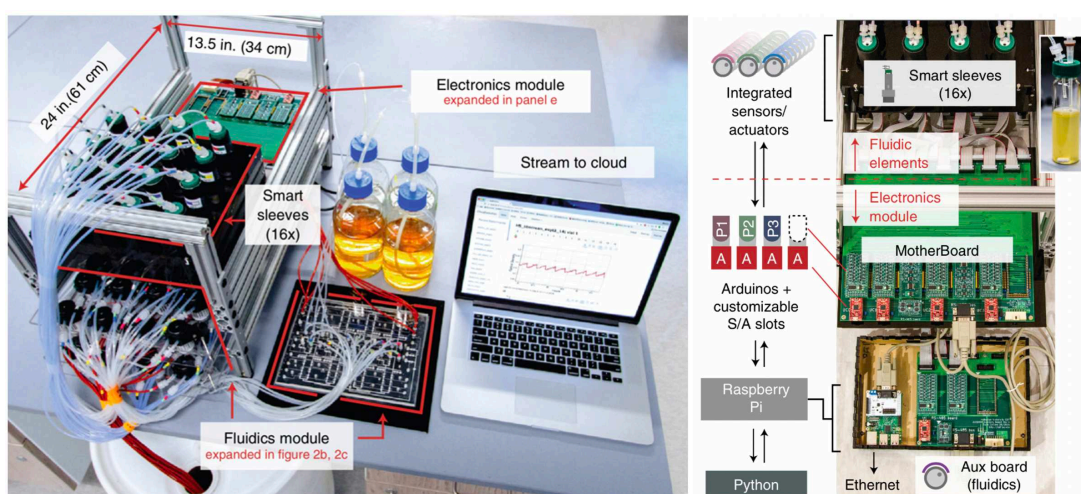


Figure 36. The original eVOLVER setup⁹ is composed of 4 main modules: the 4x4 small bioreactor array where experiments are carried out (further left), the electronic module, bridging all modules (detailed on the right), the fluidics module, comprising tubes and a programmable pneumatically-valved setup; and the software module, supervising all experiments.

Focus on one sleeve. A sleeve is a receptacle, an adaptor, that will host the culture glass vial (Fig. 37). It is composed of a base plate, a small fan, Plexiglas pieces, a 3D printed hollow holder, a hollow printed circuit board (mount board), and a machined-aluminum tube. Then comes all the small electronics components: stirring is controlled via the fan, where two round magnets are glued; the culture glass vial contains a rotating magnet that will rotate as the fan is turned on. Temperature is controlled via the two heaters connected in series to a 12V power source and measured via a thermistor: those three components lay against the aluminum tube, itself touching the glass of the culture vial to best control the temperature of the medium. Optical density (OD) is measured using an infra-red (IR) LED (900nm) and a photodiode placed at a 135° horizontal angle. The more cells, the more light scattering, and the higher the read OD value. Fluidics are placed in the hollow lid of the glass vial.

In addition to those components, the original sleeve design anticipated the need to add extra components, which we exploited for optogenetics and possibly for beta-carotene production monitoring. For that, a blue LED (460nm) was added, and a photoresistor was also added and positioned at a 135° horizontal angle. This way, the blue light can be controlled to activate the optogenetic system, and as more beta-carotene will absorb more blue light (given the orange color of beta-carotene), the signal from the photoresistor will decrease. In addition, I have made further improvements to add more blue LEDs to the design via the lid, which I will discuss later on.

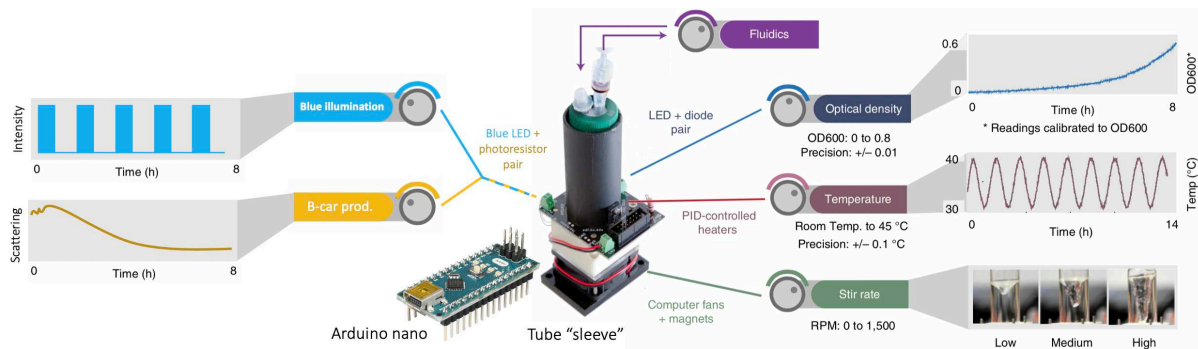


Figure 37. *eVOLVER sleeve functionalities*⁹. Each sleeve can independently monitor its optical intensity via a pair of infrared LED and photodiode placed at an angle. Its temperature is controlled using a pair of heaters placed again an aluminum tube enclosing the culture glass vial; The heaters are activated given the temperature measured by a thermistor. Stirring rate is set using a small fan where two magnets are glued and rotate to control the small rotating magnet inside the glass vial. The blue LED on the side can serve optogenetic purposes while also helping monitor beta-carotene production during the culture process: its light is absorbed by beta-carotene and the absorbance can be measured using a photoresistor; All electronic components are soldered at hollow printed circuit board and encased into a 3d-printer holder.

The motivation to build such a platform in the lab was manifold. First, we planned from the beginning to make complex illumination patterns and therefore needed a good system to control the illumination of a culture. Second, the possibility to measure the OD and the beta-carotene production was extremely promising in our initial quest to investigate trade-offs between growth and production. Third, the throughput obtained could be key to carrying out many experiments at the same time, with replicates and parameter variations. And fourth, with this culture scale, we are getting close to what can be done with small bioreactors, hence, a possibly more relatable step for further scaling up. For all those reasons, we sought to develop the eVOLVER in the lab, and we ended up developing our own version, with adapted hardware, new connectics, no fluidics, and a new user-friendly open-source software.

4.6.2. Unit development

New platform structure. Instead of sleeves connected to a large motherboard with complex connectics, we aimed to develop a simpler (as in for someone with limited knowledge in electronics) and more modular system. For this, each sleeve was connected to a single Arduino, and all Arduinos connected to a centralizing computer. This design might appear less efficient, less integrated and more costly in terms of electronic components; but it is easier to start with, and each unit can be used independently from the whole system. Here, we refer to a “Unit” as composed of a sleeve and of an Arduino nano (Fig. 38).

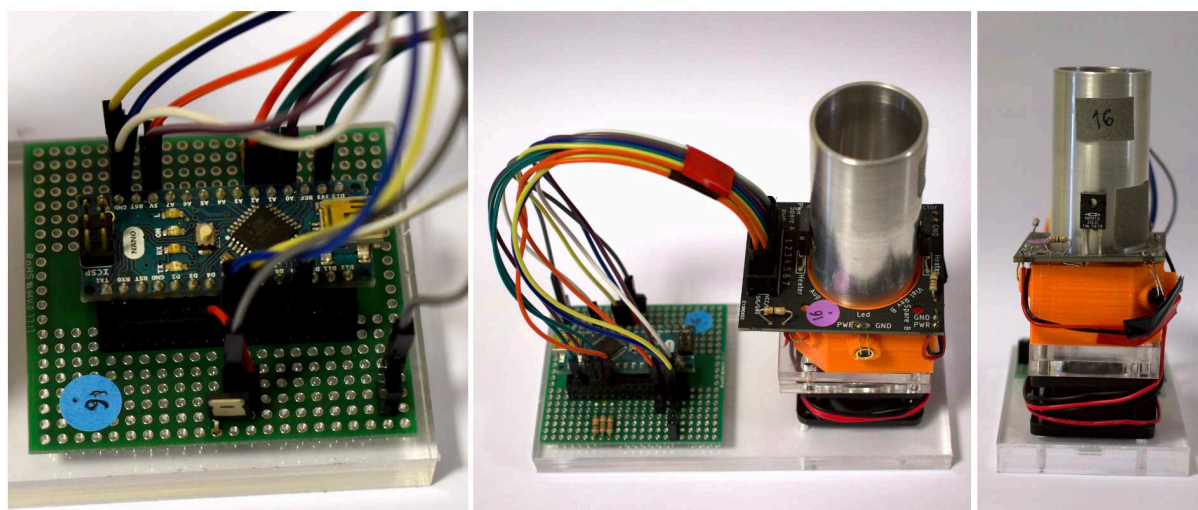


Figure 38. Adapted eVOLVER unit in our lab. With our design, instead of connecting to sleeve to a large motherboard, each sleeve is connected to its own controller (Arduino here). Each “unit” is therefore composed of an Arduino (left) and an eVOLVER sleeve (right). It renders the design simpler to implement in the lab, and each unit can be tested and modified independently. The connections to the Arduino for the electronic components have been standardized to facilitate code implementation (see next figure).

With this design, one Arduino controls and monitors all the parameters of a single sleeve. Although one could become limited by the capacities of the Arduino (number and types of pins), an Arduino Nano proved sufficient. PWM pins were allocated to components that require potential intermediate values (blue LEDs and stirring), simple digital pins to the IR LED (needs to be either full on or off), and analog pins used to receive information from the photoresistor (beta-carotene production), IR photodiode (OD) and thermistor (temperature) (see Fig. 39).

Optical Density measurement is performed as indicated in the original paper. The IR LED is connected to D5 pin and a 39Ω resistor is soldered on the hollow mount board. The IR photodiode was soldered opposite to the current, fed constantly with 3V3, it is connected to the A1 analog pin and to the ground with a $1M\Omega$ resistor. Although it was indicated in the eVOLVER documentation that changing this later resistor could change/improve the OD detection range, we did not manage to improve the range any further and remained with this original design. The two components are placed at a 135° angle from each other, such that it is light scattering that is measured with this setup.

Temperature control is made via the two ceramic-based heaters lying against the aluminum tube. The Arduino is not able to provide enough power for the temperature to rise sufficiently, such that a 12V power source needs to be brought in. For that, four 12V plugs are used, each feeding 4 units. The power is brought through electric wires running along the main Arduino power source cable (Fig. 40). The activation of the heaters is controlled in real-time given the temperature given by the thermistor (connected to the 5V and to the A0 analog pin and ground with a 10K Ω resistor). It is a bang-bang controller that turns on the heater when the temperature goes below the setpoint and off when above. The control is carried out by the Arduino D4 pin via a MOSFET transistor, as presented in section 3.6 of this manuscript.

Stirring occurs via the round magnet glued to the fan placed at the bottom of the sleeve, below the culture glass vial. Note that round magnets should be glued well centered on the fan, otherwise it may create disturbances and difficulties to operate the fan under certain conditions. The fan is controlled by the PWM D9 pin. The PWM input values range from 0 to 255 (corresponding to outputs of 0 to 5V, with a maximum of 40mA per pin).

Illumination is carried out via a blue LED soldered in the available empty slot on the sleeve mount board. It is connected to the PWM D11 pin and protected with an 82 Ω resistor. The LED, therefore, illuminates the culture medium from the bottom *side* of the glass vial. To accommodate for this addition, the 3D printed holder was redesigned with the addition of two supplementary holes, one for the LED, and one for the photoresistor. We take this opportunity to thank the authors of the original paper for anticipating the needs of others in their designs and purposefully leaving empty slots, which truly allowed us to adapt their design. Further improvements for illumination are presented below, with notable 2 extra blue LEDs connected to D7 and D8 (illuminating from the top).

A **photoresistor** was also added to the original design, similarly to the side blue LED: a second empty slot was available on the mount board, and the holder and aluminum tube were modified accordingly. The photoresistor takes 5V and inputs a voltage measured by the A7 analog pin, and also exits via a 1.2K Ω resistor connected to the ground.

This new electronic design is presented below (Fig. 39). Once established, 16 units were constructed.

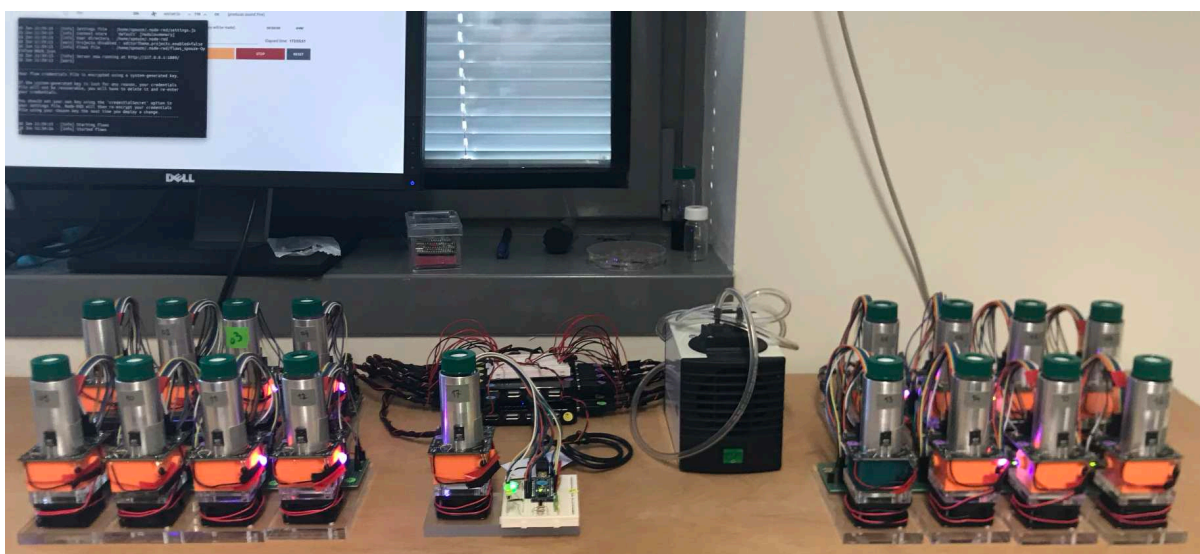
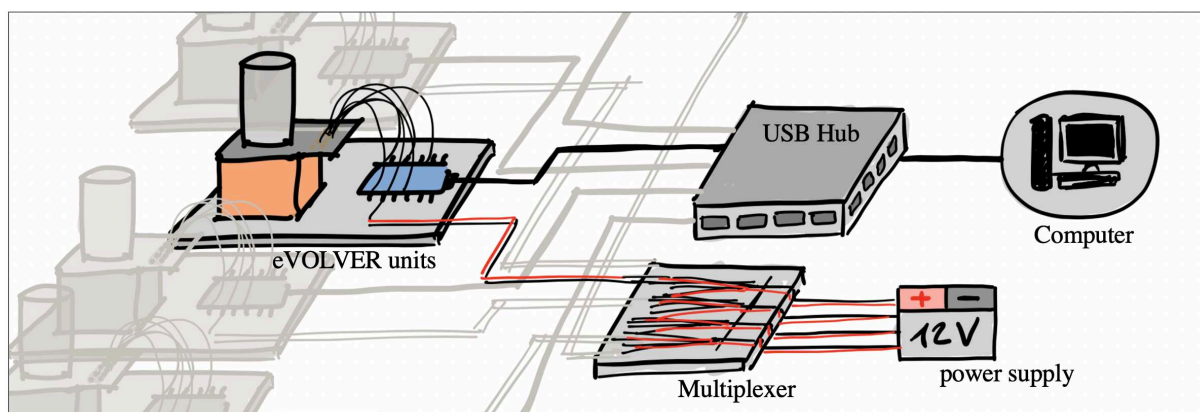


Figure 40. *The full adapted eVOLVER setup. (top): Connection scheme: each unit's Arduino is connected to a powered-USB hub connected to a computer. For the heaters, each unit needs a 12V input, provided by a "power hub": there 4 12V power each supply 4 units. (bottom): general view of the setup: 4 units on the left, 4 units on the right, with a 17th test unit in the middle. Each unit is labeled and independently recognized by the computer.*

4.6.4. Software

Node-red was chosen to develop the running code, the user interface, and to communicate with the Arduinos. This language rests upon the Node.js framework of the JavaScript language. Node-red is a web-based, flow-based programming language. This visual programming environment makes it easy to program without writing code, but by connecting nodes together to obtain more and more complex flows (Fig. 41). Node-red is convenient to make different hardware seamlessly interact together as well as with diverse online services via the use of specific nodes transmitting standardized information. It has many available modules (i.e., packages or plugins) containing many nodes for various applications; and new nodes can be easily coded to fit it this environment and communicate with other parts of the code. A node can be simply considered either as a function, with standardized input and output, that can be used over and over, in different circumstances, by being connected to other nodes (like assigning a value to a variable, a counter...); or be considered as a device part, to which information will be sent to or received from (typically, a pin of an Arduino). Although it is developed by IBM for industry-oriented purposes, it has been recently expanded to include

more simple hardware. In the lab, it was originally used to connect various microscopic equipment together, and to other lab equipment.

For **eVOLVER**, we used most especially the basic set of nodes to run an experiment, creating loops, editing variables, and writing outputs; the `Arduino` modules to communicate with the eVOLVER units via each Arduino pin, and the `dashboard` module to create the user interface. For node-red to be able to communicate with an Arduino, the Arduino is loaded with the Firmata template code (available by default in the Arduino IDE) such that it can receive and send instructions or information from and back to node-red. The code developed is usable by one single unit. For 16 units, the code is duplicated 16 times. To add another unit, the code simply has to be duplicated, the Arduino nodes modified with the new Arduino identified, and a few other minor changes (which can all be carried out in the raw JavaScript code for simplicity). Automatically, a new unit will be added to the user interface and a new experiment can be readily started. The code can be separated into 3 parts: i. the user interface and the setting up of the experiment, ii. the initialization, iii. the running code for the experiment.

The user interface is created to easily set up a standard experiment, while varying some parameters. OD measurement (“Measure OD”) can be set up at regular intervals. Similarly, the blue light can be quickly activated at regular intervals to measure the beta-carotene production (“Measure BL”). The third option (“Illuminate BL”) allows to set up a duty cycle and period for blue illumination of the culture via the side-LED, placed at the bottom of the eVOLVER. Besides the duty cycle and period, the intensity of the LED can be tuned. Temperature control can be turned on or off, and set to a desired value (here expressed in equivalent to voltage unit (0 to 5V detected corresponds to 0 to 1023 u.a.), 550 u.a. corresponding to 30°C). The stirring (“fan”) can also be set to intermediate values. Another option (“Growing delay”) was implemented, which allows for a non-illuminated period before the activation of the illumination, *i.e.*, the onset of the illumination pattern (be it constant or pulsed) can be set. Finally, additional notes and the experiment name can be edited. Additional information is displayed on the user interface (counters, measured values). Once all set, the experiment can be started, and initialization begins. At any time, the experiment can be stopped, and the user-interface reset (Fig. 41-42).

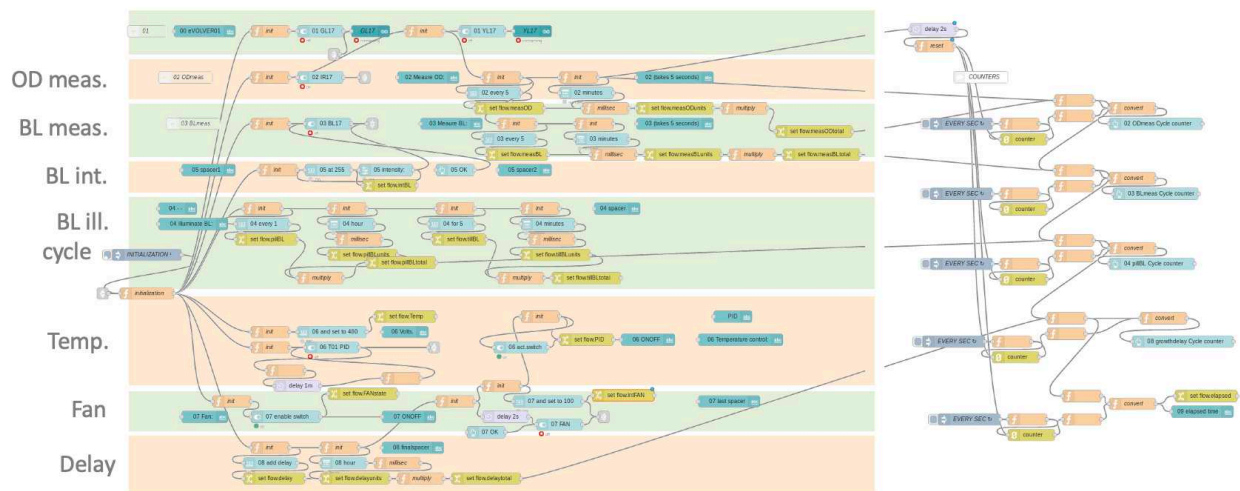


Figure 41. *The user-interface code in node-RED* combines a set of entry nodes that will create specific boxes on an interface (light-blue and teal-blue nodes), distributes the experiment's variables (in yellow - OD measurement frequency and corresponding units, intensity of the blue light illumination etc.) and allows for the start and reset of experiments independently. Initial values are set (blue/grey nodes) and other custom function nodes can be implemented (orange nodes). Besides floating variables (yellow), grey-arrowed nodes (hidden connections for visual clarity) also feed to the actual experiment code (see later).

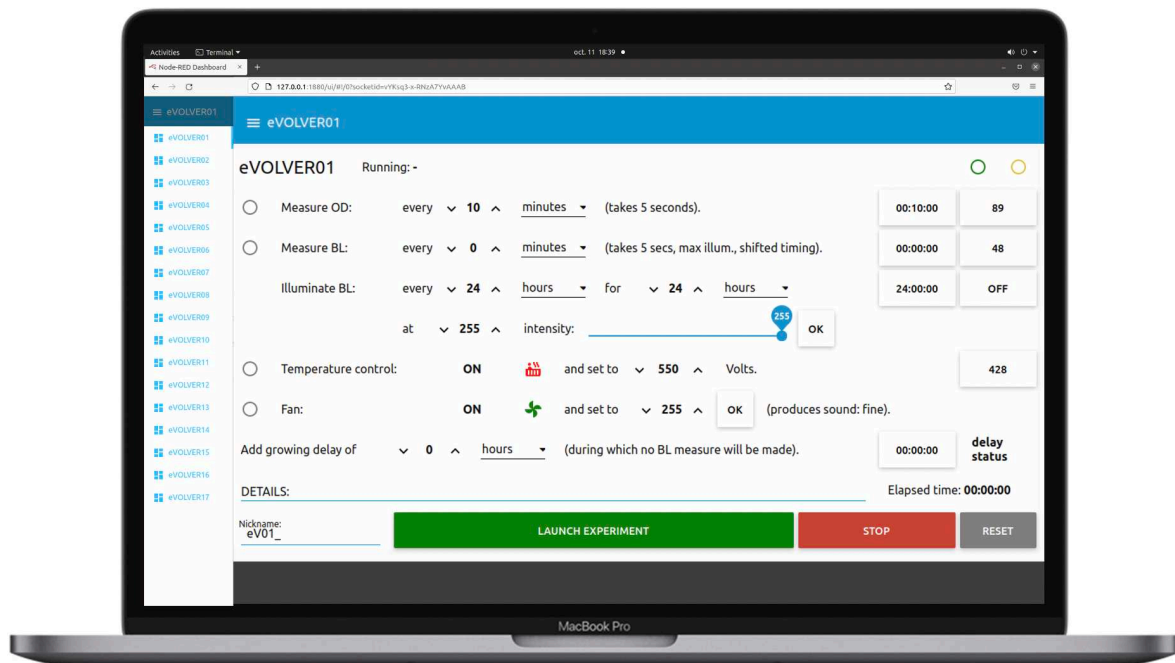


Figure 42. *The user interface to launch experiments.* For each unit, different parameters can be chosen: the frequency of the optical density measure (Measure OD), the density of the beta-carotene measure (Measure BL), the frequency and the intensity of the blue light illumination (Illuminate BL). Here, temperature control is set to 550 u.a., corresponding to 30°C, and stirring (fan) to its maximum. A growing delay can be added to start illumination only after a certain time. More details can be noted to be stored in the readme file of the experiment and a nickname given to facilitate post-experimental data processing and recover replicates. For each parameter, a counter displays the state and real-time measure. After filling in the parameters, and the experiment can be launched, stop and/or reset by hand. Each experiment works independently.

Initialization is automatically started upon launching the experiment. It consists mainly in setting up the output files that will contain the experimental data. For each eVOLVER launched, a folder will be created, named with the date and hour followed by the name specified in the user interface if any. In this folder, 4 files are created: a readme file containing all the experimental variables set up for the experiment as a list and 3 .csv files containing data coming from the sensors: the IR photodiode (OD), the photoresistor (blue light absorbance from potential beta-carotene), and the thermistor (temperature). In each file, the value recorded is followed by a timestamp, to prevent any time inconsistency during data treatment (Fig. 43). Note that, in this design, information is recorded at all times every 3 seconds: if the IR or blue LED is not on, only a baseline signal is recorded, which will have to be filtered out during data processing.

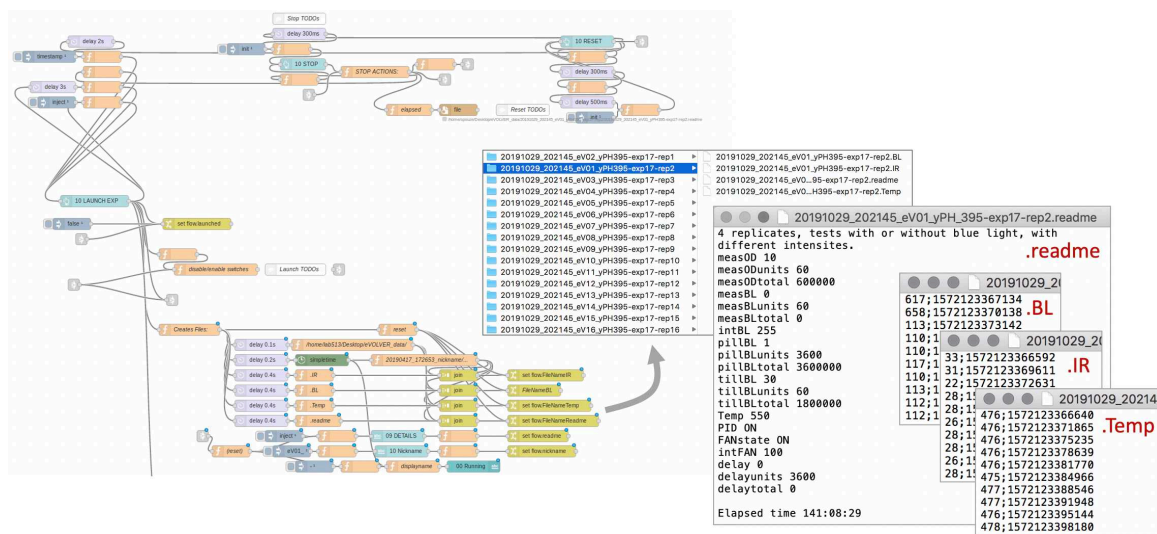


Figure 43. **Initialization and data handling.** After the experiment is launched, initialization occurs, i.e., creating a new folder that will contain standardized data for a single experiment. Each folder is named by the date and hour of the launch followed by its given nickname. In the folder will be 3 CSV files labeled “.BL”, “.IR”, “.TEMP” for the data coming from the photoresistor, the IR photodiode, and the thermistor respectively. Each line contains the measured value followed by its timestamp. Besides, a readme files father all parameters used for the experiment and notes written in the user interface.

The code running the experiment is then launched after the initialization (Fig. 44). First the stirring and the heaters are turned on. Then, the outputs from the sensors via the Arduino are recorded in the appropriate .csv files. The OD measure starts and will restart periodically according to the chosen time. For the OD measure, the fan is turned off, the blue LED is turned off, and the IR LED turns on for 5 seconds, during which a data point is recorded, without disruption from the stirring liquid swirl (vortex). After the 5 seconds, the IR LED turns off, the fan turns back on, and the blue LED recovers its previous state: ON if it was ON, OFF if it was OFF. Meanwhile, a counter is started if a growth delay was set. If not, or when the time is over, the blue light measurements start. Besides, blue light illumination will also start with the chosen pattern (which can be a cycle if the illumination is pulsed, otherwise it is constant illumination).

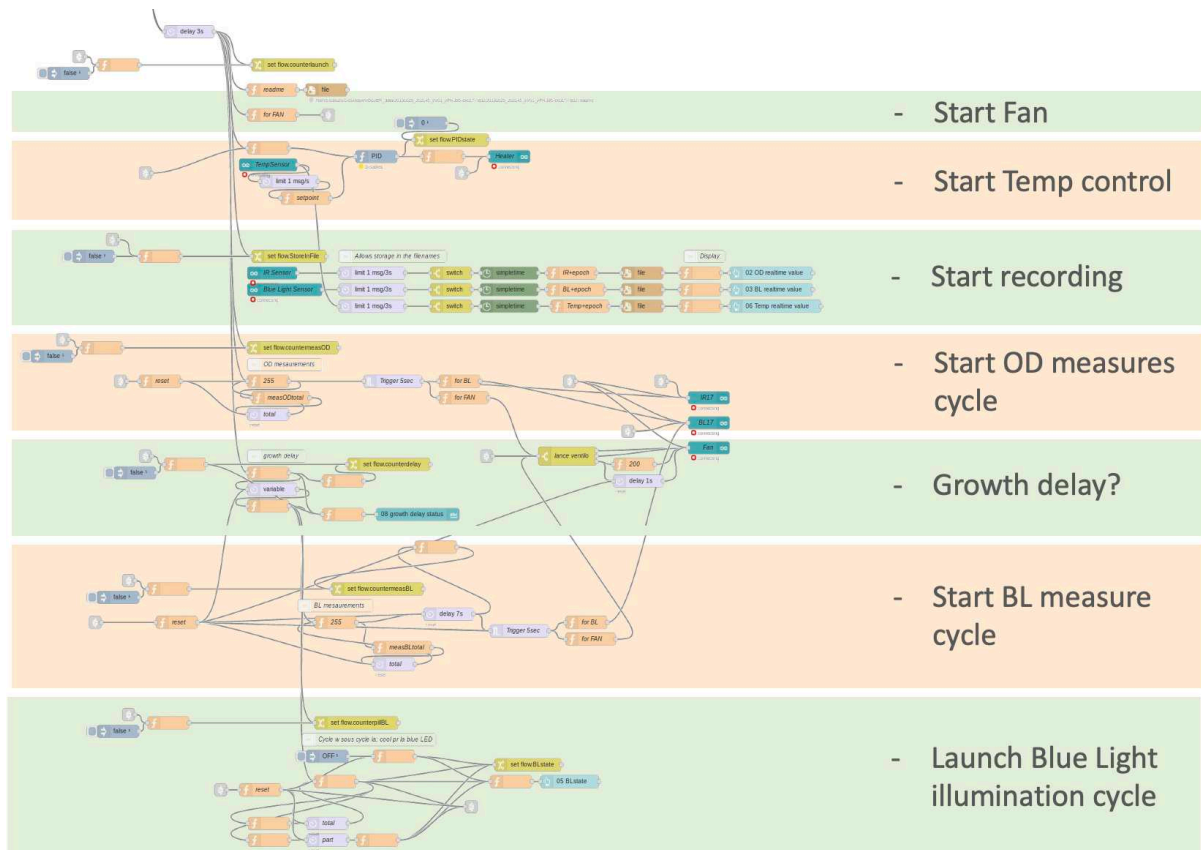


Figure 44. **Experiment running code.** Once the experiment launched and the initialization carried out, the actual experiment starts given the parameters, the fan starts to begin the stirring, the temperature control starts the control based on a PID node, and data recording starts. OD measure sequence can also start, at each defined time period: for this, blue illumination and fan are turned off, then the IR LED is turned on for 5 seconds. Finally, every component gets back to its previous state. Similarly, the illumination sequence or BL measure can start once the growth delay, if set, is over. Here, the experiment will run until interrupted by the user.

A set of R functions was developed to facilitate displaying the data coming from experiments and all code is available at https://github.com/Lab513/DIY_Optogenetics.

4.6.5. Type experiment

For an **experiment**, culture medium is prepared beforehand, glass vials with lids and rotating magnets are autoclaved and cooled down. Precultures are set overnight before starting the experiment; they can be diluted in the morning to obtain an exponentially growing culture at the beginning of the experiment and skip as much lag phase as possible. An appropriate amount of culture volume is inoculated to reach a 0.05 OD600 and is spread across eVOLVER glass vials. Lids are only slightly screwed on top of vials to allow gas exchanges to occur. Then, culture glass vials are dispatched in the eVOLVER unit sleeves.

For each culture, with the 3 output files, a summary of the growth can be drawn (Fig. 45). First, one can verify that the **temperature** indeed remained constant at 30°C (*i.e.*, 550 u.a.) during the entire culture.

Growth is detected thanks to the IR LED and photodiode and plotted here in blue. As explained before, OD is measured only at set intervals, but the signal is read every 3 seconds, such that a baseline at about 150 u.a., which corresponds to the photodiode signal without any IR light, can be seen in the raw data. Only when the IR light turns on, the measured value has meaning. The growth pattern is as expected: an exponential phase, and a stationary phase. However, one should not be misled by the familiar pattern here: the plateau reached here is a technical plateau, it is the result of the detection range of the coupled IR LED and photodiode. Therefore, in our conditions, only a small portion of the growth detected can be used to compute growth rates.

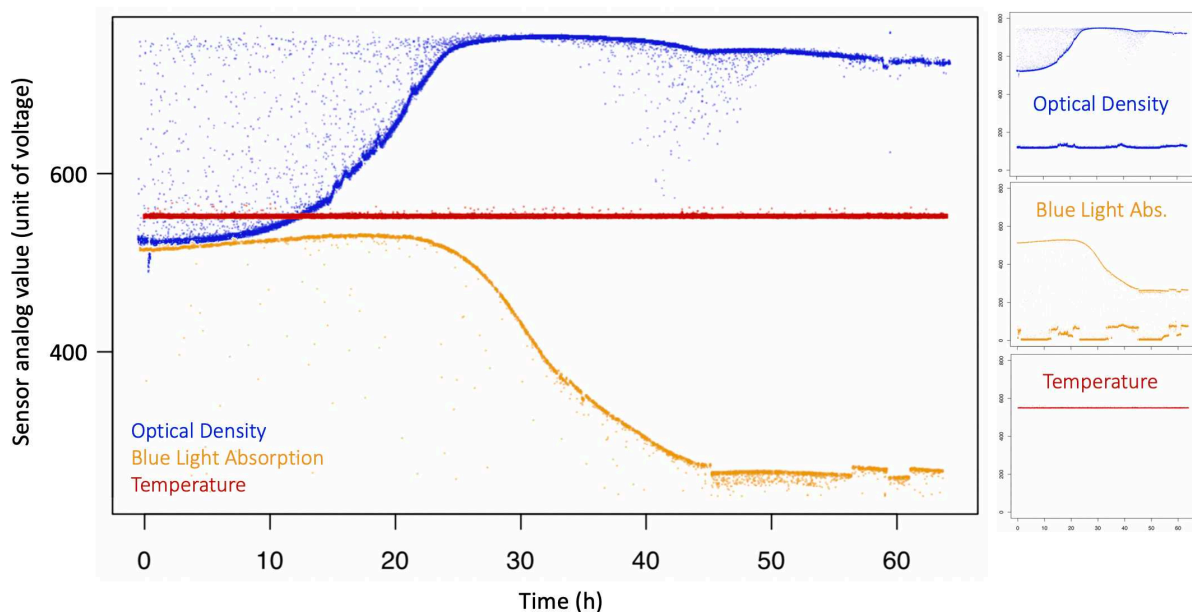


Figure 45. *Type experiment* output from the adapted eVOLVER. (Left). In blue, the infra-red signal conveys the optical density, it increases and reaches a technical (detection) plateau. In red, the temperature, measured by the thermistor, is controlled and remains constant. In yellow, the photoresistor data detecting blue light from the side LED: the signal decreases as the optical density increases and beta-carotene production occurs, increasing the absorbance further, and decreasing the signal. (Right). Raw data with baselines: the photodiode and photoresistor constantly record data, creating a baseline, only when the IR or Blue LED turns on, the signal becomes relevant: baselines are then filtered.

Beta-carotene detection follows a similar detection pattern but with a different sensitivity. Blue light detection from the photoresistor is more sensitive to variations in absorbance by cells. Similar to the OD detection, a baseline is constantly recorded for beta-carotene detection (fig. 45 – Right middle): we can see variations in the baseline (that also appear in the main figure) which corresponds to fluctuations in ambient light in the room where the experiment was carried out, impacting light detection in the photoresistor. Indeed, while the IR photodiode is specialized in IR detection, the photoresistor is more sensitive to a broad range of wavelengths.

Below (Fig. 46), as an example, are two different strains grown in the same unit successively. CEN.PK2-1C is a WT strain, and yPH_554 is the constitutive beta-carotene producer.

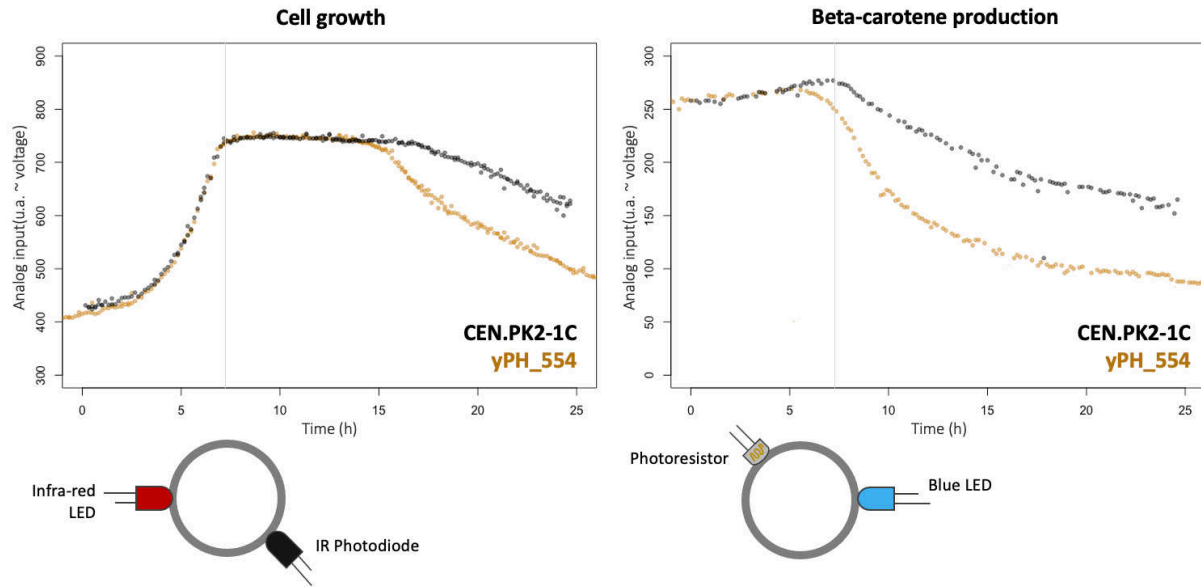


Figure 46. *eVOLVER* outputs. **(Left)** Cell growth can be measured using the IR LED and photodiode pair. The angle between the two electronic components allows for light quantification, first via light scattering (from 0 to ~7h, the more cells, the more light scattering, the higher the signal), then absorbance takes over, reducing the signal. **(Right)** Beta-carotene production can be observed in the *eVOLVER*, using the side blue-LED used to activate the optogenetic system. Here, using the photoresistor, only absorbance is considered, and the less received light leads to a lower signal. With the beta-carotene producer strain, as beta-carotene absorbs specifically blue light, more light is absorbed, leading to an even lower signal. The two strains were obtained from the same *eVOLVER* unit. In the scheme, the central hole represents the glass vial seen from above.

4.6.6. Calibrations

Beyond illumination control and automated cultures, one motivation to build *eVOLVER* was to measure growth rate, in an experiment, and possibly in real-time.

We first assessed **reproducibility**: we ran the same experiment in all the units several times. Here is shown growth in YPD at 30°C (Fig. 47). We found that reproducibility appeared overall satisfactory, except in units 1 and 2. Other units presented similar unit-specific growth profiles, but variations in-between units remain present: the detection range for growth measurement varies from unit to unit, likely due to the position (distance, angle of the component) of the IR photoresistor relative to the IR LED, both soldered and placed by hand in the 3D-printed holder.

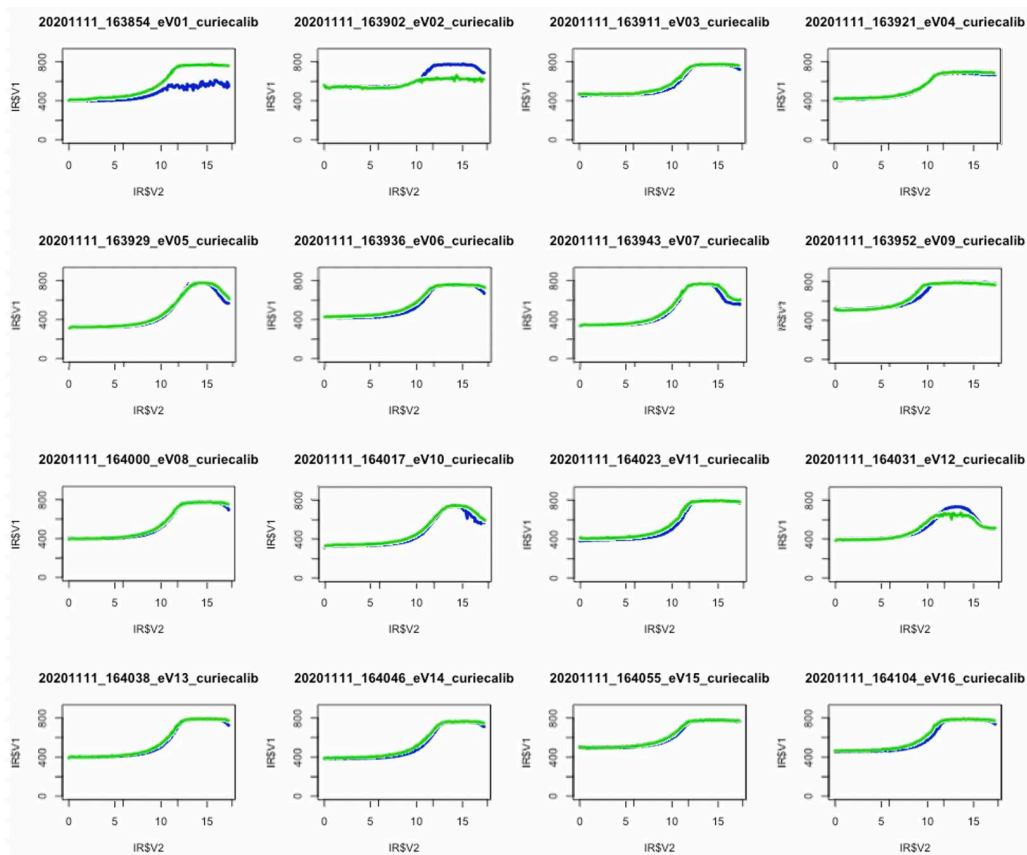


Figure 47. **Testing reproducibility** in the different eVOLVER units. Here, two experimental replicates of the Optical Density measure over a culture of a WT yeast strain in YPD at 30°C are overlapped to showcase potential intra-unit reproducibility difficulties, and inter-unit variability: all units do not all have the same dynamic range, which makes comparisons between units hardly coherent.

Comparing units. Because of this inter-unit variability, even more exemplified in figure 48, the conversion of the sensor value to an actual OD600 value meaningful in lab setting was carried out independently for each unit. For this, a saturated culture was used for different dilutions in order to test various known cell densities in each unit. From this, eVOLVER data to OD600 equivalence curves were obtained and each growth profile could be converted to the corresponding OD600 values.

Growth rate computation. From the cell number increasing in time, the growth rate can be computed. For this, the log of the cell number is plotted, which will display a period of linear increase. The derivative of the log of the cell number is then computed, and the maximal value of the plateau is used to compute the actual growth rate in cell/hour. It is then converted into a doubling time in hours. In most evolver units we built, we found results with growth rates at mostly 90 and 100 minutes (Fig. 48D), which is the expected range. Some other units displayed values outside of this range, which is likely the trace of which grew relatively slowly compared to others, or far too quickly (unit 12).

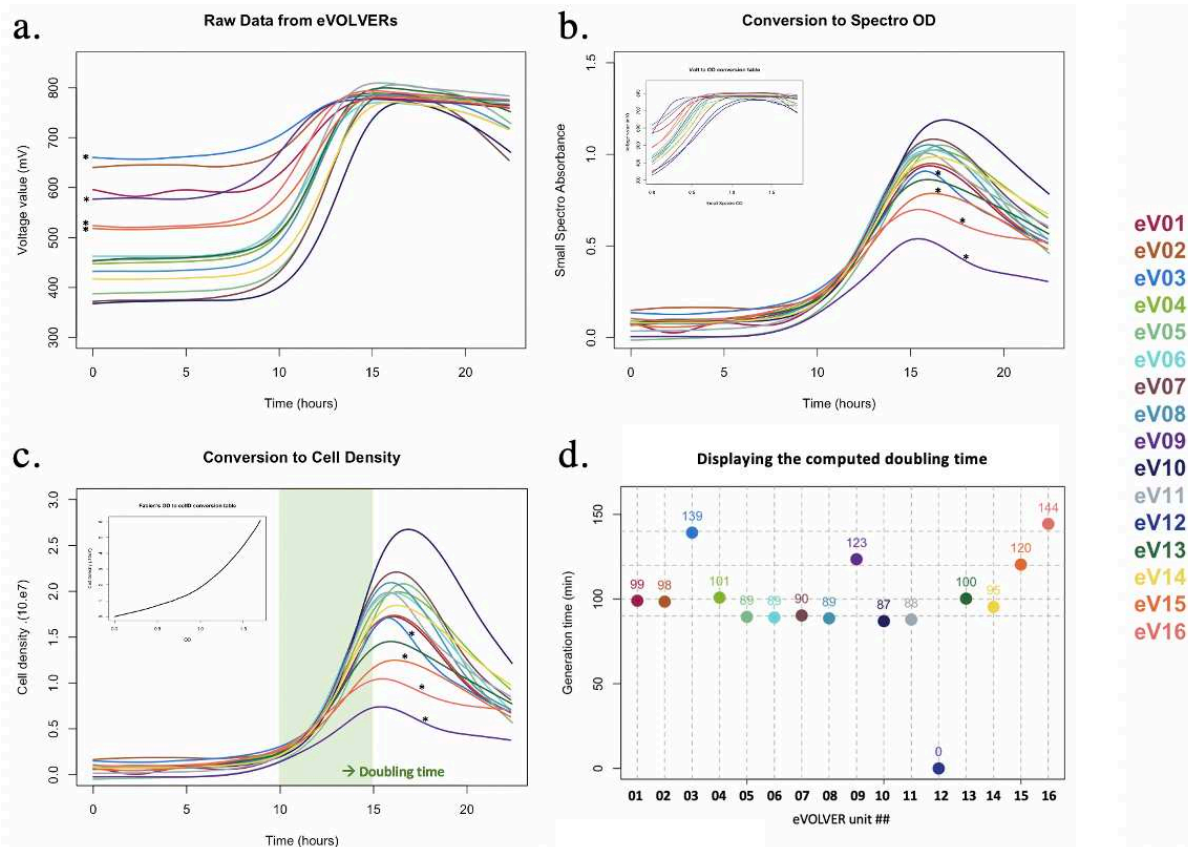


Figure 48. **Computing doubling times** from eVOLVER optical density measurements (tentative). The raw data measured with the IR LED and photodiode pairs in each unit (a.) is converted to an actual equivalent cell density (b.) thanks to calibration curves made by hand for each unit (b. top-left). The converted OD data is then converted to cell densities (c.) thanks to standard calibration curves (c. top-left). From cell densities, with the slope of the log, the actual doubling time can be recovered independently for each unit (d.). Here, data correspond to a WT strain grown in minimum medium (SC) +glucose at 30°C, therefore, a doubling time of about 90min is expected. Note inter-unit variations, and the difficulty to obtain homogeneous doubling times.

However, although rather coherent overall, a better calibration process needs to be developed to determine a growth rate over the whole experiment, or during the actual experiment. We suspected that given the hand-made nature of the devices, the components might shift in place in time and therefore impact measures and reproducibility. Confronting growth rate and production would indeed be a very interesting measure to obtain, but I finally chose not to focus my work on this aspect, but more on the illumination design. As mentioned earlier, the blue LED / photoresistor pair could be used to quantify beta-carotene production in eVOLVER. This measure would also require some calibrations of its own and need to be compared to the actual optical density. This remains a promising perspective today.

All in all, we used eVOLVER in batches, for the volumes it allows us to manipulate during an experiment, for the controllability over the stirring rate, and especially over the illumination. Besides, its throughput and ease of programming make it ideal to test many culture parameters. We will now discuss how to further improve illumination in eVOLVER, besides simply adding a side-LED to the original design.

4.6.7. Illumination

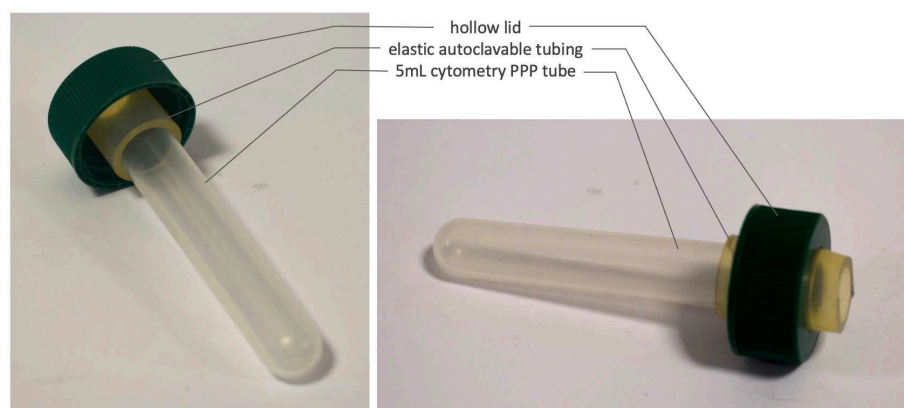


Figure 49. Custom lid for internal culture illumination. To add more light to the culture medium, the lid was modified such that LEDs can be inserted right into the medium without the need for a complete redesign of the eVOLVER sleeve. The hollow lid is normally sealed with a silicon septum. Instead, we used a cytometry polypropylene autoclavable tube to reach inside the medium and a piece of autoclavable tubing to adapt the tube and hold it to the lid hermetically.

Improving illumination came out as important for optogenetic activation. Although the original eVOLVER sleeve had an empty slot in the original design, illumination from the side of the sleeve with a resistor restricting the LED intensity was shown to be limiting in terms of activation (see results in [chapter 3](#)). Since the eVOLVER sleeve has an aluminum tube as base design, setting more illumination from the outside would require an entire redesign and reassembly. Thus, we sought to add illumination within the inside of the culture. One possibility was to take advantage of the hollow lid to get LEDs inside the culture. To prevent contact with the sterile medium and protect the LED from getting wet, different systems were tested using basic lab equipment. The requirements were simple: get the LED sufficiently inside the culture, protect it with autoclavable material, and make sure that the junctions keep everything airtight and preserve sterility. After a few tests, we settled with a customized lid in which a cytometry tube (5 mL Polypropylene Round-Bottom Tubes from BD Falcon REF 352063) is maintained inside the hole of the lid via an autoclavable cut piece of tubing large enough to keep the junction airtight ([Fig. 49](#)). The new lid can therefore be autoclaved like any other type of lab equipment.

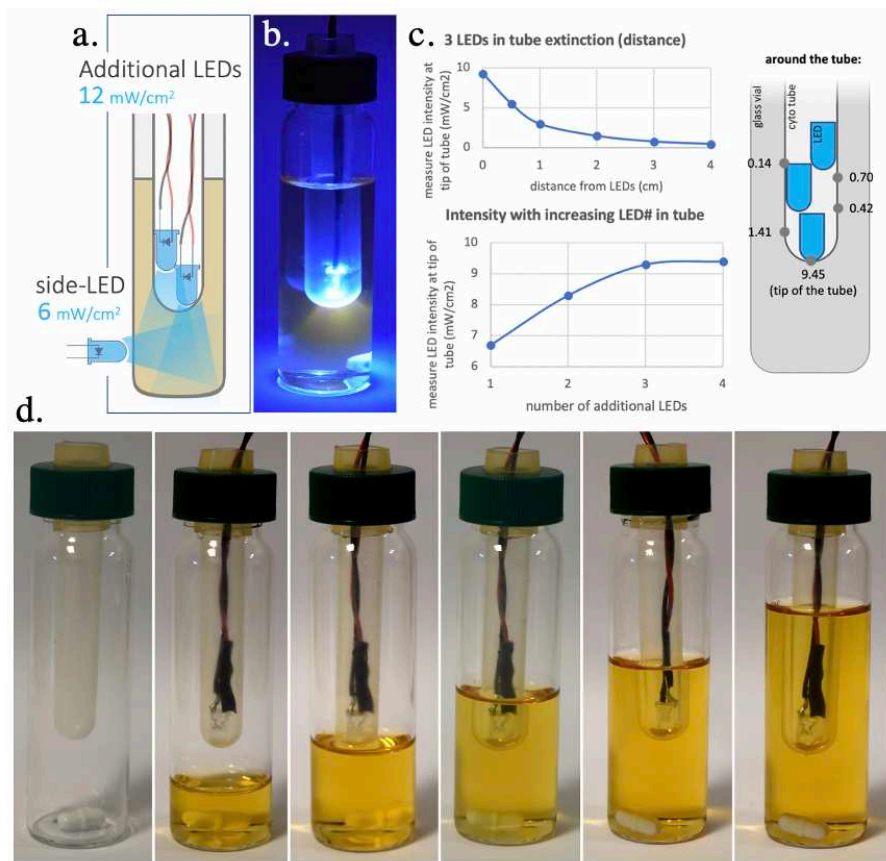


Figure 50. **Glass vial internal illumination** using the custom-lid. (a.) Schematic of a glass vial illuminated with the side LED + 2 additional LEDs (internally), referred to as “s+2”. (b.) Picture showing the light cone emanating from the LED (25mL). (c.) light intensities measured for different LED numbers and distances. (d.) Showcasing where culture medium stands relative to the internal illuminating LED given the culture volume poured in the glass vial: 5, 10, 15, 20 and 25mL: with 25mL, most culture volume actually stands above the LED, i.e., more than half of the culture volume is not actively illuminated with this configuration.

Technicalities. With this arrangement, what is mostly illuminated is what is below the LED, *i.e.*, sometimes only a certain portion of the culture volume (Fig. 50). As such, the volume of the culture can have an impact on the cell-to-cell illumination / per-cell amount of light. We used only “naked” LEDs, with no extra piece of plastic or other equipment to improve the light dissipation (such as light deflectors, or lampshades of any kind that could help to homogenize illumination). We measured the light intensity that was received through the tube, and on the sides, to confirm that light beams were mostly oriented downstream. We measured the light intensity emitted with 1 to 4 additional LEDs placed in the tube (Fig. 50C). While each LED can independently emit 12mW/cm², we found that the maximum was reached with 3 LEDs at 9.45 mW/cm² (measured through the plastic of the tube).

With this system, we did improve illumination in the eVOLVER system, and optogenetic quantifications are presented in chapter 3 of this thesis.

4.6.8. Other systems

eVOLVER⁹ was initially developed as a lab device, and indeed, we have seen that this DIY type of equipment makes it a very versatile instrument and highly adaptable for various lab applications. The eVOLVER platform actually led to the creation of a startup commercializing the instrument for other labs, as well as a forum to share information and build up an active community of users (evolver.bio). The company is called fynchbio (after Darwin's finches), and it sells for about \$11 000 to \$15 000 (including the fluidics kit) to academics for a full 16 sleeves kit (individual parts can also be ordered separately). With our design, we estimated the price to be 75€ per unit, making the 16-unit platform 1 200€ (more details in [protocol 8.9.8](#)). eVOLVER is not the only small bioreactor platform on the market though.

Chi.Bio¹² is a similar small bioreactor array developed for lab use and is also being commercialized after publication by Steel *et al.* 2020¹². As eVOLVER, Chi.Bio consists of a main controller board to which bioreactors and pumps can be connected. The bioreactors also include a glass vial inserted into a sleeve, but the Chi.Bio sleeve has a more sophisticated, compact and miniaturized design, which makes it more performant, but also less modular. While eVOLVER is regarded as a DIY instrument and was published with the idea that each user can build and tune it, Chi.Bio (although it is fully open source) requires more electronics knowledge if one wants to tweak the equipment. One big advantage of Chi.Bio compared to eVOLVER is its 7-color LED + UV LED, and especially also its small spectrophotometer that can detect various wavelengths as well ([Fig. 51](#)). This makes it usable for many optogenetic systems, and especially for fluorescence analyses such that many parameters can be controlled and monitored simultaneously! It also offers a fluidics module that can be used for similar functions as eVOLVER. Although less tunable, Chi.Bio is a strong competitor to the eVOLVER platform, and it is also available for sale online at similar prices.

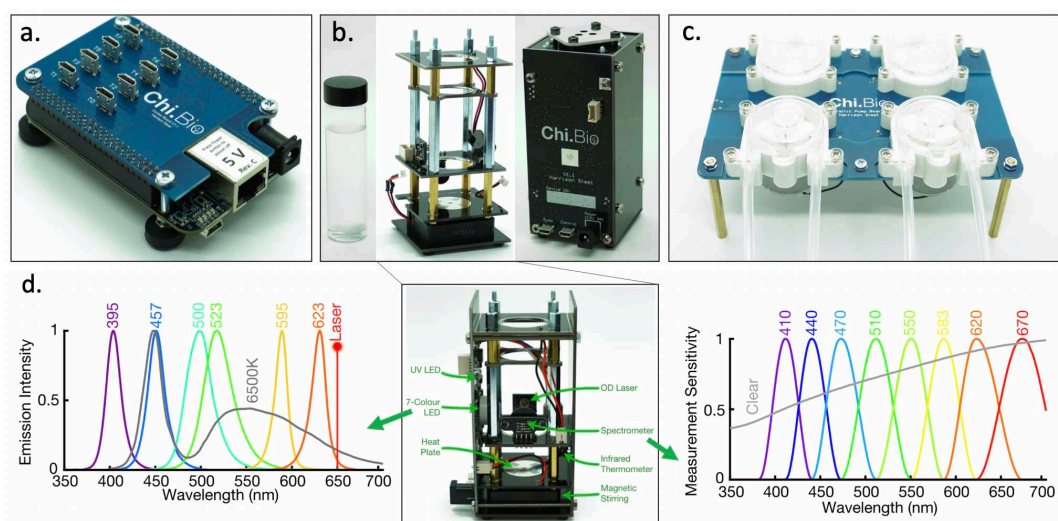


Figure 51. *The Chi.Bio system*¹² is similar to *eVOLVER*. It is composed of a controller (a.), a bioreactor / sleeve, where a glass vial is placed and encased (b.), and a fluidics system (c.). One non-negligible advantage of the Chi.Bio over *eVOLVER* is the large optic system (d.) available which makes various measurements possible, including different fluorescent proteins, but also different illumination wavelengths for different potential optogenetic systems.

ReacSight¹³ is an open-source general framework that has been shown to interface different lab instruments and have them work seamlessly together, including bioreactors (be it a custom setup, or the actual Chi.Bio mentioned earlier), with automatic sampling and perform potentially other types of quantifications. It can therefore augment the capability of the bioreactor arrays and perform even more complex tasks. At the heart of the system is the OT-2 Opentron, a low-cost pipetting robot that allows more and more for the democratization of automation in standard biological laboratories, as it is highly tunable and programmable. In the paper, the authors exemplify the use of the ReacSight framework with real-time control of gene expression using optogenetics, metabolic studies in yeast, control of microbial consortia strain proportions, and investigating changing antibiotics concentrations dynamically in plate-reader cultures (Fig. 52).

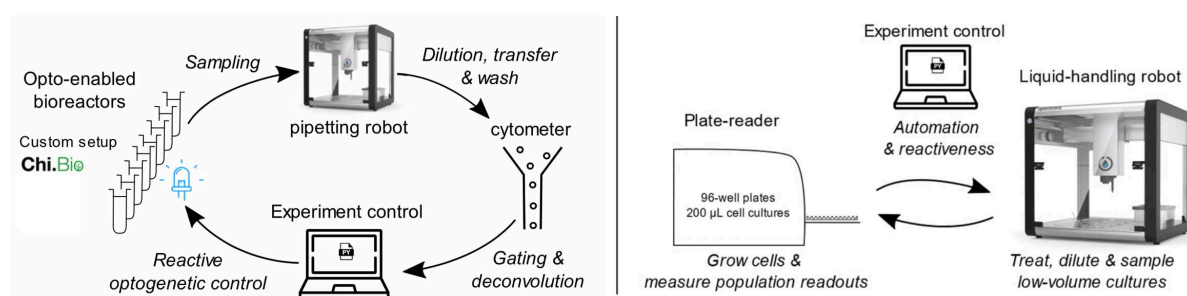


Figure 52. **ReacSight**¹³ builds further on sets of bioreactors to connect them to other devices in the lab in a more integrated and automated fashion. **(Left)**: the automated cultures are regularly sampled and transferred to a cytometer via a pipetting robot. Measurements from the cytometer can then feed control algorithms that will adjust culture parameters in the small bioreactors. **(Right)**: connecting a pipetting robot to a plate-reader to expand experiment possibilities, all in a lab-automation framework.

Industrial bioreactor arrays, finally, are without surprise what actually gets the closest to the actual industrial process. Here it is not a matter of DIY or versatility, but a matter of robustness and parameter control (Fig. 53). Indeed, in arrays of small bioreactors of each 500mL, pH is monitored (where it was not for the previous arrays), bubbling might be the preferred way to oxygenate cultures, anti-foaming agents, therefore, might be needed, and samples will be taken out regularly for analyses, but not real-time measure via optical devices are generally carried out in such bioreactors. Those systems are obviously not adapted for lab usage, for research, or even for optogenetics yet. However, they are what is used in process development, and light will have to be able to penetrate those bioreactors if one wants to bring optogenetics to the industrial scale. An example is Eppendorf which offers small-scale parallel bioreactor systems. Also, Culture Biosciences offers online booking and usage of bioreactors in a “cloud lab”-based fashion.

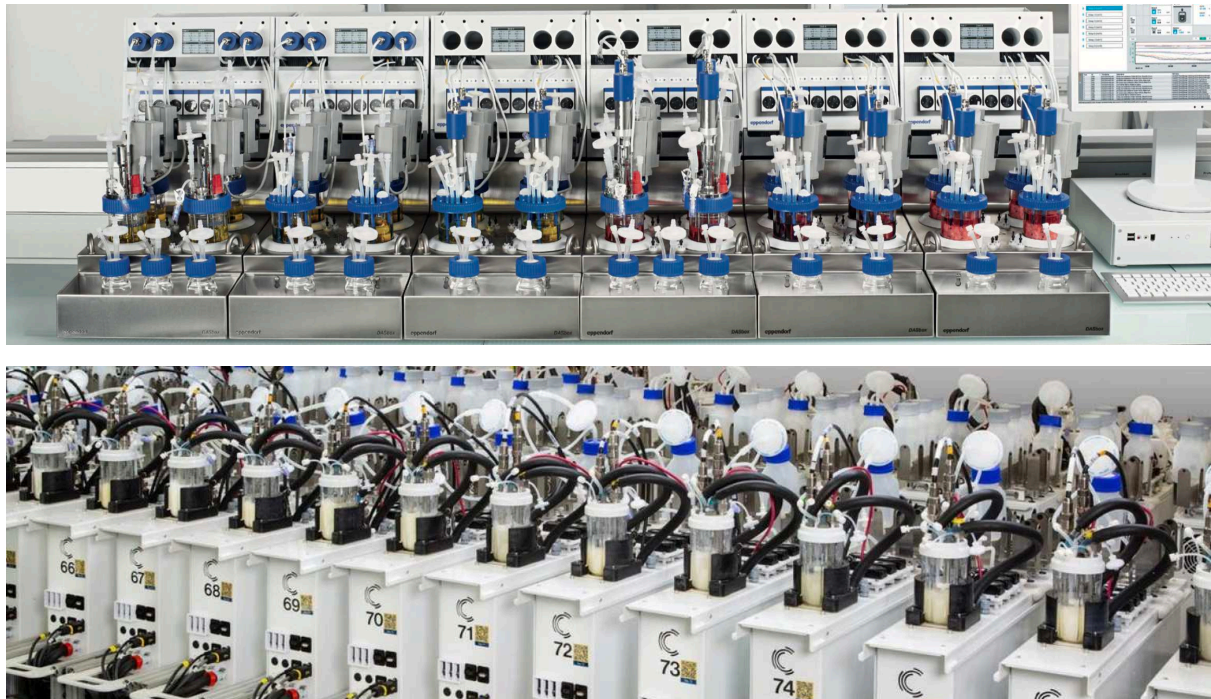


Figure 53. Arrays of small bioreactors are commonly employed in the industrial sector. (top) DASbox Mini Bioreactor System for Eppendorf¹⁴. Up to 24 vessels, from 65 to 250mL. (bottom): Culture Biosciences setup¹⁵.

4.7. Lab-scale fermenters

Pilot-scale bioreactors are generally lab-scale 2-10L bioreactors used as proof of concept to show that a strain developed at the small scale can perform at larger scales and may be fit for even more scaling-up. With pilot-scale bioreactors, we are reaching a scale where microbial optogenetics has been only used in a limited amount of papers^{16,17}.

Illumination is carried out externally, most of the time. As for algal photobioreactors, light panels can be placed around the bioreactor (or photobioreactor), and light can be user controlled. Light panels can be neon tubes to procure white light (Fig. 54A), or LED arrays for more precise wavelengths (Fig. 54B). Besides, wrapping a LED strip around the transparent glass bioreactor can also be an efficient method to illuminate a culture, but the contact of the LED with the glass might make it more difficult to control the temperature as LEDs emit heat when turned on (Fig. 54C). Another way to illuminate is with internal illumination (Fig. 54D). Internal and external illumination can be used together to maximize the amount of light received by each cell. This can be challenging as cell density reached with yeast can be very high, such that light will not go through the culture medium in most industrial cultures.

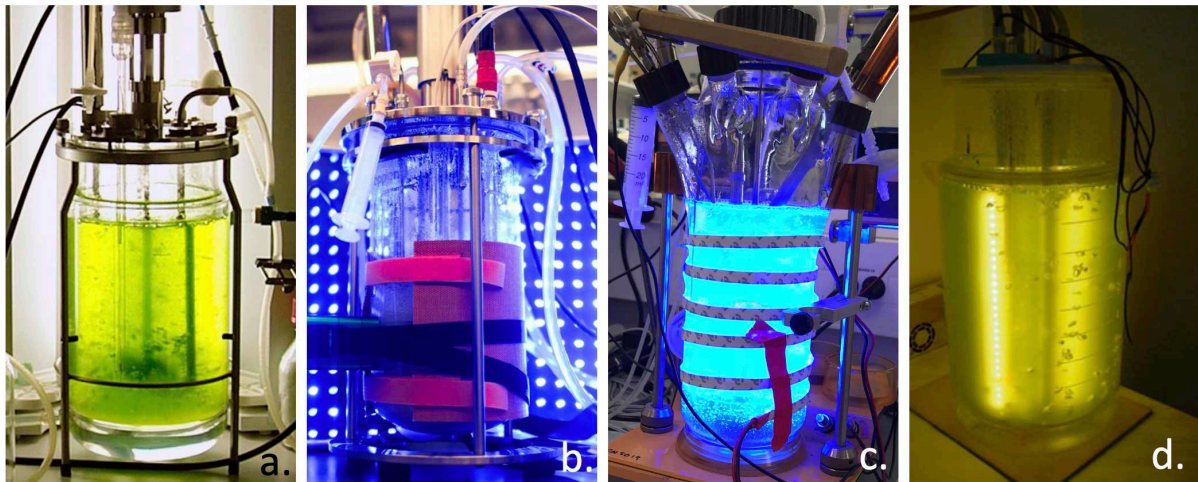


Figure 54. *Pilot-scale bioreactors (5-10 L here) with different illumination modalities. (a). Algal photobioreactor¹⁸ with white back-panel illumination. (b). LED-panel external illumination from Zhao et al. 2018¹⁶. (c). LED strip around the bioreactor, attempted in Gilles Truan's team at Toulouse Biotech Institute, with Thomas Lautier and Guillermo Nevot. (d). Internally illuminated algal photobioreactor¹⁹.*

At those pilot scales, control is carried out in terms of pH, temperature and dissolved gas, such that cultures are much closer to the actual industrial settings. With such volumes, larger-scale issues can really start to be anticipated, one important being the question of cell density and light penetration in the medium, which still remains an open question.

4.8. Industrial-scale bioreactors

While pilot-scale bioreactors are often made of glass, large-scale bioreactors used for the yeast bioproduction industry are mostly stainless-steel bioreactors and are used to carry out the actual “real” production. Besides, as the culture volume increases, the surface area/volume ratio decreases dramatically, impacting external illumination capacities. Large-scale photobioreactors do exist for algal cultures, with various designs (Fig. 55A). However, **external illumination**, although enough for algal cultivation, might become insufficient for high cell densities obtained with yeast cultures. To solve this issue, new bioreactor designs, or adapted systems will have to be developed.

External-loop illumination carrying a flow of cells through a light source could be considered as an alternative to classical external illumination. It has the advantage of being potentially adaptable to already-in-use bioreactors, *i.e.*, be considered as an external module without needing bioreactor redesign, which would equate to major spending. This strategy may come with a cost, however: not all cells will be illuminated at the same time, and the bioreactor whole volume might have to go through the loop several times to consider that carry out a homogenized illumination (Fig. 55). Consequently, quick illumination patterns might be challenged, impacting the precision of the control the user can have on the cells. **Internal illumination** was also mentioned earlier. It may be an interesting strategy also for large-scale bioreactors and may be more efficient for strong short homogeneous illumination. More imagination and work are needed to find how to implement this in actual bioreactors.

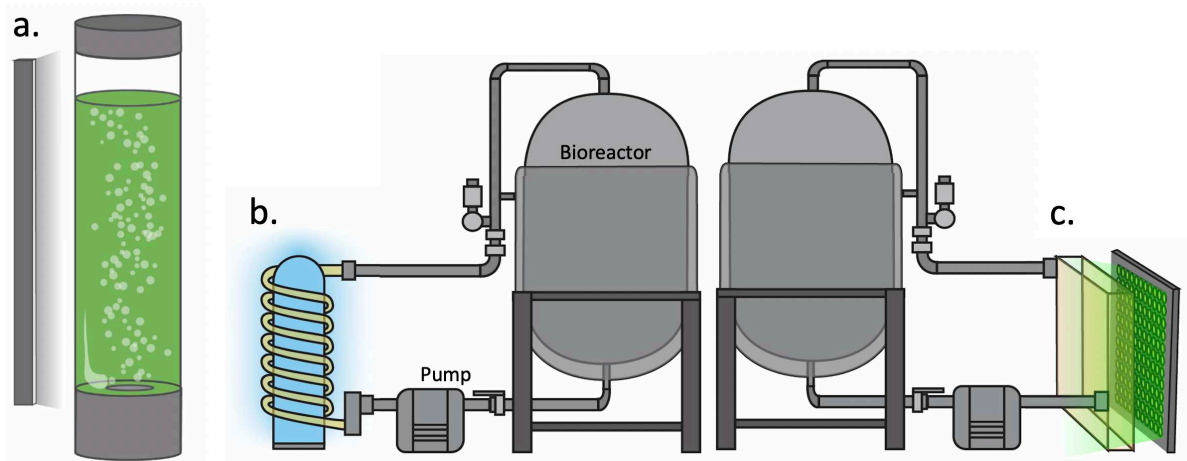


Figure 55. **Larger scale bioreactors.** (a.) Airlift algal photobioreactor, (b.) bioreactor with external loop illumination design, coiling around a light source (technique originating from photochemical engineering), or (c.) using a flat surface with LED array panel. Adapted from Pouzet et al. 2020¹.

Industrial photobioreactors. I would like to finish here by touching upon the various algal photobioreactor designs existing, some of which deployed at impressive massive scales (Fig. 56). Although those designs might not be adaptable to yeast or bacterial cultures used for bioproduction because of density, gas exchanges or light quantity issues, they bring new perspectives on how illumination can be carried out and may help inspiring new designs to scale up optogenetics for bioproduction.

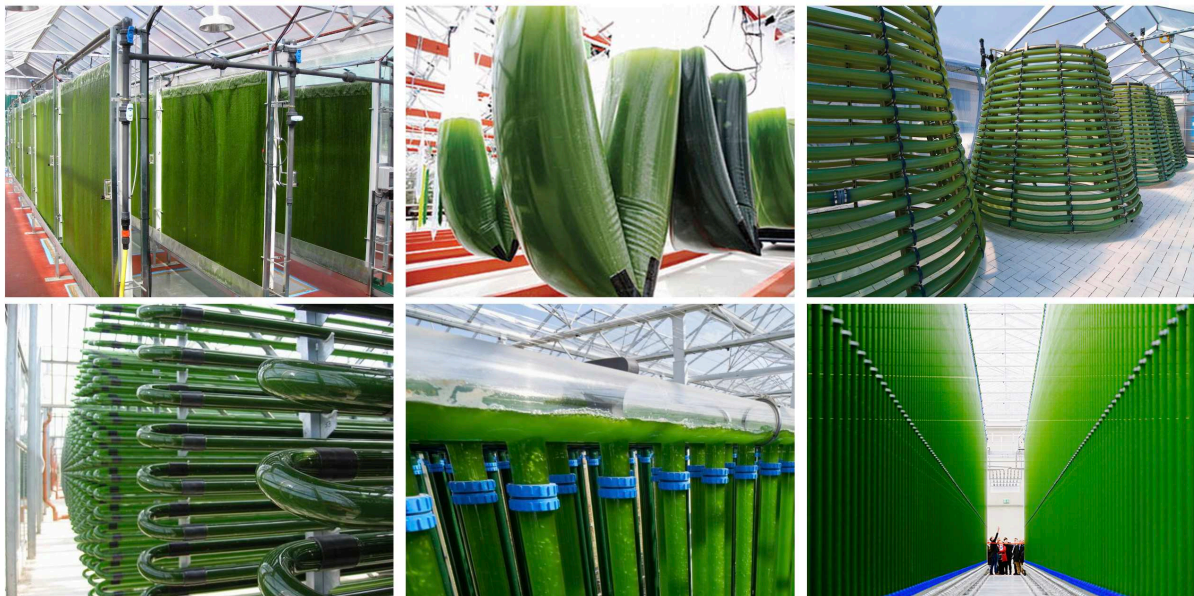


Figure 56. Types of **large-scale algal photobioreactors**. From left to right, top to bottom: flat panels or flat plates, culture bags, “christmas tree”¹⁹, tubular manifold serpentine horizontal, tubular vertical, overview of an algal farm.

4.9. Conclusion and Perspectives

We approached the question of optogenetic devices by scaling up across the different devices that are used nowadays.

Summary. We presented here different ways to carry out optogenetic studies applied to bioproduction using different illumination devices. At the smallest scale, we discussed using microfluidics and time-lapse microscopy to follow in detail optogenetics activation dynamics and the influence of other factors thanks to the fluorescent channel included in most microscopes. At the population level, a small-scale culture classically used in the lab are imaging plates: many LEDs arrays are available today to illuminate 24 to even 96-well plates, and more sophisticated systems emerge to be able to read a cell output, similar to what a plate reader can do. We focused on the OptoBox developed in our lab, adapted for blue illumination for the EL222 optogenetic system. Then, I presented the OptoTubes, used to illuminate simple starter cultures in test tubes. I also developed the OptoFlaks, an illuminating stand to illuminate cultures in shake flasks. We discussed also the ways to illuminate flat surfaces, with simple designs, or more advanced ones using video-projectors. I then presented the eVOLVER design that I adapted for optogenetics: for that, a LED and photoresistor pair was added in the initial design, the lid was modified to accommodate for internal illumination in the culture glass vial, and a whole software was developed to handle the data and launch automated cultures. Finally, we discussed pilot-scale and industrial-scale bioreactor designs, and future challenges regarding optogenetic implementation.

Strain design and development. At the lower-scale, emphasis was put on the throughput, *i.e.*, being able to screen for various strains and various illumination conditions at the same time. This offers the good versatility needed for initial optogenetic experiments. But this small scale also results in limited controllability and therefore in limited experiment complexity. Increasing in scale, with mini bioreactors, the focus is put on the controllability of the system, and how much information can be extracted from the culture (cellular state, production level), as well as fluidics that allow for more complex cultivation processes. Thus, those relatively small-scale systems are convenient for research purposes, allow for throughput, and also enable to get closer to industrial settings; although pilot scale (bioreactors) remain necessary²⁰. At larger scales, however, questions of light penetration become crucial, and with decreasing surface area to volume ratio and high densities, bringing light inside the culture remains a major challenge.

There is a real stake in optogenetic translation between culture scales. Cell behavior changes across scales are a major limitation to bringing a strain and production process to the next level. Indeed, each device at each scale has its unique characteristics, in terms of geometry, illumination input, cell exposure to light, etc. Therefore, to anticipate those challenges between larger scales, we can already start to investigate discrepancies between lab-scales devices to anticipate larger-scale challenges.

For this, we are now armed with four lab-scale illumination devices I have made during my PhD: the OptoBox, the OptoTubes, the eVOLVER and the OptoFlasks. In the next chapter, I will present the strain constructions leading to the optogenetic control of beta-carotene

production in *S. cerevisiae*. Then, we will discuss using this strain to test culture scales and the impact of the different optogenetic implementations in those devices.

Bibliography

1. Pouzet S, Banderas A, Bec M Le, Lautier T, Truan G, Hersen P. The promise of optogenetics for bioproduction: Dynamic control strategies and scale-up instruments. *Bioengineering*. 2020;7(4):1-17. doi:10.3390/bioengineering7040151
2. Rullan M, Benzinger D, Schmidt GW, Miliadis-Argeitis A, Khammash M. An Optogenetic Platform for Real-Time, Single-Cell Interrogation of Stochastic Transcriptional Regulation. *Mol Cell*. 2018;70(4):745-756.e6. doi:10.1016/j.molcel.2018.04.012
3. Chiron L, Bec M Le, Cordier C, et al. CyberSco . Py an open - source software for event - based , conditional microscopy. *Sci Rep*. Published online 2022:1-12. doi:10.1038/s41598-022-15207-5
4. Gerhardt KP, Olson EJ, Castillo-Hair SM, et al. An open-hardware platform for optogenetics and photobiology. *Sci Rep*. 2016;6(June):1-13. doi:10.1038/srep35363
5. Bugaj LJ, Lim WA. High-throughput multicolor optogenetics in microwell plates. *Nat Protoc*. 2019;14(7):2205-2228. doi:10.1038/s41596-019-0178-y
6. Richter F, Scheib US, Mehlhorn J, et al. Upgrading a microplate reader for photobiology and all-optical experiments. *Photochem Photobiol Sci*. 2015;14(2):270-279. doi:10.1039/c4pp00361f
7. Datta S, Benman W, Gonzalez-Martinez D, et al. High-throughput feedback-enabled optogenetic stimulation and spectroscopy in microwell plates. *bioRxiv*. Published online 2022. doi:10.1101/2022.07.13.499906
8. Duplus-Bottin H, Spichy M, Triqueneaux G, et al. A single-chain and fast-responding light-inducible cre recombinase as a novel optogenetic switch. *Elife*. 2021;10:1-52. doi:10.7554/eLife.61268
9. Wong BG, Mancuso CP, Kiriakov S, Bashor CJ, Khalil AS. Precise , automated control of conditions for high- throughput growth of yeast and bacteria with eVOLVER. *Nat Publ Gr*. 2018;36(April). doi:10.1038/nbt.4151
10. Olson EJ, Hartsough LA, Landry BP, Shroff R, Tabor JJ. Characterizing bacterial gene circuit dynamics with optically programmed gene expression signals. *Nat Methods*. 2014;11(4):449-455. doi:10.1038/nmeth.2884
11. Fernandez-Rodriguez J, Moser F, Song M, Voigt CA. Engineering RGB color vision into Escherichia coli. *Nat Chem Biol*. 2017;13(7):706-708. doi:10.1038/nchembio.2390
12. Steel H, Habgood R, Kelly C, Papachristodoulou A. In situ characterisation and manipulation of biological systems with Chi.Bio. *PLoS Biol*. 2020;18(7):1-12. doi:10.1371/journal.pbio.3000794
13. Bertaux F, Sosa-Carrillo S, Gross V, et al. Enhancing bioreactor arrays for automated measurements and reactive control with ReacSight. *Nat Commun*. 2022;13(1):1-12. doi:10.1038/s41467-022-31033-9
14. Eppendorf DASbox Mini Bioreactor System. Published 2022. https://www.eppendorf.com/product-media/doc/en/788453/Fermentors-Bioreactors_Poster_Microbiome_Standardizing-Microbiome-research.pdf
15. Culture Biosciences Website. <https://www.culturebiosciences.com/applications-cell->

- culture
16. Zhao EM, Zhang Y, Mehl J, et al. Optogenetic regulation of engineered cellular metabolism for microbial chemical production. *Nature*. 2018;555(7698):683-687. doi:10.1038/nature26141
 17. Raghavan AR, Salim K, Yadav VG. Optogenetic Control of Heterologous Metabolism in *E. coli*. *ACS Synth Biol*. 2020;9(9):2291-2300. doi:10.1021/acssynbio.9b00454
 18. Photobioreactor wikipedia page. <https://en.wikipedia.org/wiki/Photobioreactor>
 19. Masojídek J, Sergejevová M, Malapascua JR, Kopecký J. *Algal Biorefineries*. Vol 2. (Prokop A, Bajpai RK, Zappi ME, eds.). Springer International Publishing; 2015. doi:10.1007/978-3-319-20200-6
 20. Kumar S, Khammash M. Platforms for Optogenetic Stimulation and Feedback Control. *Front Bioeng Biotechnol*. 2022;10. doi:10.3389/fbioe.2022.918917

5. CHAPTER 2 – The making of a strain

The last chapter presented the instrumentation necessary to carry out optogenetics at different lab scales. This chapter details how the “opto-beta-carotene” strain was constructed, the technical and theoretical problems that arose, and experiments that were carried out to investigate the behavior of the strain that we observed at different steps of strain development.

I will detail here the construction of 2 strains:

The first strain, the **slow-opto-beta-carotene** was the one I worked with during the first part of my PhD, which successfully produced beta-carotene under optogenetic control. It produced however only in specific conditions that made it hard to efficiently work with, but which raised interesting questions in terms of resource allocation in cells. I will present here its genetic makeup, and its specific slow production characteristics that made it hard to work with. The initial genetic design was then questioned, leading to the production of the second strain.

The second strain was developed from the previous first slow optogenetic producer strain. In contrast to the previous strain, it proved to be effective in standard lab conditions, making it ideal to study its production dynamics easily. With such a functional strain, we will then be able to investigate the impact of culture scale and device on its controllability and performance, which will be discussed in the next chapter.

5.1. Strain construction

To construct a strain in which beta-carotene production is induced by light, we used the EL222 opto-EXP optogenetic system, changed the GFP reporter to an RFP, and connected the optogenetic system to the beta-carotene heterologous pathway using the pC120 optogenetic promoter.

5.1.1. Optogenetics

After a few tries with the CRY2-CIB1 and the PHY-PIF optogenetic systems, we quickly settled with the EL222 optogenetic system (Fig. 57) which showed the best activation range and dynamics. One big advantage of the EL222 optogenetic system compared to the others is the fact that it is a single-component system (that then dimerizes), which does not require exogenous cofactors (like phycocyanobilin for PHY-PIF) and was shown to be very effective in yeast as shown in Zhao *et al.* 2018¹. For this, Prof. Jose Avalos kindly agreed to send the EL222-based optogenetic systems to the lab.

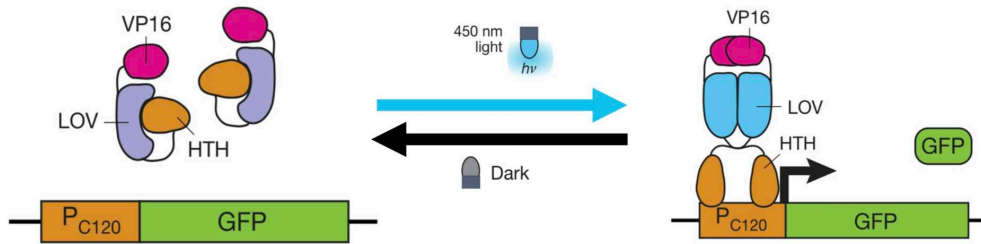


Figure 57. *The EL222 optogenetic system*, where light activates the production of GFP reporter. The EL222 light-activated transcription factor uncages its DNA binding domain (HTH) upon blue illumination, allowing it to dimerize and bind to its cognate pC120 promoter to activate the transcription of the downstream genes.

We remind briefly here that the EL222 optogenetic system from *Erythrobacter litoralis* consists in a light-activated transcription factor that dimerizes upon blue illumination. When blue light is present, the FADH cofactor is excited and binds covalently to the protein, triggering a change in conformation that uncages the Helix-Turn-Helix (HTH) DNA binding domain from the Light-Oxygen-Voltage (LOV) domain. There, the protein dimerizes, binds to the pC120 promoter and the VP16 transactivational domain interacts with the RNA polymerase to favor transcription of the gene under the control of this promoter. In this strain, the downstream gene is simply a Green Fluorescent Protein (GFP) (Fig. 57). This system is inserted in the auxotroph CEN.PK2-1C *Saccharomyces cerevisiae* strain at the *his* locus in its genome, via homologous recombination. The inserted cassette is *his3ΔI::(pPGK1-EL222, pC120-GFP, CgHIS3)*, selected on medium lacking histidine.

5.1.2. Changing to mCherry

Spectral overlaps. First, the GFP reporter of the optogenetic activation was changed to a mCherry red fluorescent protein (RFP). Indeed, we realized quickly, while imaging the cells under the microscope, that the production of beta-carotene in cells led to the production of small foci (lipid droplets) containing beta-carotene², which emitted strongly in the GFP channel. This resulted in a spectral overlap, where the GFP signal, reporter of the optogenetic activation, was mixed up with the signal coming from the beta-carotene production. To alleviate this issue, we used the mCherry RFP, imaged in the RFP channel.

Cloning. We edited the GFP directly in the genome of a transformed strain. Based on Laughery *et al.* 2015³ (Fig. 58), we designed a gRNA targeting the GFP gene (see also protocol 8.9.3). Besides, we designed a template sequence (repair strand) with the mCherry gene placed between two homology sequences corresponding to the pC120 promoter and the tADH1 terminator of the GFP open reading frame (ORF). Using the yeast transformation LiAc protocol from Gietz & Schiestl 2007⁴ (protocol 8.9.4), both the plasmid and the template strand are transformed. Plasmid selection is performed on synthetic minimal medium (protocol 8.9.1) lacking uracil. Once transformed, cas9 is expressed, hybridizes with the gRNA and targets the designed locus to trigger a double-strand break. Upon this, the homologous recombination (HR) machinery acts, and uses the repair strand as a template strand for the repair, thus inserting, deleting or replacing the sequence of interest. If HR or non-homologous end joining

(NHEJ) machinery make the sequence back to what it originally was, then cas9 will cut repeatedly (negative selection). This is the powerful negative selection by cas9. If NHEJ repairs with a mistake, cas9 might not cut anymore and this will create a false positive. By screening transformants, good clones can rather easily be identified, sequenced and tested experimentally.

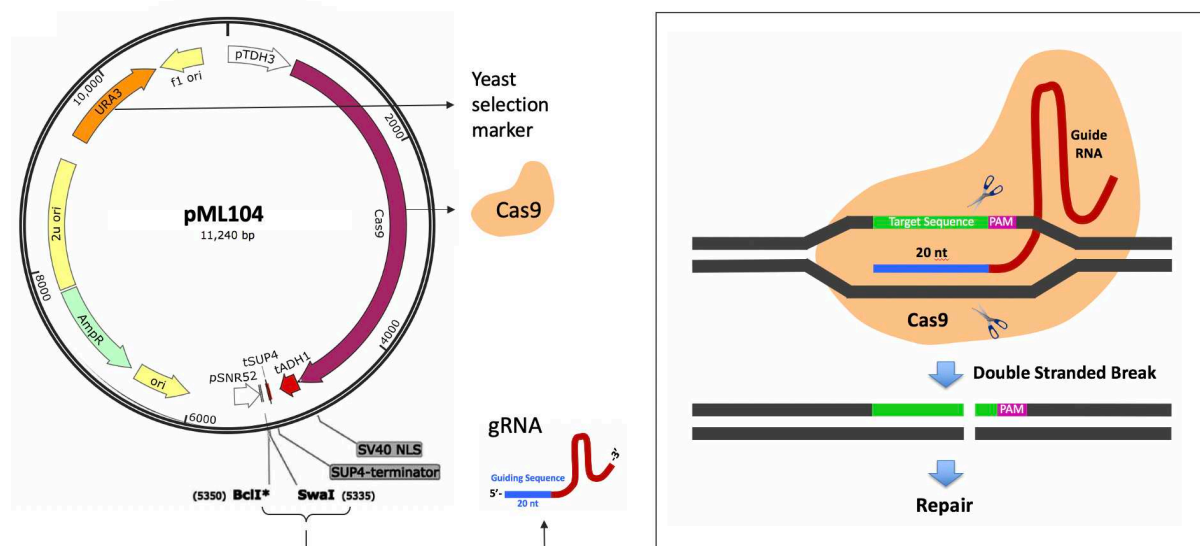


Figure 58. **CRISPR in yeast** is based on the use of the portable Cas9 protein and the designed gRNA transformed and selected via the pML104 plasmid (left) containing also a URA3 selection marker. After transformation, the cas9 protein interacts with the gRNA to generate a double-strand break which will prompt the homologous repair machinery to act and use a repair strand as a template, thereby inducing an insertion, deletion, or modification. If the repairing generates the original unmutated sequence, CRISPR will cut again. System developed by Laughery et al. 2015³, image courtesy: Fabien Duveau.

5.1.3. Beta-carotene

Beta-carotene is a terpene molecule of importance for its sun-protectant and antioxidant properties. More importantly, it is the precursor to vitamin A and represents the major source of pro-vitamin A from the human diet. Besides, its coloring qualities are significant for the food industry, but they especially make this molecule easy to detect when produced, making it a widely used proxy for bioproduction studies. Besides, focusing on improving beta-carotene bioproduction in microorganisms and in yeast, in particular, is relevant as its production rests on the mevalonate (MVA) pathway (Fig. 59) and precursors that are also of importance for the production of certain drugs (more details in the introduction).

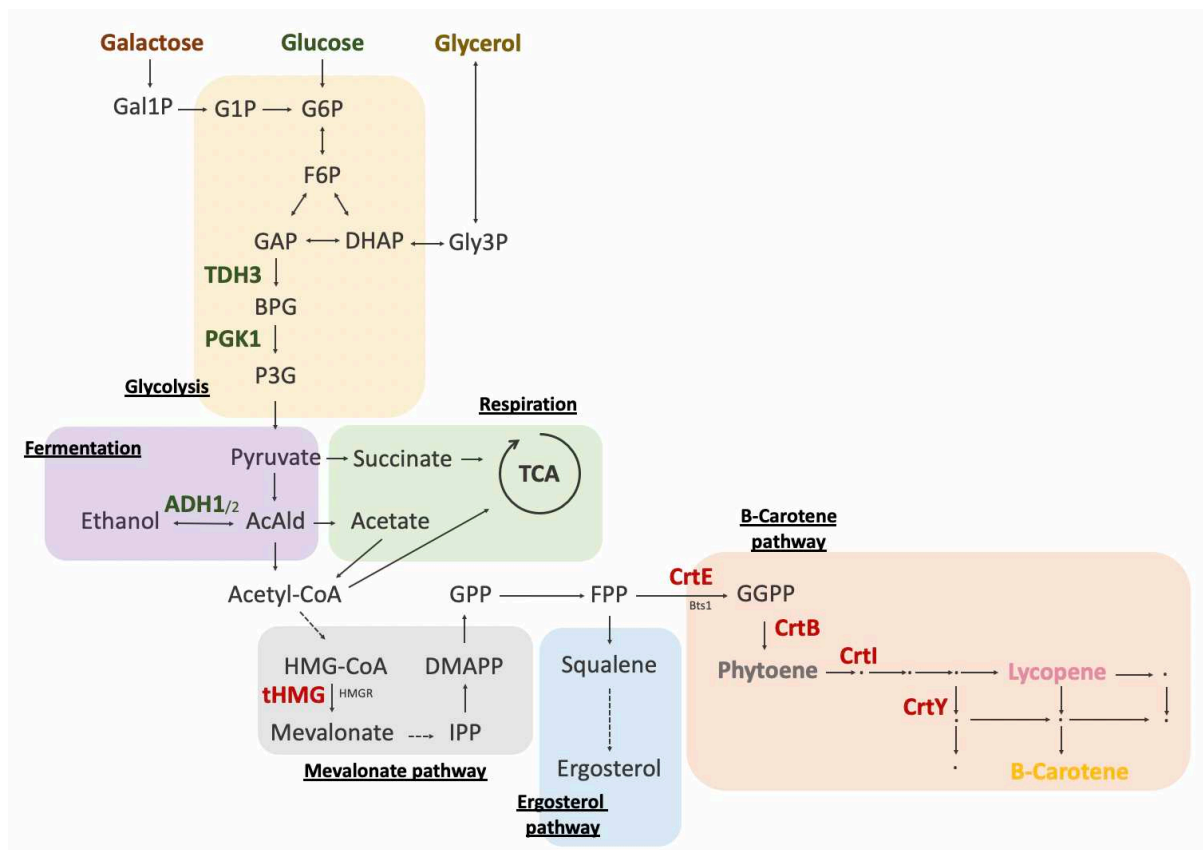


Figure 59. **Beta-carotene production in yeast.** To produce beta-carotene, glucose (or glycerol or galactose) is turned into pyruvate via the glycolysis; From there, it is the pool of acetyl-coA that is key to enter the mevalonate (MVA) pathway, leading to the production of the GGPP precursor. GGPP is turned into first phytoene, and then other carotenoids including the re-color lycopene, and finally into beta-carotene. To carry out these reactions, our design includes CrtE and tHMG which boost the production of GGPP by increasing the carbon flux entering the MVA and the FPP conversion to GGPP, and the final beta-carotene pathway reactions carried out by CrtYB and CrtI, fused into CrtYBekI in the initial design we used.

Genetic engineering. Although the beta-carotene production pathway was presented in the introduction of the thesis, we take the opportunity here to elaborate a bit more on the chemical species produced and precursors along the pathway. The design we used originates from Rabeharindranto *et al.* 2019⁵.

It consists of two modules:

- Boosting the production of precursors using the tHMG (facilitates the conversion of HMG-coA to MVA) and CrtE (FPP conversion to GGPP) enzymes, inserted at the *dpp1* locus, which knocks out the production of DPP1p (which channels FPP flow towards farnesol production).
- Converting the GGPP precursor into beta-carotene thanks to the CrtYBekI trifusion enzyme, inserted at the *ho* locus. While the CrtYB bifunctional enzyme is a naturally fused bicatalytic enzyme, it was proposed that with the appropriate “ek” linker, a trifusion enzyme could be more efficient to produce beta-carotene thanks to the coordinated localization of the 3 catalytic domains⁵.

Origins. The authors in Rabeharindranto *et al.* 2019⁵ used a strain where all this design is under the control of pGAL1-10 promoters, in a $\Delta gal80$ strain (the antagonist of the GAL4 transcription factor, activating pGAL1-10). This way, the system is poorly activated during active growth in glucose due to the glucose repression mechanism at the pGAL1-10 promoters via MIG1p, but turns on after the exponential pause, when glucose repression is alleviated. With this design, beta-carotene production was increased with the trifusion compared to the natural bifusion + CrtI on its own⁵. Therefore, also given the simplicity of the design (one gene instead of two), we naturally decided to turn to this design.

Beta-carotene quantifications were made in different ways. Initially, we use the visual cue provided by beta-carotene to estimate the production. When real quantifications became required, we turned to HPLC. Then, as more throughput was needed, we adapted the protocol from Reyes & Kao 2018⁶ which allowed us to easily make beta-carotene production estimations using a bead-beater to extract beta-carotene in dodecane, and measure the characteristic beta-carotene absorbance using a plate-reader. (see [protocol 8.9.5 and next chapter](#)).

5.1.4. Opto-beta-carotene

To optogenetically control beta-carotene production in the yeast *S. cerevisiae* ([Fig. 60](#)), we proceeded in three steps:

1. Make the opto-EXP strain mCherry (as detailed before).
2. Insert booster genes at the *dpp1* locus with constitutive promoters. We adapted the DNA material from Rabeharindranto *et al.* 2019⁵ to make the insertion using also CRISPR, targeting the DPP1 gene, so that no antibiotic selection marker is needed for the selection (and no need for additional transformation for marker removal afterward).
3. Insert CrtYBekI under pC120 promoter at the *ho* locus. For this, the plasmid containing CrtYBekI in the original paper's library was modified to replace the pGAL1-10 promoter with the pC120 promoter isolated from Zhao *et al.* 2018¹ plasmids containing the EL222 optogenetic system. The promoter was cloned in CrtYBekI plasmid using Gibson Assembly⁷.

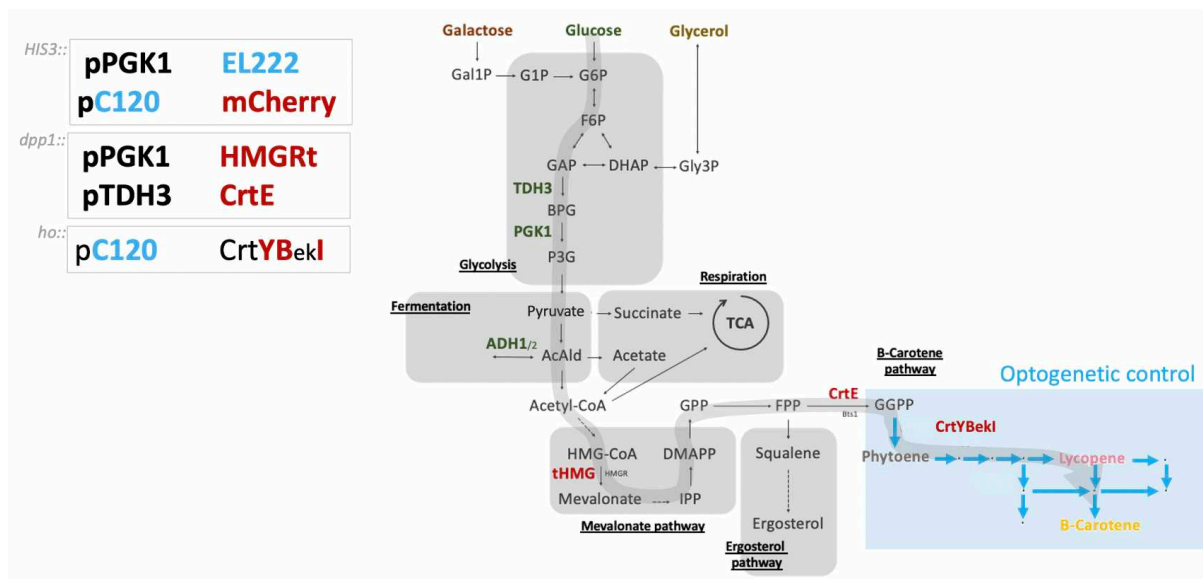


Figure 60. Setting beta-carotene production under optogenetic control. For this, the *CrtYBekI* enzyme was put under the *pC120* optogenetic promoter in the *mCherry* optogenetic strain. There, the last step of GGPP to beta-carotene production can only occur when blue light shines on EL222, activating the transcription of *CrtYBekI*. The protein acts as a valve, controlling the beta-carotene production.

After DNA extraction, PCRs and sequencing to verify strain construction, the resulting strain was validated in terms of genetics. We sought to characterize this strain, which we will refer to as “slow producer” in the following sections.

5.2. A slow producer strain

Once the strain built, we set out to characterize it, and investigate to what extent we could control its production using light. We will see here the results showing the peculiar behavior of this strain that does not produce much under standard growth conditions.

5.2.1. Early observations

Agar plates are the most basic way to observe the strain. It is easy to expose them to ambient light, or just protect them from light using aluminum foil. **That is the way we started and quickly found that, at room temperature, production was indeed light dependent.** We also found that the production varied with the type of carbon source we used. Indeed, YPD (glucose) plates are used to cultivate strains and YPG (Glycerol) plates are typically used to thaw strains from stocks stored at -80°C . We saw that production was higher on glycerol compared to that on glucose. However, the light control was sharp: no production at all was observed in the absence of light (Fig. 61-Left).

Then, **liquid cultures** were set up in eVOLVER to confirm these results, with or without light, in YPD and YPG, and at standard (30°C) or low (23°C) temperatures. Interestingly, we not only confirmed the previous results but also found that temperature impacted the production as well. In liquid cultures, this “carbon-source and temperature production phenotype”

appeared even stronger than on agar plates: there was no detectable production even in YPD, while it was the case using agar cultures (Fig. 61-Right). There, production occurred only in YPG, when illuminated (only the side-LED of eVOLVER here), and at low temperature, *i.e.*, in an eVOLVER-controlled 23°C.

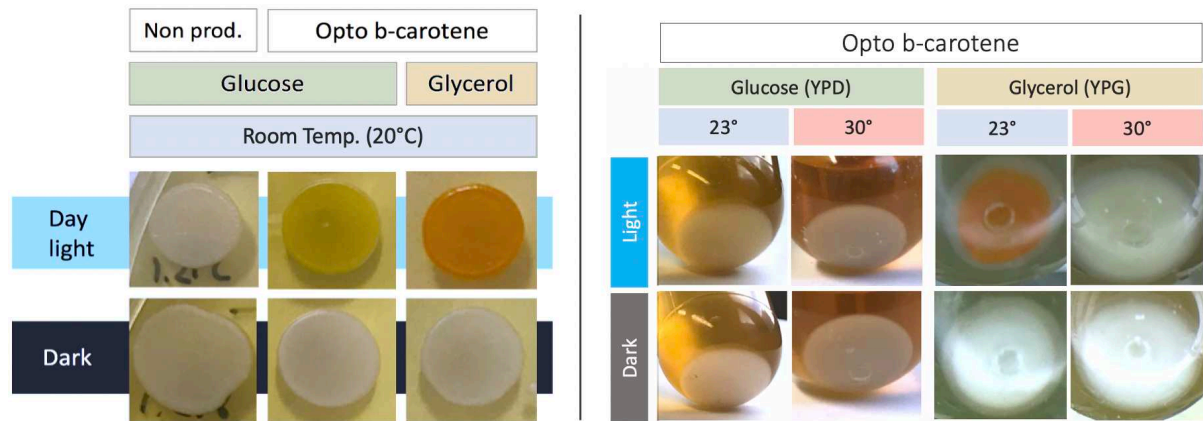


Figure 61. *Light-controlled beta-carotene production on agar (left) and liquid cultures (right). The opto-beta-carotene strain was grown on two carbon-sources (glucose and glycerol), at different temperatures (room temperature / 23°C and 30°C) and with or without light. Light-induced production appeared efficient, but the general production profile appeared surprisingly weak or non-existent in fast-growing conditions, we therefore referred to the strain as slow-opto-beta-carotene.*

In definitive, we found 3 parameters that appeared to influence the production of beta-carotene: light, carbon-source, and temperature. This result is interesting in manifolds. First, it means that the optogenetic control is successful and that our initial goal to control the production of beta-carotene using light was achieved. Second, we know that the growth in glycerol and at low temperature influence cell physiology and most importantly, growth rate is reduced in those conditions compared to growth in YPD and at 30°C. Therefore, we can start to appreciate a trade-off between growth and production here.

With the throughput offered by the eVOLVER platform, we decided to further investigate the production dynamics of this strain and find the best production conditions.

5.2.2. Multidimensional analyses with eVOLVER

Experiment setup. In order to further investigate the influence of each parameter on production, we sought to gradually vary parameters and screen for various culture parameter combinations. We set the carbon-source to glycerol for all experiments here, as it is the only one that appeared permissive to production with this strain in liquid cultures, even though it makes for much longer experiments (1 to 3 weeks cultures!). Besides illumination and temperature, another parameter we varied was the stirring in eVOLVER. Below is shown an experiment with varying temperature (23°C and 30°C), illumination (0, 2h, 10h and 23h every 24h - defining the period), and stirrings (100 and 150 here -but the maximum is actually 255). After almost 3 weeks of culture (19 days), we checked the resulting culture color, the pellet colors, the resulting optical density, and acquired images in Bright Field (BF), in the red (RFP)

channel to see the mCherry, and the GFP channel to see beta-carotene accumulation in cells (Fig. 62).

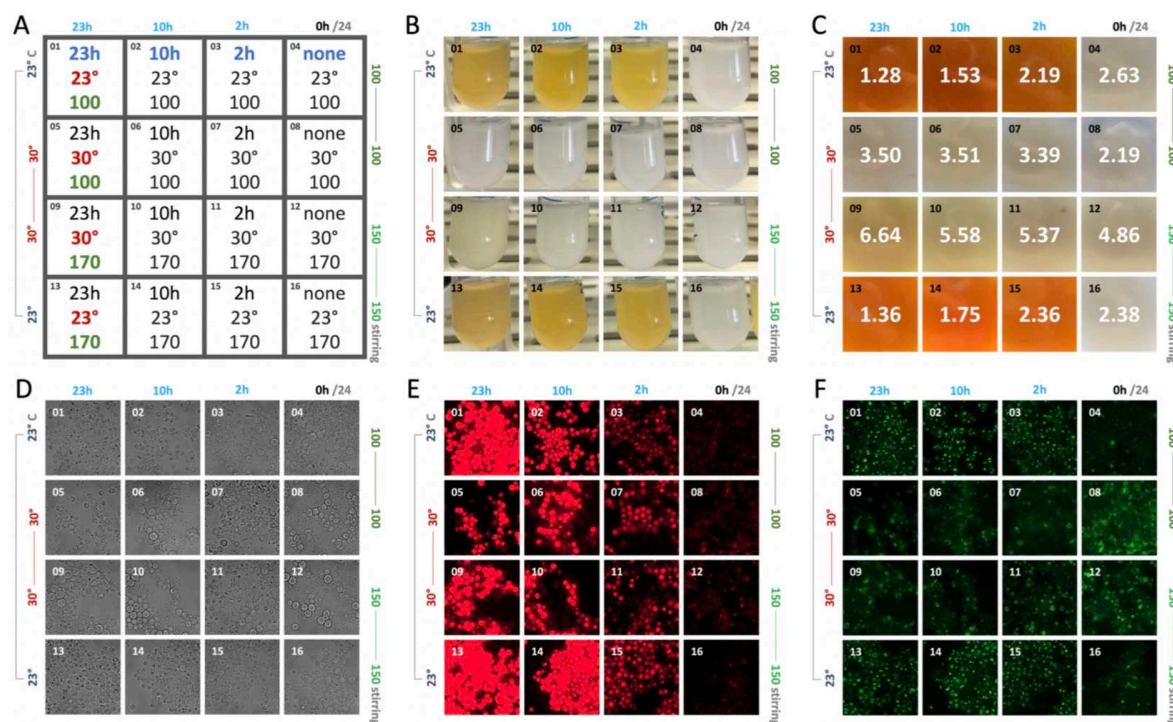


Figure 62. *Multi-dimensional testing with eVOLVER.* To further characterize the slow opto-beta-carotene strain, experiments were carried out in glycerol. The experiment design was set to vary culture temperature, stirring intensity and illumination time over a 24h period using the side-LED of the eVOLVER units (A). After 2.5 weeks of culture in eVOLVER, we captured the culture aspect (B), pellet color and optical density (C) and acquired microscopy image (60x): snapshots in bright field (D), in the RFP channel to witness the activation of the optogenetic system via the mCherry reporter (E), and the GFP channel to visualize the fluorescent beta-carotene carrying lipid droplets in cells (F).

Light was confirmed strictly necessary for beta-carotene production, comforting the fact that control by light is efficient, and does not seem leaky at all. Interestingly, a small amount of light (2/24h) appeared enough to activate production. At low temperature, the impact of light on cell density seems quite detrimental, it is to be determined if this is because of a higher production of other physiological reasons. In non-producing conditions (at 30°C), interestingly, illumination appears beneficial for cell density.

Stirring displayed an overall beneficial effect on cell density: more stirring led to high cell density in all conditions. Indeed, more oxygenation can be important for growth, and it could even impact production (see chapter 3 for more details). Since glycerol is respired by cells, diluted oxygen, which can be improved via stirring, can become significant.

Temperature again was shown to impact beta-carotene production, with only low temperature being permissive to production. Here we chose 23°C since this is slightly above room temperature (eVOLVER can only heat up) and can therefore be controlled. It would be interesting to test intermediate temperatures to see how production responds (see below, section 5.2.3). Temperature also impacted cell physiology, even without light: while cells grown at 23°C present a classical yeast cell phenotype in BF images, cells grown at 30°C appear swollen, and lots of cell debris are present in the medium.

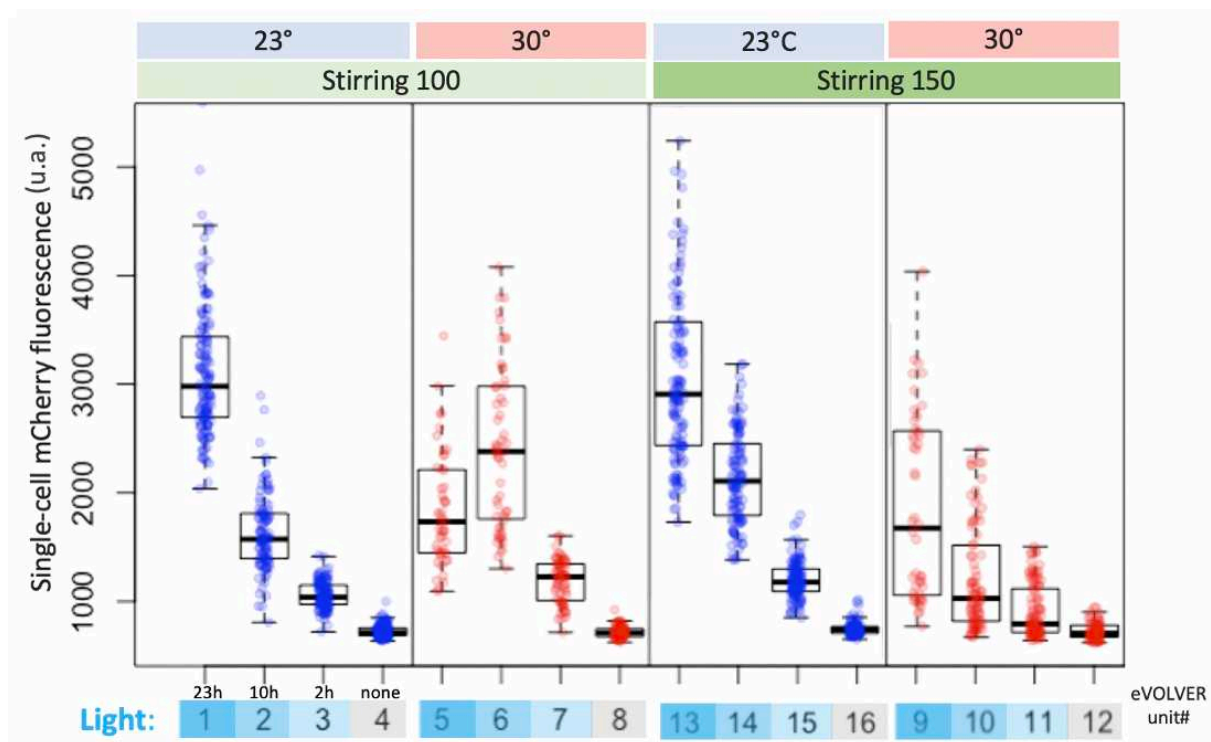


Figure 63. **Optogenetic activation given culture conditions.** mCherry is under the pC120 promoter and therefore acts as a proxy for optogenetic activation. Displayed data are quantifications from the previous figure's panel E. For each image, 50 cells were quantified using ImageJ – fluorescence in arbitrary units. Illumination corresponds to 23, 10, 2 or 0 hours of illumination over 24h periods using the side-LED. Temperature and stirring were kept constant in eVOLVER.

Optogenetic activation. Quantification from RFP images showed that optogenetic activation was light-dependent, but also temperature-dependent (Fig. 63). This could be due to the accumulation and dilution of mCherry in cells growing at different speeds. However, it remains difficult to acknowledge this, given that cells growing at different speeds may be at different phases of their growth profile, and therefore different medium compositions and cell aging can impact this phenotype.

Beta-carotene production detected in the GFP channel images concurred with the color observations. While quantification by image analysis did not yield relevant results because of the localization of beta-carotene in droplets, one can clearly see that fluorescent droplets are only visible in orange-colored cultures.

To conclude on this 3-week culture experiment, we found that only 2h of light per day was sufficient to activate production and that without light, in a sharp manner, cells do not produce beta-carotene. Temperature effect was shown to impact not only production, but also cell physiology, besides the fact that cell mass is increased at higher temperature. However, interpreting this effect can prove challenging. Indeed, comparing cell physiology at a single time point while the growth rate must be different would result in biases. Those results would therefore require not only to be reproduced, and beta-carotene properly quantified here, but also to find how to make measures that are well comparable between conditions.

5.2.3. Temperature Effects

Setup. To understand better the relationship between temperature and beta-carotene production, in an attempt to vary the growth rate at different ends of the temperature spectrum, we tried production under a range of different temperatures. We again took full advantage of the eVOLVER system to test simultaneously 17 different growth temperatures, from 20 to 35°C. It is generally recognized that *Saccharomyces cerevisiae* has its peak growth at 30°C⁸, after which the heat shock response is activated, and growth rate decreases because of stress. Below the 30°C optimum, growth rate also decreases. Growth was carried out for 2 weeks, in YPG medium, at different temperatures, with 12/24h illumination and stirring set to 100. After this time, cultures were pelleted, and pictures of the pellet colors were taken (Fig. 64A).

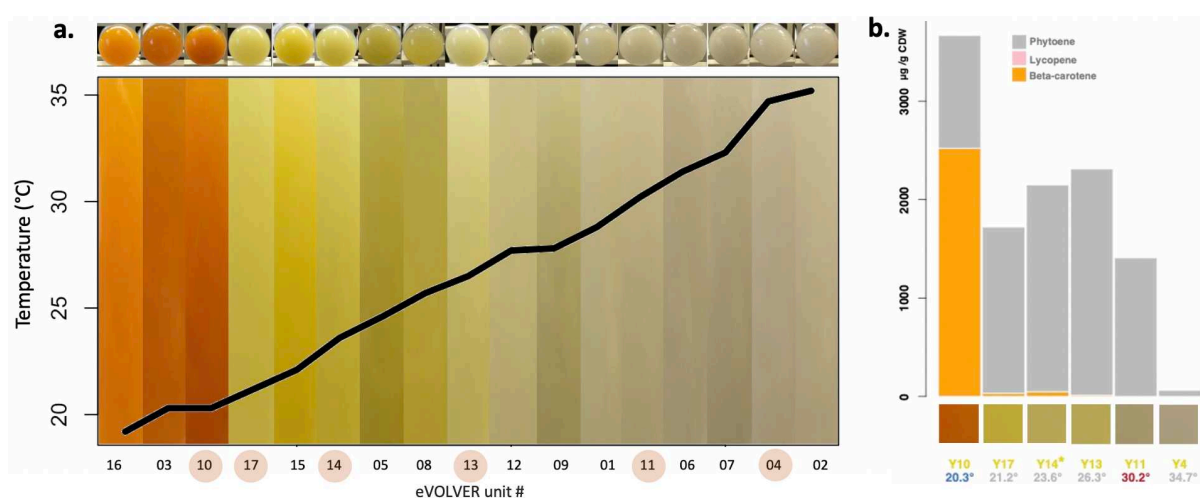


Figure 64. **Temperature effect on beta-carotene production.** The slow opto-beta-carotene strain was set to grow in eVOLVER in glycerol culture medium over two weeks at different temperatures with a 12h hour illumination over 24h periods and stirring of 100. At the end of the culture, cell pellets colors were taken as pictures and assembled to display pellet color as a function of the temperature (eVOLVER units reordered given temperature). Highlighted eVOLVER unit numbers correspond to samples that were used for HPLC quantification (right).

Results. The output production pattern is very clear: the lower the temperature, the higher the production. Interestingly, the temperature culture difference between eVOLVER unit 10 and 17 is only 1°C (20.3 and 21.2°C respectively), but there is a clear difference in beta-carotene production in those two conditions, which is confirmed by the HPLC quantification (Fig. 64B). We have seen in the previous experiment that beta-carotene production was possible at 23°C after a 3-week experiment, such that it is likely that beta-carotene production would happen at some point at higher temperature: meaning this color would change in time. Those results capture however a single time point in the production process at different temperatures.

TESTING OTHER STRAINS

We asked if this effect of temperature was specific to our strain, or if it was a property of the pathway and design that we used. To answer this question, we decided to use the original strains from Rabeharindranto *et al.* 2019⁵, and have them grow and produce at high and low temperatures (here, at 30°C in the incubator, or at room temperature – 20°C). We tested the original CrtYBekI trifusion strain, which has the same design compared to our strain except the promoters controlling carotenogenic genes are pGAL1-10; and we tested another strain, which only produces lycopene via the CrtBekI enzyme. Strains were grown in YPD or in YPGal (Galactose 2%) for 48h and photographed and quantified using HPLC (Fig. 65).

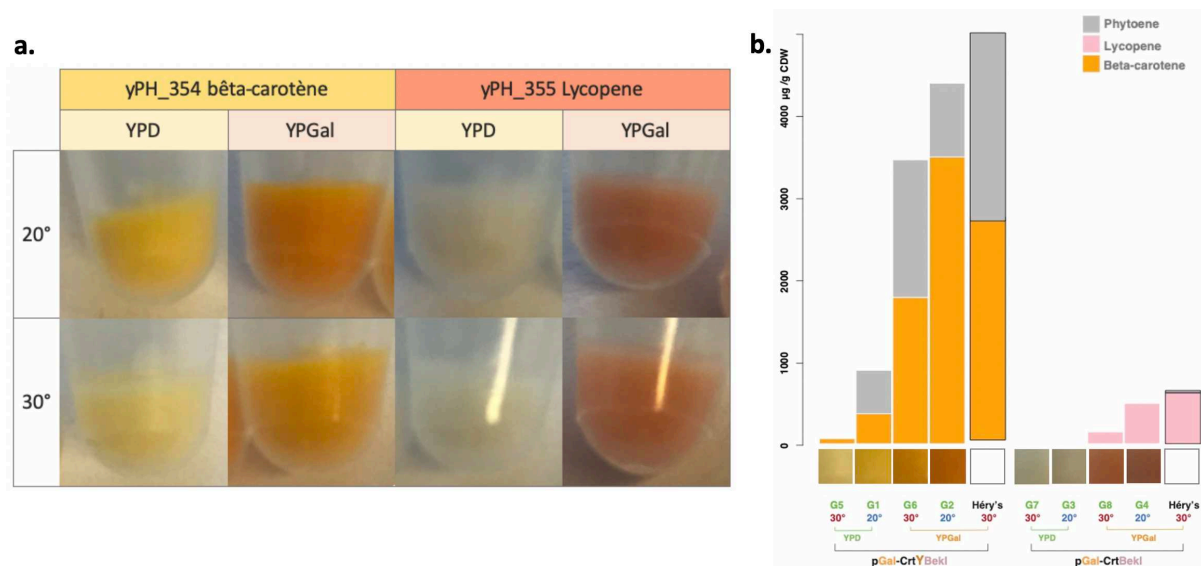


Figure 65. **Galactose inducible strains** originating from Rabeharindranto *et al.* 2019⁵ were used to test the effect of the culture temperature and medium composition on other strains than ours. We compared 20 and 30°C and culture in glucose (fast growing) and galactose (slower growing). Cells were grown for 2 days and pellet pictures were taken. Besides, samples were also quantified using HPLC (b.). Note that those strains are galactose inducible, such that the production dynamics are hardly comparable to our optogenetic strain, but the effect of culture temperature on production is nevertheless undeniable for beta-carotene production, allowing the strain from the original paper⁵ to produce even more than what was indicated in the paper. The lycopene strain (yPH_355) does not have the CrtY catalytic activity, such that lycopene cannot be converted to beta-carotene.

We observed the same profile as before, showing that this effect is not a specificity to our strain but a more general phenomenon: those strains too produce more beta-carotene and lycopene at low culture temperature. This is the case in YPD and YPGal for the beta-carotene strain, and also for the lycopene strain, which actually failed to produce in YPD, probably given its weaker overall production (Fig. 65B). We can note here that, compared to the production results from Rabeharindranto *et al.* 2019⁵, cells produced more (content per cell) in 2 days of cultures compared to 3 days in the paper.

Although those results comfort us in thinking that this temperature effect is not an artifact, they do not explain why our optogenetic strain controlling beta-carotene production does not produce in standard growth conditions, *i.e.*, in YPD and at 30°C.

5.3. Questioning the phenotype

This “slow producer” strain is indeed efficient to control beta-carotene production by light. However, its **slow production dynamics make it particularly difficult to work with**: indeed, long experiments limit throughput. They are also more prone to contamination, and to computer crashes. Besides, and most importantly, we know of beta-carotene producer strains that do produce well in glucose and at standard cultivation temperature (30°C), although beta-carotene production in those strains is controlled with other genetic systems, constitutively or via other inducers.

Therefore, we started to question the design used for the strain construction. We tested **two of the simplest hypotheses that could explain this slow production**: the optogenetic control could be too weak, or the trifusion design (which is specific to Rabeharindranto *et al.* 2019⁵, and not a generally used design) could have an impact on production dynamics.

5.3.1. Expression strength from pC120

First, we questioned the responsibility of the optogenetic system: optogenetic activation could be rather weak (Zhao *et al.* 2018⁹ and quantifications in chapter 3) and not allow for production in standard culture conditions. Indeed, during fast growth, the produced enzymes and few beta-carotene molecules could be too quickly diluted between newly formed cells and fail to accumulate, such that beta-carotene would not be detected in samples.

We have seen that Rabeharindranto *et al.* 2019⁵'s strains are also temperature and c-source sensitive. However, the role of pGAL1-10 promoter, which is inducible and strongly subjected to metabolism, is rather unclear. Consequently, we decided to replace the pC120 promoter in our optogenetic strain with constitutive promoters, *i.e.*, pADH1, pTDH3 and pTEF1. To change pC120 to the constitutive promoters, a CRISPR guide was designed to target pC120, and repair strands were produced thanks to the MoClo promoter library.

The Molecular Cloning system (MoClo) was published by Lee *et al.* 2015¹⁰ as the “Yeast Toolkit” (Fig. 66, protocol 8.9.2). This toolkit consists of an array of parts (promoters, coding sequences, terminators, connectors, etc.) that can be assembled in a quick and modular fashion. The MoClo is based on the Golden Gate Assembly system, using the class II restriction enzymes BsaI and BsmBI which cut after their recognition sites such that overhangs can be intentionally designed, here to make the system modular. The combination of those two restriction enzymes allows for the construction of plasmids carrying simple parts (level 0), carrying an assembled cassette (promoter-CDS-terminator – level 1), or an assembly of multiple cassettes (level 2), with various plasmid backbone possibilities. For our purposes, pTDH3 and pTEF1 were cloned from the MoClo, while the weak constitutive promoter pADH1 was cloned from a WT strain and included in the MoClo library as a new part for later use.

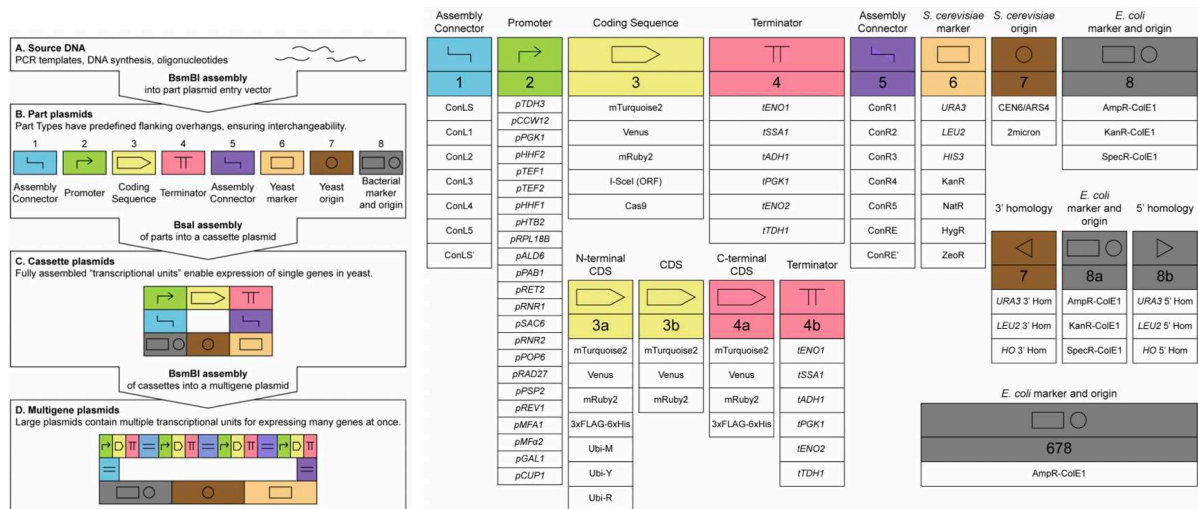


Figure 66. The *Molecular Cloning (MoClo) Yeast Toolkit*¹⁰ consists in a library of standardized parts that are assembled using Golden Gate assembly (using type II restriction enzymes). Those parts can be assembled in plasmids containing single gene cassettes and be further combined into multigene plasmids using standardized simple reactions.

Results. Observations on agar plates (Fig. 67) showed that, by using constitutive promoters instead of the optogenetic pC120 promoter, we recovered production in YPD but only at low temperature and that production with strong promoters might be higher on YPG, except for pADH1, a rather weak promoter that seems to display even less production than pC120 in YPG at 20°C. These transformations and observations were carried out with or without the presence of the optogenetic system in the genome, and the results were identical (not shown).

opto	CrtE - tHMGR	CrtYBekI	yPH_	YPD		YPG	
				30	20	30	20
EXP	pTDH3-pPGK1	pC120	524				
-	pTDH3-pPGK1	pADH1	531				
-	pTDH3-pPGK1	pTHD3	532				
-	pTDH3-pPGK1	pTEF1	533				

Figure 67. Replacing the pC120 promoter in the slow-opto-beta-carotene strain, using constitutive promoters of different strengths: pADH1 is considered weak, pTDH3 and pTEF1 strong. For this, promoters from the MoClo library were used, and a gRNA targeting the pC120 promoter was designed for the cas9 to target the promoter and repair with the appropriate template strand containing the sequence of one of the three constitutive promoters. After transformation, clones were isolated, and grown on plates of different agar media (YPD or YPG) and placed at different temperatures (20 and 30°C). Colonies were then captured.

Conclusions here are relatively straightforward: even with strong constitutive promoters, we failed to recover beta-carotene production in standard growing conditions. However, we know from older papers that this should be possible: the work in Rabeharindranto *et al.* 2019⁵

is based on Verwaal *et al.* 2007¹¹, where beta-carotene is produced at relatively high and detectable levels in YPD at 30°C. Therefore, it should be possible to produce in those standard conditions.

Given those results and knowing that the major divergence compared Verwaal *et al.* 2007 made in Rabeharindranto *et al.* 2019 is the presence of the trifusion, we focused on this particular aspect of the design, and decided to deconstruct it back to the classical Verwaal *et al.* 2007 design.

5.3.2. Questioning the trifusion design

Hypothesis. In the previous HPLC quantifications, we noticed the presence of a lot of phytoene, especially in the temperature range experiment (Fig. 64). We can suggest that phytoene accumulation could be the result of a poor CrtI (phytoene desaturase) activity or low expression (see Fig. 68 for more details). The mere presence of phytoene signifies that trifusion is actually expressed since the CrtB activity is efficient. This reinforces the idea that the problem may lie with CrtI, because of its fusion in the CrtYBekI protein. It is known that CrtI can be limiting when it comes to producing beta-carotene in *S. cerevisiae*¹¹ but the large amounts of phytoene with no beta-carotene in Fig. 8 led us to wonder if the trifusion, where CrtI has been fused to CrtYB could lead to CrtI limitation in some conditions.

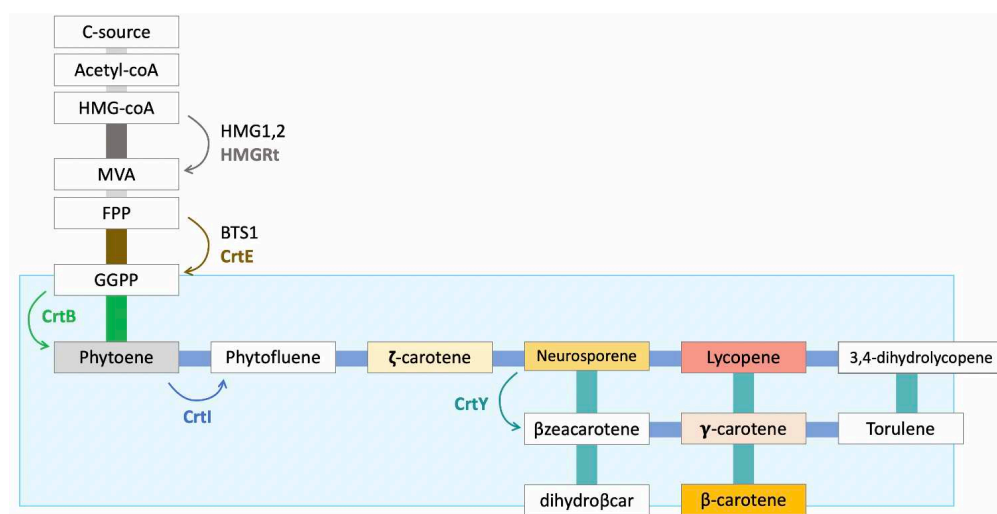


Figure 68. **Focus on the beta-carotene heterologous production pathway.** Here are displayed the specific reactions carried out by the different enzymes (colors of the links between chemical species corresponding to its enzyme). Here we see phytoene conversion to lycopene rests on the CrtI enzyme, included in the trifusion design in CrtYBekI.

To test this, the trifusion was removed from the optogenetic strain and from the constitutive producer strains as well (made in the previous section to test the effect of the promoter controlling the trifusion). For this, a gRNA targeting the “ek” linker of the CrtYBekI trifusion was designed, and a repair strand containing the tADH1 terminator, and the pTDH3 promoter was used to create two independent genes from the trifusion.

opto	CrtE - tHMGR	CrtYBekI	YPD 30	
EXP	pTDH3-pPGK1	pC120	CrtYBekI trifusion 524	CrtYB, I 2 enzymes 551
-	pTDH3-pPGK1	pADH1	531	553
-	pTDH3-pPGK1	pTHD3	532	554
-	pTDH3-pPGK1	pTEF1	533	555
			yPH_	

Figure 69. **Breaking down the trifusion design.** Since *CrtI* was suspected to be impacted by the trifusion design, the fusion was severed in the different strains (slow-opto-beta-carotene and constitutive strains). For this, a gRNA targeting the *ek* linker between the *CrtYB* and *CrtI* protein was designed and appropriate repair strands prepared from genetic material from Verwaal *et al.* 2007¹¹. After transformation and selection, the clones were cultivated in YPD (glucose) medium directly at 30°C. After an overnight culture, cells were pelleted, and pictures were taken.

The results speak for themselves: we completely restored production in YPD and at 30°C, *i.e.*, in standard culture conditions (Fig. 69). With an overnight culture, beta-carotene production can be detected with constitutive promoters and also with the optogenetic control of production.

At least **one question** arises from these results: we showed here that production is better without the trifusion with optogenetic and constitutive promoters, but the opposite conclusion was drawn with Rabeharindranto *et al.* 2019⁵'s strains and culture conditions. There, GAL promoters were used: could the pGAL1-10 confer some specific qualities making the trifusion more efficient?

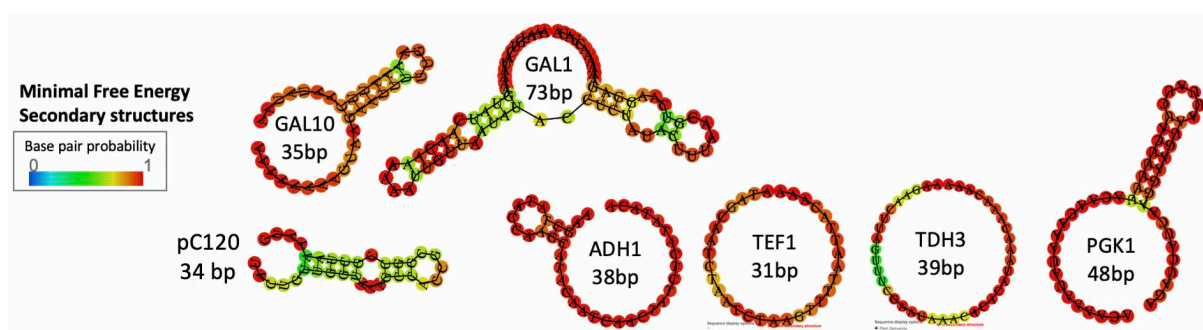


Figure 70. **5' Untranslated Regions (UTRs)** of a few genes: the UTRs were detected using transcriptomics data in JBrowse (Hypothetical for pC120), and 2D structure using RNAfold. This shows different UTR secondary structures that could impact the lifetime of the resulting mRNA.

To explain the fact that the trifusion is more efficient than the bifusion + *CrtI* when controlled under pGAL promoters, we may suggest that the one major difference with the use of a promoter may be the 5' untranslated regions (UTR) that are different for each promoter: while pADH1, pTDH3 and pTEF1 (tested here) are poorly structured and pC120 basically non-

existing, we can see that the 2D structure of pGAL1 and pGAL10 contain hairpins which may contribute to the stabilization of the mRNA and hence produce different results (Fig. 70). Another reason could be the way that GAL promoters are regulated and behave in regard to the cell physiology, such that another expression timing and strength can be more appropriate than strong constitutive expression.

5.3.3. Conclusions

We identified a limiting factor for the beta-carotene production controlled by optogenetics and finally managed to produce a strain that produces in standard growth conditions. This means from now on that we will be able to use this new strain (yPH_551) to carry out quicker experiments and start to investigate its behavior regarding growth and production more easily than before.

Although we have found a way to improve our strain and circumvented the low production issue, this solution is not completely satisfying as it does not really explain why this inefficient construction would only work at low temperature and with glycerol as carbon-source.

5.4. A new functional strain

In our previous “slow producer” strain, we broke down the trifusion protein, which produced a new strain, in which beta-carotene production is also controlled by blue light, but importantly, in which production seems to occur in standard culture conditions: in YPD medium (glucose) and at 30°C. This results in a higher growth rate, hence much shorter experiments.

After the obtention of this strain, we decided to characterize it better, verify if the light control was efficient, and how it reacted to different culture conditions.

5.4.1. Early checks

First, we checked in the OptoTubes how the strain reacted to the presence and absence of light in an overnight culture at 30°C in different growth media, to compare to the previous trifusion strain.

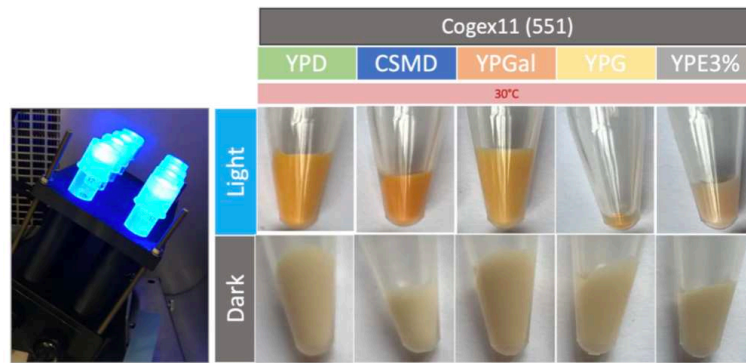


Figure 71. Testing different carbon sources with the new opto-beta-carotene strain. The strain was grown at 30°C overnight in different culture media: Rich medium (YP) with glucose 2% (YPD), galactose 2% (YPGal), glycerol 5% (YPG), ethanol 3% (YPE), or minimal medium with glucose (CSMD). Tubes were either illuminated in the OptoTubes at maximal intensity (255) or kept in the dark. After overnight culture, cultures were pelleted, and pictures taken.

We saw that the production of beta-carotene was still sharply light-dependent and that the biomass and production varied in different carbon sources, but also given the richness of the medium (YP-D, rich, versus CSMD minimal medium) (Fig. 71). In ethanol, we saw no production, probably because all carotenogenic genes except the CrtYB (under pC120) are under glycolytic promoters and glycolysis does not occur when ethanol is consumed, such that those genes are downregulated.

5.4.2. Device and illumination

Next, we tried the strain in YPD 30°C all the time, in the different optogenetic devices and with different illumination.

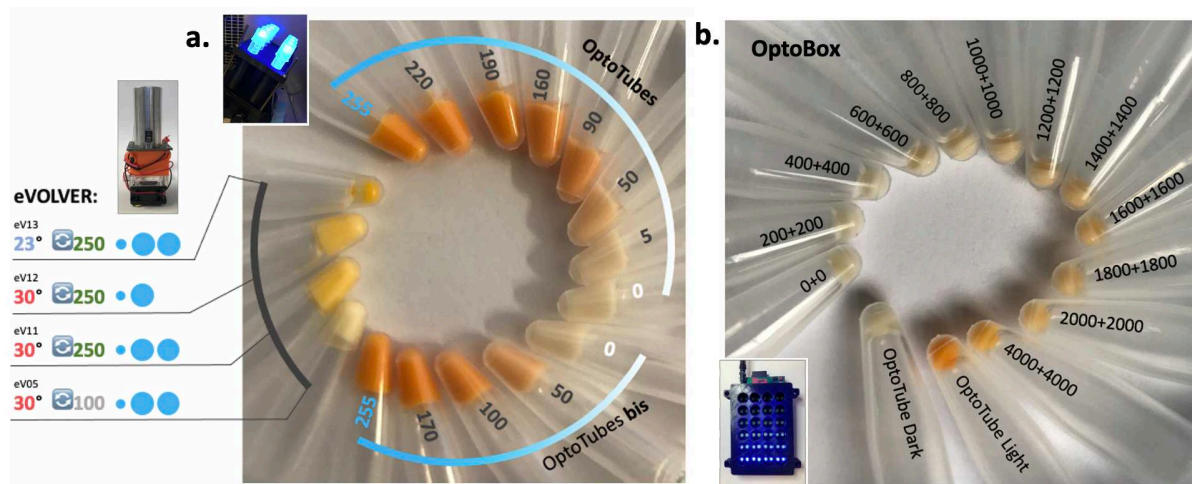


Figure 72. Testing production in the different illumination devices. Early tests of the new opto-beta-carotene strain. It was cultured in YPD with different illumination intensities in the different devices (eVOLVER, OptoTubes and OptoBox), and with different culture conditions in eVOLVER. After 24h culture, samples were pelleted, and pictures taken.

In each device, we managed to produce beta-carotene under illumination (Fig. 72). We saw that not all devices had the same ability to activate production to the same level, and that they each had different thresholds and activation ranges. For example, maximal illumination in the OptoBox seemed to lead to lower production compared to mid illumination in the OptoTubes. Also, we found that temperature still could impact the production. Finally, we noticed that other parameters such as stirring had a significant impact on production.

We characterize all those aspects in the next chapter of this manuscript.

5.5. Conclusions

In this chapter, we have seen how to connect the beta-carotene production pathway to the optogenetic system. The first “slow producer” strain we obtained had indeed its beta-carotene production placed under blue light control, but it did manage to produce only in low growing culture conditions, *i.e.*, at low temperature and in glycerol medium. To understand this particular phenotype, we questioned the optogenetic system, and the heterologous pathway: although the activation strength of EL222 is considered relatively low, it does not justify this phenotype. On the other hand, by deconstructing the trifusion design leading to beta-carotene production, beta-carotene production in standard growth conditions was successfully restored. Thereby, we obtained a new functional strain, which produces beta-carotene under optogenetic control in glucose medium and at 30°C.

I show here that adapting an optogenetic system to a heterologous pathway can lead to unexpected complications. Although here not necessarily linked to optogenetic *per se*, simply changing a promoter or the induction system can lead to unexpected strain behavior. Therefore, although being a widespread recommendation, we suggest systematically constructing precisely-corresponding control strains (with constitutive promoters for example) when adapting a heterologous system to optogenetics. Also, we demonstrated here the throughput power of eVOLVER and started to envision how different scales and devices can impact the production of a single strain.

These results led us to wonder about the relationship between optogenetic activation and beta-carotene production with this last functional strain, and to investigate how each device impacts both optogenetic activation and beta-carotene independently and together. Those questions guide us to the main article of this PhD, reproduced in the next chapter. It consists of the presentation of 4 optogenetic devices developed in the lab (the OptoBox, the OptoTubes, the eVOLVER and the OptoFlasks), the characterization of optogenetic activation in each given illumination, the culture conditions in each device impacting beta-carotene production, and finally how optogenetic control of this production can be established with all the different constraints in each device. There, we will relate optogenetic control of bioproduction with the scaling-up challenges across devices.

Bibliography

1. Zhao EM, Zhang Y, Mehl J, et al. Optogenetic regulation of engineered cellular metabolism for microbial chemical production. *Nature*. 2018;555(7698):683-687. doi:10.1038/nature26141
2. Bu X, Lin JY, Duan CQ, Koffas MAG, Yan GL. Dual regulation of lipid droplet-triacylglycerol metabolism and ERG9 expression for improved β -carotene production in *Saccharomyces cerevisiae*. *Microb Cell Fact*. 2022;21(1):1-13. doi:10.1186/s12934-021-01723-y
3. Laughery MF, Hunter T, Brown A, et al. New vectors for simple and streamlined CRISPR-Cas9 genome editing in *Saccharomyces cerevisiae*. *Yeast*. 2015;32(12):711-720. doi:10.1002/yea.3098
4. Gietz RD, Schiestl RH. High-efficiency yeast transformation using the LiAc/SS carrier DNA/PEG method. *Nat Protoc*. 2007;2(1):31-34. doi:10.1038/nprot.2007.13
5. Rabeharindranto H, Castaño-Cerezo S, Lautier T, et al. Enzyme-fusion strategies for redirecting and improving carotenoid synthesis in *S. cerevisiae*. *Metab Eng Commun*. 2019;8(December 2018):1-11. doi:10.1016/j.mec.2019.e00086
6. Reyes LH, Kao KC. Growth-coupled carotenoids production using adaptive laboratory evolution. *Methods Mol Biol*. 2018;1671:319-330. doi:10.1007/978-1-4939-7295-1_20
7. Gibson DG, Young L, Chuang R, et al. Enzymatic assembly of DNA molecules up to several hundred kilobases. 2009;6(5):12-16. doi:10.1038/NMETH.1318
8. Salvadó Z, Arroyo-López FN, Guillamón JM, Salazar G, Querol A, Barrio E. Temperature adaptation Markedly Determines evolution within the genus *Saccharomyces*. *Appl Environ Microbiol*. 2011;77(7):2292-2302. doi:10.1128/AEM.01861-10
9. Zhao EM, Suck N, Wilson MZ, et al. Light-based control of metabolic flux through assembly of synthetic organelles. doi:10.1038/s41589-019-0284-8
10. Lee ME, DeLoache WC, Cervantes B, Dueber JE. A Highly Characterized Yeast Toolkit for Modular, Multipart Assembly. *ACS Synth Biol*. 2015;4(9):975-986. doi:10.1021/sb500366v
11. Verwaal R, Wang J, Meijnen JP, et al. High-level production of beta-carotene in *Saccharomyces cerevisiae* by successive transformation with carotenogenic genes from *Xanthophyllomyces dendrorhous*. *Appl Environ Microbiol*. 2007;73(13):4342-4350. doi:10.1128/AEM.02759-06

6. CHAPTER 3 – Optogenetic control of beta-carotene bioproduction across multiple lab-scales

Sylvain Pouzet¹, Jessica Cruz-Ramon¹, Matthias Le Bec¹, Céline Cordier¹, Alvaro Banderas¹, Simon Barral¹, Sara Castano-Cerezo², Thomas Lautier², Gilles Truan² and Pascal Hersen^{1*}

¹ Institut Curie, Université PSL, Sorbonne Université, CNRS UMR168, Laboratoire Physico Chimie Curie, 75005 Paris, France

² Toulouse Biotechnology Institute, Université de Toulouse, CNRS, INRAE, INSA, Toulouse, France

* **Correspondence:** Pascal Hersen (pascal.hersen@curie.fr)

Keywords: Optogenetics, bioproduction, *Saccharomyces cerevisiae*, beta-carotene, synthetic biology, metabolic engineering

Foreword

Thanks to the illumination devices developed and presented in the first chapter of this thesis, and with an efficient strain producing beta-carotene upon illumination, we were able to start investigating the interplays between optogenetic activation, beta-carotene production, and device scale.

This chapter is the manuscript of the article under revision. In its introduction, it therefore recalls our introduction and presents the four optogenetic devices used in this study in the first part of the results. Then, the optogenetic activation alone is investigated in the different devices, while varying illumination and other culture parameters. Following, we investigate constitutive beta-carotene production in the different devices. Only in the third part, after optimization of both optogenetic activation and constitutive beta-carotene production, the optogenetically-controlled beta-carotene producer strain is tested in the different devices.

Abstract

Optogenetics arises as a valuable tool to precisely control genetic circuits in microbial cell factories. Light control holds the promise of optimizing bioproduction methods and maximizing yields, but its implementation at different steps of the strain development process and at different culture scales remains challenging. In this study, we aim to control beta-carotene bioproduction using optogenetics in *Saccharomyces cerevisiae* and investigate how its performance translates across culture scales. We built four lab-scale illumination devices, each handling different culture volumes, and each having specific illumination characteristics and cultivating conditions. We evaluated optogenetic activation and beta-carotene production across devices and optimized them both independently. Then, we combined optogenetic

induction and beta-carotene production to make a light-inducible beta-carotene producer strain. This was achieved by placing the transcription of the bifunctional lycopene cyclase / phytoene synthase CrtYB under the control of the pC120 optogenetic promoter regulated by the EL222-VP16 light-activated transcription factor, while other carotenogenic enzymes (CrtI, CrtE, tHMG) were expressed constitutively. We show that illumination, culture volume and shaking impact differently optogenetic activation and beta-carotene production across devices. This enabled us to determine the best culture conditions to maximize light-induced beta-carotene production in each of the devices, reaching a content of up to 880 $\mu\text{g/gCDW}$. Our study exemplifies the stakes of scaling up optogenetics in devices of different lab scales and sheds light on the interplays and potential conflicts between optogenetic control and metabolic pathway efficiency. As a general principle, we propose that it is important to first optimize both components of the system independently, before combining them into optogenetic producing strains to avoid extensive troubleshooting. We anticipate that our results can help design both strains and devices that could eventually lead to larger scale systems in an effort to bring optogenetics to the industrial scale.

6.1. Introduction

Advances in bioproduction using yeast and bacteria as microbial cell factories have enabled significant feats in metabolic engineering to be showcased^{1,2} and allow for the unprecedented production of complex chemicals through more sustainable processes. However, despite impressive progress, the compound of interest is often produced at relatively low levels³. To increase production yields, forward metabolic engineering (rational design and Design-Build-Test-Learn Cycles)³ and reverse metabolic engineering (mutagenesis and directed evolution)⁴ have emerged as preferred strategies to increase the carbon flux and redirect more cellular resources toward the production of the compound of interest. These strain engineering strategies are increasingly benefiting from progress in computational approaches (multiomics^{5,6}, genome-wide metabolic models⁵, machine learning⁷).

To improve yields, complementary strategies mostly focus at the bioprocess level. There, the key is to best cope with metabolic burden, *i.e.*, the potential metabolic load and stress created during production, such that growth is least impaired, and productivity maintained. To this end, tools and methods to decouple growth from production have been continuously perfected since the first production of antibiotics from fungi⁸. Inducible systems (usually relying on transcriptional activation) are often employed to control the shift from the growth phase (building up biomass without production or burden) to the production phase (which focuses on production with minimal growth).

Moving beyond this two-step cultivation strategy, several recent studies showed that controlling growth *versus* production in a dynamic manner can further increase production yields^{9,10}. Finely controlling the induction of the metabolic pathways leading to production is critical for such “dynamic regulation”¹¹ strategies. The inducer must be reversible, responsive, easy to handle, and cheap. Today, mostly chemical inducers are used. But once injected in large volumes, chemical inducers take time to diffuse uniformly, which leads to potential induction

heterogeneity, and cumbersome medium changes are usually required to reverse their action. Besides, metabolizable carbon-sources used as inducers (galactose, methanol, arabinose) exhibit slow response dynamics and are expensive at larger scales. In contrast, the use of light as an inducer (optogenetics) is a very attractive strategy since the responsiveness and its reversibility are instantaneous.

Optogenetics has already been applied to bioproduction, though only in a handful of lab-scale studies. Light has mostly been used to control transcription irreversibly¹² or reversibly^{9,13–15}, to direct the assembly of enzymatic clusters¹⁶, or to tune the composition of microbial consortia¹⁷. The development of an optogenetic producer strain at the lab scale requires the use of specific illumination devices. In this paper, we present and compare four devices that can be used at every step of the strain development process: from 24-well plate systems (OptoBox¹⁸), to simple small-scale starter cultures (OptoTubes), larger-scale batch cultures (OptoFlasks), and devices that allow multiple-parameter control of the culture conditions (eVOLVER¹⁹).

We used the EL222 optogenetic system, a single-component light-oxygen-voltage-sensing (LOV)-based light-activated synthetic transcription factor derived from the bacteria *Erythrobacter litoralis*. EL222 offers rapid activation ($\tau_{\text{on}} = 5\text{sec}$) and deactivation kinetics ($\tau_{\text{off}} = 30\text{sec}$)²⁰ and is an established system in yeast⁹.

Beta-carotene is a terpene known for its characteristic yellow/orange color. Its photochemical and antioxidant properties make this carotenoid a valuable molecule in a wide range of industries, including cosmetics (sun protection), health (antioxidant, dietary supplement as provitamin A), feed and food (health and coloring)²¹. Major sources of beta-carotene are chemical synthesis (enol-ether condensation or Wittig condensation of beta-ionone²²) and extraction from plants (carrots, oil of palm fruit, and sweet potato) or naturally producing microorganisms (mostly the algae *Dunaliella spp.* and fungus *Blakeslea trispora*)²¹. Beyond its industrial relevance, beta-carotene and other compounds of economic importance (artemisinine²³, taxol²⁴, celastrol²⁵) originate from the isoprenoid pathway. Therefore, new improvements obtained using beta-carotene could also benefit the production of other compounds. In addition, production of a colorful compound that can be detected with the naked eye is a particularly convenient output for bioproduction studies. Hence, beta-carotene is often used as a proxy for various proofs-of-concept and genetic systems^{26–29}.

In this study, we use the EL222 optogenetic system and the beta-carotene synthesis pathway to explore the importance of different culture parameters at various scales using four illumination devices. The constraints encountered at these different scales of lab culture foreshadow larger-scale potential challenges. Indeed, differences in illumination (light input, medium penetration, and device geometry) and the culture conditions (stirring and shaking, culture volume, gas exchange) between these scales can independently impact both genetic components: the activation of the optogenetic system and the bioproduction by the metabolic pathway. First, we detail the constructions of these four illumination devices and investigate how optogenetics translates across lab scales. Second, we optimize culture conditions to maximize beta-carotene production across devices and identify production constraints. Only then, as a third step, we combine optogenetic control with beta-carotene production. We investigate to what extent this optogenetic control of bioproduction recapitulates constraints

identified independently for both genetic components and discuss the relationships between optogenetic activation and the resulting production. In a nutshell, we demonstrate how this three-step approach can help identify optogenetic, metabolic and scaling constraints to define the optimal parameters to drive beta-carotene production in response to light in the budding yeast *Saccharomyces cerevisiae* in multiple lab culture scales.

6.2. Results

6.2.1. Setting-up optogenetics in different lab-scale culture devices

OptoBox

The OptoBox, (*a.k.a.* The Light-Plate Apparatus¹⁸ – Fig. 73A) was developed to illuminate 24-well imaging plates in a shaking incubator. Each well of the OptoBox contains two interchangeable LEDs connected to a Printed Circuit Board (PCB). Although the two LEDs can be different in order to be compatible with various optogenetic systems, we connected two blue LEDs (461 nm) to maximize light exposure for the EL222 optogenetic system. Programming of the device is particularly easy: the program can be set up online using the user-friendly software Iris, uploaded to an SD card, and plugged into the PCB. The programming consists of assigning each of the two LEDs an arbitrary value between 0 and 4000 (for a given illumination pattern), corresponding, in our case, to an intensity of 0 to 4mW/cm² per LED (Fig. S1). The OptoBox provides a convenient tool to screen various strains or illumination conditions. The 24-well plates generally hold a culture volume of 1 mL per well and can be sealed with aluminum foil to prevent light leaking, culture spilling and evaporation. At the bottom of the well-plate we use (see Methods), lies a 25 µm film that allows for gas exchanges and light penetration.

OptoTubes

To illuminate simple culture tubes with light, we designed a set of OptoTubes by positioning LEDs at the bottom of 14 mL glass test tubes (Fig. 73B). The LEDs are directly connected to an Arduino's Pulse-Width Modulation (PWM) pin for intermediate light intensities (from 0 to 255, corresponding to 0 to 12 mW/cm² - Fig. S1 and S2). This is the simplest system to illuminate simple cultures of typically 3 mL, for either overnight cultures or specific, programmed, durations. Specific illumination patterns can also be accommodated by programming the Arduino. The inclination of the tubes and LEDs was designed to increase gas exchange during shaking in the incubator (See Fig. S2 and Supplementary File 1).

eVOLVER

The eVOLVER platform, adapted from Wong *et al.* 2018¹⁹, comprises 16 independent culture units, in which a glass vial can be inserted (Fig. 73C), each allowing a single automated yeast culture of 10-25 mL. For each unit, the temperature (heaters and thermistor) and stirring (rotating magnet in vial combined with disc-magnets on a rotating fan) are controlled and the growth rate (infra-red LED and photodiodes) can be monitored semi-quantitatively.

Optogenetics was not included in the original design of the eVOLVER platform, but the addition of a LED in their culture unit PCB to illuminate the culture from the side of the device was anticipated, and we indeed took advantage of this option. We also added a photoresistor so that the absorption of blue light in the medium can be monitored. Given that beta-carotene interacts with blue light³⁰, its production in cells could be estimated using the blue-LED-photoresistor pair ([Supplementary File 2](#)) to obtain qualitative estimations of the cell density and beta-carotene production within the eVOLVER. To further increase the illumination of the cultures, we designed a custom lid: in the hollow lid normally sealed using a removable silicon septum, an autoclavable cytometry tube is placed. Additional LEDs can be stacked inside this tube to illuminate the inside of the medium. Here, we distinguish between the side-LED of the original eVOLVER design (6mW/cm² – external illumination) and the additional LEDs inserted from the top (internal illumination). Adding 1, 2, 3, or 4 additional LEDs was found to correspond to adding 6.7, 8.3, 9.3 and 9.4 mW/cm² of intensity, respectively, in the culture medium.

In our design, each eVOLVER unit is controlled by an individual Arduino Nano and each Arduino is connected to a computer via USB. Compared to the Khalil lab's fully integrated eVOLVER platform¹⁹, we propose this more DIY and straightforward design for biologists with minimal knowledge of electronics, since our design circumvents the need to order and assemble various cards and PCBs (see [Supplementary File 2](#)). In terms of software, we developed a Node-Red program (detailed in [Supplementary File 2](#) and available on Github) to communicate with the Arduinos in real-time, via the Firmata Arduino Template. This software handles the user interface used to set up and launch experiments, PID used to control temperature, illumination control and data-output. Using this platform containing 16 functional units and an efficient user-interface, we are able to quickly and easily vary multiple parameters at the same time (illumination, volume, stirring, temperature, strain) and thus achieve high experimental throughput.

OptoFlasks

Flasks are the standard culture container used to test strains before scaling up to pilot-scale bioreactors. In order to illuminate flasks, we arranged LEDs into petri-dishes, which were used as illumination stands to illuminate them from the bottom ([Fig. 73D, S3](#)). LEDs were soldered in a circular pattern such that they line the outermost area of the bottom of the flask. Thus, in a shaking incubator, when the culture medium is driven to the sides of the flask and rotates along the round bottom of the flask, the exposure of the culture to light will be maximized. LEDs are soldered such that each receives 20mA current, resulting in a measured 12mW/cm² intensity per LED, similar to the additional LEDs of eVOLVER and the maximal value of the OptoTubes' LEDs. Here, we used both flat-bottom flasks and indented-bottom (baffled) 250 mL flasks: the indentation creates turbulences in the liquid flow, which in turn incorporates more air in the culture medium and improves gas transfer. We tested volumes of 25 and 50 mL in 250 mL flat and indented flasks.

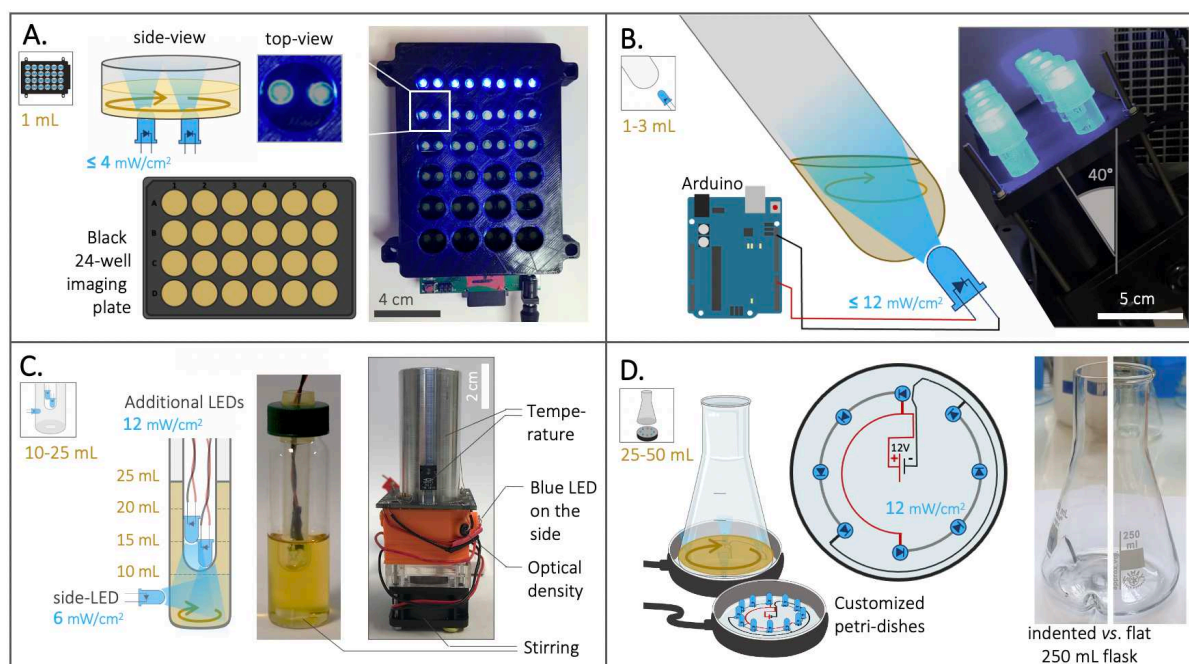


Figure 73. Description of the four optogenetic devices used in this study. (A) The OptoBox (adapted from Gerhardt et al. 201618) can independently illuminate 1 mL cultures in a 24-well plate placed in a shaking incubator. Two LEDs (0 to 4 mW/cm²) illuminate each well from below and can be programmed. (B) The OptoTubes are used to illuminate 14 mL tubes (generally 3 mL cultures) using a LED (0 to 12 mW/cm²) placed at the bottom of each tube. The OptoTubes can be programmed with an Arduino (0 to 255 u.a.) and be placed in a shaking incubator thanks to a dedicated 3D printed opaque holder. (C) The eVOLVER culture platform adapted from Wong et al. 201819 uses a DIY “sleeve” (right) where a glass vial (center) can be inserted, all connected to an Arduino. We built 16 of these units, and the temperature, stirring and illumination (via an additional side-LED: 6 mW/cm²) can be controlled for each unit, while the growth rate and production of beta-carotene can be monitored. The lid of the glass vial was adapted to accommodate the input of more light using additional LEDs (12 mW/cm² each). (D) The OptoFlasks, in which custom-made illumination stands were built to hold different numbers of LEDs (12 mW/cm² each), on top of which the flasks (indented/baffled or flat) are positioned and can hold 25 to 50 mL cultures.

6.2.2. Devices and culture conditions influence optogenetic activation

To investigate how optogenetics translates at different scales, we tested the four optogenetic devices presented above. Each device has its own intrinsic properties: illumination modalities (disposition, number, controllability of the LEDs), geometries (which impact light diffusion and shaking), and range of culture volumes. Illumination, culture volume and shaking can be altered within each device, so that the influence of these factors on optogenetic activation can be identified.

We used the strain OPTO-EXP from the Avalos Lab⁹, a *Saccharomyces cerevisiae* CEN.PK2-1C-derived strain that contains the light-activated EL222-VP16 transcription factor under constitutive expression (pPGK1 promoter). Upon blue light illumination, a change of conformation induced via its flavin chromophore allows EL222 to dimerize, bind to its synthetic cognate pC120 promoter and activate the transcription of the downstream Green Fluorescent Protein (GFP) thanks to its VP16 transactivation domain (Fig. 74A).

To test optogenetic activation in different devices and growth conditions, YPD medium was first inoculated with the OPTO-EXP strain at 5.10⁶ cells/mL (OD₆₀₀=0.05), spread across culture containers, placed in illumination devices and illumination started at t₀. During growth, as cell density increases, light penetration may be impaired and the amount of light received

by each cell may decrease, leading to lower optogenetic activation. Therefore, to determine the best timepoint to obtain a readout of optogenetic activation during growth, we performed a time course experiment, measuring GFP levels every hour using cytometry (Fig. S4 and Methods). We determined that the highest activation per cell was reached at 6 h post-inoculation. Therefore, we standardized the optogenetic experiments using these parameters. As references, we measured fluorescence levels of GFP expressed from the strong and medium constitutive promoters pTDH3 and pADH1 (Fig. 74B). To estimate background fluorescence, the autofluorescence of a WT non-producer strain (CEN.PK2-1C) was also measured in the different devices, averaged and subtracted to all datapoints.

By varying the intensity of the LEDs in the Optobox and OptoTubes and measuring the production of GFP (Fig. 74C,D), we determined light-response curves. The shaking (250 rpm) and volumes (1 mL and 3 mL) were constant for each device. We obtained two sigmoidal response curves; the dynamic ranges started at 110 arbitrary units of fluorescence (a.u.) and increased to 1014 and 1236 a.u. for the OptoBox and the OptoTubes, respectively, resulting in 9.2- and 11.2-fold, a ~18% differences in max fluorescence between those two devices. In the OptoBox, maximal activation could almost be reached with one single LED operating at maximal intensity (4000 – 4 mW/cm², for 1 mL). In the OptoTubes, the maximum activation threshold was reached when using maximum intensity (255 – 12 mW/cm², for 3 mL). The effective amount of light reaching the culture volume can be difficult to evaluate due to the geometry of the devices, the type of material and the thicknesses of the materials or media the light has to pass through. However, it is necessary to determine the minimal amount of light needed for maximal optogenetic activation as high doses of blue light can result in phototoxic effects^{31,32}.

For eVOLVER and the OptoFlasks we not only varied the illumination but also the culture volume and the agitation properties, *i.e.*, the stirring speed in eVOLVER and the presence or absence of indentation (*i.e.*, baffles) in the culture flasks for the OptoFlasks system. Fig. 74E shows that the additional LEDs increase activation compared to the side-LED alone and that the maximal activation is obtained with the side-LED and two to three additional LEDs (s+2 and s+3), reaching about 1190 a.u. Volume also has an impact on optogenetic activation: using a 10 mL culture, activation corresponds to 990 a.u., but only 526 a.u. for 25 mL. Here, reducing the volume 2.5 times yields a 1.9-fold increase in fluorescence. Moreover, in eVOLVER, stirring also proved significant: no stirring leads to an activation of 233 a.u., and low and high stirring (100 to 255 – Arduino PWM values) lead to activation of 730 a.u., corresponding to a 3.1-fold increase. Interestingly, the absence of the stirring appears detrimental, while any other stirring value restores the optogenetic activation level: there, cells don't simply sit at the bottom of the glass vial.

We reached up to 2453 a.u. in the OptoFlasks (Fig. 74F), the highest optogenetic activation of the four devices. Although the impact of the tested volumes (50 and 25 mL) does not appear significant, activation in 25 mL cultures seems to respond more to higher illumination. In general, maximal activation is reached using eight LEDs (12mW/cm² per LED). Using flat or indented flasks did not yield any significant difference in activation.

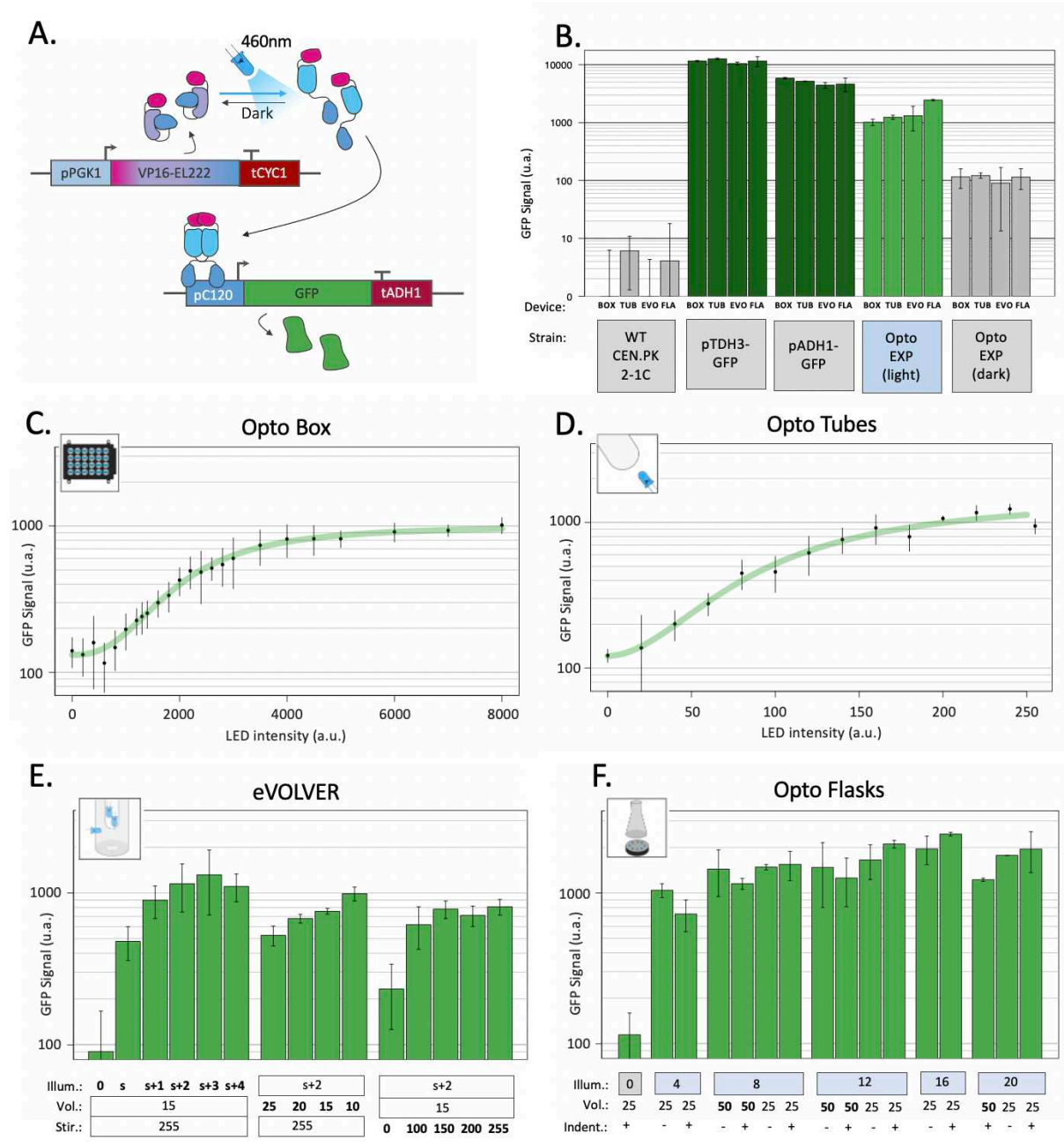


Figure 74. Optogenetic activation in different devices. (A) The EL222 optogenetic system responds to blue light which activates the transcription of genes under the control of the pC120 promoter (here a GFP, in the OPTO-EXP strain). Adapted from Zhao et al. 20189. (B) Fluorescence GFP levels of the background strain CEN.PK2-1C; strains carrying GFP under the strong pTDH3 and medium pADH1 constitutive promoters; and highest levels of fluorescence reached with the OPTO-EXP strain in the light and in the dark in each of the four different illumination devices (BOX: OptoBox, TUB: OptoTubes, EVO: eVOLVER, FLA: OptoFlasks). (C) OPTO-EXP optogenetic activation in the OptoBox. Cumulative LED intensities from 0 to 8000 u.a. correspond to 0 to 4 mW/cm² per LED. (D) OPTO-EXP optogenetic activation in the OptoTubes. LED intensities from 0 to 255 u.a. correspond to 0 to 12 mW/cm² (Fig.S1) (E) OPTO-EXP optogenetic activation in the eVOLVER, with variation of illumination (number of LEDs: s+2 corresponds to the side-LED and 2 additional LEDs inserted via the lid), volume (mL) and stirring (u.a., 0 to 255). The side-LED corresponds to 6 mW/cm², and 1, 2, 3, and 4 additional LEDs add 6.7, 8.3, 9.3 and 9.4 mW/cm² of intensity in the medium. (F) OPTO-EXP optogenetic activation in OptoFlasks. Illumination (0, 4, 8, 12, 16 or 20 LEDs on the illumination stand, 12 mW/cm² each). Volume (25 and 50 mL) and the presence of indentation in the 250 mL flask (+ is indented, - is flat) were tested. For all measures, the levels of GFP were determined using cytometry (n > 3); error bars represent the standard deviation.

In general, while the OptoBox, OptoTubes and eVOLVER reach similar maximal activation values of 1015 a.u., activation in OptoFlasks reached an average of 1652 a.u., 1.63-fold higher (Fig. 74B), suggesting that the optogenetic activation in the three first devices has potential for improvement. Compared to the basal optogenetic expression in the dark (110 a.u. - leaking), optogenetic activation yielded a 13.7-fold increase in GFP fluorescence. In most of the devices, the optimal activation level (1505) corresponds to 30% of the pADH1 (5021) and 13% of the pTDH3 promoter activity (11578 a.u.).

6.2.3. Beta-carotene production is impacted at different scales

Before investigating the efficiency of the optogenetic control of beta-carotene production, we carefully characterized and optimized constitutive beta-carotene production under different culture conditions and across scales. For these experiments, the strain yPH_554, in which the beta-carotene pathway is placed under constitutive expression (*no* optogenetic control), was assayed in the different devices. Culture volume, stirring and light-side-effects have been quantified.

The synthesis of beta-carotene relies on the isoprenoid / mevalonate metabolic pathway. First, acetyl-CoA is channeled towards mevalonate production, then to production of IPP and DMAPP, which are precursors to many other high value-added molecules³³. Condensation of IPP and DMAPP produces geranyl-pyrophosphate (GPP) and the addition of a second IPP molecule gives farnesyl-pyrophosphate (FPP). FPP can be converted to either farnesol (FOH) via DPP1p; two FPP molecules can condensate to form squalene via ERG9p (the pathway for synthesis of ergosterol and other sterols, essential for cell membranes) or via the addition of another IPP molecule to GGPP, the precursor of the beta-carotene pathway (Fig. 75A). To increase GGPP synthesis by yPH_554, the enzymes tHMG1 and CrtE were placed under control of the strong constitutive promoters (pPGK1 and pTDH3 respectively) at the DPP1 locus, while the DPP1 gene was knocked out. Thus, the conversion of acetyl-CoA to mevalonate is increased and the conversion of FPP to FOH is prevented, thus favoring GGPP production. GGPP can then be converted to phytoene (uncolored) by the bi-functional CrtYB enzyme, and subsequently converted to lycopene (red pigment) by CrtI and finally into beta-carotene by CrtYB again. In yPH_554, the genes encoding the CrtYB and CrtI enzymes are inserted at the *ho* locus and both under the strong constitutive promoter pTDH3 (see Methods for more details). This design is based on Rabeharindranto *et al.* 2018³⁴, which originated from Verwaal *et al.* 2007³⁵.

yPH_554 cell pellets appear orange, and cells observed under fluorescence microscopy display numerous fluorescent foci, which are likely to be lipid droplets^{36,37} enriched in beta-carotene (Fig. 75B). In fact, these droplets that emit in the GFP channel are orange when observed using a color camera (Fig. S5). A time course of production was carried out to compare production in the different devices: we found that no more beta-carotene was produced after 24 h of culture (Fig. S6). Thus, we standardized our protocol such that cultures are launched at OD₆₀₀ 0.05 and left to grow and produce for 24 h in YPD at 30°C in batches before extraction in dodecane and quantification of beta-carotene via spectrophotometric analysis (based on Reyes & Kao 2018³⁸, see Methods).

The effect of culture volume varied across devices (Fig. 75C). In the OptoTubes, reducing the culture volume from 3 mL to 1.5 mL yielded a 16% increase in the beta-carotene content, from 1150 and 1330 $\mu\text{g/gCDW}$ (cell dry weight), respectively. Similarly, decreasing the volume in eVOLVER from 25 mL to 10 mL also improved production by 2.2-fold from 515 to 1145 $\mu\text{g/gCDW}$, respectively. However, this increase was not observed at low stirring, meaning that the limiting factor is probably a combination of low stirring and volume, hence indicating probable differences in aeration between the conditions. At low stirring in eVOLVER (corresponding to the Digital PWM value of 100 sent by the Arduino; the maximum being 255), production is strongly impaired, resulting in an average of 355 $\mu\text{g/gCDW}$ (3.2 times less than the maximum, Fig. 75C) and a faintly yellow cell pellet (Fig. 75B). In the OptoFlasks, neither the culture volume (50 and 25 mL) nor the presence of indentation in the flasks appeared to affect production. All OptoFlasks conditions yielded slightly less beta-carotene (about 1000 $\mu\text{g/gCDW}$) than all other devices under their respective optimal conditions.

Beta-carotene is sensitive to blue light: its peak absorption wavelength is about 450 nm^{30,39} and the blue LEDs used to activate the EL222 optogenetic system peak at 461 nm (see Methods). In plants, beta-carotene is even considered to function as a protective molecule against excessive illumination, given its photo-oxidative properties⁴⁰. Therefore, there might be some incompatibility between the blue light-activated optogenetic system and the molecule we wish to produce. Thus, we investigated the impact of blue light on constitutive beta-carotene production (*i.e.*, *no* optogenetic activation) across devices with the illumination conditions used to activate the optogenetic system. As shown in Fig. 75D, in the OptoTubes and OptoFlasks, strong illumination does not impact beta-carotene production. However, strong illumination impacted production in the OptoBox and in eVOLVER, resulting in a drop from 1070 to 845 $\mu\text{g/gCDW}$ (21%) in OptoBox and from 905 to 705 $\mu\text{g/gCDW}$ (22%) in eVOLVER; this effect does not appear to be light dose dependent. It is important to bear these results in mind when interpreting the forthcoming results of the experiments combining optogenetics and beta-carotene production.

In conclusion, we optimized the culture conditions such that the constitutive level of beta-carotene production varied only moderately across devices, ranging from 1000 to 1200 $\mu\text{g/gCDW}$. The culture conditions were especially improved in the eVOLVER and we showed that culture volume and stirring impacted the production the most. Moreover, beta-carotene production and/or accumulation was only mildly impacted by illumination in OptoBox and eVOLVER.

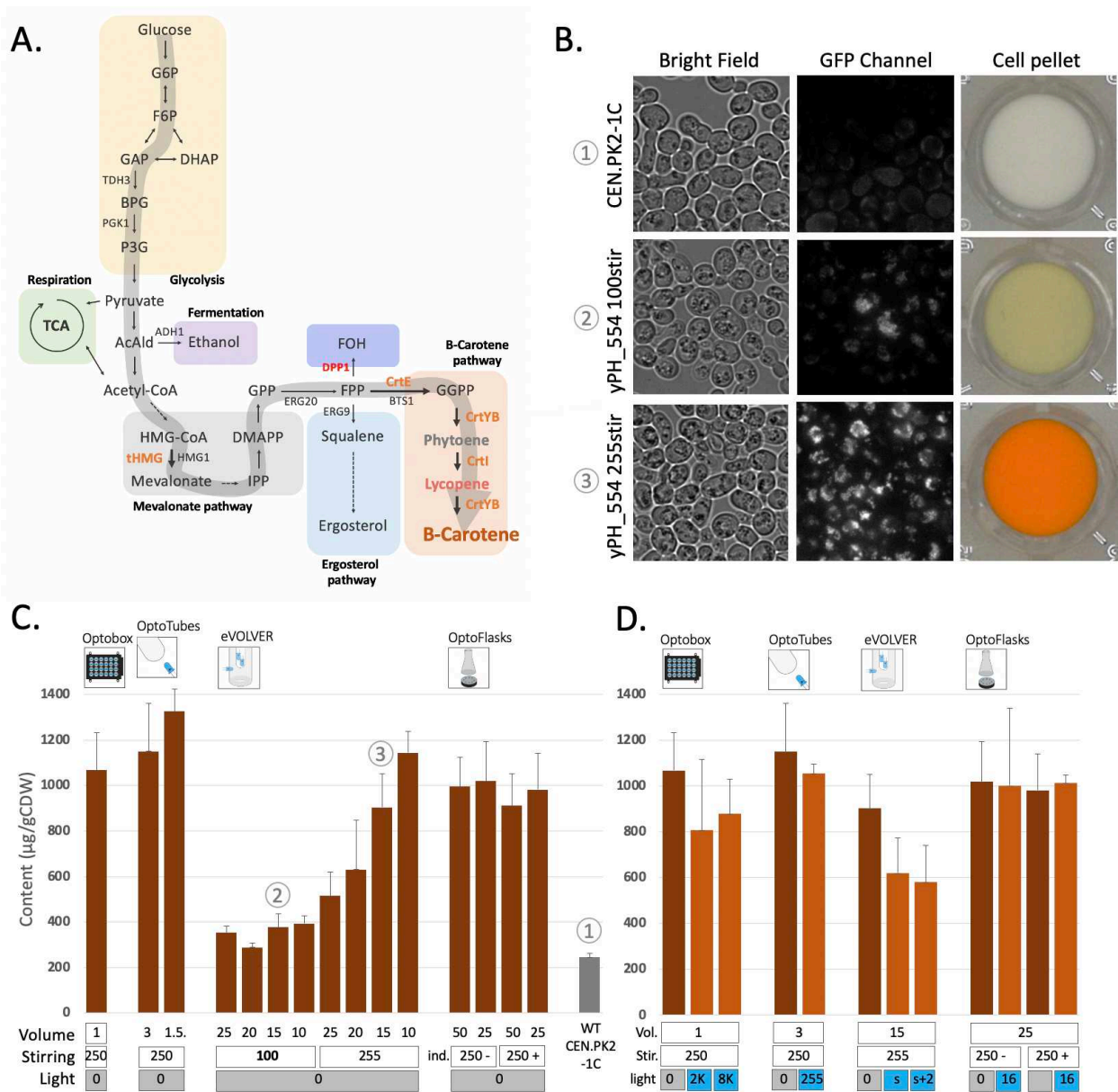


Figure 75. Constitutive beta-carotene production and analysis of the effect of light on beta-carotene accumulation in yeast. (A) Beta-carotene pathway. Arrows point to chemical species (see Figure S8 for more details), genes names are indicated in capital letters beside arrows. The large grey arrow represents the carbon flux leading to beta-carotene production. Orange: heterologous genes inserted under constitutive promoters. Red: endogenous gene deletion. (B) Microscopic observations and corresponding cell pellets. CEN.PK2-1C (top) strain and constitutive beta-carotene production (yPH_554 – middle and bottom). Growth in YPD at 30 °C for 24 h with low stirring (100 – middle) versus high stirring (255 – bottom). Bright field images and GFP images showing beta-carotene localized in lipid droplets and emitting in the GFP channel (100X objective). See also Fig.S5 (C) Constitutive beta-carotene production (content – μg beta-carotene / g cell dry weight) measured after growth in the different devices (see Methods). Volume (mL), stirring/shaking (rpm except for eVOLVER, which is given in arbitrary units, + and - in OptoFlasks represent the presence or absence of indentation, respectively). In this panel, all experiments were performed in the dark (non-optogenetic strain). The WT non-producer strain is CEN.PK2-1C. Sample numbers indicated in encircled numbers in (C) match images in (C). (D) Effect of light on constitutive beta-carotene production in the different devices. Dark-orange bars are cultures in the dark, light-orange bars are illuminated cultures. Volume (mL), stirring (rpm or u.a. and indentation presence) are the same as in (C) and light (u.a.) as in Fig.2.

6.2.4. Optogenetic control of beta-carotene production in different devices

In the two previous parts, to assess the influence of illumination, volume and stirring across devices, we used two different strains: the OPTO-EXP strain, in which GFP transcription is controlled by the EL222 optogenetic system via its pC120 promoter; and the constitutive beta-carotene producer strain yPH_554, which expresses all four carotenogenic genes under strong constitutive promoters.

Now, we combine these genetic systems into the strain yPH_551, in which the EL222 optogenetic system controls beta-carotene production. tHMG, CrtE, and CrtI were inserted into OPTO-EXP under the control of the constitutive promoters, similarly to the genetic design of yPH_554. However, CrtYB, which recapitulates two enzymatic reactions necessary to produce beta-carotene, was placed under the control of the pC120 optogenetic promoter (see Methods). Thus, in strain yPH_551, the expression of CrtYB acts as a light-activated valve for beta-carotene production (Fig. 76A).

Fig. 76B shows that beta-carotene production by strain yPH_551 was indeed successfully made light-dependent. The average production of 215 $\mu\text{g/g}$ CDW in the dark corresponds to no production of beta-carotene (as confirmed by white cell pellets – see Fig. 75C), *i.e.*, this value is our detection threshold (see Methods).

In the OptoBox and OptoFlasks, optogenetically controlled beta-carotene production saturates at 550 and 610 $\mu\text{g/gCDW}$ respectively. In the OptoTubes and eVOLVER, production increases with the amount of light, to reach a maximum of 780 $\mu\text{g/gCDW}$ in the OptoTubes and 880 in the eVOLVER. The maximal production values in each device were lower than their respective maximal values achieved by constitutive beta-carotene production shown in Fig. 75C (52%, 68%, 79%, 62% - for OptoBox, OptoTubes, eVOLVER and OptoFlasks, respectively). Reaching 50 to 80% of constitutive beta-carotene production while optogenetic activation reaches 11% activation of the pTDH3 promoter (Fig. 74B) reveals that light induction is efficient, despite the detrimental effects of light on beta-carotene production in the OptoTubes and eVOLVER (Fig. 75D)

For most of the conditions tested here, the light-induced production can be related to the previously measured amount of optogenetic activation (Fig. 76C), such that conditions yielding more optogenetic activation result in higher beta-carotene production. Here, the production is proportional to the \log_{10} of the optogenetic activation value. The consequence of this relationship is that only about 8% of the strength of the pTDH3 promoter is required to reach 50% of the possible beta-carotene production. In other words, even though the Opto-EXP optogenetic system has comparatively low transcriptional strength, in our case, this system produces a good amount of beta-carotene compared to production from a strong constitutive promoter, perhaps because the controlled enzyme, CrtYB, does not conduct the rate-limiting step of the pathway³⁵. Finally, the outliers in Fig. 76C suggest that culture conditions could probably be further improved to increase production even more.

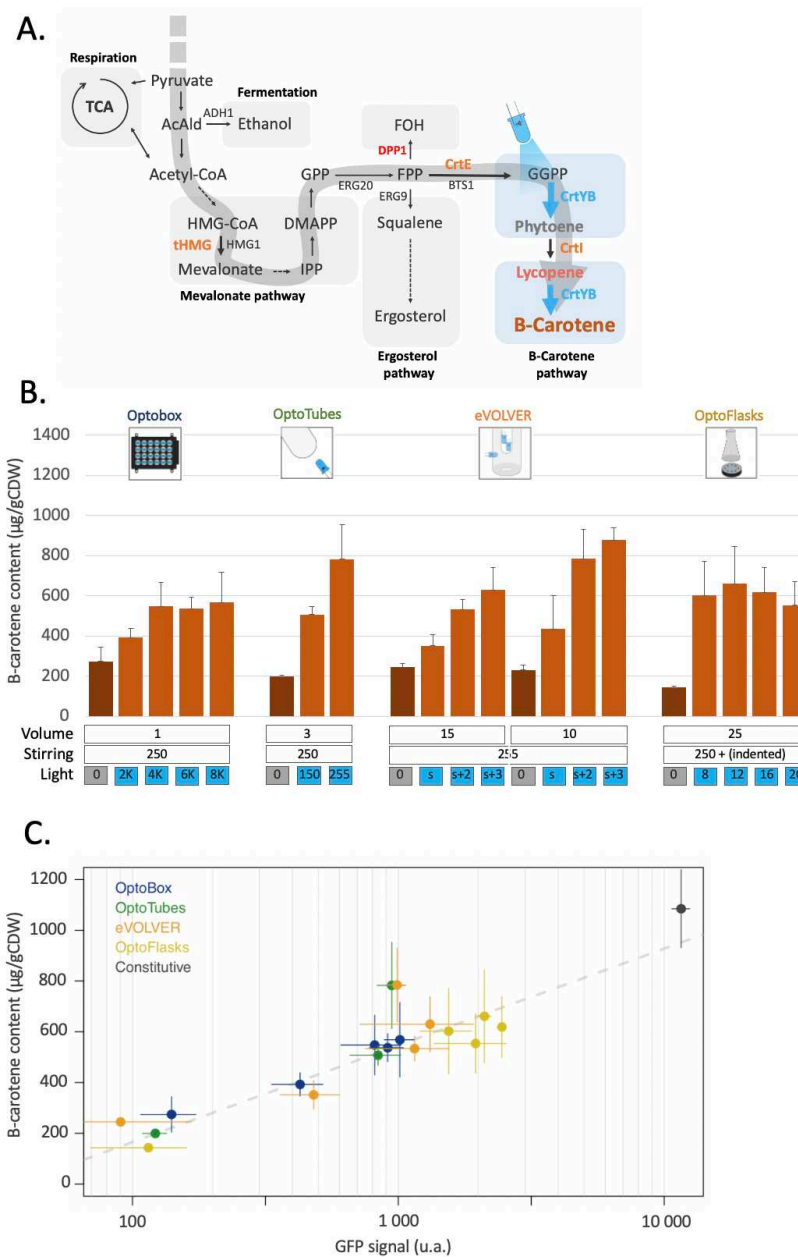


Figure 76. Light-activated beta-carotene production. (A) Design leading to light controlled beta-carotene production: in the optogenetic strain, only *CrtYB* is under the control of the *pC120* promoter (*yPH_551*). Blue arrows represent light-induced enzymatic reactions. Orange: heterologous carotenogenic genes inserted under constitutive promoters. Red: deleted endogenous genes. Blue: optogenetically controlled reaction. (B) Beta-carotene production quantification from the different devices. Dark-orange bars correspond to cultures in the dark, light-orange bars correspond to illuminated cultures. Volumes (mL), stirring (rpm except u.a. for eVOLVER) and illumination (u.a.) are indicated ($n > 3$). (C) Light-activated beta-carotene production (Fig.4B) versus corresponding optogenetic activation strength (from Fig.2C-F) in the different devices. Grey dashes represent the linear regression fit (adjusted $R^2 = 0.81$). The black constitutive point represents the *pTDH3* promoter GFP signal and production by the constitutive beta-carotene production strain (*yPH_554* - Fig.3C). Error bars are standard deviations.

6.3. Discussion

To test the scalability of the use of optogenetics to control bioproduction and identify its challenges, we built four illumination devices at different lab scales. These devices mainly vary with respect to the culture volumes they hold (from 1 to 50 mL); in their geometry, which impacts shaking and illumination; and in their illumination modalities, which impacts cell exposure to light. Each optogenetic device corresponds to a standard lab-scale culture device, and alternative designs exist for each device and purpose: screen straining in imaging plates like the OptoBox^{18,41–43}, illumination of starter cultures in OptoTubes⁴⁴, monitoring multiple culture parameters in minibioreactors such as eVOLVER^{19,45,46}, or use of larger culture volumes for various purposes in OptoFlasks⁴⁷. Measuring the intensities of the LEDs allows us to compare the relative amounts of input light across these devices. However, due to the unique geometry of each device (position of the LEDs, light absorption, diffraction, and reflection) and their different culture volumes (light penetration), it remains difficult to precisely estimate the actual quantity of light received by each cell; thus, testing the activation of a reporter gene like GFP remains the best way to take these technical aspects into consideration in combination with potential biological limitations.

We concluded that optogenetic activation reached an average maximum of 13% of the pTDH3 promoter across devices. Estimations of the quantity of light per milliliter of culture revealed that between 1 and 4 mW/cm²/mL was sufficient for maximal activation in the different devices. The variations across devices indicate that other factors impact optogenetic activation in addition to the amount of light, even though measuring the effective amount of light entering and staying in the media remains difficult. Light distribution has been actively studied using single-particle and fluid dynamics models to optimize illumination of photobioreactors (mostly cultures of photosynthetic microorganisms) and predict the amount of light received by each cell over time^{48,49}; and microbial optogenetics could indeed profit from such approaches.

In eVOLVER, the volume and stirring parameters strongly impacted optogenetic activation. Indeed, reducing the volume from 25 to 10 mL with maximum stirring and s+2 illumination improved activation by almost 2-fold. Furthermore, a lack of stirring resulted in a 3-fold decrease in activation, while it remained constant between low (100) and strong (255) stirring. One can interpret these results from two points of view: in terms of gas exchange in the medium and in terms of light availability. On one hand, a decrease in volume will increase the surface-to-volume ratio in the vial and improve gas exchange, and more specifically the oxygen transfer rate (OTR), a crucial element taken into consideration in bioreactors. Similarly, increasing the stirring will create a bigger vortex, resulting in comparable effects. Since only the absence of stirring (and not an increase in stirring) impacts activation, we suggest that the limitation of the OTR may be relatively low in this case, justified by the fact that the cultures measured in our experiments were only 6 h old. On the other hand, these effects may relate to the amount of light received per cell. For a set amount of light, a lower culture volume (lower cell number) could result in a higher amount of light per cell. Moreover, in eVOLVER, a high volume (25 mL) implies that some parts of the culture volume (and therefore, cells) are lying above the LEDs (*i.e.*, the poorly illuminated area - Fig.1C) and a higher volume also leads to

lower light penetration; both of these factors result in a decrease in the amount of light per milliliter. In addition, in the absence of stirring, the cells lie still on the bottom of the glass vial and remain far from the light sources due to the position of the LEDs, which are placed at the top and on the side in eVOLVER. These results emphasize the importance of the illumination design within each of the different devices, which may not necessarily be well-suited for larger culture volumes.

Using our genetic design, constitutive beta-carotene production achieved a content of 1000 to 1300 mg/gCDW in the different devices. Beta-carotene production was sensitive to the culture volume and stirring. Reducing stirring in eVOLVER resulted in a 3-fold drop in production and increasing the volume to 25 mL led to a 2-fold drop (compared to production at 255 stirring of 10 mL). Culture volume also had an effect in the OptoTubes, but not in the OptoFlasks. This highlights the need to optimize the culture conditions of every device to obtain a functional strain in each and across scales. Since both higher stirring and lower volume impact beta-carotene production, we suggest that improved gas-exchange favors beta-carotene production by impacting cellular metabolism. At a sufficient concentration of oxygen (which is constrained by gas-exchange), *S. cerevisiae*, a Crabtree-positive species, undergoes both fermentation and also respiration⁵⁰, which consequently increases the acetyl-CoA pool directed to the Krebs cycle as well as other precursors to beta-carotene.

The effects of volume and stirring on our two different genetic components were found to overlap: more stirring and a lower volume improved both optogenetic activation (for optimal illumination reasons) and beta-carotene production (for metabolic reasons), making those two genetic components easily compatible. This compatibility may not always be consistent for every system; hence, it is crucial to anticipate and evaluate these effects independently before combining optogenetic control with the pathway of interest.

We saw that the constraints of the optogenetic system and the beta-carotene pathway in each device are recapitulated in the optogenetic beta-carotene strain: in general, more light resulted in more production, and a smaller volume in eVOLVER favored the light-activated production. Production levels reached 50 to 80% of those from constitutive production. Since we saw that production was proportional to the \log_{10} of the expression of the enzyme, this lower production reached using optogenetics is likely due to the relatively low transcriptional strength of the pC120 optogenetic promoter. This could be solved by adding more copies of pC120-CrtYB or by using a different⁹ or more recent and stronger optogenetic system⁵¹⁻⁵³.

Although we found that more activation (optogenetic or constitutive) yielded more beta-carotene production, this straightforward relationship may not always stand^{54,55}. Indeed, relative enzymatic levels can have an impact on the production of different metabolites (and this has even been demonstrated for beta-carotene production^{34,56}). Therefore, fine-tuning the optimal enzyme concentration with optogenetics could result in higher yields in different designs and for different metabolic pathways. More importantly, if higher expression yields more production, it can also lead to a higher burden and impact growth and strain stability, and therefore impact the production titers. Using optogenetics could enable precise control of the levels of enzymes using dynamic control based on feedback from the expression levels and growth rate⁵⁷.

Optogenetics also allows for precise control of gene expression in terms of timing. Here, we activated the cells constantly during a 24 h culture. Nevertheless, other studies have indicated that starting the illumination at later phases of growth or using pulsed patterns of illumination can improve production: Zhao *et al.* 2021⁵¹ distinguished the growth, induction and production phases and differently optimized the illumination patterns to produce specific chemicals and Raghavan *et al.* 2020¹² defined the optimal illumination onsets to start the production.

This question of timing can be especially important when the production of the chemical of interest creates a burden on the cell and therefore slows down growth and/or creates a stress. In our study, beta-carotene production did not appear to produce a burden (Fig. S7); however, if this were the case, the ease of timing optimization and control using optogenetics could allow for improved titers (g/L of culture) and yields (g/g of carbon source), not only content (g/gCDW - shown in this study). To further reduce this burden, dynamic control of bioproduction could be employed to let the cells recover from the production stress and then resume production with a renewed high productivity⁵⁷.

The four optogenetic devices presented here are lab-scale culture devices. Scaling-up optogenetics to industrial culture volumes will generate different constraints on optogenetic activation and yeast metabolism, although bioreactors often have better control over culture parameters than lab-scale devices (pH, dissolved O₂ and CO₂, temperature). Other papers have already demonstrated optogenetic control of bioproduction in up to 5 L bioreactors⁵¹ and we look forward to seeing how optogenetics can be scaled-up to industrial settings⁵⁷.

6.4. Conclusion

We suggest a three-step approach to apply optogenetics to bioproduction control: characterize and optimize each of the optogenetic and the bioproduction components independently, before combining them. Indeed, optogenetic activation can vary across devices and the production behavior of a strain can be significantly affected by seemingly minor differences in culture conditions. Overall, this approach can help to reveal incompatibilities between the genetic components and eliminate optogenetic-dependent or pathway-dependent confounding factors.

While optogenetic systems are becoming better and illumination devices more widespread, the use of optogenetics to control microbial systems and its application to bioproduction is still a biotechnology in its infancy. Scalability remains a technical challenge and this study sets the stage for every step of the strain development process at the lab scale. Coming up next will be small and larger bioreactors before industrial scales. The promises of optogenetics for bioproduction lie in the controllability it offers to achieve more robust bioprocesses and apply real-time dynamic control of growth *versus* production, wherein lies an important resource allocation trade-off, with the overall goal of improving yields and making bioproduction an economically viable technology for sustainable production of any type of chemical or protein for multiple industrial sectors.

6.5. Materials and methods

6.5.1. Construction of yeast strains

The GFP optogenetic strain **OPTO-EXP** originated from Zhao *et al.* 2018⁹. Using the **CEN.PK2-1C** background, pPGK1-EL222 (constitutive expression of the light-activated transcription factor) and pC120-GFP (optogenetic promoter to which EL222 binds to activate the GFP transcription) were inserted at the *His3* locus, with a functional HIS3 copy (*CgHIS3*).

For constitutive beta-carotene production, constructs were made using Rabeaharindranto *et al.* 2019³⁴'s DNA material in which a trifusion enzyme CrtYBekI was developed. In plasmid **pHR0016**, the pGal1-10 promoter was replaced with pTDH3 using the Gibson assembly⁵⁸, to obtain plasmid **pPH_386**. Similarly, the bidirectional pGAL1-10 controlling the expression of CrtE and tHMG1 in plasmid **pMRI34** was replaced with pPGK1-pTDH3 to build plasmid **pPH_350**.

In strain **CEN.PK2-1C**, the trifusion CrtYBekI was inserted at the *ho* locus using CRISPR⁵⁹. In brief, a gRNA targeting the *ho* locus was designed and inserted into the pML104 plasmid containing cas9, the gRNA expression cassette and the URA3 marker (**pML104-ho**, built using restriction enzyme digestion and ligation according to Laughery *et al.* 2015⁵⁹). The template DNA strand was amplified from the plasmid **pPH_386**, containing pTDH3-CrtYBekI and two homologous arms of 90 bp targeting the *ho* locus. Upon transformation using the LiOAc Gietz method⁶⁰, both the **pML104-ho** plasmid and the template strand were added to the mix. In brief, Cas9 will cut repeatedly at the *ho* locus and favors homologous recombination with the template DNA at this locus, which acts as selective pressure against perfect double stranded break repair. After transformation, cells were plated on Complete Synthetic Medium (CSM)-URA. Clones were isolated and screened using OneTaq DNA polymerase (NEB). The **pML104-ho** plasmid was then cured using 5-fluoroorotic acid (5-FOA) CSM. The trifusion design³⁴ was broken down to the natural bifusion CrtYB and CrtI using the same CRISPR method (**pML104-ek**, and template from **YIplac211**), resulting in pTDH3-CrtYB-pTDH3-CrtI at the *ho* locus. In addition, using a gRNA targeting the *DPP1* locus (**pML104-DPP1**), CrtE and tHMG were inserted under the constitutive pPGK1 and pTDH3 promoters (**pPH_350**), both of which favor carbon flux to increase production of the GGPP precursor (at the same time, *DPP1* was deleted, which was shown to improve production³⁴).

To achieve optogenetic control of beta-carotene production (**yPH_551**), the background strain was **OPTO-EXP-mCherry** (**yPH_463**), in which the GFP reporter of the optoEXP system at the *HIS* locus of the **OPTO-EXP** strain was replaced with mCherry (using **pML104-GFP**) to prevent spectral overlap in microscopy (beta-carotene localizes in lipid droplets that are visible in the GFP channel and would therefore overlap with the GFP signal). The CrtYBekI trifusion was placed under the control of the pC120 optogenetic promoter in plasmid **pHR0016** (amplified from the plasmid **EZ-L83**) using the Gibson assembly⁵⁸. Then, the CrtYBekI trifusion was inserted at the *ho* locus in strain **OPTO-EXP-mCherry** (**yPH_463**) and broken down using CRISPR, similarly to the constitutive **yPH_554** strain. In addition, as for **yPH_554**, CrtE-pTDH3-pPGK1-tHMG was inserted at the *dpp1* locus.

Plasmids used in this study

Plasmid	Derived from	Description	Source
pHR0016	-	pGAL1-10-CrtYB(ek)I	Rabeharindranto 2019 ³⁴
pPH_386	pHR0016	pTDH3-CrtYB(ek)I	This study
pPH_371	pHR0016	pC120-CrtYB(ek)I	This study
pMRI34	-	CrtE-pGal1-10-tHMG1	Rabeharindranto 2019 ³⁴
pPH_350	pMRI34	CrtE-pTDH3-pPGK1-tHMG1	This study
YIplac211	-	pTDH3-CrtYB,pTDH3-CrtI, pTDH3-CrtE	Verwaal 2007 ³⁵
EZ-L83	-	pC120-GFP	Zhao 2018 ⁹
pML104	-	Cas9, gRNA scaffold (URA3)	Laughery 2015 ⁵⁹
pML104-ho	pML104	gRNA targeting <i>ho</i> promoter	This study
pML104-DPP1	pML104	gRNA targeting DPP1 CDS	This study
pML104-GFP	pML104	gRNA targeting GFP CDS	This study
pML104-ek	pML104	gRNA targeting the (ek) linker	This study

Strains used in this study

Yeast strain	Genotype	Source
CEN.PK2-1C	<i>MATa; ura3-52; trp1-289, leu2-3_112; his3D1;; MAL2-8c; SUC2</i>	Euroscarf (ref 30000A)
yPH_545	<i>CEN.PK2-1C</i> <i>ho::pTDH3-GFP</i>	This study
yPH_550	<i>CEN.PK2-1C</i> <i>ho::pADH1-GFP</i>	This study
OPTO-EXP (YEZ139)	<i>CEN.PK2-1C</i> <i>his3D1::pPGK1-EL222-pC120-GFP (CgHIS3)</i>	Zhao 2018 ⁹
yPH_463 (OPTO-EXP-mCherry)	<i>CEN.PK2-1C</i> <i>his3D1::pPGK1-EL222-pC120-mCherry (CgHIS3)</i>	This study
yPH_554	<i>CEN.PK2-1C</i> Δ <i>ho::pTDH3-CrtYB-pTDH3-CrtI</i> Δ <i>dpp1::CrtE-pTDH3-pPGK1-tHMG</i>	This study
yPH_551	OPTO-EXP-mCherry (yPH_463) Δ <i>ho::pC120-CrtYB-pTDH3-CrtI</i> Δ <i>dpp1::CrtE-pTDH3-pPGK1-tHMG</i>	This study

6.5.2. Growth conditions

All strains were grown in standard, home-made, filter-sterilized YPD [yeast extract 1% w/v (BD 212750), peptone 2% w/v (BD 211677) and D-glucose 2% w/v] at 30 °C. All devices except for eVOLVER, were placed in incubators with shaking at 250 rpm and protected from ambient light. For strain selection after transformation, CSM-URA was made with Yeast Nitrogen Base (YNB) without amino acids 0.67% w/v (BD 291940), D-glucose 2% w/v, CSM dropout-URA 0.08% (MP Bio 114500022). To prepare 5-FOA medium, 50 mL/L of 1g/L uracil solution and 0.8 g/L 5-FOA were added to CSM-URA.

6.5.3. Illumination devices

LED intensity. Würth Elektronik 151054BS04500 LEDs with a peak wavelength of 461 nm were used for all devices. Intensity measurements were conducted using a power meter (TOR Labs S120C) and divided by the sensor surface (0.7088 cm²). The intensities of the LEDs depends on their connection. Optobox LEDs have a maximum intensity of 4 mW/cm² due to the resistance present in the PCB design. Similarly, in eVOLVER, the side-LED intensity is limited to 6 mW/cm² by the 82 Ohm resistance. The additional LEDs in the eVOLVER and the OptoTubes LEDs are directly connected to the digital pins of an Arduino, such that their current is only dependent on the Arduino, reaching about 20 mAmp and yielding 12 mW/cm² intensity. In the OptoFlasks, the illumination stand was designed with the 20 mAmp constraint mentioned earlier; four LEDs in series was computed to reach a similar current per LED, such that their intensity was also 12 mW/cm².

OptoBox. Based on Gerhardt *et al.* 2016¹⁸, the OptoBox (*a.k.a.* the Light Plate Apparatus) was assembled using ordered PCBs, soldered LED-sockets, inserted blue LEDs and 3D-printed cases. LED calibration was performed using a power meter (TOR Labs S120C) and increasing illumination steps to achieve homogeneous illumination between all LEDs and wells at the same illumination intensity. Black 24-well cell imaging plates (Eppendorf 0030741005) were used to prevent light leaking between wells and sealed with aluminum foil to prevent light leakage and culture spillage and evaporation. A 25- μ m film lies at bottom of the well plate to allow high gas permeability and UV-light transparency, according to the manufacturer. For an experiment, 1 mL of inoculated medium is placed into each well. A sticking aluminum sheet is used to seal the wells, and the lid is placed in top. The imaging plate is placed in the previously programmed (via its SD card) OptoBox, which is then connected to a 5 V power supply. The device sits in a 30 °C incubator shaking at 250 rpm.

OptoTubes. LEDs are encased in a box at regular intervals (4 x 2 LEDs) and the tubes are held on top, with their bottom almost touching the LED, via a 3D printed holder (Fig.S2 and Supplementary File 1). LEDs are directly connected to an Arduino PWM pin and were measured to result in a LED intensity of 12 mW/cm². Pictures and schemes are shown in Fig.S2. To run an experiment, 3 mL (generally) of inoculated medium is placed into a 14 mL glass test tube. The tubes are closed with a cellulose cap, placed in the OptoTubes device, and the Arduino (previously programmed with the Arduino software for the chosen light

intensities) is connected to 12 V power supply. The device also sits in a 30 °C incubator shaking at 250 rpm.

eVOLVER. eVOLVER was built following the instructions of Wong *et al.* 2018¹⁹. To launch an experiment, autoclaved vials are filled with inoculated medium and closed with a simple lid or with the custom-lid (briefly detailed below and more extensively described in [Supplementary File 2](#)). The lid is loosely placed on top of the vial, *not* tightly screwed on, to allow for gas exchange. The vials are then placed in the aluminum sleeves (which are used for temperature control) of each eVOLVER unit. There, the additional LEDs, are placed and stacked by hand into each custom-lid. Using Node-RED software on the user interface, the culture parameters can be set (stirring, illumination from the side-LED, temperature), measure cycles modified, and names and notes added for each unit independently.

The lid of the glass vial used in eVOLVER is a hollow cap, normally closed with a removable silicone septum. To improve illumination, the cap was modified to accommodate insertion of LEDs that reach into the medium (custom-lid). For this, autoclavable cytometry tubes (5 mL Polypropylene Round-Bottom Tubes; BD Falcon REF 352063) are held tightly inside the cap hole using a larger piece of silicon (autoclavable) tubing. Using this design, additional LEDs can be placed inside the culture vial without getting wet and while maintaining sterility ([Supplementary File 2](#)). In the intensity measurements, we distinguished the side-LED of the original eVOLVER design (6 mW/cm² - a 82 Ohm resistor sets its intensity¹⁹) from the additional LEDs inserted from the top (12 mW/cm² each, independently). However, combining several additional LEDs in the custom-lid does not result in a linear increase in total intensity. Since the LEDs are stacked on top of each other in a plastic (quite opaque) cytometer tube, adding 1, 2, 3, or 4 additional LEDs was measured to correspond to adding 6.7, 8.3, 9.3 and 9.4 mW/cm² of intensity, respectively, (measured at the tip of the tube – [Fig.S1](#)) in the culture medium.

OptoFlask. The OptoFlask illumination stand is made by connecting standard LEDs in series of four in order to have 20 mA per LEDs (similar to the Arduino output, and recommended in the LED specs datasheet) with a 12 V input (DC power connector socket). Several series of four LEDs can be connected in derivation such that all LEDs remain at 20 mA per LED, resulting in a proportional increase in light intensity in the different illumination stands containing 4, 8, 12, 16 or 20 LEDs. To set up an experiment, 250 mL flasks (flat or indented -baffled – bottom) are filled with inoculated media and sealed with a cotton-cap, held with a thin rubber-band. The 250 mL flasks are positioned on the illumination stand, then placed in an oversized metal flask holder in a 30 °C shaking incubator (250 rpm) and held in place with a metal string and lab tape. Then, the stand is connected to the 12 V power supply. See [Fig.S3](#).

6.5.4. Quantification of optogenetic activation (cytometry)

To quantify the activation of the optogenetic system in the different devices under different growth and illumination conditions, the YEZ139 strain (OPTO-EXP⁹) was streaked onto YPD from a glycerol stock and incubated at room temperature for 48 h. For the preculture,

a single colony was picked from the plate and incubated overnight in the dark. The next morning, an aliquot of the preculture was inoculated into YPD to obtain a OD_{600} of 0.05 ($5 \cdot 10^6$ cells/mL) and then dispensed into the different containers for the illuminated cultures. The cultures and illumination were set for 6 hours: 2 Optoboxes, 8 OptoTubes, 5 Flasks, and 16 eVOLVER units can be tested in parallel. After culture, 200 μ L of cultures were diluted in 200 μ L of PBS and the levels of GFP resulting from the optogenetic activation were quantified using a BD LSR II flow cytometer (BD Biosciences) at an excitation wavelength of 488 nm and emission wavelength of 530 nm. The acquisition settings (voltage) for fluorescence quantification were identical for all experiments. Data were collected for 10,000 cells in each culture and analysis was performed in R using the FlowCore⁶¹ package.

6.5.5. Beta-carotene extraction and content estimation

Beta-carotene quantification was adapted from Reyes & Kao 2018³⁸. In brief, after inoculation of the media at OD_{600} 0.05 and growth for 24 h, each yeast culture sample was diluted 1:100, the OD_{600} was read and Cell Dry Weight was estimated accordingly using a calibration curve (of equivalences between spectrophotometer and actual freeze-dried weighed samples). Then, 1 mL of culture was transferred to a collection tube (MP Bio). The cells were collected by centrifugation at 11 000 x g for 2 min, the supernatant was discarded, 250 μ L of acid-washed glass beads (Sigma 425-600um – G8772) and 1 mL of dodecane were added to the cell pellet and the yeast cells were lysed using a FastPrep bead-beater (MP Bio) for five times for 1 min to ensure maximal carotenoid recovery. After cell disruption, the samples were centrifuged (11 000 x g, 2 min) to separate cell debris and glass beads, 200 μ L of the supernatant was transferred to a 96 well plate and scanned from OD_{200} to OD_{700} using a Spark TECAN analyzer. The A_{454} of the scan was used to estimate the beta-carotene of the dodecane solution using calibration curve prepared with hexane and beta-carotene's extinction coefficient. By comparing the determined beta-carotene concentration in the dodecane solution with the actual OD and culture volume, the content, yield and titer can be calculated. Note that *non*-beta-carotene-producing cells yield a production value of about 200 μ g/g CDW, even though the colonies will appear white, *i.e.*, this value is the limit of detection.

To view the color of the cell pellets, cultures were concentrated to OD 50 by centrifugation, 200 μ L was poured into a 96-well-plate, allowed to sit for 15 minutes, then the plate was color-scanned using a desktop scanner.

6.5.6. Microscopy

Bright field (BF) and fluorescence images were acquired with MetaMorph software from an Olympus IX83 inverted epifluorescence microscope paired with an Andor CMOS Zyla camera using an 100x objective. Samples were illuminated using a CoolLED pE4000 fluorescence lamp. An exposure time of 200 ms was used to acquire BF images. Images of GFP fluorescence were acquired using excitation and emission wavelengths of 470 and 525 nm, respectively, and an exposure time of 250 ms at 25% light intensity. To acquire images, a small volumes of culture were centrifuged and the cells were simply loaded into a custom-made PDMS chip⁶² to obtain a monolayer of cells. The chip was then placed under the 100x objective for image acquisition.

Bibliography

1. Srinivasan P, Smolke CD. Biosynthesis of medicinal tropane alkaloids in yeast. *Nature*. 2020;585(7826):614-619. doi:10.1038/s41586-020-2650-9
2. Galanie S, Thodey K, Trenchard IJ, Filsinger Interrante M, Smolke CD. Complete biosynthesis of opioids in yeast. *Science (80-)*. 2015;349(6252):1095-1100. doi:10.1126/science.aac9373
3. Chen R, Yang S, Zhang L, Zhou YJ. Advanced Strategies for Production of Natural Products in Yeast. *iScience*. 2020;23(3):100879. doi:10.1016/j.isci.2020.100879
4. Oud B, Van Maris AJA, Daran JM, Pronk JT. Genome-wide analytical approaches for reverse metabolic engineering of industrially relevant phenotypes in yeast. *FEMS Yeast Res*. 2012;12(2):183-196. doi:10.1111/j.1567-1364.2011.00776.x
5. Pereira F, Lopes H, Maia P, et al. Model-guided development of an evolutionarily stable yeast chassis. *Mol Syst Biol*. 2021;17(7):1-18. doi:10.15252/msb.202110253
6. Subramanian I, Verma S, Kumar S, Jere A, Anamika K. Multi-omics Data Integration, Interpretation, and Its Application. *Bioinform Biol Insights*. 2020;14:7-9. doi:10.1177/1177932219899051
7. Sahu A, Blätke MA, Szymański JJ, Töpfer N. Advances in flux balance analysis by integrating machine learning and mechanism-based models. *Comput Struct Biotechnol J*. 2021;19:4626-4640. doi:10.1016/j.csbj.2021.08.004
8. Martin JF, Demain AL. Control of antibiotic biosynthesis. *Microbiol Rev*. 1980;44(2):230-251. doi:10.1128/membr.44.2.230-251.1980
9. Zhao EM, Zhang Y, Mehl J, et al. Optogenetic regulation of engineered cellular metabolism for microbial chemical production. *Nature*. 2018;555(7698):683-687. doi:10.1038/nature26141
10. Lalwani MA, Zhao EM, Wegner SA, Avalos JL. The *Neurospora crassa* Inducible Q System Enables Simultaneous Optogenetic Amplification and Inversion in *Saccharomyces cerevisiae* for Bidirectional Control of Gene Expression. *ACS Synth Biol*. 2021;10(8):2060-2075. doi:10.1021/acssynbio.1c00229
11. Tan SZ, Prather KL. Dynamic pathway regulation: recent advances and methods of construction. *Curr Opin Chem Biol*. 2017;41:28-35. doi:10.1016/j.cbpa.2017.10.004
12. Raghavan AR, Salim K, Yadav VG. Optogenetic Control of Heterologous Metabolism in *E. coli*. *ACS Synth Biol*. 2020;9(9):2291-2300. doi:10.1021/acssynbio.9b00454
13. Lalwani MA, Ip SS, Carrasco-López C, et al. Optogenetic control of the lac operon for bacterial chemical and protein production. *Nat Chem Biol*. Published online 2020. doi:10.1038/s41589-020-0639-1
14. Senoo S, Tandar ST, Kitamura S, Toya Y, Shimizu H. Light-inducible flux control of triosephosphate isomerase on glycolysis in *Escherichia coli*. *Biotechnol Bioeng*. 2019;116(12):3292-3300. doi:10.1002/bit.27148
15. Ding Q, Ma D, Liu GQ, et al. Light-powered *Escherichia coli* cell division for chemical production. *Nat Commun*. 2020;11(1):1-14. doi:10.1038/s41467-020-16154-3
16. Zhao EM, Suck N, Wilson MZ, et al. Light-based control of metabolic flux through

- assembly of synthetic organelles. *Nat Chem Biol.* 2019;15(6):589-597. doi:10.1038/s41589-019-0284-8
17. Lalwani MA, Kawabe H, Mays RL, Hoffman SM, Avalos JL. Optogenetic Control of Microbial Consortia Populations for Chemical Production. *ACS Synth Biol.* 2021;10(8):2015-2029. doi:10.1021/acssynbio.1c00182
 18. Gerhardt KP, Olson EJ, Castillo-Hair SM, et al. An open-hardware platform for optogenetics and photobiology. *Sci Rep.* 2016;6(June):1-13. doi:10.1038/srep35363
 19. Wong BG, Mancuso CP, Kiriakov S, Bashor CJ, Khalil AS. Precise , automated control of conditions for high- throughput growth of yeast and bacteria with eVOLVER. *Nat Publ Gr.* 2018;36(April). doi:10.1038/nbt.4151
 20. Motta-Mena LB, Reade A, Mallory MJ, et al. An optogenetic gene expression system with rapid activation and deactivation kinetics. *Nat Chem Biol.* 2014;10(3):196-202. doi:10.1038/nchembio.1430
 21. Bogacz-Radomska L, Harasym J. β -Carotene-properties and production methods. *Food Qual Saf.* 2018;2(2):69-74. doi:10.1093/fqsafe/fyy004
 22. Ribeiro BD, Barreto DW, Coelho MAZ. Technological Aspects of β -Carotene Production. *Food Bioprocess Technol.* 2011;4(5):693-701. doi:10.1007/s11947-011-0545-3
 23. Paddon CJ, Westfall PJ, Pitera DJ, et al. High-level semi-synthetic production of the potent antimalarial artemisinin. *Nature.* 2013;496(7446):528-532. doi:10.1038/nature12051
 24. Nowrouzi B, Li RA, Walls LE, et al. Enhanced production of taxadiene in *Saccharomyces cerevisiae*. *Microb Cell Fact.* 2020;19(1):1-12. doi:10.1186/s12934-020-01458-2
 25. Hansen NL, Miettinen K, Zhao Y, et al. Integrating pathway elucidation with yeast engineering to produce polypunonic acid the precursor of the anti-obesity agent celastrol. *Microb Cell Fact.* 2020;19(1):1-17. doi:10.1186/s12934-020-1284-9
 26. Benzinger D, Ovinnikov S, Khammash M. Synthetic gene networks recapitulate dynamic signal decoding and differential gene expression. *Cell Syst.* 2022;13(5):353-364.e6. doi:10.1016/j.cels.2022.02.004
 27. Shaw WM, Yamauchi H, Mead J, et al. Engineering a Model Cell for Rational Tuning of GPCR Signaling. *Cell.* 2019;177(3):782-796.e27. doi:10.1016/j.cell.2019.02.023
 28. Liu R, Liu L, Li X, Liu D, Yuan Y. Engineering yeast artificial core promoter with designated base motifs. *Microb Cell Fact.* 2020;19(1):1-9. doi:10.1186/s12934-020-01305-4
 29. Duplus-Bottin H, Spichy M, Triqueneaux G, et al. A single-chain and fast-responding light-inducible cre recombinase as a novel optogenetic switch. *Elife.* 2021;10:1-52. doi:10.7554/eLife.61268
 30. Pénicaud C, Achir N, Dhuique-Mayer C, Dornier M, Bohuon P. Degradation of β -carotene during fruit and vegetable processing or storage: Reaction mechanisms and kinetic aspects: A review. *Fruits.* 2011;66(6):417-440. doi:10.1051/fruits/2011058
 31. Enwemeka CS, Baker TL, Bumah V V. The role of UV and blue light in photo-eradication of microorganisms. *J Photochem Photobiol.* 2021;8:100064. doi:10.1016/j.jpap.2021.100064

32. Grangeteau C, Lepinois F, Winckler P, Perrier-Cornet JM, Dupont S, Beney L. Cell death mechanisms induced by photo-oxidation studied at the cell scale in the yeast *Saccharomyces cerevisiae*. *Front Microbiol.* 2018;9(NOV):1-8. doi:10.3389/fmicb.2018.02640
33. Clomburg JM, Qian S, Tan Z, Cheong S, Gonzalez R. The isoprenoid alcohol pathway, a synthetic route for isoprenoid biosynthesis. *Proc Natl Acad Sci U S A.* 2019;116(26):12810-12815. doi:10.1073/pnas.1821004116
34. Rabeharindranto H, Castaño-Cerezo S, Lautier T, et al. Enzyme-fusion strategies for redirecting and improving carotenoid synthesis in *S. cerevisiae*. *Metab Eng Commun.* 2019;8(December 2018):1-11. doi:10.1016/j.mec.2019.e00086
35. Verwaal R, Wang J, Meijnen JP, et al. High-level production of beta-carotene in *Saccharomyces cerevisiae* by successive transformation with carotenogenic genes from *Xanthophyllomyces dendrorhous*. *Appl Environ Microbiol.* 2007;73(13):4342-4350. doi:10.1128/AEM.02759-06
36. Zhao Y, Zhang Y, Nielsen J, Liu Z. Production of β -carotene in *Saccharomyces cerevisiae* through altering yeast lipid metabolism. *Biotechnol Bioeng.* 2021;118(5):2043-2052. doi:10.1002/bit.27717
37. Jing Y, Guo F, Zhang S, et al. Recent Advances on Biological Synthesis of Lycopene by Using Industrial Yeast. *Ind Eng Chem Res.* 2021;60(9):3485-3494. doi:10.1021/acs.iecr.0c05228
38. Reyes LH, Kao KC. Growth-coupled carotenoids production using adaptive laboratory evolution. *Methods Mol Biol.* 2018;1671:319-330. doi:10.1007/978-1-4939-7295-1_20
39. Scita G. The stability of β -carotene under different laboratory conditions. *J Nutr Biochem.* 1992;3(3):124-128. doi:10.1016/0955-2863(92)90104-Q
40. Telfer A, De Las Rivas J, Barber J. β -Carotene within the isolated Photosystem II reaction centre: photooxidation and irreversible bleaching of this chromophore by oxidised P680. *BBA - Bioenerg.* 1991;1060(1):106-114. doi:10.1016/S0005-2728(05)80125-2
41. Bugaj LJ, Lim WA. High-throughput multicolor optogenetics in microwell plates. *Nat Protoc.* 2019;14(7):2205-2228. doi:10.1038/s41596-019-0178-y
42. Repina NA, McClave T, Johnson HJ, Bao X, Kane RS, Schaffer D V. Engineered Illumination Devices for Optogenetic Control of Cellular Signaling Dynamics. *Cell Rep.* 2020;31(10):107737. doi:10.1016/j.celrep.2020.107737
43. Heo J, Cho DH, Ramanan R, Oh HM, Kim HS. PhotoBiobox: A tablet sized, low-cost, high throughput photobioreactor for microalgal screening and culture optimization for growth, lipid content and CO₂ sequestration. *Biochem Eng J.* 2015;103:193-197. doi:10.1016/j.bej.2015.07.013
44. Olson EJ, Hartsough LA, Landry BP, Shroff R, Tabor JJ. Characterizing bacterial gene circuit dynamics with optically programmed gene expression signals. *Nat Methods.* 2014;11(4):449-455. doi:10.1038/nmeth.2884
45. Wang H, Yang YT. Mini Photobioreactors for in Vivo Real-Time Characterization and Evolutionary Tuning of Bacterial Optogenetic Circuit. *ACS Synth Biol.* 2017;6(9):1793-1796. doi:10.1021/acssynbio.7b00091
46. Steel H, Habgood R, Kelly C, Papachristodoulou A. In situ characterisation and

- manipulation of biological systems with Chi.Bio. *PLoS Biol.* Published online 2020:1-12. doi:10.1371/journal.pbio.3000794
47. Nedbal J, Gao L, Suhling K. Bottom-illuminated orbital shaker for microalgae cultivation. *HardwareX.* 2020;8:e00143. doi:10.1016/j.ohx.2020.e00143
 48. Pires JCM, Alvim-Ferraz MCM, Martins FG. Photobioreactor design for microalgae production through computational fluid dynamics: A review. *Renew Sustain Energy Rev.* 2017;79(May):248-254. doi:10.1016/j.rser.2017.05.064
 49. Loomba V, Huber G, Von Lieres E. Single-cell computational analysis of light harvesting in a flat-panel photo-bioreactor. *Biotechnol Biofuels.* 2018;11(1):1-11. doi:10.1186/s13068-018-1147-3
 50. Pfeiffer T, Morley A. An evolutionary perspective on the Crabtree effect. *Front Mol Biosci.* 2014;1(OCT):1-6. doi:10.3389/fmolb.2014.00017
 51. Zhao EM, Lalwani MA, Chen J-M, Orillac P, Toettcher JE, Avalos JL. Optogenetic Amplification Circuits for Light-Induced Metabolic Control. *ACS Synth Biol.* 2021;10(5):1143-1154. doi:10.1021/acssynbio.0c00642
 52. Zhao EM, Lalwani MA, Lovelett RJ, et al. Design and Characterization of Rapid Optogenetic Circuits for Dynamic Control in Yeast Metabolic Engineering. Published online 2020. doi:10.1021/acssynbio.0c00305
 53. Benzinger D, Khammash M. Pulsatile inputs achieve tunable attenuation of gene expression variability and graded multi-gene regulation. *Nat Commun.* 2018;9(1). doi:10.1038/s41467-018-05882-2
 54. Looser V, Bruhlmann B, Bumbak F, et al. Cultivation strategies to enhance productivity of *Pichia pastoris*: A review. *Biotechnol Adv.* 2014;33(6):1177-1193. doi:10.1016/j.biotechadv.2015.05.008
 55. Aw R, Polizzi KM. Can too many copies spoil the broth? *Microb Cell Fact.* 2013;12(1):128. doi:10.1186/1475-2859-12-128
 56. López J, Bustos D, Camilo C, Arenas N, Saa PA, Agosin E. Engineering *Saccharomyces cerevisiae* for the Overproduction of β -Ionone and Its Precursor β -Carotene. *Front Bioeng Biotechnol.* 2020;8(September):1-13. doi:10.3389/fbioe.2020.578793
 57. Pouzet S, Banderas A, Bec M Le, Lautier T, Truan G, Hersen P. The promise of optogenetics for bioproduction: Dynamic control strategies and scale-up instruments. *Bioengineering.* 2020;7(4):1-17. doi:10.3390/bioengineering7040151
 58. Gibson DG, Young L, Chuang R, et al. Enzymatic assembly of DNA molecules up to several hundred kilobases. 2009;6(5):12-16. doi:10.1038/NMETH.1318
 59. Laughery MF, Hunter T, Brown A, et al. New vectors for simple and streamlined CRISPR-Cas9 genome editing in *Saccharomyces cerevisiae*. *Yeast.* 2015;32(12):711-720. doi:10.1002/yea.3098
 60. Gietz RD, Schiestl RH. High-efficiency yeast transformation using the LiAc/SS carrier DNA/PEG method. *Nat Protoc.* 2007;2(1):31-34. doi:10.1038/nprot.2007.13
 61. Ellis B, Haaland P, Hahne F, et al. flowCore: Basic structures for flow cytometry data. *R Packag version 280.* Published online 2022.
 62. Llamosi A, Gonzalez-Vargas AM, Versari C, et al. What Population Reveals about Individual Cell Identity: Single-Cell Parameter Estimation of Models of Gene

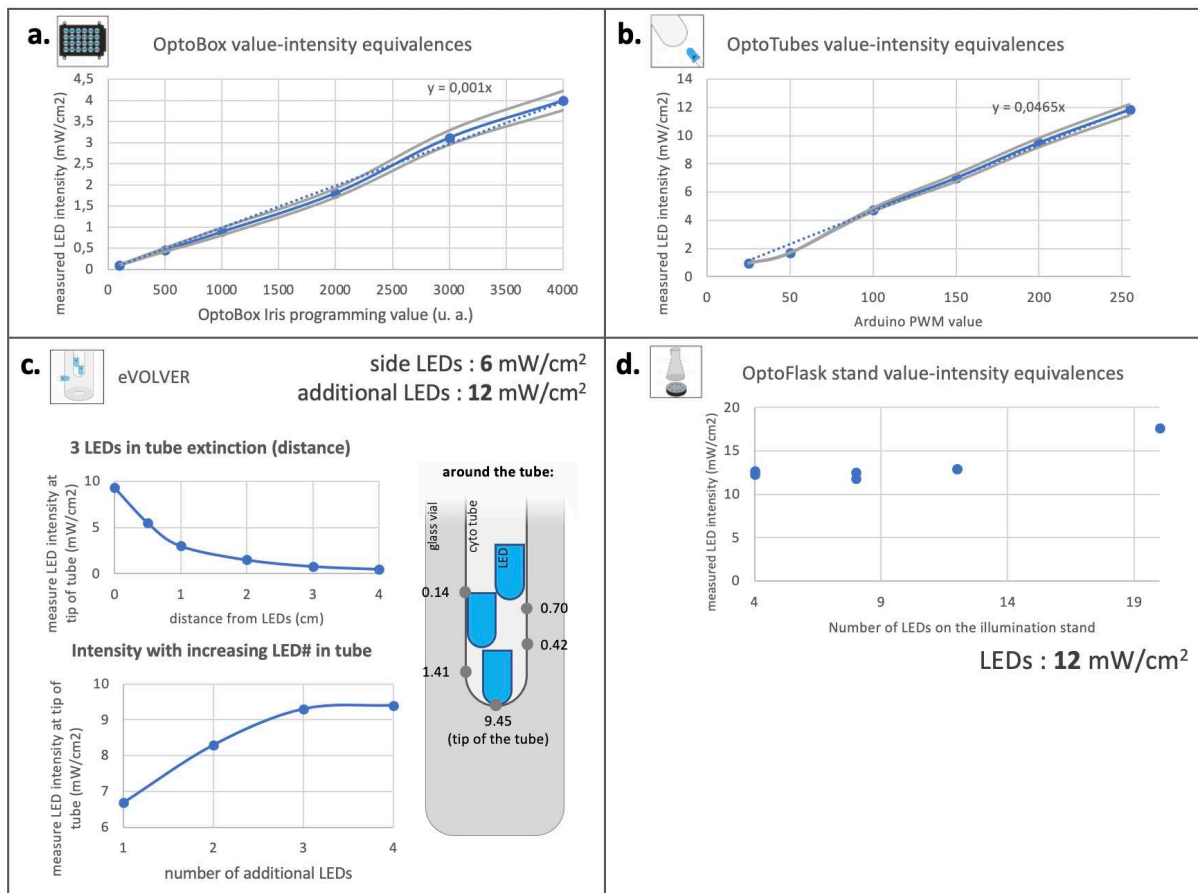
Supplementary information

Supplementary Figure S1: Illumination quantifications across devices
Supplementary Figure S2: OptoTubes design
Supplementary Figure S3: OptoFlasks illumination stands designs
Supplementary Figure S4: Optogenetic activation timelines
Supplementary Figure S5: Lipid droplets microscopic observations
Supplementary Figure S6: Beta-carotene production timeline
Supplementary Figure S7: Yeast strains growth curves
Supplementary Figure S8: Beta-carotene pathway

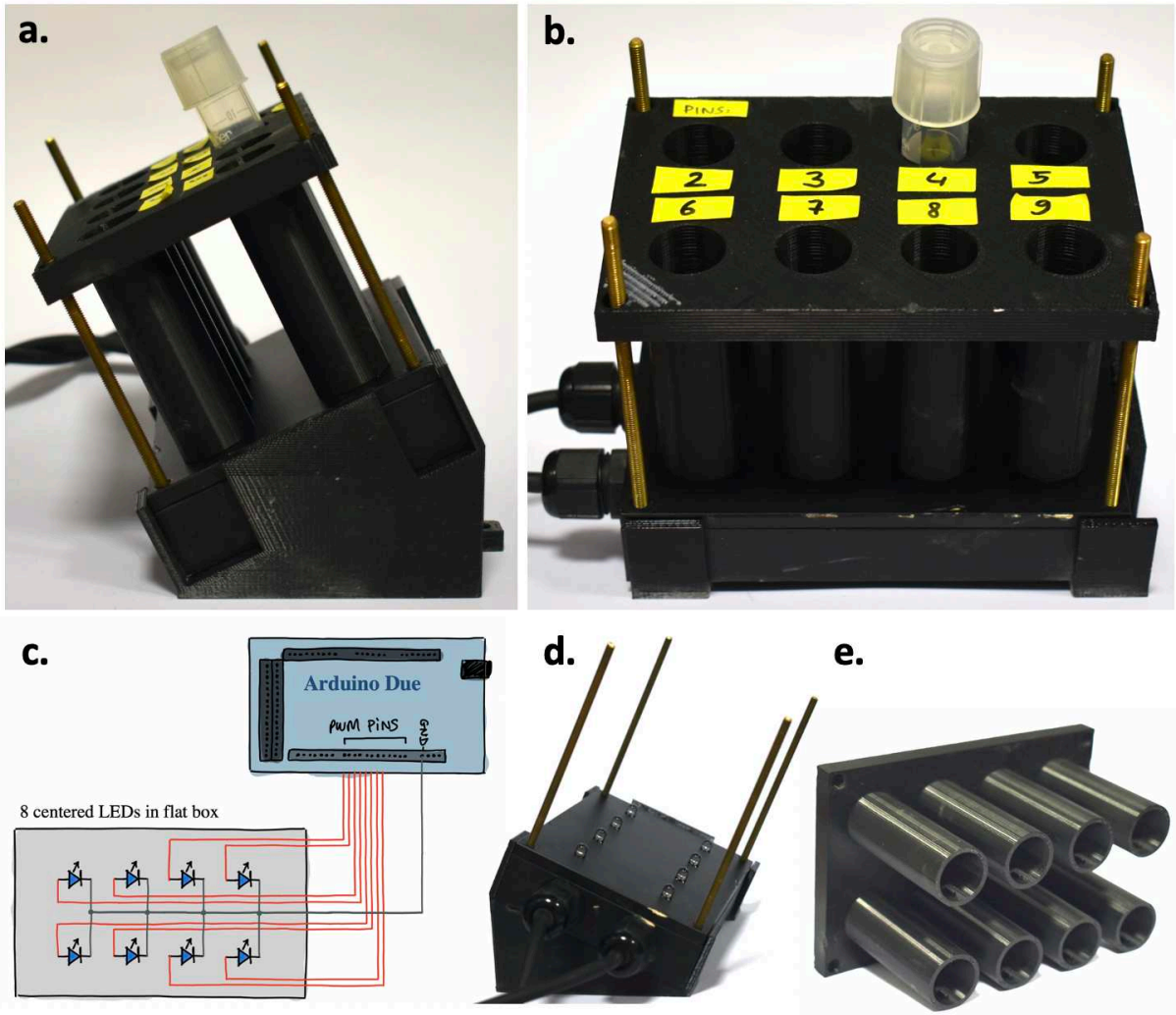
Other files:

Supplementary File 1: OptoTubes STL Files
Supplementary File 2: eVOLVER design, hardware and software
Supplementary File 3: eVOLVER 3D-printed holder STL File

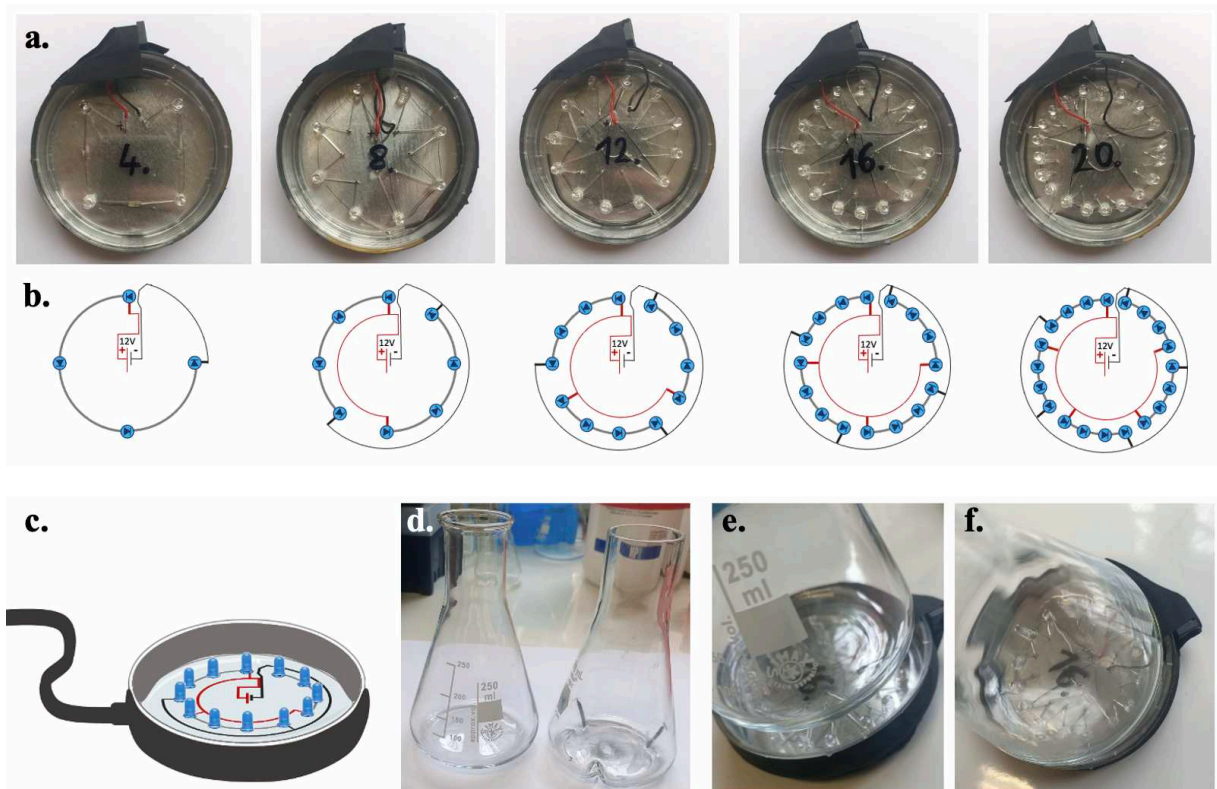
→ https://github.com/Lab513/DIY_Optogenetics



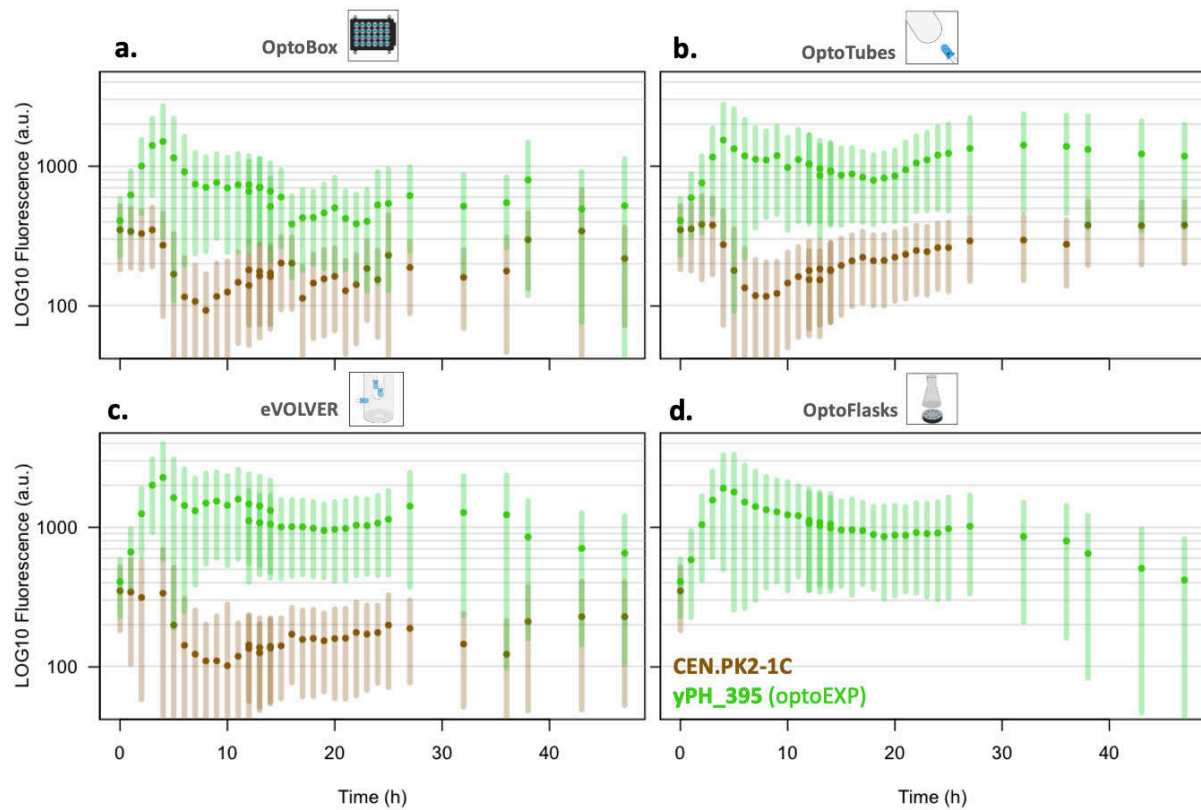
Supplementary Figure S1. Quantification of illumination across devices: set values (a.u.) vs. intensity (mW/cm²). (a) OptoBox equivalences were measured using a sensor placed directly above the LEDs, at the distance the imaging plate receives light. (b) The intensity of OptoTubes LEDs linearly increases with the PWM Arduino value up to a maximum of 12 mW/cm². Values were measured directly above (touching) the LED. (c) In the eVOLVER, intensity, and therefore illumination, decrease exponentially with the distance between the LED and the tip (base) of the tube containing the additional LEDs. Data for 3 additional LEDs are presented (top left). Bottom-left: increasing the number of LEDs in the tube increases the intensity but saturates at 3 LEDs. Right-side: scheme of the arrangement of the LEDs in the tube in the glass vial, and intensity values measured by sensor touching the tube at different locations around the tube. Note that to compute the total intensity in the medium, the 6 mW/cm² (the intensity set by a resistor) of the side-LED should be added to these measures. (d) Measured intensity in the OptoFlask illumination stand: all LEDs display 12 mW/cm². The higher value observed for 20 LEDs is due to light leaking from nearby LEDs. Measures were taken on top of the petri-dish covering the LEDs.



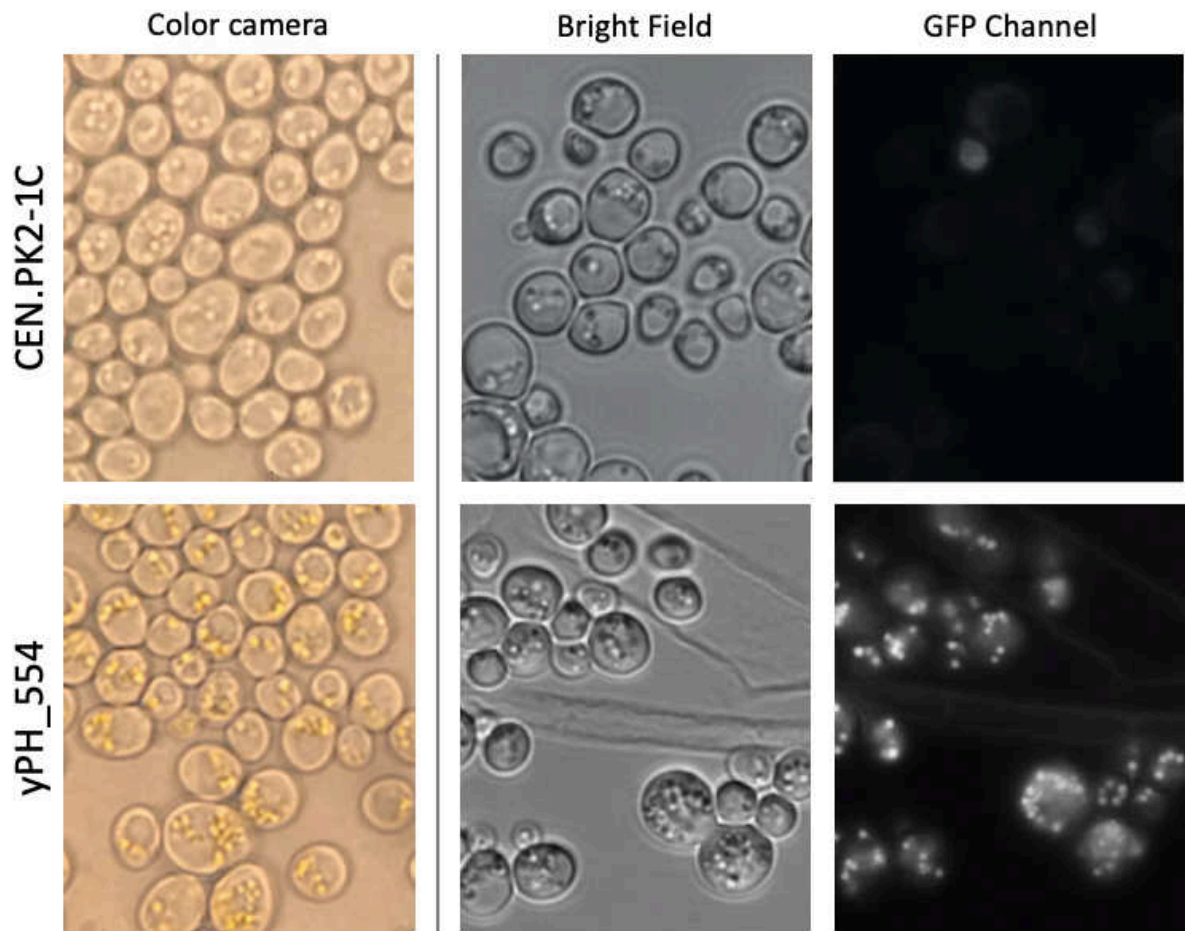
Supplementary Figure S2. Design of the OptoTubes. (a) Side-view and (b) front view of the device. (c) Electronic connection inside the flat box containing the LEDs, positioned on its 3D-printed stand in (d). (e) 3D-printed tube holder (which holds and positions the culture tubes above the LEDs). Long screws are used to secure the entire structure. The STL files for the 3D-printed parts are available in Supplementary File 1.



Supplementary Figure S3. Designs of OptoFlasks illumination stands. (a) Pictures of the five types of illumination stands with 4, 8, 12, 16 and 20 LEDs. The hump on top corresponds to the DC power supply jack connector (12V). (b) Corresponding electrical designs that fit inside Petri dishes and ensure same light intensities between LEDs and between illumination stands. (c) Side-view scheme of the illumination stand in which 250 mL flasks, either flat or indented/baffled (d) are placed. (e., f.) To maximize illumination, the circular pattern of LEDs lines up with the edges of the flask, where the medium will localize in a shaking incubator.

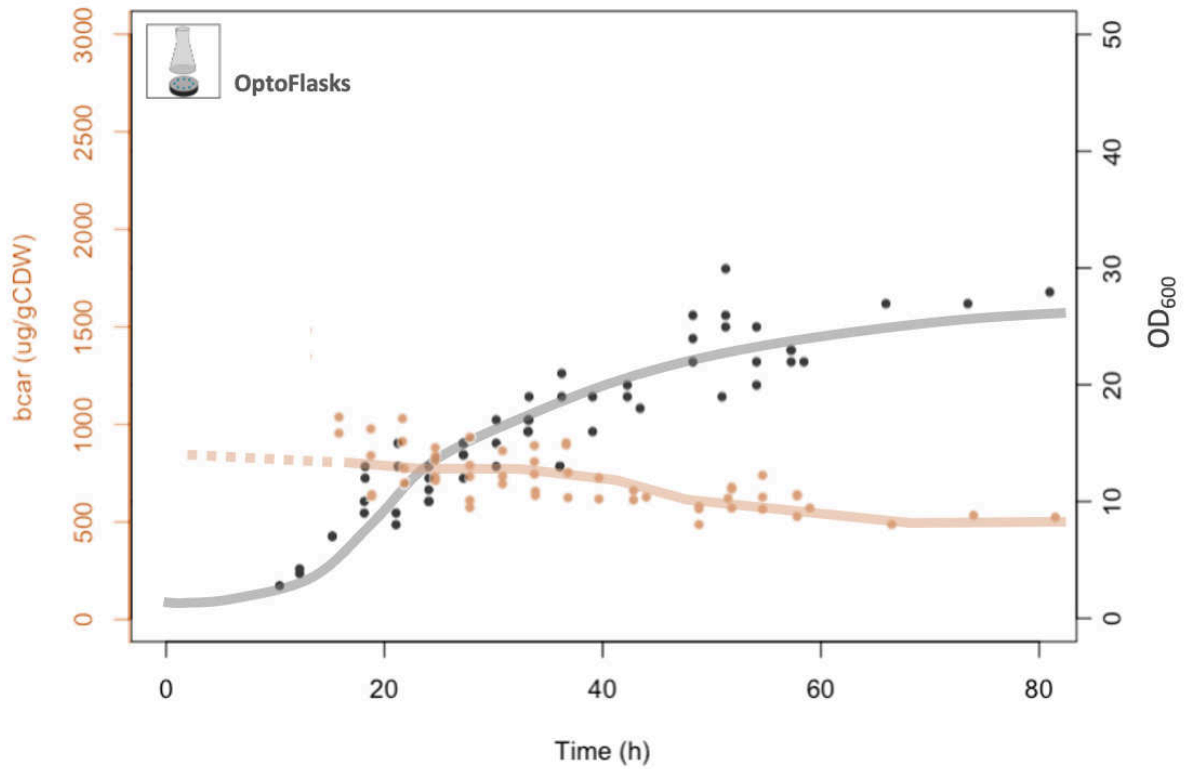


Supplementary Figure S4. Timelines of optogenetic activation in the different devices. Brown points are the CEN.PK2-1C WT strain. Green points are the OPTO-EXP strain. Error bars represent the standard deviation fluorescence value of the 10 000 cells quantified. The exposure to light of a culture with an OD600 0.05 starts at T0; GFP level was measured every hour up to 25 hours, then at 27, 32, 36, 38, 43 and 47 hours. (a) Activation in the OptoBox, 1 mL cultures, illumination is 8000 (max). (b) Activation in the OptoTubes: 3 mL cultures, illumination 255 (max). (c) Activation in eVOLVER: 15 mL cultures, stirring 255, s+2 illumination. (d) Activation in OptoFlasks: 50 mL cultures in 250 mL indented flasks, 12 LED illumination stand.

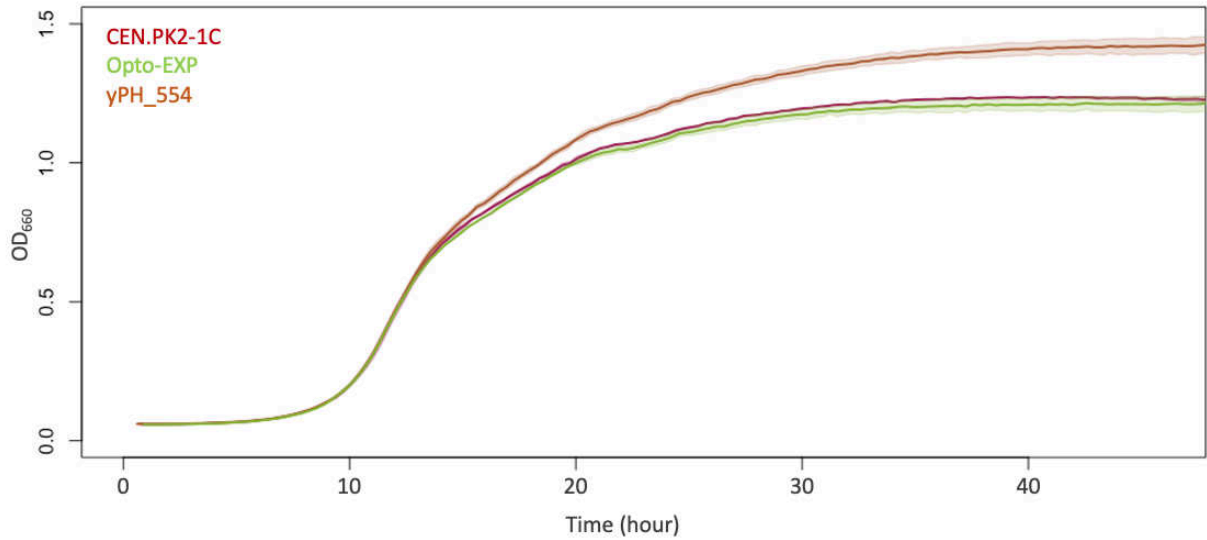


Supplementary Figure S5. Microscopic observations of lipid droplets (100X). Beta-carotene localizes in lipid droplets. (Left) Color camera view (does not correspond to the other microscopic pictures). Note the golden droplets are only present in the cells of the constitutive producer strain yPH_554. It is necessary to adjust with the microscope diaphragms to obtain a lighting setting that display the yellow color, besides using a color camera (these images were taken with a phone through an ocular lens). (Middle) Bright field (exposure 1 sec) image and corresponding fluorescent (exposure 1 sec) image (Right).

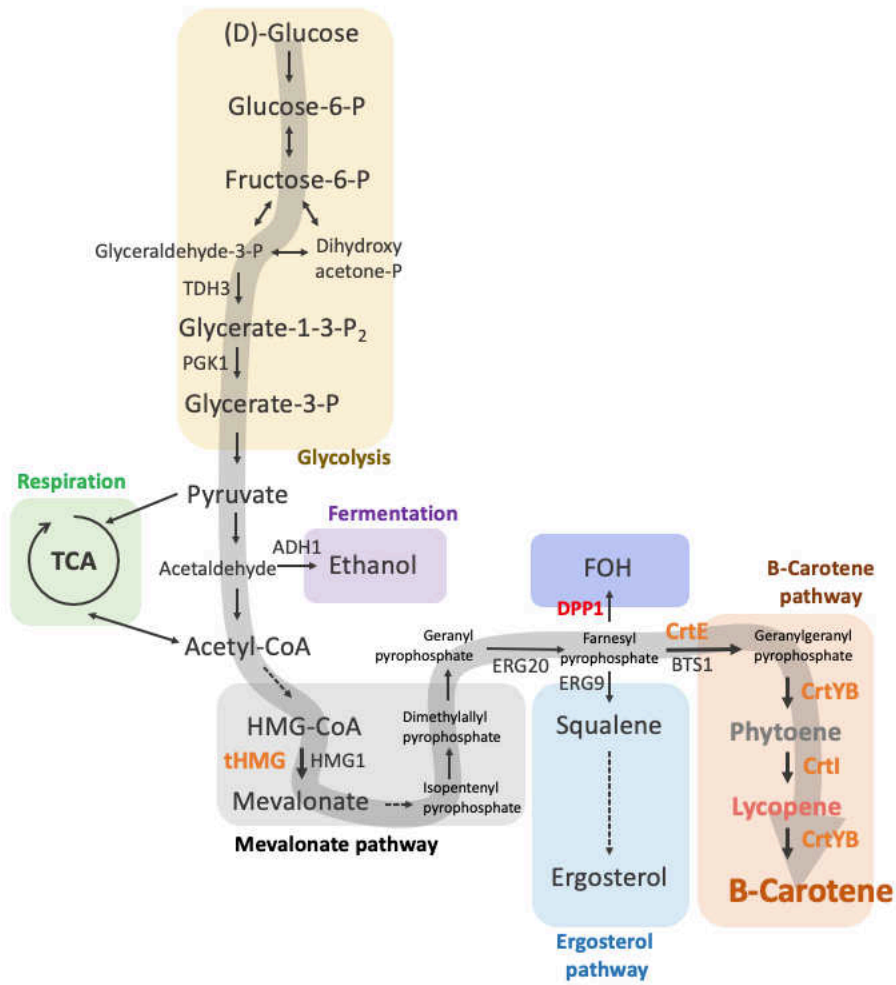
yPH_554 – Constitutive beta-carotene production



Supplementary Figure S6. Beta-carotene production during cultivation of strain yPH_554. Each point corresponds to one measure, beta-carotene content was estimated as described in the materials and methods. OD₆₀₀ was measured by hand using a spectrophotometer. The small number of cells at the beginning of the culture prevented early quantification of beta-carotene (dashed line). The hand-drawn solid lines illustrate proposed trends – the grey line is estimated from Figure S7. Growth and production in the dark, 50 mL culture in a 250 mL indented flask; 24 h was chosen as appropriate timepoint to estimate beta-carotene production under different conditions.



Supplementary Figure S7. Yeast strain growth curves. Cultures were performed in filter sterilized YPD and growth was quantified by reading optical density values using a plate reader. No burden was detected for the beta-carotene constitutive producer strain yPH_554 compared to the non-producer strains, i.e., the control CEN.PK2-1C and the optogenetic strain OPTO-EXP: the exponential growth phase was not impacted, and the other phases of growth appear to lead to increased total biomass, perhaps due to lower overflow metabolism in the fermentation phase. N=2.



Supplementary Figure S8. Yeast metabolic pathways. With detailed chemical names.

7. Conclusions

7.1. Conclusions

7.1.1. Summary

During my PhD, I investigated how to apply optogenetic control to beta-carotene production in the yeast *Saccharomyces cerevisiae* and how this translates at different lab-scales.

In the **introduction**, I presented bioproduction techniques and stakes, leading to the realization of the need for better control tools. With its high versatility, reversibility and controllability, optogenetics comes as an ideal inducer for bioproduction purposes. In the published review following the introduction, I presented how optogenetics is already being applied for bioproduction in a handful of studies and started to discuss devices used at the lab-scale to cultivate and control producer microbes controlled by light.

Indeed, **using optogenetics comes with challenges**. Mainly, in terms of strain construction and regarding the scalability of the process and strain development. Most importantly, we focused on how to scale up optogenetic control for bioproduction at the lab scale and how various illumination devices could impact the performance of a strain producing beta-carotene controlled by light.

In the **first chapter**, I presented the work I have done to develop optogenetic devices in the lab and discussed other available illumination systems in increasing culture scales. This included mainly the development of the OptoBox (imaging plates), OptoTubes (test tubes), OptoFlasks (shake flasks), and finally, adapting the eVOLVER platform for optogenetics: improving its illumination capacity and developing the framework and software allowing for automated experiments with high control. For those various culture devices, each with different but complementary purposes along the strain development process, we discussed advantages and drawbacks, which encompasses mainly a trade-off between experimental throughput, controllability, and feedback from the experiment, *i.e.*, being able to monitor various parameters during the cultivation and production process. Besides, the amount of light put in the system as well as the geometry of the device will impact cells' exposure to light, and this remains hard to anticipate, though important to develop a robust process. Now that we have developed those devices, it is therefore necessary to test optogenetic activation across scales to understand those interplays.

In **chapter 2**, I detailed the construction of an optogenetically controlled beta-carotene producer strain. For this, we proceeded by combining an already working beta-carotene production design with the light-activated transcription factor EL222 via the use of the pC120 optogenetic promoter, activated by EL222. The first "slow producer" strain was characterized in various devices and proved to produce beta-carotene only in the presence of light. The impacts of temperature, stirring and carbon-source feedstock were tested in a combinatorial fashion thanks to the throughput and controllability offered by the eVOLVER system. From this, we concluded that only at low temperature and in glycerol medium (low growth conditions) would the strain produce beta-carotene. Driven by such a slow growth rate and

slow production dynamics, we sought to improve this strain. By deconstructing part of our previous design, we succeeded in obtaining a strain in which beta-carotene production was occurring in standard growing conditions and only in the presence of blue light. This showed that adapting a heterologous genetic design with optogenetics is not trivial and that specific precautions are needed to obtain functional strains. We observed also that production seemed to vary across devices, drawing questions about the impact of device and culture scale on the optogenetic activation and light-controlled production.

Finally, the manuscript of my paper under revision is placed as **chapter 3**. There, to study the impact of culture parameters and scale on optogenetic control of bioproduction, we first treated separately optogenetic activation and beta-carotene production. Both were independently tested in the various devices. We found that they could be independently optimized in every device, mostly by reducing culture volume and/or increasing stirring when possible. We also determined the minimum amount of light in each device to obtain the maximal optogenetic activation. Finally, the optogenetically-controlled beta-carotene producer strain was tested in the different devices and found that, once all devices beta-carotene production was not necessarily proportional to the optogenetic activation, highlighting the importance of finely controlling heterologous systems.

7.1.2. Contribution

With this work, we can now propose answers to our original questions:

How to scale up optogenetics?

Various illumination devices are now available, and while some are more difficult to build than others, each has advantages and drawbacks in terms of ease to build in a DIY fashion, controllability, throughput and feedback. The way to implement optogenetic to a culture device will impact how the light enters, stays and exits the medium, hence varying illumination per cell. Therefore, the geometry of the device and the light implementation will impact the optogenetic activation. For devices to be comparable to one another, it is important to calibrate them: not necessarily given the quantity of light in the medium *per se* but given the optogenetic activation reported by an optogenetic strain with a simple GFP reporter as we did in chapter 3. This way, light input and activation levels can be compared between devices. Besides, each device can also be optimized for optogenetic activation: indeed, not only the light will impact optogenetic activation, but also other culture parameters like the volume and stirring rate. Finally, while most small-scale traditional culture devices can be adapted to optogenetics with DIY methods, implementing optogenetics for industrial scale cultures remains an open question, but the results presented in this manuscript can help foreshadow the difficulties and challenges that will be encountered.

How to apply optogenetics for bioproduction?

Making a producer strain controlled using optogenetics is technically (in terms of molecular biology) rather easy: it relies on classical molecular cloning techniques. However, it is a new way of controlling the biological process that can sometimes be unpredictable, like

any other biological system. In our case, we saw that it created difficulties. This emphasizes the need to have precise controls to confront a newly constructed optogenetic strain and never take for granted that a strain will work. Besides, optogenetic devices must be ready and well-characterized to make sure they do not add any uncertainty regarding optogenetic activation.

Indeed, when combining production with optogenetics (2 different genetic systems, each with its specific characteristics, sensitivities and limitations), all those parameters are intertwined such that it may be hard to disentangle the factors that impact the overall strain performance. To alleviate this issue, we proposed to characterize optogenetic activation and the heterologous pathway in the used devices, and optimize them independently before combining them; in other words: first solve independent uncertainties before merging them. This is also important to test the compatibility of both genetic systems. In our case, we saw that reducing volume and increasing stirring both increased optogenetic activation and beta-carotene production. This is convenient for us, but that may not always be the case.

Besides this step, it is important to simply test the effect of light on the heterologous pathway and final product, without the use of the optogenetic system. Here again, this is a way to limit the confounding factors that may impact strain production. For example, beta-carotene is sensitive to blue light, but not so much that it really hinders bioproduction. Had it been more sensitive, we maybe should have considered another optogenetic system (with a different activation wavelength), or another heterologous pathway to use as our model.

This work gives insights into the implementation of optogenetic devices in the lab, their constructions, limitations and comparative characteristics. It also details strain construction and finally the strategies to test a newly constructed optogenetic producer strain with a systematic 3-step method: first characterize and optimize both systems independently in the optogenetic devices, then combine to validate and further experiment.

7.2. Perspectives

We intentionally include the perspectives here before the discussion, just to be able to include those perspectives and a few supplementary results in the final discussion.

We have discussed already in the introduction that different control modalities can be used for bioproduction, and that optogenetics is a very versatile and controllable induction system. Initially, a main part of my PhD was intended to investigate the relationship between growth and production and try various induction patterns to maximize bioproduction. However, as the project unfolded, it became clear that a more thorough investigation regarding illumination device development, strain construction and optogenetic scalability was necessary before reaching this step. *In fine*, this is what applying optogenetics to bioproduction aims for: better controlling biological systems, with an emphasis on cells' trade-off between growth and production to mitigate burden and maximize production yields.

would result in a more “reddish” cell pellet). This hints again at the importance of finely controlling the induction level controlling the level of the protein of interest. It has been shown many times that the expression ratio of enzymes of a metabolic pathway can impact the resulting production^{2,3}.

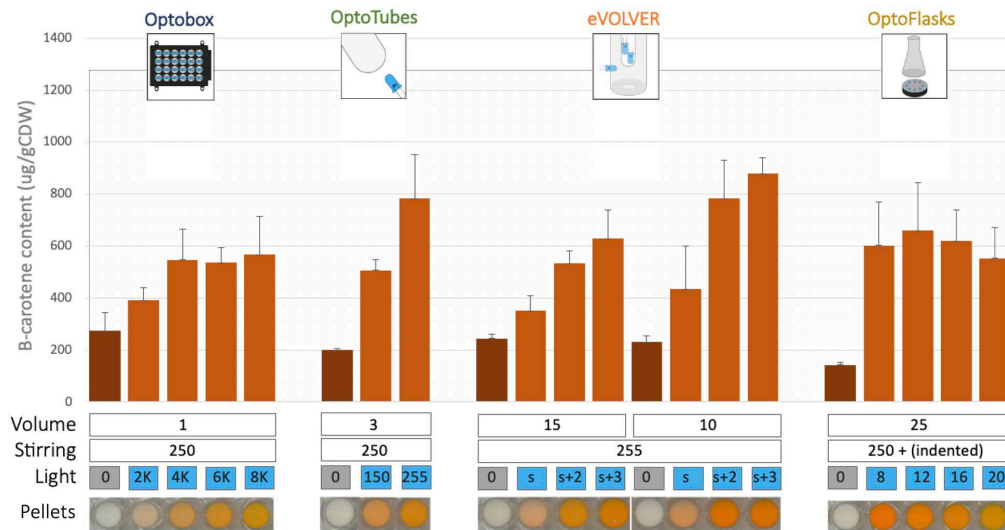


Figure 78. **Induction strength and metabolic effects:** beta-carotene production in the different devices (fig. 4B of chapter 3) with pellet colors displayed for each tested condition. The different cell pellet colors are the results of the different chemical species: for example, beta-carotene appears yellow-orange, and lycopene red. Note especially in the OptoFlasks, while different illuminations lead to similar beta-carotene content, cell pellet color varies significantly.

Besides inductions strength, in the interest of working with optogenetic and resource allocation, we asked if other activation patterns could increase production. Indeed, varying illumination, in terms of timing and pattern has potential to increase production yields by alleviating burden intermittently.

7.2.2. Illumination onset

Another way to tune the illumination is to vary the induction time, *i.e.*, the time of the switch from growth to production (like this is the case in a classical two-step cultivation process). This strategy is widely spread, and it was shown several times that changing the induction onset time could impact production, in terms of production titer (g/L) but also in terms of content (g/gDCW)^{4,5}. It could for sure impact the production titer (trade-off biomass and content – g/L), but we mostly focused on the content so far, *i.e.*, the quantification of beta-carotene produced per cell because it gives us information regarding the cell’s state.

Here, the experiment was launched in the OptoBox, with only 1 LED illumination (4000) in YPD with our functional strain yPH_551 (Fig. 79).

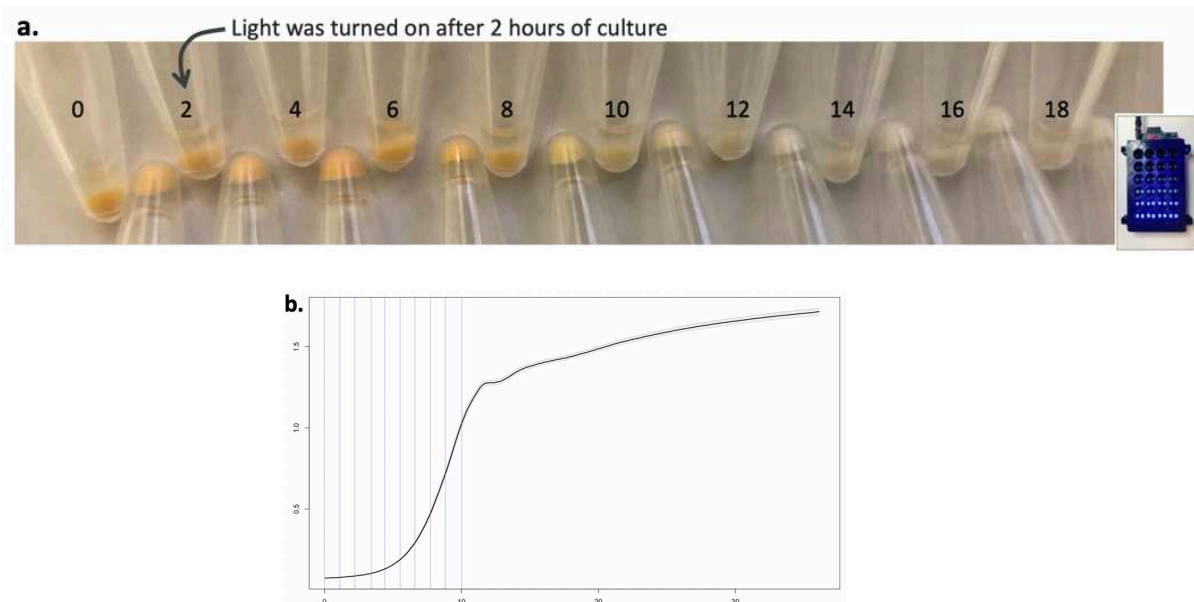


Figure 79. **Different illumination onsets in the OptoBox.** Each well of the OptoBox was programmed to turn on the illumination after a certain amount of time. At the end of the 24h growth, cells were removed from the wells, pelleted and pictured. Pellets are displayed according to the onset time (a.), which can be interpreted when aligned on the corresponding growth profile (b.).

We see that after 9 or 10h post-inoculation, turning on the light has no effect on production. That is, passed a certain time, production does not occur anymore, regardless of the activation. There seems to be only a decreasing production trend with induction time here, but Raghavan *et al.* 2020⁴ found an induction peak at 5h in terms of titer with their system. Those production dynamics could be explained with fermentation profiles: as cells grow, the medium becomes depleted in certain nutrients, and with an auxotroph strain like ours, after a certain time, not only growth but production could stop.

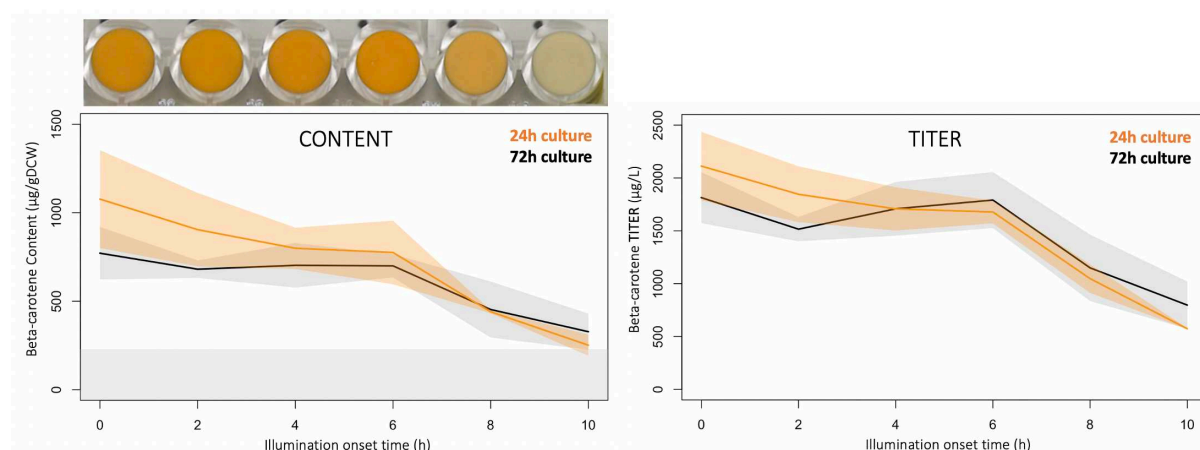


Figure 80. **Different illumination onsets in the eVOLVER.** As in figure 3, different onset times were chosen (at 0, 2, 4, 6, 8, and 10h) and beta-carotene quantifications were carried out at the end of the culture. 24h and 72h cultures were tested. The content (left) and the titer (right) can be compared. Besides, cell pellets were captured (top left). Measures were done in triplicates; standard deviation is shown as transparent colors.

We did those experiments in eVOLVER and found a similar decreasing trend (Fig. 80). Content and titer appeared to have a similar decreasing profile with induction time, meaning that the number of cells, and hence the growth rate, is not impacted by the production. This may suggest that there is no burden upon beta-carotene production in our strain, and therefore, illumination cells for the longest time will always be best to maximize beta-carotene production.

7.2.3. Pulse activation

One control modality, often hard to set up with other inducers (compared to optogenetics) is induction pulses. Indeed, chemical inducers might necessitate burdensome changes of medium to reverse induction, and other metabolizable carbon-source-based inducers might present slow activation and deactivation dynamics. With light, one can reach a very fast and sharp reversibility. Using pulses is attractive, as it has the potential to alternate easily and quickly between producing and non-producing states, which may be beneficial for the cell to cope with burden.

Besides, one goal can also be to find the minimum amount of light yielding the maximum production. We may suggest that high light intensity shone intermittently can yield the same production content, and therefore reducing the level of potential phototoxicity (for which more studies are actually required), if we are to consider this aspect. Therefore, we also tested the impact of different periods of illumination of a same 50% duty cycle. This can be easily programmed with the eVOLVER software (Fig. 81).

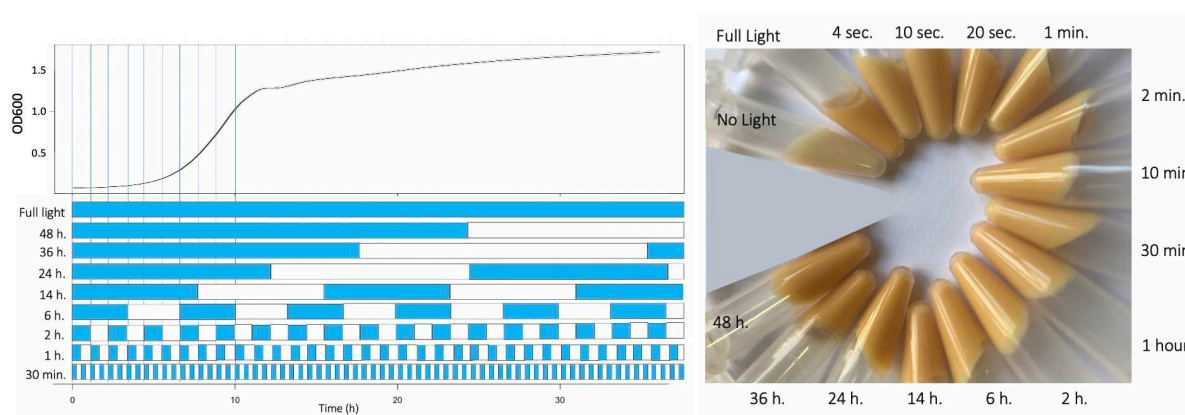


Figure 81. Varying light-pulse duration does not increase production in our case. (Left) illumination patterns compared to the corresponding growth profile in batch. (Right) resulting cell pellets colored in light orange. All illumination patterns have a 50% duty cycle (only the side-LED for illumination), 25 mL cultures were 4 days at 23°C in eVOLVER, fan at 100.

With these settings, no difference appeared between all those conditions. One could even argue that the colors appear less powerful than compared to the “Full Light” condition. To draw real conclusions here would require quantification as well as replicates. But two things may be suggested: first, compared to the previous experiments, since periods all start with the illuminated part of the duty cycle, it will not mimic a difference in illumination onset. Second, since all samples seem to have produced similarly, perhaps illumination can indeed be reduced.

Reducing illumination without impacting too much the production could be dependent on the quantity of production, the accumulation in the cells (growth rate), and of the lifetime of the RNA and/or of the protein. Consequently, we can expect a short-lived mRNA/protein to be more affected by those fluctuations in illumination. In our case, it does not seem to be the case, but remains to be better characterized.

7.2.4. Resource allocation

Controlling the production in a strain is important to control the inflicted burden. However, we suggested earlier that there may be no burden in our strain, hence the results showing no improvement when testing lower illuminations or different light patterns. This can easily be checked using the plate-reader and comparing growth profiles from a WT strain compared to a constitutive beta-carotene producer (where we expect a maximal burden if there was one to be detected - Fig. 82).

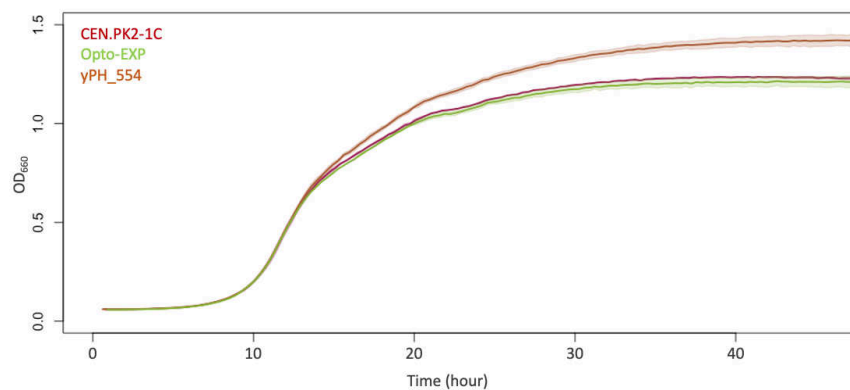


Figure 82. **Growth curves** of various strains. No burden can be detected in a strain producing beta-carotene constitutively (yPH_554) compared to a wild-type strain (CEN.PK2-1C) or a strain containing only the optogenetic system (opto-EXP). However, after the exponential phase, we see that the beta-carotene producer strain accumulates more overall biomass, hinting that heterologous pathway producing beta-carotene, which redirects cell resources to the mevalonate pathway can influence cell metabolism, perhaps limiting overflow metabolism.

In this figure, the exponential phase of the three strains appears identical, such that no slower growth rate is detected here. The exponential phase is brief here because the strains are auxotrophs for uracil, resulting in a phase of linear growth. Interestingly, this phase is different for the beta-carotene producing strain, resulting in more biomass accumulation overall. We conclude here that there is indeed **no burden** triggered by the beta-carotene production, and that perhaps, with tHMG and CrtE or $\Delta dpp1$, carbon fluxes may vary, resulting in either a better resource usage allowing for more biomass formation, or either alleviating some overflow metabolism or other kind of less energetically efficient cell processes.

As a conclusion, without any burden, it is only interesting to always seek to maximize production by any given means. The limitation, therefore, does not lie with burden and despite many efforts to better control this design version of the heterologous pathway, strong constitutive promoters are always producing more than any optogenetically controlled design. Thus, the strain could produce even more, and more metabolic engineering efforts can be made to improve production. In this work, we showed a production of 1-2mg/gDCW of beta-carotene, but more recent papers do better. Much better. While Verwaal *et al.* 2007¹ went up to 6 mg/gDCW, the *status quo* remained for a few years at about 20 mg/gDCW⁶⁻⁸ in *S.*

cerevisiae, it reached 60 mg/gDCW⁹ in *E. coli*, 50¹⁰ and 90¹¹ mg/gDCW in *Yarrowia lipolytica* (an oleaginous yeast with high lipid metabolism), with a recent record breaking 494 mg/gDCW published in early 2022¹².

Therefore, there is room for improvement, and controlling an actual burden will be necessary to better understand the interplays between growth and production and find ways to improve production using a fine control of the biological processes leading to bioproduction.

7.2.5. Real-time control

We discussed about various types of control that can be carried out using optogenetics here. We also mentioned, in the introduction, systems that can detect burden inside cells. To mitigate burden, controlling cells in real-time is one of the promises of optogenetics, detailed in the review I wrote. Indeed, ideally, the user would actually rely on specific cellular cues to decide when to activate and repress production or growth. This would mean setting up a feedback control. With a real-time sensor of cell burden combined with optogenetic control, this could be achievable.

This idea relies on bridging control engineering with biological systems, termed “**Cybergenetics**”. This corresponds to control engineers’ “attempts to design and commission [their] own control systems in living cells”¹³. Those approaches would require computer models, continually monitoring bioproduction processes, and taking decisions as to how to best control the production induction for example. This can be achieved using various control methods, some directly coming from control engineering, others based on biological models.

Although various cell processes have been already controlled in real-time (mostly growth rate and fluorescent protein level – at the single cell scale), using microfluidics systems^{14,15}, **for bioproduction**, this kind of approach remains mostly a perspective – though some examples do exist: in Shabestary *et al.* 2021¹⁶, to increase lactate bioproduction in *Synechocystis sp.*, the authors interrupted biomass formation by inducing the expression of a gRNA-dCas9 targeting the essential *gltA* citrate synthase (resulting in decreasing ATP and NADH pools), and let cell recover by addition of L-glutamate after a few days (before cell metabolism stalls), and inhibit growth again only when max growth rate is reached, maintaining production for 30 days (3 cycles). This is a great example of user-guided real-time dynamic feedback control.

7.3. Discussion

7.3.1. The choice of the optogenetic system

In this work, we have used the EL222 optogenetic system, which binds to its cognate pC120 promoter upon illumination, acting as an activator for transcription. This straightforward regulation system, resulting in blue light activating gene transcription, is called the Opto-EXP system¹⁷. The reverse version of this system, where transcription is inhibited by blue illumination, is the opto-INVRT system, which also relies on EL222. Instead of EL222

directly targeting the gene of interest (GOI – in our case, the CrtYB enzyme), EL222 activates the GAL80 repressor, which binds and represses the GAL4 transcription factor, which is constitutively produced and activates GOI under pGAL promoters (see the review after the introduction for more details). This system is particularly convenient because it rests on the use of the GAL system, already widely used in yeast and GAL4 is a stronger transcriptional activator than EL222. I have actually constructed strains that control the production of beta-carotene with this opto-INVRT system but decided not to focus on those. Even though those opto-INVRT-bcar strains produce actually more than opto-EXP-bcar strains, the activation and activation dynamics are slower, leading to less controllability, and we observed more cell-to-cell heterogeneity in terms of production. Besides, as we want to control the production finely, having cells producing while kept in the dark (which is the default cultivation process in the lab: it is easy to shelter a culture from light) makes the strain more difficult to handle and more prone to leaking. Based on EL222, more recent opto-EXP-derived systems have been published, some relying again on the use of the GAL system in yeast: for example, Zhao *et al.* 2021⁵ put the GAL4 transcription factor under the pC120 optogenetic promoter, such that upon illumination, GAL4 is expressed and targets pGAL genes, acting as a signal amplifier system and facilitating designs. By also creating a set of pGAL synthetic promoters, it is a full optogenetic toolkit that has been developed and is promising for future studies.

LiCRE. Another way to control the production of beta-carotene using optogenetic I tried during my PhD was through a system where a CRE recombinase has been made light inducible (LiCRE)¹⁸ (Fig. 83). Upon illumination, the LiCRE monomer is able to tetramerize to carry out recombination at targeted lox sites. With the genetic design presented in Duplus-Bottin *et al.* 2021¹⁸, after illumination, a terminator is excised irreversibly from the genomic region containing the carotenogenic genes, allowing for the expression of CrtYB and therefore unleashing beta-carotene production in the newly modified clones. Using this technique of light-inducible cell “differentiation”¹⁹, the ratio between growing cells and producing cells could be controlled and modified along the culture process, and tuned in order to maximize production titer.

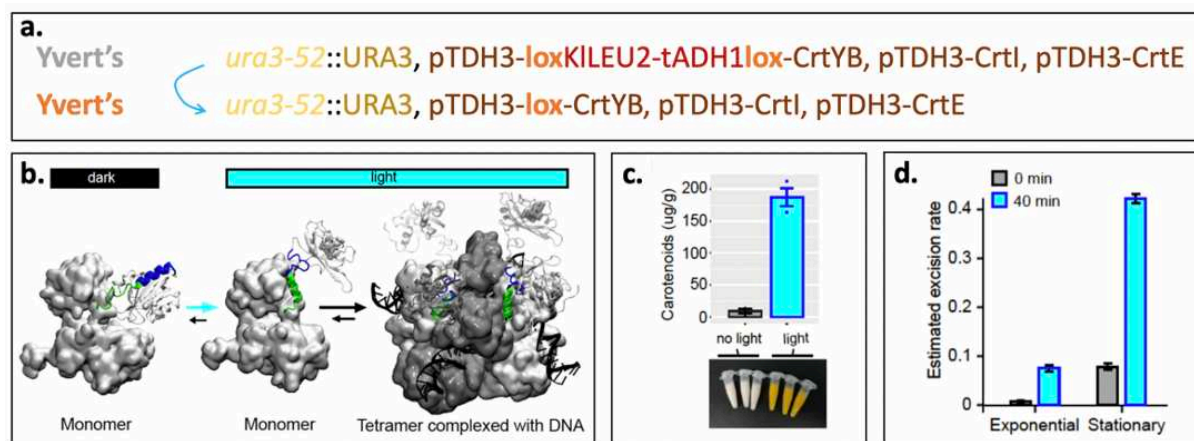


Figure 83. **Light-inducible CRE (LiCRE)** system From Duplus-Bottin2021¹⁸. (a.) Strain genotypes: top is the non-excised original genotype. Upon recombination by the CRE activated by light, the LEU2 cassette and the terminator tADH1 will be excised, creating a new genotype, where the CrtYB gene is under the control of the pTDH3 promoter. (b.) Structure of the LiCRE: upon illumination, each monomer is uncaged and allowed to tetramerize to carry out DNA recombination at lox sites. (c.) beta-carotene quantification and demonstration from the original paper. (d.) Excision rate reaches 40% in non-growing cells.

Similar to what we did, we could have varied the time of illumination onset at different, vary illumination to see how the population behaves in time and how production follows. However, given the max 40% excision rate (which we confirmed experimentally) and the fact that the producing cells have no production burden created limited sense with this configuration. Besides, the irreversibility of this system makes it, *in fine*, less versatile than our current system, but the possibility to perform another type of population control is attractive. Indeed, balancing two cell populations (growers and producers) could have been a great demonstration of control in biological systems, which has been extensively demonstrated and discussed in papers similar to Aditya *et al.* 2021¹⁹.

7.3.2. The heterologous production pathway

One of the promises of using optogenetics is to be able to control biological systems very precisely and to go as far as forcing the cell to produce up to a certain point for example, but there is no question that the cell metabolism will always interfere with this control. For example, we have seen that beta-carotene production was dependent on growth conditions (stirring and volume) and also on the carbon source used for growth. That is, production relies a lot on the metabolic state of the cell. So even though we could control this production, with a metabolic valve like in our case, regardless of the control we may have, the production will always be subjected to the cell's very own metabolism.

Indeed, even with similar genetic designs, strains can show different production dynamics. This has actually been the case in our very hands, without *no* optogenetic control for two different strain designs: one from Verwaal *et al.* 2007¹ and the other derived from Rabeharindranto *et al.* 2019²⁰ – used to construct our optogenetic strain in this manuscript. While the strain from Verwaal *et al.* 2007 proved more efficient with constitutive production on a long cultivation run, when this design was adapted for optogenetic control, it proved actually less efficient (not shown). This illustrates the importance and how much the controlled bioproduction system actually will always rely on the host's metabolism.

Therefore, it is important not to neglect metabolic effects and always work with well-characterized strains. It is better to adapt already well-working systems to optogenetic control. As we have seen before, there is much room for improvement to increase light-induced beta-carotene production, and another step would perhaps be not to necessarily only control the expression of a single enzyme of the heterologous metabolic pathway, but higher order processes in the cell: controlling either many genes at the same time (using variations of promoters responding to light for example, or via guide-arrays-based CRISPR systems), or a certain metabolic module, like controlling a regulator of the lipid metabolism, which has been shown to be important for beta-carotene accumulation in *S. cerevisiae*²¹.

7.3.3. Controlling: production vs. growth?

Besides controlling production or higher cell processes involved in production, growth could also be directly controlled with optogenetics. This has been demonstrated already using

optogenetics in continuous cultures²¹, and controlling growth for bioproduction via fed-batch methods (mostly feeding carbon-source) is already applied for bioproduction to tune cell metabolism²². Indeed, instead of only focusing on the activation of the production itself, working with growth is an attractive strategy as it can reflect the cell's state and we suggested before that maintaining a slow but consistent growth rate was necessary for the cell to keep an active metabolism while allocating enough resources to production and not to ribosome formation. Therefore, we can suggest that approaches based on resource allocation could benefit more from controlling growth.

There are different ways to control growth: we can mention the use of an essential gene (e.g., an auxotrophy²³, a key enzyme of the glycolysis pathway¹⁷), or genes involved in the cell cycle, or cell cycle arrest, like FAR1¹⁹. In Zhao *et al.* 2018¹⁷, the authors controlled optogenetically actually both growth and production as antagonist systems. Light allowed for growth via the control of the PDC1 protein expression under the control of the opto-EXP system, and dark enabled production via the control of the ILV2 protein expression, using the opto-INVRT system, which led to isobutanol production in *S. cerevisiae*. With such a system, resources are either allocated to growth or to production and very tightly controlled. With an open loop control approach, they found that illuminating at regular intervals during the production phase allowed to maintain production over days of culture.

7.3.4. Auto-induction vs. external control

Along this work, we mostly discussed how to carry out external control using light as an inducer, which may ultimately be applied to balance resource allocation in cells to maximize bioproduction. However, in the introduction, we also mentioned systems where the control is embedded / internal, relying on the host's gene regulatory networks and embracing the fact that the cell may be able to autoregulate the heterologous production system based on internal cues. Those approaches are very promising, and I do not know if they have yet been applied at larger scales, although they have demonstrated promising results already in the lab²⁴.

With this work in mind, we can question to a certain extent the actual use of optogenetics to control cells. We suggested that those embedded control systems are actually hard to tune and may not exploit the full potential given by an organism, notably as production relies on the actual cell metabolic state: with such embedded systems, cells cannot be coerced to produce beyond certain points, which might be also what could be envisioned to a certain extent with external control. Besides, no correction could be carried out if the system behaves unexpectedly. Finally, in current studies, no distinction between a biomass accumulation phase and production was made, which is an essential part for larger scale processes.

Those embedded control systems seem to be very powerful to deal with how the heterologous pathway pulls on a certain key metabolite in the cell, or to detect a general or specific stress and repress the production to limit burden. Perhaps it is another layer of control onto this embedded control system that is needed to enable the user to actually decide when to activate the production, define a production setpoint and be able to correct the system's trajectory.

7.3.5. Scaling-up

Finally, we mentioned several times that scaling-up optogenetics to industrial settings remains an open question. One of the main technical challenges will be to tune already existing bioreactors so that they can enable light to reach cells or develop brand-new systems. We mentioned the possibility of drawing inspiration from current algal photobioreactors, but the cell densities reached with yeast might compromise this strategy, as light penetration is heavily reduced with high cell densities.

Indeed, most culture processes involving yeasts imply high cell densities that make the broth difficult to handle and light hard to penetrate it. Different strategies have been proposed, including internal illumination, and external illuminating loops. The question turns to how long it would take to illuminate all the cells. Indeed, using an external loop for illumination could considerably extend the time needed for each cell to receive light, with increased heterogeneity of activation, and resulting in reduced controllability. On the other hand, an internal illumination might be harder to set up technically, but potentially profit to activation dynamics. Finding the appropriate amount of light to input in bioreactors, without overheating culture medium, without creating phototoxicity and heterogeneity but for a maximized cell optogenetic activation will likely rely on fluid dynamics modeling and light intensity distribution²⁵.

While proofs of concepts of the use of optogenetics to better control and optimize bioproduction are real at increasing lab-scales, I look forward to seeing how this technology can be adapted at larger scales and help make bioproduction a more resilient and economically viable technology applied for different industrial fields; and I hope my work comes as a little contribution in this direction.

Bibliography

1. Verwaal R, Wang J, Meijnen JP, et al. High-level production of beta-carotene in *Saccharomyces cerevisiae* by successive transformation with carotenogenic genes from *Xanthophyllomyces dendrorhous*. *Appl Environ Microbiol*. 2007;73(13):4342-4350. doi:10.1128/AEM.02759-06
2. López J, Bustos D, Camilo C, Arenas N, Saa PA, Agosin E. Engineering *Saccharomyces cerevisiae* for the Overproduction of β -Ionone and Its Precursor β -Carotene. *Front Bioeng Biotechnol*. 2020;8(September):1-13. doi:10.3389/fbioe.2020.578793
3. Benzinger D, Ovinnikov S, Khammash M. Synthetic gene networks recapitulate dynamic signal decoding and differential gene expression. *Cell Syst*. 2022;13(5):353-364.e6. doi:10.1016/j.cels.2022.02.004
4. Raghavan AR, Salim K, Yadav VG. Optogenetic Control of Heterologous Metabolism in *E. coli*. *ACS Synth Biol*. 2020;9(9):2291-2300. doi:10.1021/acssynbio.9b00454
5. Zhao EM, Lalwani MA, Chen J-M, Orillac P, Toettcher JE, Avalos JL. Optogenetic Amplification Circuits for Light-Induced Metabolic Control. *ACS Synth Biol*. 2021;10(5):1143-1154. doi:10.1021/acssynbio.0c00642
6. Xie W, Ye L, Lv X, Xu H, Yu H. Sequential control of biosynthetic pathways for balanced utilization of metabolic intermediates in *Saccharomyces cerevisiae*. *Metab Eng*. 2015;28:8-18. doi:10.1016/j.ymben.2014.11.007
7. Reyes LH, Gomez JM, Kao KC. Improving carotenoids production in yeast via adaptive laboratory evolution. *Metab Eng*. 2014;21:26-33. doi:10.1016/j.ymben.2013.11.002
8. Olson ML, Johnson J, Carswell WF, Reyes LH, Senger RS, Kao KC. Characterization of an evolved carotenoids hyper-producer of *Saccharomyces cerevisiae* through bioreactor parameter optimization and Raman spectroscopy. *J Ind Microbiol Biotechnol*. 2016;43(10):1355-1363. doi:10.1007/s10295-016-1808-9
9. Zhao J, Li Q, Sun T, et al. Engineering central metabolic modules of *Escherichia coli* for improving β -carotene production. *Metab Eng*. 2013;17:42-50. doi:10.1016/j.ymben.2013.02.002
10. Gao S, Tong Y, Zhu L, et al. Iterative integration of multiple-copy pathway genes in *Yarrowia lipolytica* for heterologous β -carotene production. *Metab Eng*. 2017;41:192-201. doi:https://doi.org/10.1016/j.ymben.2017.04.004
11. Larroude M, Celinska E, Back A, Thomas S, Nicaud JM, Ledesma-Amaro R. A synthetic biology approach to transform *Yarrowia lipolytica* into a competitive biotechnological producer of β -carotene. *Biotechnol Bioeng*. 2018;115(2):464-472. doi:10.1002/bit.26473
12. Ma Y, Liu N, Greisen P, et al. Removal of lycopene substrate inhibition enables high carotenoid productivity in *Yarrowia lipolytica*. *Nat Commun*. 2022;13(1):1-11. doi:10.1038/s41467-022-28277-w
13. Khammash MH. Cybergenetics: Theory and Applications of Genetic Control Systems. *Proc IEEE*. 2022;110(5):631-658. doi:10.1109/jproc.2022.3170599
14. Uhlenendorf J, Miermont A, Delaveau T, et al. Long-term model predictive control of gene expression at the population and single-cell levels. *Proc Natl Acad Sci U S A*. 2012;109(35):14271-14276. doi:10.1073/pnas.1206810109
15. Lugagne JB, Sosa Carrillo S, Kirch M, Köhler A, Batt G, Hersen P. Balancing a genetic toggle switch by real-time feedback control and periodic forcing. *Nat Commun*. Published online 2017. doi:10.1038/s41467-017-01498-0
16. Shabestary K, Hernández HP, Miao R, et al. Cycling between growth and production

- phases increases cyanobacteria bioproduction of lactate. *Metab Eng.* 2021;68(October):131-141. doi:10.1016/j.ymben.2021.09.010
17. Zhao EM, Zhang Y, Mehl J, et al. Optogenetic regulation of engineered cellular metabolism for microbial chemical production. *Nature.* 2018;555(7698):683-687. doi:10.1038/nature26141
 18. Duplus-Bottin H, Spichy M, Triqueneaux G, et al. A single-chain and fast-responding light-inducible cre recombinase as a novel optogenetic switch. *Elife.* 2021;10:1-52. doi:10.7554/eLife.61268
 19. Aditya C, Bertaux F, Batt G, Ruess J. A light tunable differentiation system for the creation and control of consortia in yeast. *Nat Commun.* 2021;12(1). doi:10.1038/s41467-021-26129-7
 20. Rabeharindranto H, Castaño-Cerezo S, Lautier T, et al. Enzyme-fusion strategies for redirecting and improving carotenoid synthesis in *S. cerevisiae*. *Metab Eng Commun.* 2019;8(December 2018):1-11. doi:10.1016/j.mec.2019.e00086
 21. Jiang W, Li C, Li Y, Peng H. Metabolic Engineering Strategies for Improved Lipid Production and Cellular Physiological Responses in Yeast *Saccharomyces cerevisiae*. *J Fungi.* 2022;8(5). doi:10.3390/jof8050427
 22. Cannizzaro C, Valentinotti S, von Stockar U. Control of yeast fed-batch process through regulation of extracellular ethanol concentration. *Bioprocess Biosyst Eng.* 2004;26(6):377-383. doi:10.1007/s00449-004-0384-y
 23. Miliás-Argeitis A, Rullan M, Aoki SK, Buchmann P, Khammash M. Automated optogenetic feedback control for precise and robust regulation of gene expression and cell growth. *Nat Commun.* 2016;7(May):1-11. doi:10.1038/ncomms12546
 24. Yuan J, Ching CB. Dynamic control of ERG9 expression for improved amorpha-4,11-diene production in *Saccharomyces cerevisiae*. *Microb Cell Fact.* 2015;14(1):1-10. doi:10.1186/s12934-015-0220-x
 25. Luzi G, McHardy C. Modeling and Simulation of Photobioreactors with Computational Fluid Dynamics—A Comprehensive Review. *Energies.* 2022;15(11):3966. doi:10.3390/en15113966

8. Appendix

8.1. Résumé substantiel en français	199
8.2. Résumé grand public.....	203
8.3. Cybersco.py (paper)	206
8.3.1. Introduction	206
8.3.2. Results	207
8.3.3. Discussion	212
8.3.4. Materials and Methods	215
Bibliography	216
8.4. Table of strains	218
8.5. Protocols	219
8.5.1. Culture media for yeast	220
8.5.2. MoClo for Yeast (YTK)	224
8.5.3. CRISPR for yeast	229
8.5.4. Yeast LiAc transformation	236
8.5.5. Beta-carotene quantification.....	239
8.5.6. Optobox	240
8.5.7. OptoTubes	245
8.5.8. eVOLVER – list of components	247
8.5.9. eVOLVER – installing	251

8.1. Résumé substantiel en français

La bioproduction permet la production de différents composés à partir de ressources renouvelables. Ceux-ci peuvent être des molécules chimiques naturellement produites par les organismes, des protéines thérapeutiques ou enzymes industrielles, ou encore d'autres molécules hétérologues produites par voies métaboliques exogènes, qui peuvent aujourd'hui être assemblées grâce aux techniques de biologie moléculaire modernes. Plusieurs paramètres vont impacter la production : le niveau d'ingénierie de l'organisme, le type de procédé ou culture pendant lequel l'organisme va croître et produire, et la composition de milieu et conditions de culture. Cependant, les performances d'un organisme mesuré à l'échelle du laboratoire sont souvent non reproductibles à de grandes échelles, dites « industrielles ».

Ces organismes modifiés sont conçus pour produire, au dépend de leur propre but évolutif, qui est de se reproduire (croître) et de survivre. La production a donc un coût (« burden ») pour l'organisme : les voies métaboliques exogènes consomment des ressources cellulaires et peuvent créer différents types de stress impactant la croissance. Par conséquent, les souches productrices souffrent d'un défaut de croissance, qui tend à favoriser les échappements évolutifs et réduisent l'efficacité des procédés de bioproduction. Pour pallier ces problèmes, des procédés spécifiques ont été développés, reposant sur un découplage de la croissance et de la production lors d'un même procédé. Avec des systèmes génétiques inductibles, il est possible de séparer la culture en deux phases : une première phase de croissance où la souche se multiplie, sans production et sans « burden » ; et une seconde phase de production, après induction, où la souche produit tout en ratisant sa croissance. De cette façon, un compromis est trouvé entre croissance et production à l'échelle du procédé. Cependant, le « burden » causé par la production entraîne lui-même une réduction de la production sur le long terme. En effet, plus la cellule produit, plus elle augmente son risque de stress qui va impacter négativement alors la santé de la cellule et par conséquent la bioproduction. Il devient alors nécessaire de contrôler le niveau et/ou le timing d'induction du système de production de façon à maximiser la production en réduisant son impact sur la santé de la cellule. Pour cela, des systèmes inductibles efficaces et contrôlables sont nécessaires. Il existe de nombreux systèmes génétiques inductibles détaillés dans l'introduction, et un de ceux qui gagne en popularité en ce moment est l'optogénétique. Contrôler des processus du métabolisme cellulaire grâce à la lumière a en effet l'avantage d'être rapide, réversible et contrôlable finement : dans l'espace, le temps et en intensité. Appliquer un contrôle optogénétique sur un système de bioproduction a le potentiel de permettre d'augmenter la compétitivité de cette biotechnologie. Bien que plusieurs études aient déjà montré des débuts prometteurs en la matière, cette idée se heurte encore à un problème de mise à l'échelle, et des contraintes, tant au niveau génétique qu'au niveau technique restent à être caractérisées.

Pour répondre à ces interrogations, pendant ma thèse, j'ai mis en place différents systèmes de culture de laboratoire de différentes échelles pour tester ces contraintes et poser une réflexion sur le passage à l'échelle de cette technique : comment concevoir des systèmes de culture permettant un contrôle optogénétique du métabolisme cellulaire ? Quelles est

l'impact de différentes échelles de culture ? Comment normaliser à travers ces échelles ? Comment concevoir une souche optogénétique ?

Comme mentionné précédemment, un des freins au développement de l'optogénétique pour la bioproduction est la nécessité d'avoir des moyens d'illumination à différentes échelles de culture. Pour cela, une des premières étapes de ma thèse a été le développement et l'adaptation de ces différents systèmes. A la plus petite échelle, celle de la cellule unique, les travaux en microfluidiques permettent de contrôler précisément l'illumination de monocouches de cellules grâce aux lampes déjà en place pour l'épifluorescence. Les plaques multi-puits, qui contiennent des volumes de généralement 200 à 1000 microlitres, permettent de cultiver différentes souches et/ou dans différentes conditions. Nous avons exploité ce débit expérimental en adaptant un socle d'illumination permettant d'illuminer indépendamment chaque puits de nos plaque 24 puits avec deux LED chacun. A l'échelle de culture supérieure, des rangs de cultures pour tubes de culture de 14 millilitres peuvent aussi être illuminés avec un socle dédié où sont fixées des LEDs contrôlable indépendamment via un Arduino. Pour illuminer des erlenmeyers de différentes contenances, permettant d'illuminer des volumes de culture plus large, j'ai développé des socles dédiés, où différent nombre de LEDs arrangées circulairement s'alignent avec le volume de culture se déplaçant lors les rotations dans un incubateur à agitation. Enfin, le plus gros du développement d'équipement de culture concernait le système « eVOLVER », une plateforme composée d'une série de 16 mini-bioréacteurs, chacun contrôlé par un Arduino permettant de mesurer et contrôler différents conditions de culture comme la température, l'agitation, l'illumination, et la densité optique, indiquant le taux de croissance, ainsi que potentiellement la production en bêta-carotène de la culture, puisque la couleur orange des bêta-carotène permet l'absorption de la lumière bleue utilisée pour l'activation du système optogénétique EL222. En plus des branchements prévus dans le système d'origine, le bouchon du tube a été modifié de façon à augmenter la quantité de lumière apportée au système de culture, avec ajout d'une illumination interne. Avec cette plateforme, plusieurs combinaisons de de conditions de culture peuvent être testées simultanément, accélérant largement le temps de développement nécessaire pour trouver les meilleures conditions permettant une activation optogénétique maximale pour une illumination minimale, ainsi que pour la production de bêta-carotène. Au-delà de cet aspect purement technique et électronique, le code de lancement d'une expérience, l'acquisition automatique des données et une interface utilisateur a été développée pour permettre le lancement simple et rapide de 16 expériences en parallèle. Des perspectives sont ensuite apportées concernant les potentielles adaptations de plus gros bioréacteurs pour faire de l'optogénétique, qui auront alors encore besoin de développement pour adapter l'optogénétique à de telles échelles de culture.

Ces instruments ont des avantages et des inconvénients propres : approche single-cell, haut débit expérimental, volumes réduits facile à utiliser, contrôlabilité de l'illumination, capacité de contrôle et mesure de certains paramètres de culture en temps réel etc. Tous ces aspects font de chaque système de culture un système unique. De plus, avec ces instruments de culture de différents volumes, différentes modalités d'illumination apparaissent, pour différents volumes, avec donc différentes quantités et pénétration de la lumière, et aussi différentes conditions de la culture. D'où le besoin de tester indépendamment d'abord les

limites de chaque instrument en termes d'activation optogénétique, puis de production constitutive de bêta-carotène.

La construction d'une souche de levure *Saccharomyces cerevisiae* où la production de bêta-carotène est contrôlée par la lumière via le système optogénétique EL222 est détaillée dans le chapitre 2 de la thèse. Pour faire cela, seule une enzyme trifonctionnelle (CrtYBekI) a été placée sous control du promoteur pC120, activé optogénétiquement. Les autres gènes nécessaires pour la production de bêta-carotène (tHMG, CrtE) sont placés sous control de promoteurs constitutifs. La synthèse du promoteur optogénétique avec la CDS de CrtYBekI a été réalisée par Gibson assembly. La souche de départ contient le système optogénétique EL222 contrôlant l'expression d'une GFP. Afin d'éviter des chevauchements en termes de longueur d'onde pour imagerie sous microscope (le signal de la GFP chevauche celui du bêta-carotène observable dans les cellules), nous avons remplacé la GFP par une mCherry via une approche CRISPR. Les deux gènes sous control constitutif ont été insérés au locus *dpp1* et la trifusion sous contrôle optogénétique au locus *ho*. Avec cette souche, la production de bêta-carotène activé par la lumière ne fonctionnait que sur milieu respirable (et non fermentable) et à basse température de culture (température ambiante au lieu de 30°C). Pour comprendre ce phénotype, nous avons questionné l'efficacité de transcription de pC120 comparé à d'autres promoteurs constitutifs plus ou moins forts, mais surtout questionné le design de trifusion CrtYBekI qui était établi dans notre design de base. Ce design de trifusion synthétique, basé sur de précédentes recherches, peut être reconverti en design plus classique, résultant en CrtYB + CrtI. Cela fait, via une approche CRISPR, le phénotype de production seulement dans certaines conditions a été résolu, donnant une souche capable de produire du bêta-carotène sous contrôle de la lumière dans des conditions de culture classiques, c'est à dire à 30°C en YPD (milieu riche avec glucose), permettant de faire des expériences bien plus rapides grâce à un taux de croissance bien plus élevé dans ces conditions.

Grâce aux instruments optogénétique développés et la souche fonctionnelle, nous avons pu passer aux tests afin d'optimiser pour chaque instrument 1. L'activation optogénétique, 2. La production constitutive de bêta-carotène, et enfin 3. La production de bêta-carotène contrôlée par la lumière. C'est ce qui constitue le troisième chapitre de cette thèse et le papier récemment publié dans *Frontiers in Bioengineering and Biotechnology*. En premier lieu, nous avons optimisé et quantifié, l'activation optogénétique de la simple souche optogénétique, où une GFP est sous contrôle optogénétique. Pour chaque instrument après une illumination de 6 heures, le niveau de GFP des cellules est mesuré grâce à la cytométrie de flux. Nous observons alors que le niveau d'activation tend à saturer, bien que ce soit au-dessous de l'expression de promoteurs constitutifs, et que la quantité de lumière à laquelle cela sature dépend de chaque instrument. Nous avons ainsi déterminé la quantité de lumière minimale pour une activation maximale, ce qui est important car la lumière peut s'avérer toxique pour les cellules. Ensuite, la production constitutive de bêta-carotène a été testée dans les différents instruments pour tester l'impact de l'échelle de culture et définir les meilleures conditions de production. En particulier, dans eVOLVER, l'agitation du milieu et le volume de culture se sont avérés cruciaux pour optimiser la production (mesuré en « content », *i.e.* ug/gCDW). En plus de cela, l'impact de la lumière sur la production et/ou accumulation de bêta-carotène (produite de façon constitutive) a été testée : en effet, le bêta-carotène est une molécule connue pour être sensible

à la lumière, particulièrement à la lumière bleue, et cela pourrait impacter nos résultats. Nous avons ainsi déterminé que l'illumination a un impact sur la production de bêta-carotène seulement dans certains instruments de culture et peut provoquer une réduction de 20% de production. Avec ces observations, nous concluons que les contraintes de chaque système génétique (optogénétique et bioproduction) sont compatibles et devraient fonctionner ensemble.

Enfin, après avoir évalué et déterminé de manière indépendante l'activation optogénétique et la production constitutive de bêta-carotène entre instruments de culture, nous avons testé la production de bêta-carotène contrôlée par la lumière dans les différents instruments grâce à la souche détaillée plus tôt. Nous observons alors que les contraintes observées précédemment et indépendamment pour les deux systèmes génétiques se rencontrent aussi quand ils sont combinés : réduire le volume de culture et augmenter l'agitation permet d'augmenter la production contrôlée par la lumière. De plus, la comparaison du signal GFP, donnant la quantité de protéine produite, à la production de bêta-carotène donne une relation logarithmique, signifiant qu'un autre paramètre de notre système est limitant, non pas la production de l'enzyme CrtYB en elle-même. De cette façon, même si le niveau d'enzyme issu de l'activation optogénétique est relativement faible comparé à des systèmes d'expression constitutifs, il s'avère suffisant dans notre cas : avec 10 fois moins d'enzymes, on obtient seulement 2 fois moins de bêta-carotène.

En conclusion, dans cette thèse, j'ai adapté et développé plusieurs instruments de culture pour systèmes optogénétiques afin de tester le passage à l'échelle de son utilisation pour la bioproduction et identifier les contraintes techniques mais aussi génétiques de construction et d'utilisation via une souche contrôlant la production de bêta-carotène par le système optogénétique EL222. Ce travail fournit un large aperçu et des propositions concernant l'utilisation de l'optogénétique pour la bioproduction à différentes échelles de culture : leurs constructions, limitations et caractéristiques comparatives, dans l'espoir de pouvoir utiliser l'optogénétique à des échelles de culture encore plus grandes afin d'optimiser la bioproduction à partir de microorganismes pour rendre cette biotechnologie plus compétitive encore.

8.2. Résumé grand public

La levure est utilisée par les Hommes depuis les milliers d'années pour faire notamment du pain et de la bière. Aujourd'hui, tous les pains levés sont faits avec la levure *Saccharomyces cerevisiae*, et chaque goutte d'alcool que nous buvons dans nos boissons a été produite par ce microorganisme (microscopique) unicellulaire (une seule cellule) de la famille des champignons (et ses cousins proches).

Pour faire cela, la levure transforme les sucres présents dans le moût du raisin, dans la farine, ou dans le malt d'orge. C'est la fermentation : ces sucres sont convertis en dioxyde de carbone (CO₂ - qui fait lever le pain) et en alcool (éthanol, à proprement parlé - qui s'évapore lors de la cuisson du pain mais reste dissout dans les boissons alcoolisées), et en biomasse. Ce processus est bien connu, bien décrit et domestiqué depuis longtemps, et c'est grâce à cela que nous sommes capables de le remanier.

La bioproduction est une biotechnologie qui se propose de dérouter les résultats de la fermentation : au lieu de produire du CO₂ + éthanol à l'issue de la fermentation, on veut pouvoir favoriser la production d'autre composés, utiles pour d'autre applications. Pour cela, nous sommes aujourd'hui capables de modifier génétiquement les levures et autres microorganismes pour leur donner de nouvelles capacités. Par exemple, en insérant dans le génome de la levure les instructions codant pour l'insuline, celles-ci vont interpréter cette nouvelle information pour produire l'insuline à partir du sucre. Un fois purifiée, cette insuline peut être injectée aux patients atteints de diabète. Ainsi, on produit un médicament à partir de simples sucres, au lieu de devoir l'isoler à partir d'autres animaux comme c'était le cas auparavant.

Aujourd'hui, à partir de microorganismes, nous sommes capables de produire non seulement des médicaments et des vaccins, mais aussi des colorants textiles, des plastiques biodégradables, des biocarburants, des parfums, des molécules rentrant dans la composition de différentes crèmes qui provenaient avant d'huiles animales, etc. Bref, les possibilités sont larges, et le potentiel de cette technologie est en expansion, notamment du fait qu'elle repose sur un matériel de base biosourcé et renouvelable : des sucres, ou, mieux encore, des déchets végétaux de différentes industries. Cette technologie fonctionne aujourd'hui. Cependant, elle ne fonctionne pas assez bien pour concurrencer les façons traditionnelles que nous avons d'obtenir divers produits issus notamment de l'industrie pétrolière.

Pour la faire mieux, il faut mieux comprendre et mieux manier ces microorganismes pour augmenter les rendements et diminuer les coûts. C'est une entreprise intéressante car appliquée, mais aussi d'un point de vue fondamentale car elle pousse les limites de compréhension que nous avons des systèmes biologiques. Ma thèse se focalise sur l'augmentation de ces rendements en appliquant de meilleurs systèmes de contrôle sur la levure. Pour mon étude, j'utilise des levures qui sont modifiées génétiquement pour produire du bêta-carotène, une molécule qui donne la vitamine A une fois ingérée, et qui donne sa couleur orange aux carottes. Ainsi, les levures, qui donnent normalement une couleur beigeâtre quand elles sont cultivées, apparaissent orange lorsqu'elles sont modifiées pour produire du bêta-carotène.

En pratique, la production a lieu. Mais elle a un cout. La cellule alloue des ressources à cette production, et fournit alors moins de CO₂, d'éthanol, et de biomasse. Pire encore, cette production va impacter la santé de la cellule : la cellule produit, ce qui crée du stress, qui réduit alors sa productivité. Ici, c'est comme si l'on demandait à un employé de travailler 24h/24, 7 jours sur 7 : ce rythme n'est pas tenable, et un employé a besoin de diverses périodes de repos, au moins 1 fois par jour pour dormir, ainsi qu'un weekend pour faire de l'aikibudo et se promener au jardin des plantes. Exactement de la même façon, la cellule a besoin de récupérer de son effort de production. Dans ce contexte, il est alors nécessaire de réguler son activité de production : produire du bêta-carotène puis croître et produire de nouveau éthanol et CO₂, reprendre la production, et arrêter de nouveau etc.

Pour faire cela finement, on a alors besoin de systèmes de contrôle génétique performants. Un des meilleurs systèmes existants est l'optogénétique : *opto* pour lumière, et *génétique* pour des systèmes encodés par des gènes. Pour ma thèse, l'optogénétique me permet alors de contrôler la production de bêta-carotène chez la levure : quand j'allume la lumière (lumière bleue), la cellule produit du bêta-carotène (devient orange). En absence de lumière, cette production s'arrête. Ma thèse a alors consisté à développer cette levure particulière pour qu'elle soit performante, mais aussi à tester d'usage de ce contrôle génétique à différentes échelles de culture. En effet, les levures peuvent être cultivées dans des tubes à essai de quelques millilitres, dans des bouteilles de quelques litres, ou encore, à l'échelle industrielle, dans les bioréacteurs de milliers de litres. Un des freins principaux dans le développement de ces nouveaux microorganismes produisant des composés d'intérêt est le passage à l'échelle. En effet, il n'est pas rare qu'une levure développée et cultivée dans des conditions de laboratoire soit efficace à cette échelle, mais échoue dans des conditions industrielles car les contraintes et conditions de cultures changent alors. Pour augmenter les rendements et permettre ce passage à l'échelle, il devient important d'identifier les paramètres clés qui influent sur la performance du microorganisme.

A cette fin, pendant ma thèse, j'ai développé et adapté des systèmes de culture de levure de façon à apporter de la lumière pour contrôler la production des levures. J'ai aussi modifié génétiquement des levures pour qu'elles puissent 1. répondre à la lumière, 2. faire du bêta-carotène, ou 3. faire du bêta-carotène sous control de la lumière. Dans un premier temps, il a fallu mettre au point ces instruments électroniques pour pouvoir contrôler l'arrivée de la lumière dans les réceptacles dans lesquelles vont croître les levures. Une fois cela fait, j'ai pu commencer les tests.

J'ai testé la réponse des levures à la lumière dans ces différents instruments : comment, en combien de temps et de combien celles-ci vont avoir la capacité de réagir à telle ou telle quantité de lumière, et quel est l'impact de l'échelle de culture et de la façon dont est apporté la lumière sur cette réponse. Il a fallu notamment aussi déterminer la quantité minimale de lumière apportant une réponse maximale, car trop de lumière peut potentiellement être nocif pour les cellules.

Ensuite, la production de bêta-carotène entre les différents instruments a été testée et a été cruciale pour harmoniser les conditions de culture indispensable pour le passage à l'échelle entre instruments de laboratoire, et donc pour de plus grandes échelles encore. Ainsi, on a pu

obtenir une production de bêta-carotène satisfaisante entre chaque échelle, démontrant l'importance d'un volume réduit et d'une bonne aération dans notre système. Ces contraintes identifiées sont compatibles avec celles du système optogénétique, et donc la combinaison de l'optogénétique et de la production de bêta-carotène apparaît possible.

Enfin, j'ai donc combiné optogénétique et production pour construire une levure où la production de bêta-carotène est contrôlée par la lumière. Cela s'est avéré plus compliqué que prévu car, même en minimisant les incertitudes en étudiant chaque système indépendamment (détaillé juste avant), il reste une incertitude sur le comportement de deux systèmes mis ensemble. Une fois fonctionnelle, j'ai donc pu tester cette levure dans les différents instruments de cultures, avec les bonnes conditions de culture et d'illuminations identifiées précédemment. La souche se comporta alors relativement comme attendu et varier l'intensité de la lumière résulte en une plus faible production. De plus, la relation entre la quantité de lumière et la production de bêta-carotène nous informe sur les propriétés de la façon dont les modifications génétiques ont été faites et peuvent suggérer de meilleurs designs. Enfin, j'ai pu tester différentes façons d'illuminer : varier le timing d'illumination ou alterner des périodes d'illumination (de production de bêta-carotène) et d'obscurité (croissance cellulaire), qui permettent de tester les limites de mon système et suggèrent que la coût de production pour la levure est faible et donc la production ne pourra pas être optimisée véritablement grâce à l'optogénétique avec mon design génétique. Ainsi, pour continuer le projet, il faudra reprendre la génétique, optimiser la production de base et refaire des tests de contrôle avec la lumière, et cela assez facilement, puisque tous les instruments et levures ont été caractérisés, discuté, et publié.



OPEN

CyberSco.Py an open-source software for event-based, conditional microscopy

Lionel Chiron^{1,3}, Matthias Le Bec^{1,3}, Céline Cordier¹, Sylvain Pouzet¹, Dimitrije Milunov¹, Alvaro Banderas¹, Jean-Marc Di Meglio², Benoit Sorre¹ & Pascal Hersen¹✉

Timelapse fluorescence microscopy imaging is routinely used in quantitative cell biology. However, microscopes could become much more powerful investigation systems if they were endowed with simple unsupervised decision-making algorithms to transform them into fully responsive and automated measurement devices. Here, we report CyberSco.Py, Python software for advanced automated timelapse experiments. We provide proof-of-principle of a user-friendly framework that increases the tunability and flexibility when setting up and running fluorescence timelapse microscopy experiments. Importantly, CyberSco.Py combines real-time image analysis with automation capability, which allows users to create conditional, event-based experiments in which the imaging acquisition parameters and the status of various devices can be changed automatically based on the image analysis. We exemplify the relevance of CyberSco.Py to cell biology using several use case experiments with budding yeast. We anticipate that CyberSco.Py could be used to address the growing need for smart microscopy systems to implement more informative quantitative cell biology experiments.

Microscopy imaging is an invaluable tool in quantitative cell biology. Recent years have seen the emergence of increasingly sophisticated techniques to probe the dynamics of living systems at high spatio-temporal resolutions. These technological developments have mostly been obtained using novel optical methods that structure the illumination of biological samples in space and time, the rise of optogenetics that facilitates real-time interactions with living samples, and the development of deep learning algorithms to analyze images and segment cells. Many microscopes are now powerful semi-automated systems that can acquire pre-programmed timelapse sequences, usually via a process called Multi-Dimensional Acquisition (MDA), to observe and characterize the behaviors of single cells over extended periods of time. To define a MDA protocol, the user typically has to select several locations within the biological sample (X and Y coordinates) and focal planes (Z positions), as well as the illumination settings that will be applied to every position (wavelengths, intensities, exposure times) and then, choose how often images should be captured by the camera. Automation microscopy software is used to ensure synchronization of the devices attached to the microscope, by periodically looping through these dimensions (space, time, imaging parameters). MDA has become very popular and is used routinely in cell biology laboratories. While the value of this approach has been well-demonstrated for the study of time-varying phenomena at play in biological systems, MDA drastically limits the capacity of fluorescence timelapse microscopy to monitor complex, multiscale biological processes. Indeed, for every experiment, a balance must be found between the number of positions imaged, the spatial resolution (magnification of a given objective), the time resolution, and additional effects such as phototoxicity, the duration of the experiment, cell density, etc. The tradeoffs between these factors are not trivial to setup and are usually not known at the beginning of experiments. Moreover, a simple MDA cannot typically deal with all of these factors; for example, studies of fast, intermittent processes (e.g., mitotic events) require imaging at both a high framerate and over a long period of observation, which lead to either phototoxicity or improper sampling.

Such basic workflows have become outdated at the time when smart systems and artificial intelligence are being used to improve the functioning of many (scientific) devices. A key practical limitation of MDAs is the fact that the images are only analyzed at the end of the experiment, which sequentially separates the workflows of image acquisition and image analysis. The ability to employ real-time image analysis to inform and optimize

¹Institut Curie, Université PSL, Sorbonne Université, CNRS UMR168, Laboratoire Physico Chimie Curie, 75005 Paris, France. ²Laboratoire Matière et Systèmes Complexes, UMR 7057 CNRS, Université Paris Diderot, 10 rue Alice Domon et Léonie Duquet, 75013 Paris, France. ³These authors contributed equally: Lionel Chiron and Matthias Le Bec. ✉email: pascal.hersen@curie.fr

or adjust the settings of ongoing image acquisition would be a game changer for studying complex, dynamic cellular processes. Although this strategy requires a deep dive into the software programming and automation of microscopy devices, transformation of a conventional timelapse automated microscope into a powerful unsupervised automaton that is able to acquire data from a live biological sample at the right place and at the right timing could empower researchers in the biomedical sciences.

Building on existing automation microscopy software, several groups have started to explore how smart microscopy automate can benefit the life sciences^{1–5}. In 2011, MicroPilot⁵ used LabVIEW (a proprietary systems engineering automation software) to interface μ Manager^{6,7} (the most popular open source and cross platform software used to pilot a large variety of microscopy devices) and other commercial vendor automation software with a machine learning algorithm to identify and only focus on cells in a specific phase of mitosis. This strategy increased the throughput and decreased the time required to screen the desired cells. Since then, the rise of machine learning and the popularization of simple automation strategies—using low cost prototyping microcontroller boards (Arduino⁸) or compact single-board computers (Raspberry Pi⁹) and Python programming—have made it easier to build simple open-source solutions to achieve the same goals. For example, μ Magellan⁴ and NanoJFluidics¹ were built directly on μ Manager to achieve some level of feedback loop control and automation of image acquisition. μ Magellan focuses on creating content-aware maps to adapt imaging modalities to a 3D biological sample. NanoJFluidics¹ homemade array of Arduino-controlled syringe pumps combined with μ Manager can perform automated fixation, labeling and imaging of cells; notably, this system could be triggered by real-time detection of the rounding of mitotic cells through a basic image analysis algorithm. More recently, Pinkard et al.³ established PycroManager, a Python library that can interact with μ Manager to program a microscope in a very flexible way, though at the expense of a prerequisite for expert-level Python coding skills and the knowledge of additional software or programming language. Overall, these examples harness the capability of μ Manager to pilot microscopy instruments and home-made image-analysis tool suites to trigger pre-programmed actions, and thus facilitate the development of complex or time-consuming microscopy experiments.

In addition, recent advances in the application of control theory to biology led to the development of external feedback loops, in which cells are analyzed and stimulated in real-time to force the cell state (e.g., expression of a gene^{10–17}, activity of a signaling pathway¹⁸) to follow a user-defined (time varying) profile. Such feedback loops require the ability to perform real-time image analysis, in order to extract cellular features to feed an algorithm that decides how to stimulate the cells in live mode via microfluidics^{14,15} and/or optogenetics^{10–13,16}. This novel and active field of research, called *cybergenetics*, harnesses the possibility of creating interactions between cells and a numerical model in real-time, and thus opens novel areas of both applied and fundamental research. To demonstrate the power of cybergenetics, we and others have developed various software to implement feedback loop-controlled microscopy systems. These solutions combine μ Manager and/or MATLAB with dedicated image analysis and control algorithms to close the feedback loop^{14,15}. However, in practice, these solutions are difficult for non-experts to implement and cannot be easily transposed to a broad range of biological problems. More recently, several groups proposed Python and μ Manager-based software to develop cybergenetic experiments^{19,20}, though these approaches remain specific to the control of gene expression in cells over time and do not meet all of the varied needs of cell biologists.

Here, we present CyberSco.Py software, which is a follow-up to our contributions to piloting gene expression in real-time in yeast and bacteria^{14,15}. CyberSco.Py is written in Python, has been designed with automated, real-time feedback loops in mind, and includes deep learning image analysis methods as an integral part of image acquisition. We focused on achieving a proof-of-concept software with a simple, robust, user-friendly interface that can be deployed as a web application. Importantly, CyberSco.Py natively includes the ability to control basic microfluidic devices through an Arduino board that drives electro-fluidic valves (see “[Materials and methods](#)”). CyberSco.Py is, by design, oriented towards advanced timelapse experiments that include triggered events and routed tree scenarios—rather than preprogrammed sequences of image acquisition. CyberSco.py is still a proof-of-concept and, here, our main goal is to demonstrate the potential of event-based, conditional microscopy to cell biologists. To this end, we first describe the principle of CyberSco.py, and then focus on several use case scenarios to exemplify how event-based microscopy can be applied to perform more informative experiments relevant to cell biology.

Results

CyberSco.py is an open-source web application for timelapse microscopy and microfluidics automation. It is written in Python (Fig. 1) and employs real-time image analysis and decision-making algorithms to trigger changes in the imaging parameters in real-time during the experiment. At present, this proof-of-concept is operational on a fully automated Olympus microscope (IX81) equipped with brightfield and epifluorescence illumination and linked to an Arduino-based homemade microfluidic control device (Supplementary Figs. S1 and S2). A web interface allows the user to easily setup an experimental plan and/or to select pre-configured conditional experimental scenarios, together with the corresponding image analysis solutions. A local server receives these parameters and launches the experiment. During the experiment, the acquired images are constantly analyzed and used to trigger events according to the chosen scenario. In particular, the detected events can feedback on the microscopy settings and the microfluidic settings to adapt the experimental plan during the experiment (Fig. 1). Thus, CyberSco.Py transforms microscopes and their related devices into an advanced imaging automaton capable of performing unsupervised time-dependent tasks with the capacity to handle various user-defined triggers. More details of the CyberSco.Py source code and its documentation are available on the GitHub page of the project (Supplementary Information). Although the software has been developed for a given microscopy setup, it can be extended to any equipment providing there is a driver and/or

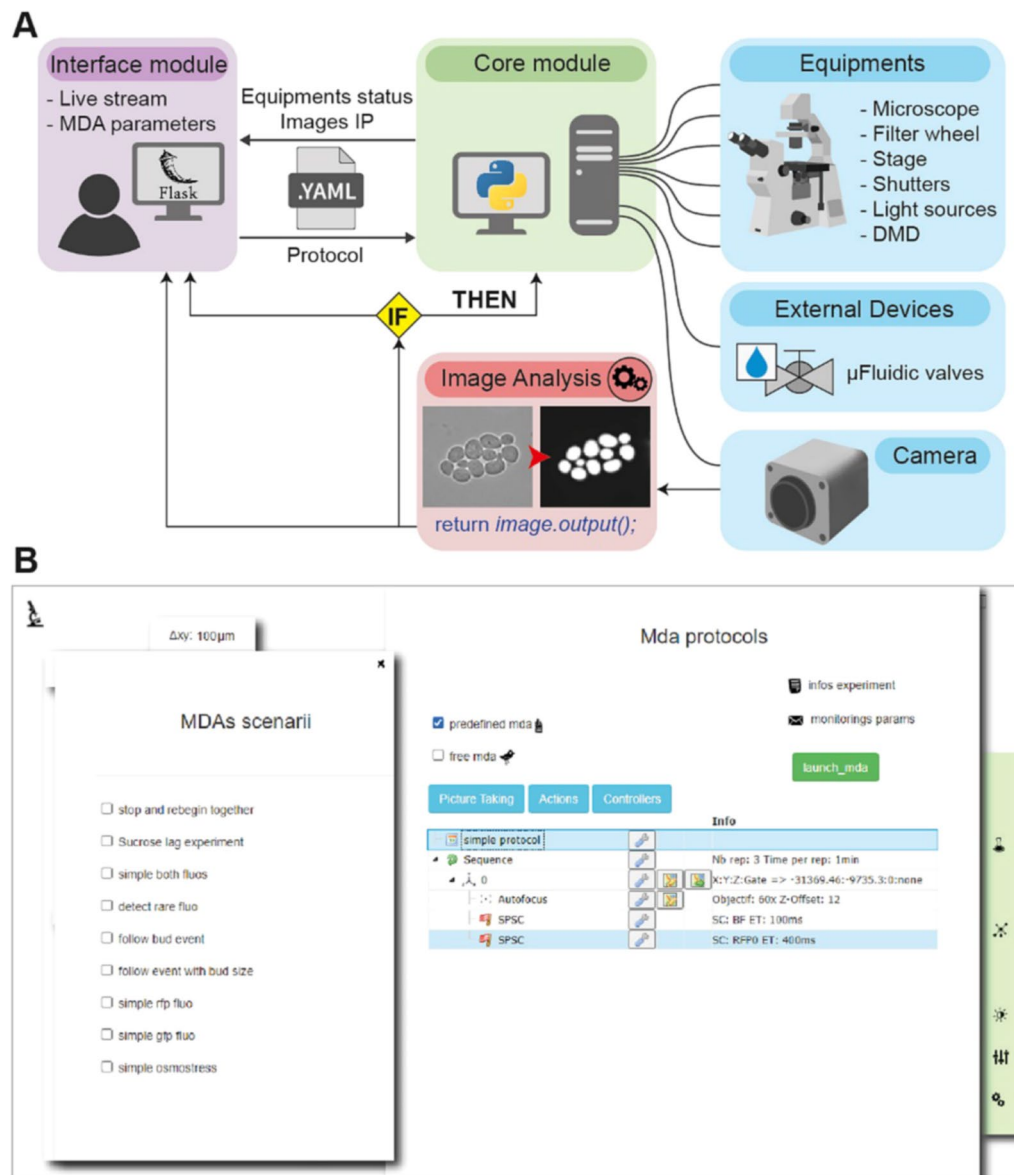


Figure 1. CyberSco.Py framework. **(A)** Architecture. CyberSco.Py is built in Python and uses the web application library Flask to create a web user interface. Microscopy protocols are written into a YAML (human readable data serialization language) file, which can be interpreted by the Python core module of CyberSco.Py, which drives the various components of a IX81 fully automated microscope. The core module also drives a set of fluidic valves that can be used to switch the media flowing into a microfluidic device. A class in Python is associated to each device. Images obtained from the camera are analyzed in real-time by a U-NET deep learning model to segment yeast cells and/or detect specific events, depending on the pre-trained model selected by the user. The result of the analysis is used by the core module to update the current state of any devices under its control (see “Materials and methods” for more information). **(B)** Snapshot of the current user interface. The user interface is very simple by design and allows the user to choose between several pre-programmed event-based scenarios, for which the user must define various relevant parameters and condition switches. The simple drag and drop interface can be used to modify a given Multi-Dimensional Acquisition protocol to give more flexibility and to create more advanced protocols. The same interface can be used in “live mode” to view what is currently being imaged and check that the live image analysis is performing correctly. Once the program is launched, the computer takes control of the microscope and will adjust the image acquisition parameters based on the event-based scenario that has been selected. It is possible to code a novel scenario directly in Python and/or to manually adjust the thresholds and parameters used to detect events (e.g., number of cells, size of cells, etc.). The structure of a scenario consists of a list of instructions for the microscope (“make the autofocus”, “take a picture”, etc.) to be serially executed at each iteration, a conditional block, and an initialization block. Each scenario corresponds to a unique Python file with the same consistent structure. The user can also enter information about the projected experiment, as well as selecting modalities for monitoring the experiment remotely via email (selecting where to send the emails and at which frequency) and/or through a discussion channel (e.g., Microsoft Teams or Slack).

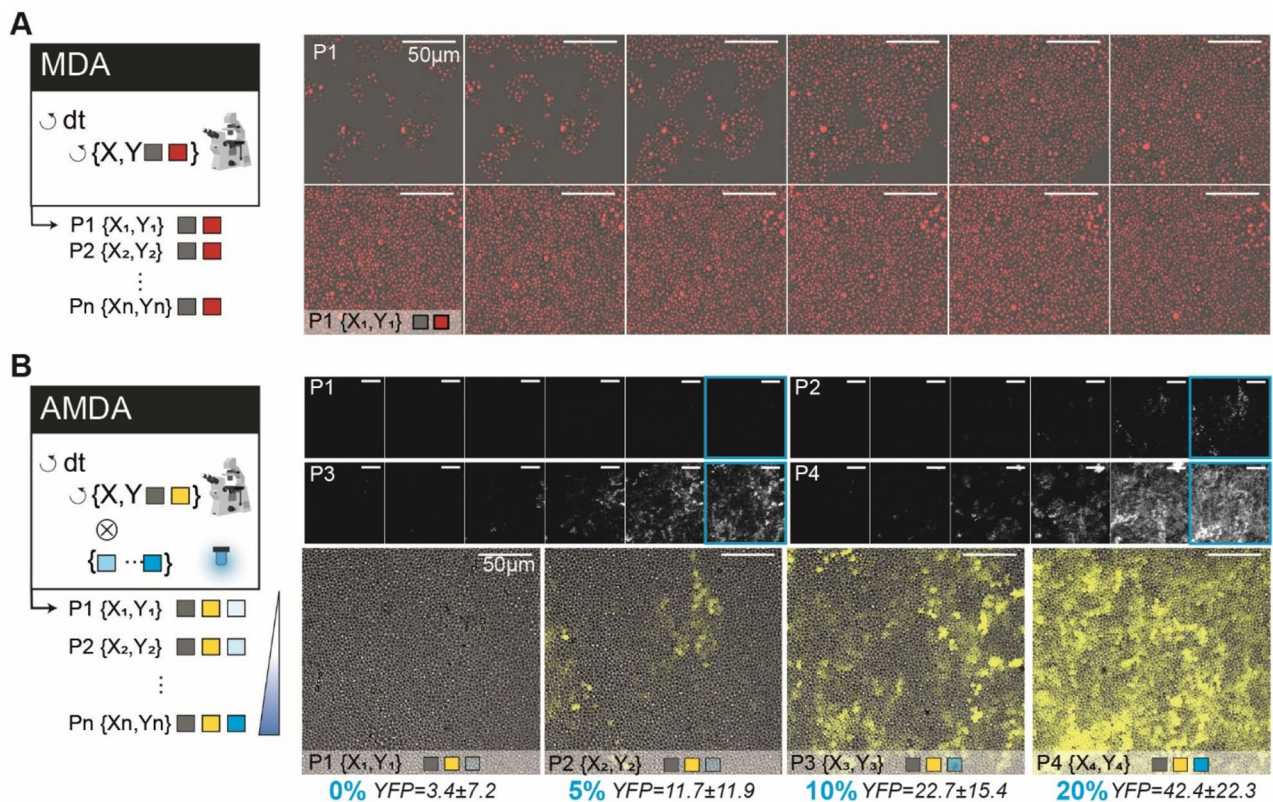


Figure 2. From simple to advanced MDA. **(A)** Example of a classic Multi-Dimensional Acquisition (MDA) protocol to observe yeast proliferation in a microfluidic chamber, with two imaging channels (brightfield and RFP) imaged every 6 min for several hours. The HTB2 protein of the yeast cells is tagged with a mCherry fluorescent reporter. A sketch of the program (nested loops) is shown on the left side: the imaging parameters are identical for every position and timepoint. **(B)** An advanced MDA, in which the user has defined several positions, but set different illumination settings in the blue channel (LED intensity: 0%, 5%, 10% and 20%). This programming was done without scripts, by just using the drag and drop interface (see Supplementary Materials). Yeast cells bearing an optogenetic gene expression system (pC120-venus) were imaged for 15 h. Each position is exposed to a different level of light stimulation, which alters the expression of a yellow fluorescent reporter both in terms of cell–cell variability, the maximum level of expression and dynamics. Thus, in one experiment, it was possible to quantitatively calibrate the pC120 optogenetic promoter using our settings without any requirement for coding (objective $\times 20$). Fluorescence levels are averaged across the field of view and the error values are the standard deviation of pixel intensity.

a documented communication protocol (see Supplementary Information and the GitHub page of the project on how to proceed).

CyberSco.Py allows to automate complex multidimensional acquisitions. CyberSco.Py can obviously be used to build classic MDA experiments. A web interface enables the imaging acquisition settings to be easily defined through a drag and drop interface (Fig. 1 and Supplementary Information). The user can define X–Y positions and the corresponding focal planes and set the illumination parameters, as in conventional microscopy software. CyberSco.Py makes it easy to perform a classic MDA experiment that follows, for example, the proliferation of a population of yeast cells in a microfluidic device (Fig. 2A). Crucially, the user can define specific imaging settings for each position (Fig. 2B). This modification of how MDA is defined through the user interface is simple but powerful: by design, the user has full control over the acquisition settings without having to follow the classic MDA patterns of nested loops, which by default impose the same imaging acquisition parameters on all time points and positions. The ability to vary the imaging modalities per position imaged allows, for example, the user to conveniently and quickly optimize the imaging conditions by varying the exposure time for each position (to screen for phototoxicity or optimal illumination, for example). To demonstrate its usefulness, we used this feature to measure the light-dose response of a light-inducible promoter (Fig. 2B and Supplementary Fig. S3) with just one timelapse experiment. Setting up this experiment was quick and simple thanks to the minimal powerful user interface. More generally, any combination of imaging parameters can be assigned to a given position using the drag and drop tools within the user interface. For advanced users, the imaging parameters and positions can also be sent directly through a configuration file to create programmatically complex acquisition scenarios. More details of the user interface and scripting possibilities are available on the GitHub repository of the project (see also Supplementary Information). Notwithstanding such flexibility,

CyberSco.Py has been programmed to include several types of protocols relevant to quantitative cell biology. Such built-in capabilities include: (1) synchronization of the image acquisition framerate with the microfluidic valve switches that apply the environmental changes; (2) detection and tracking of a cell of interest in a microfluidic device over an extended period of time; (3) cell counting, and triggering of environmental changes when the cell population reaches a certain size in the field of view; and (4) prediction of the future occurrence of a cellular event and the corresponding changes in the illumination settings and framerate required to image this event at an appropriate time interval.

External triggers and adaptive acquisition framerates enable the observation of cell signaling at the right pace. Cells use a large set of signaling pathways and gene regulatory networks to process information from their surroundings. The signaling pathways in yeast are usually activated relatively quickly, within tens of seconds, while the transcriptional responses are slower (several minutes) and cell adaptation is even slower (tens of minutes). Therefore, it is difficult to image cell growth and signaling dynamics with fluorescence microscopy at the same time. Indeed, conventional MDA only allows image acquisition on one timescale. Fast periodic acquisition is possible, but leads to phototoxicity. Ideally, several acquisition frequencies need to be defined: a fast frequency to capture signaling events at the right pace, and slower frequencies, to image physiological adaptation and monitor cell growth. Moreover, the switch from a slow to fast acquisition framerate should be synchronized with the changes in the cellular environment through microfluidics. These technical requirements can be met by a simple scenario within CyberSco.py.

As an example, we studied nuclear import of the MAPK Hog1p following hyperosmotic stress^{21,22}. Yeast cells were grown inside a microfluidic device (see “Materials and methods”) to facilitate imaging and facilitate dynamic environmental changes. We observed that an acquisition rate faster than one fluorescent image every 5–6 min led to phototoxicity and cellular arrest if performed over extended periods of time. This acquisition rate is too slow to capture nuclear localization of the Hog1p protein, which peaks 1–2 min after cells are subjected to hyperosmotic stress. We programmed CyberSco.Py to perform pulses of osmotic stress (by switching the state of an electrofluidic valve) every hour. Sending this command triggered modification of the acquisition framerate, which was increased from one frame every 5 min to one frame every 25 s (Fig. 3). No coding/ scripting was required for this modification: the user just needed to select this predefined scenario and set the desired framerates and illumination parameters. As shown in Fig. 3, we monitored several successive signaling events using this adaptive sampling rate without any user intervention. This example shows how the combination of external triggers and advanced MDA enables quantitative, time-resolved data on cellular responses and stress adaptation to be obtained without user supervision.

Live cell segmentation enables the use of conditional events to dynamically change the modalities of image acquisition based on real time cellular features. CyberSco.py also offers the possibility of operating the microscope and the attached devices in real-time based on events detected during unsupervised analysis of the cell sample. The central idea is to let the microscope focus on “interesting” events through adjustment of the imaging acquisition parameters without supervision. This task requires efficient image analysis to segment cells, measure their properties and detect cellular events of interest. Image analysis is conveniently achieved in Python using the U-NET convolutional neural network²³ (“Materials and methods” and Supplementary Information), which is trained on a set of images. Once the training is complete, CyberSco.Py can use the resulting model to segment cells, display the segmentation in the user interface, compute cellular features and trigger user-defined events. At present, CyberSco.Py comes with two U-NET-trained models for yeast segmentation at different magnifications that give the following outputs: (1) the number of cells in the field of view; (2) a segmentation map of the cells in the field of view, as well as (3) their size and (4) their fluorescence levels. These cellular features can then be used to define conditional statements and adapt the imaging acquisition parameters in real-time. The segmentation results can be instantly visualized in “live” mode as a quality control step before launching timelapse experiments (see Supplementary Material). Below, we describe three different use case scenarios to exemplify the potential of conditional microscopy.

Cells of interest can be detected and tracked in real-time. One interesting avenue of event-based microscopy is the ability to detect and focus on a particular cell of interest displaying a given phenotype at a given time. Instead of imaging many cells to find the cell of interest a posteriori, one can use real-time image analysis to identify cells with specific features and study their properties at an appropriate spatio-temporal resolution. There are two main challenges to overcome: defining the appropriate image analysis method to detect the cells of interest, and tracking those cells over time. Indeed, in an assembly of cells, growing cells push against their neighbors, often leading to large-scale displacement of the cells of interest, which may exit the field of view and be lost to subsequent imaging. Here, we demonstrate that it is possible to control the position of the X–Y stage to make sure that the cell of interest remains visible throughout the duration of the experiment. We studied a mixed population of yeast cells, in which a small fraction of the population (10%) express a fluorescent RFP histone tag. The program scans through the cells growing in a microfluidic device and once an RFP-expressing cell is detected, the scanning stops, the X–Y stage is moved to center the cell of interest and a timelapse is started to record RFP and brightfield images. The cell of interest is tracked throughout the timelapse, and the X–Y stage is moved so that this cell is always centered in the field of view. Figure 4 shows two such experiments, in different contexts, to demonstrate the efficiency of this detection and tracking scheme. Providing that the phenotype can be identified through image analysis (for example, a morphological feature or expression of a fluorescent reporter), this strategy could be employed to study rare phenotypes or, alternatively, to study long-term cellular

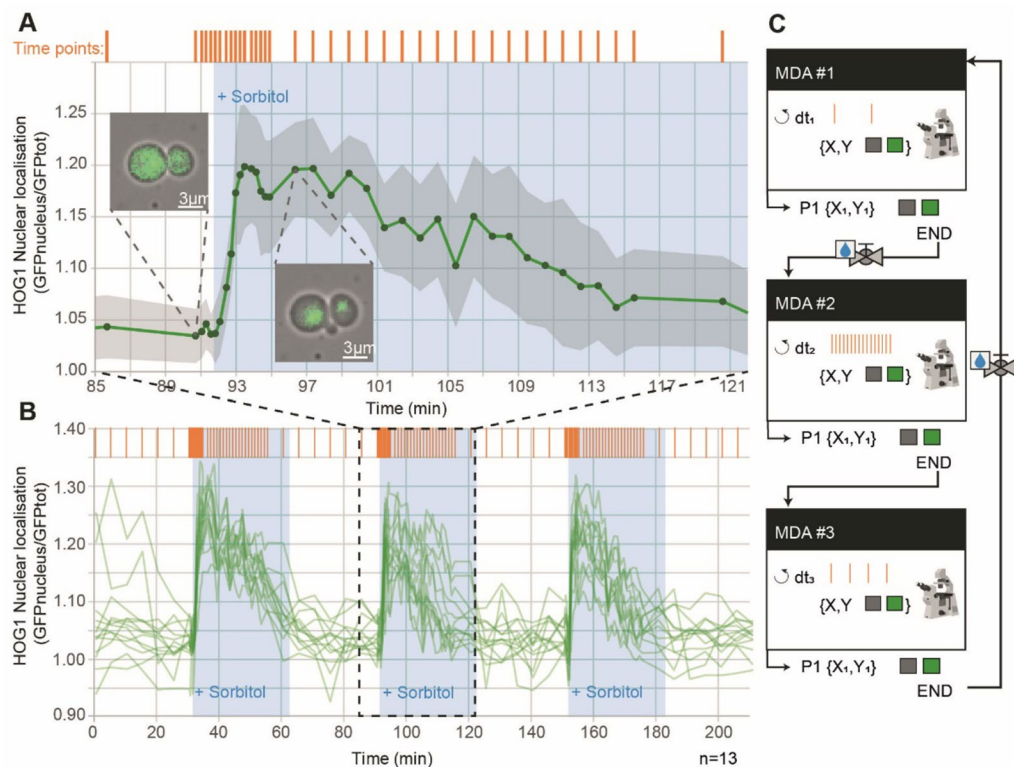


Figure 3. Synchronization of the acquisition framerate with dynamic perturbations to capture yeast cell signaling dynamics. **(A)** Time course of nuclear accumulation of Hog1p in yeast cells growing as a monolayer in a microfluidic chamber subjected to an osmotic stress (1 M sorbitol). The insets show localization of Hog1-GFP before and after the osmotic stress. The acquisition framerate (orange bars) is automatically adjusted from one frame every 5 min to one frame every 25 s (12 times faster) just before the cells are stressed osmotically. The autofocus was turned off during the first 4 min of rapid Hog1 nuclear import. Recovery of the cells was then monitored at one frame every minute for 20 min, and finally the framerate was set back to its initial value (one frame every 5 min) until the next stress. The grey area represents the \pm standard deviation of nuclear localization across 13 tracked cells from one microfluidic chamber. **(B)** The adaptive sampling rate used in **(A)** was repeated three times to demonstrate that cells exhibit reproducible dynamics in response to every stress. This experiment allowed the timescales of activation (fast) and deactivation (slow) of the HOG cascade to be measured in an unsupervised manner. **(C)** Sketch of the adaptive sampling MDA, which consists of three MDA experiments: one with a fast acquisition rate (nuclear import dynamics), one with a medium acquisition rate (nuclear export dynamics), and one with a slow acquisition rate (cell division after recovery). The switch from MDA#1 to MDA#2 is synchronized with the activation of an electrofluidic valve that delivers an osmotic stress of 30 min duration (repeated every 60 min). Nuclear localization is computed as the mean of GFP fluorescence in the nucleus normalized to the mean of GFP fluorescence in the entire cell.

behaviors (aging, cell-memory, habituation to repeated stress, etc.) within a large population of cells without user supervision. It is worth noting that this method can also compensate for spatial drift of the mechanical stage.

Cybersco.Py can trigger a change in the microenvironment in function of a threshold in cell density through microfluidic automation. Above, we showed how to control gene expression in cells based on real-time measurement of a fluorescent reporter. The same experimental strategy can be used to trigger a change in the cellular environment as a function of an observable feature in the field of view. This event-based strategy can be used to stimulate or perturb cells only when they have reached a given state. Alternative methods would require impractical, constant monitoring of the cells by the user. As a demonstration, we explored the impact of the number of yeast cells on the dynamics of recovery of cell division following a metabolic switch from glucose to sucrose. In response to glucose starvation, yeast cells produce and harbor the invertase Suc2p²⁴ in their cell wall, which hydrolyses sucrose into glucose and fructose in the extracellular environment. The yeast growth rate takes a certain amount of time to recover after a metabolic shift from glucose to sucrose. Since the benefit of Suc2p production is shared among the yeast population, we hypothesized that the size of the population of cells may impact the response time after a metabolic shift to sucrose²⁴. To test this assumption, cells growing in a microfluidic chamber were counted in real-time and, as soon as the number of cells in the chamber reached a given value ($N = 100, 500$ or 2000 ; Fig. 5), CyberSco.Py switched the perfusion from glucose to sucrose by triggering a microfluidic valve. Again, such experiments require an unsupervised, live method in order for the

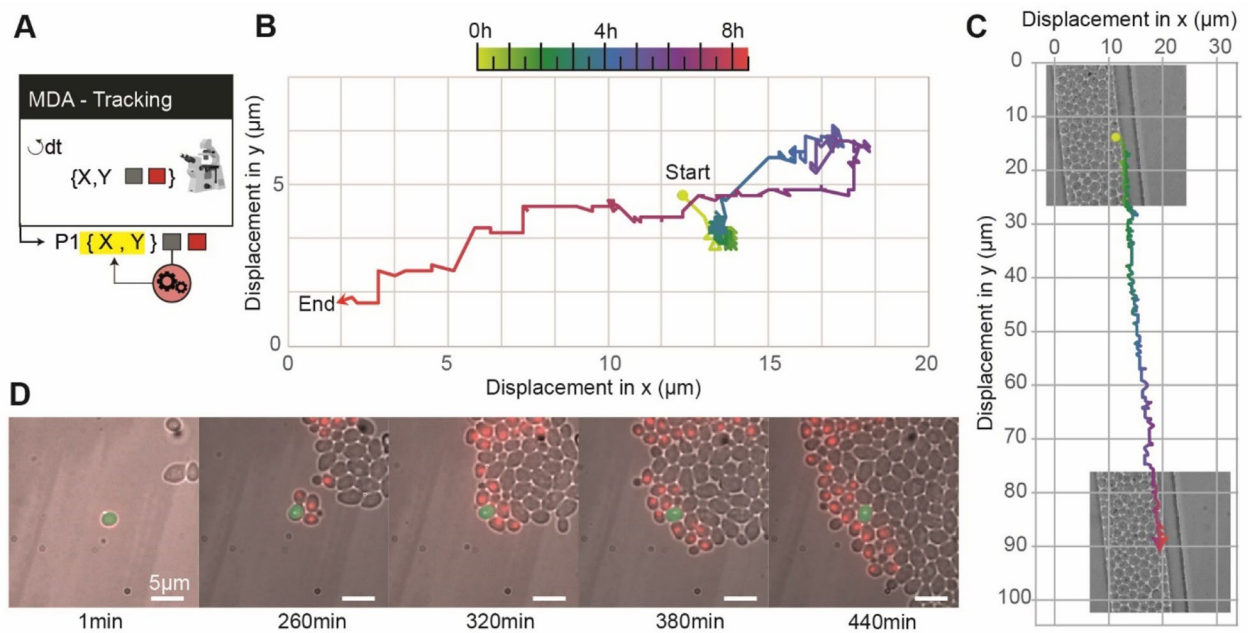


Figure 4. Detection and tracking of a cell of interest. **(A)** Sketch of the “detect and track scenario”. Once a cell of interest is found in the field of view, the field of view is centered on that cell and the stage is periodically moved to maintain this cell in the center of the field of view. **(B)** We mixed two populations of yeast cells in a microfluidic chamber, one of which express a HTB2-mCherry fluorescent reporter (1:10 cell ratio). The algorithm scans through several positions and when it detects cells with a signal in the RFP channel, picks one such cell randomly and centers it on the field of view. This cell is then tracked using brightfield segmentation, and the stage position is corrected through a feedback loop to compensate for cell displacement. **(C)** The cell of interest moves because it is pushed by the growth of neighboring cells, traveling approximately 20 μm during the course of the experiment. The real-time stage compensation keeps the cell in the center of the field of view. The duration of the experiment (around 9 h) is long enough to observe the appearance of the progeny of the cell of interest. **(D)** Tracking a non-fluorescent yeast cell growing in a dead-end narrow microfluidic chamber, leading to global directed motion of all cells. The tracked cell remains in the field of view, even though it travels approximately 80 μm ; in contrast, the field of view is only $\sim 25 \times 25 \mu\text{m}$.

switch to be made efficiently. We observed that the duration of the lag phase decreased as the size of the population in the microfluidic chamber at the time of the metabolic shift increased, indicating faster production and accumulation of the enzymatic products within larger yeast populations, and hence a better adaptability of large yeast populations to sucrose metabolic shifts. Moreover, this experiment demonstrates the capacity of CyberSco.Py to precisely control the sample size at the start of the experiment, and suggests that cell density is a biologically relevant parameter that should be considered to improve experimental reproducibility.

Imaging of mitosis in yeast can be done at high temporal resolution by conditionally switching between two predefined MDAs.

As a final example, we used CyberSco.Py to precisely image mitotic events in a population of growing yeast cells (Fig. 6). We combined cell segmentation, cell tracking, and event-based modification of the imaging parameters to achieve imaging of mitotic events in yeast at a high temporal resolution in an unsupervised manner. Cells were observed and segmented at regular intervals (3 min). We assessed the increase in the size of buds over time to predict when mitosis will occur. We detected buds using U-NET segmentation and searched for yeast cells with buds that have grown to reach a threshold size and that have been increasing in size over the past three pictures (see “Materials and methods”). Both criteria were sufficient to detect mitotic events under our conditions and to eliminate segmentation artefacts. When all conditions are fulfilled, the first MDA is stopped and a second MDA with a faster acquisition framerate, along with fluorescence imaging for the HTB2-mCherry reporter, is initiated. In this manner, mitotic events can be imaged at a much faster rate than in a classic MDA experiment (Fig. 6) without the detrimental long term effect of phototoxicity. This kind of “search and zoom” scenario is presented for mitotic events as a proof-of-principle, but could be applied to any rare event that occurs within a population of cells.

Discussion

The main goal of CyberSco.Py is to enable the design of augmented MDA experiments in which the imaging settings can be changed in real-time as a function of unsupervised image analysis conducted during the time course of the experiment. CyberSco.Py has been built as a modular web application; in addition to the modularity of the device management, both the image analysis and decision-making algorithm are separate modules that can be adjusted individually and plugged into the communication modules that drive the microscope and its

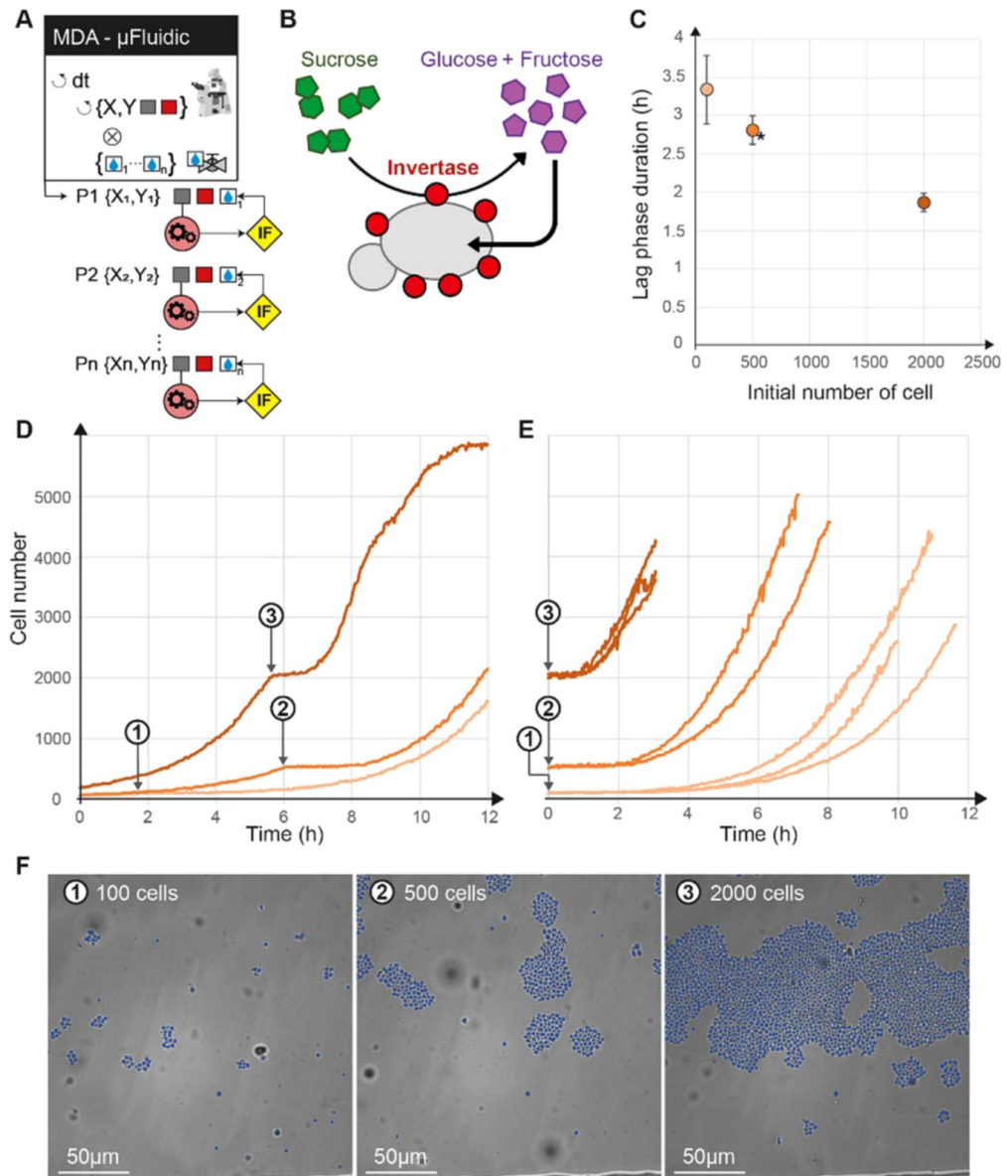


Figure 5. Conditional perturbation based on the number of cells. (A) Sketch of the protocol, showing that different positions have a different conditional statement ((IF)) on the number of cells to trigger the switch from glucose to sucrose independently of each other. (B) Sucrose conversion by yeast. The Suc2p invertase produced by cells is secreted extracellularly and can degrade extracellular sucrose into diffusible hexose. (C) Following a shift from glucose to sucrose, cells need some time to convert sucrose to glucose and restart division. We show here that this time depends on the initial cell density (the higher the number of cells, the shorter the lag phase). The duration of the lag phase was estimated as the time it took the population to reach 130% of its initial size after the switch from glucose to sucrose. Error bars represent \pm one standard deviation over three biological replicates (two replicates for the *). (D) Temporal evolution of the number of cells for different initial densities: 100 (1), 500 (2) and 2000 (3) cells (grey arrows). (E) Population growth shifted temporally to the switch time (i.e., switch = t_0), demonstrating that the lag time increases as the initial cell density decreases. (F) Cell counting is achieved by real-time segmentation, shown here as an overlay of the brightfield image with single cell masks (in blue) at the time of the valve switch.

associated components. In that respect, CyberSco.Py aims to push forward “low code” or “no code” strategies, which are becoming increasingly popular, and enable biologists without coding expertise to create complex, event-based routines and workflows using cloud-based web applications. Creation of automation protocols that contain simple logical, conditional statements such as “IF this THEN that” or “WHILE this DO that” are within the reach of CyberSco.Py and may have an impact for researchers in biology who do not want, nor have the time or expertise, to dive into programming. This goal could be reached progressively by building on the examples

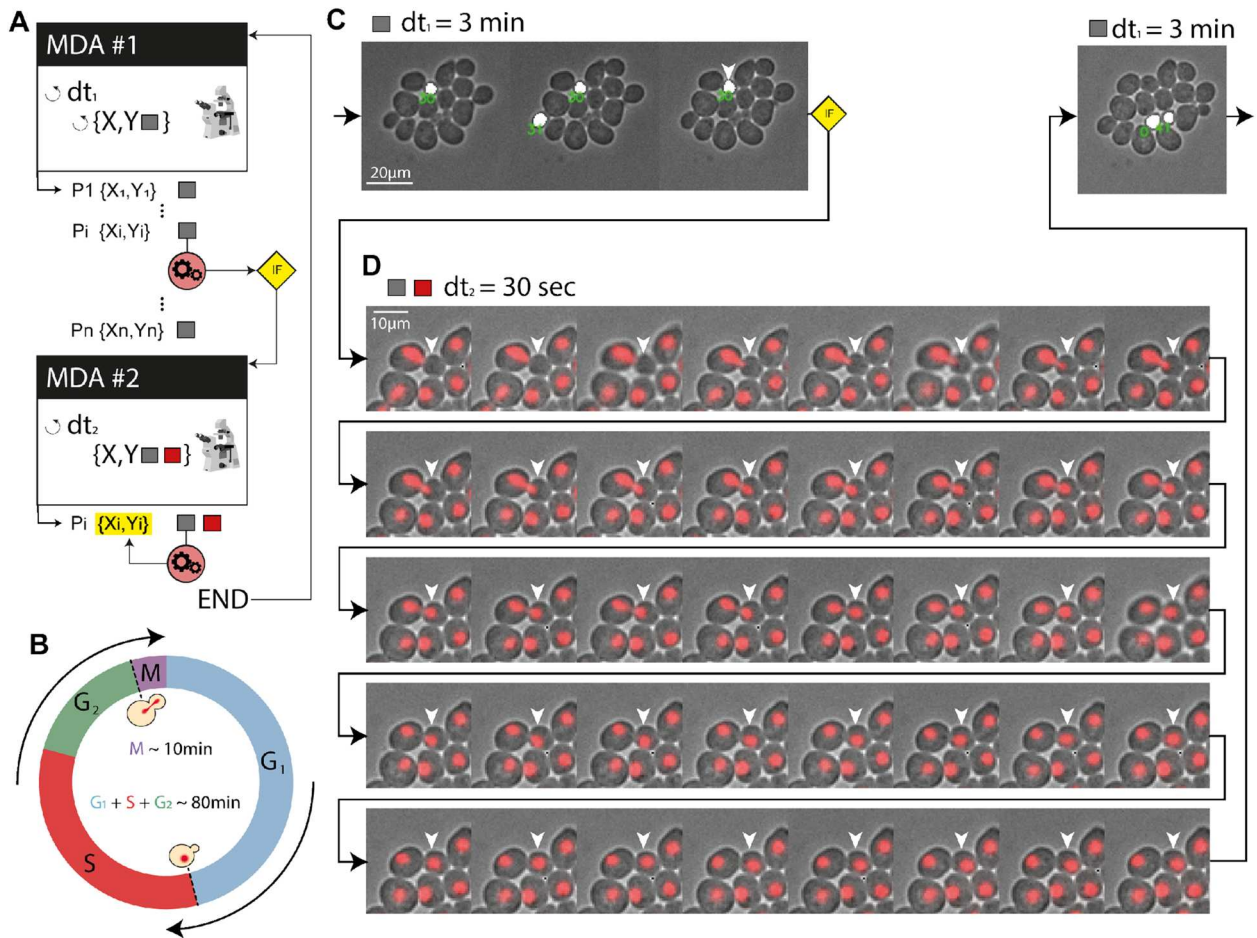


Figure 6. Bud detection and high-temporal-resolution imaging of mitosis. **(A)** Scenario used to detect and “zoom in” on a particular event (in this case, mitosis). Several positions are monitored and when a condition is fulfilled, image acquisition is performed on only this position at an adapted sampling framerate. **(B)** Cell cycle progression in yeast. The mitosis event to be captured represents a small-time fraction of the cell’s life cycle ($\sim 10\%$). **(C)** In practice, the acquisition of brightfield images of a population of budding yeast leads to a coarse timelapse with an acquisition framerate of 3 min to search for the next mitotic event. Cell segmentation is used to identify buds (size filtering), shown here as a white overlay. When a bud has reached a given size (and has been growing for at least three frames), we consider that a mitotic event is about to occur. **(D)** Then, the acquisition software “zooms in” on that cell by increasing the framerate to one frame every 30 s for 20 min and RFP imaging is added to image the nucleus (HTB2-mCherry reporter). As shown in panel **(D)**, this scenario allows the complete mitotic event and nuclear separation between the mother and daughter cells (around 10 min, as expected) to be captured at an appropriate framerate. Once this image acquisition sequence is complete, the program resumes its search at the lower framerate for another mitotic event.

proposed here and adding generic scenarios that are driven through the results of real-time image analysis. For example, the scenario developed in this work that acts on a microfluidic chip based on the number of cells could be directly reprogrammed by changing the trigger condition.

Image analysis remains the bottleneck of automation and will continue to require expertise in machine learning and coding. However, the pace at which deep learning is being adopted in laboratories and adapted into user-friendly software solutions and online tools^{25,26} suggests that an increasing number of easy-to-use methods to create UNET-trained networks will be developed in the near future and could subsequently be incorporated into CyberSco.Py. While we modified several classic experiments to demonstrate the potential of event-based microscopy, rethinking automation software for microscopy and including complete management of triggers and event detection may provide other important benefits in quantitative cell biology.

To start with, we can use our conditional microscopy framework to better prepare experiments and obtain a level of quality control before starting an experiment. Indeed, we showed that the number of cells may be an important factor when exploring the dynamics of population growth after a metabolic shift. Other processes related to cell–cell communication, metabolic gradients and cell–cell contact inhibition are also likely to be dependent on cell density. To increase experimental reproducibility, it seems reasonable to add a condition (or a set of conditions) on cell density to start a timelapse experiment. Similarly, only starting experiments, even simple timelapse studies, when a steady state is reached or when a gene has been expressed at a given level could

improve experimental reproducibility. Only stimulating cells when the system is “ready” can also help avoiding phototoxicity and bleaching due to starting an experiment too early.

Timelapse experiments are usually long and prone to failures in both the microscopy system (e.g., loss of focus, improper control of temperature, drift in the stage) and the biological sample (e.g., contamination). However, in conventional timelapse microscopy, the user only realizes these issues at the end of the experiment, when it is too late. Our framework can be extended to regularly communicate the state of both the microscope and the experiment to the user. This could be in either a trigger mode, with the software sending a status report to the user through all sorts of classic communication channels (e.g., Slack, Teams, Email, SMS) when something goes wrong or the experiment reaches a given state, or—even better—the microscope could use the output of the image analysis to correct the problem automatically (e.g., by relaunching an autofocus step). Such simple automation workflows will certainly help to achieve high-quality data, reduce the time and cost of experiments, and improve experimental reproducibility.

Another important aspect is the huge amounts of data acquired in conventional, uninformed MDA. In many cases, this is due to the fact that image analysis is performed a posteriori, which requires as much data as possible to be acquired given the constraints of the imaging system and the biological sample. The ability to perform real-time analysis and conditional acquisition will make it possible to collect much sparser data, by focusing only on precisely what matters for a given study. This would speed up the analysis, facilitate data storage and sharing, and more generally improve the life cycle of imaging data.

We envision that advanced automation could be further used to perform online learning and automatically adjust the imaging parameters and stimulation of the biological system to obtain a model of the system under study. Such applications, which we are presently developing in the field of cancer research, may represent a game changer that increases the throughput of rare event detection and the quality of the resulting analysis by “zooming in” in time and space and/or sending drugs to perturb cells as soon as these rare events are detected among a large population of cells.

Our motivation to develop this proof-of-concept software with a simple user-friendly interface was to introduce conditional microscopy to a large audience. While this first step is relatively limited, the initial framework we propose here can be improved and developed further. Ideally, a global effort to develop application programming interfaces (APIs) for lab automation would facilitate the development of no-code workflows that are accessible to all researchers and integrate with commonly used collaborative online tools such as Slack and Teams. We believe that researchers could benefit from such advanced ways of conducting experiments, especially the ability to perform event-based automated imaging. CyberSco.Py is a first step to bring such concepts to the attention of biologists.

Materials and methods

Yeast strains and growth conditions. All yeast strains used in this study are derived from the BY4741 background (EUROSCARF Y00000). The list of strains can be found in Supplementary Table 1. Yeast cells were picked from a colony in an agar plate, grown overnight in 2 mL YPD media, then the culture was diluted 1/100 in 5 mL of filtered synthetic complete media (SC; 6.7 g Yeast Nitrogen Base w/o amino acid [Difco 291940] and 0.8 g complete supplement mixture drop-out [Formedium DCS0019] to 1 L) supplemented with 2% glucose and cultured for 4–6 h at 30 °C with orbital shaking at 250 RPM (Innova 4230 incubator). The media used to perfuse the microfluidic chips during the experiments was SC supplemented with either 2% glucose or 1% sucrose. The microfluidic chips were made following a previously published protocol¹⁵ (see Fig. S8). Liquid perfusion was performed using an Ismatec IPC (ISM932D) peristaltic pump at 50 μ L/min (or 120 μ L/min for the osmotic shock experiment). A homemade Arduino-based system was used to switch the state of an electrofluidic valve to change the media that perfuses the microfluidic chip. The microfluidic chip (Supplementary Fig. S2) allows yeast cells growing in a monolayer to be imaged and has been described in previous works²⁷. Another microfluidic design²⁸ was used (in Fig. 4C) to constrain cell displacement in one direction.

Microscopy imaging. We used a fully automated Olympus IX81 inverted epifluorescence microscope equipped with a motorized stage (Prior Pro Scan III), Photometrix Evolve512 camera, and a pE-4000 CoolLED as a fluorescent light source. The objectives used in this study were either a 20 \times UPlanSApo or 60 \times PlanApo N. For the RFP channel, we used the 550 nm LED through a filter cube (EX) 545 nm/30; (EM) 620 nm/60 (U-N49005) with a 150 ms exposure time. For the GFP channel, we used the 460 nm LED through a filter cube (EX) 545 nm/30; (EM) 620 nm/60 (U-N49005) with a 150 ms exposure time. For the YFP channel, we used the 525 nm LED through a filter cube (EX) 514 nm/10; (EM) 545 nm/40 (49905-ET) with a 500 ms exposure time. Microscopy experiments were carried out in a thermostat chamber set to 30 °C.

CyberSco.Py software. CyberSco.Py is written in Python for the backend and HTML/CSS/ JS for the frontend, connected by a WebSocket channel. Communication to the different devices is made directly through serial communication and whenever necessary, the drivers provided by the vendors or a generic version from the μ Manager community. CyberSco.Py is installed on computer software that must be equipped with a recent GPU to benefit from U-NET deep learning segmentation of cells. A server can interface several microscopes running CyberSco.Py and be extended with a user manager database and image database management program such as OMERO. The current open-source release of CyberSco.Py can be found on GitHub (<https://github.com/Lab513/CyberSco.Py>).

Acquisition, segmentation and tracking. Image acquisition is preceded by an autofocus algorithm that optimizes the quality of the segmentation, as well as the sharpness of the object under scrutiny. Cell segmenta-

tion is achieved via a machine-learning algorithm based on the U-NET architecture. Twenty images of cells at different positions and containing different numbers of cells were taken to produce the training set. This dataset was then augmented as it is classically done (see Supplementary Information). For the main model for yeast segmentation, the neural network was trained on five periods using a GPU NVIDIA GeForce GTX 1080; this training only took 5 min. Predictions with this model are obtained in around 0.2 s. Cell tracking is performed using both image correlation in real-time and using a simple proximity relationship between the predicted contours.

Data availability

The datasets used and/or analysed during the current study are available from the corresponding author on reasonable request. The main datasets and code are available at the following address <https://github.com/Lab513/CyberSco.Py>.

Received: 18 March 2022; Accepted: 20 June 2022

Published online: 08 July 2022

References

- Almada, P. *et al.* Automating multimodal microscopy with NanoJ-Fluidics. *Nat. Commun.* **10**, 1–9 (2019).
- Hossain, Z. *et al.* Interactive and scalable biology cloud experimentation for scientific inquiry and education. *Nat. Biotechnol.* **34**, 1293–1298 (2016).
- Pinkard, H., Stuurman, N. & Waller, L. Pycro-manager: Open-source software for integrated microscopy hardware control and image processing. *ArXiv200611330 Q-Bio* (2020).
- Pinkard, H., Stuurman, N., Corbin, K., Vale, R. & Krummel, M. F. Micro-Magellan: Open-source, sample-adaptive, acquisition software for optical microscopy. *Nat. Methods* **13**, 807–809 (2016).
- Conrad, C. *et al.* Micropilot: Automation of fluorescence microscopy-based imaging for systems biology. *Nat. Methods* **8**, 246–249 (2011).
- Edelstein, A., Amodaj, N., Hoover, K., Vale, R. & Stuurman, N. Computer control of microscopes using μ Manager. *Curr. Protoc. Mol. Biol.* **92**, 14.20.1–14.20.17 (2010).
- Edelstein, A. D. *et al.* Advanced methods of microscope control using μ Manager software. *J. Biol. Methods* **1**, e10 (2014).
- Kondaveeti, H. K., Kumaravelu, N. K., Vanambathina, S. D., Mathe, S. E. & Vappangi, S. A systematic literature review on prototyping with Arduino: Applications, challenges, advantages, and limitations. *Comput. Sci. Rev.* **40**, 100364 (2021).
- Jolles, J. W. Broad-scale applications of the Raspberry Pi: A review and guide for biologists. *Methods Ecol. Evol.* **12**, 1562–1579 (2021).
- Milias-Argeitis, A. *et al.* In silico feedback for in vivo regulation of a gene expression circuit. *Nat. Biotechnol.* **29**, 1114–1116 (2011).
- Milias-Argeitis, A., Rullan, M., Aoki, S. K., Buchmann, P. & Khammash, M. Automated optogenetic feedback control for precise and robust regulation of gene expression and cell growth. *Nat. Commun.* **7**, 12546 (2016).
- Rullan, M., Benzinger, D., Schmidt, G. W., Milias-Argeitis, A. & Khammash, M. An optogenetic platform for real-time, single-cell interrogation of stochastic transcriptional regulation. *Mol. Cell* **70**, 745–756.e6 (2018).
- Chait, R., Ruess, J., Bergmiller, T., Tkačik, G. & Guet, C. C. Shaping bacterial population behavior through computer-interfaced control of individual cells. *Nat. Commun.* **8**, 1535 (2017).
- Lugagne, J.-B. *et al.* Balancing a genetic toggle switch by real-time feedback control and periodic forcing. *Nat. Commun.* **8**, 1671 (2017).
- Uhlendorf, J. *et al.* Long-term model predictive control of gene expression at the population and single-cell levels. *Proc. Natl. Acad. Sci.* **109**, 14271–14276 (2012).
- Harrigan, P., Madhani, H. D. & El-Samad, H. Real-time genetic compensation defines the dynamic demands of feedback control. *Cell* **175**, 877–886.e10 (2018).
- Perkins, M. L., Benzinger, D., Arcak, M. & Khammash, M. Cell-in-the-loop pattern formation with optogenetically emulated cell-to-cell signaling. *Nat. Commun.* **11**, 1355 (2020).
- Toettcher, J. E., Gong, D., Lim, W. A. & Weiner, O. D. Light-based feedback for controlling intracellular signaling dynamics. *Nat. Methods* **8**, 837–839 (2011).
- Fox, Z. R. *et al.* MicroMator: Open and flexible software for reactive microscopy. *bioRxiv*. <https://doi.org/10.1101/2021.03.12.435206> (2021).
- Pedone, E. *et al.* Cheetah: A computational toolkit for cybergenetic control. *ACS Synth. Biol.* **10**, 979–989 (2021).
- Hersen, P., McClean, M. N., Mahadevan, L. & Ramanathan, S. Signal processing by the HOG MAP kinase pathway. *Proc. Natl. Acad. Sci.* **105**, 7165–7170 (2008).
- Muzzey, D., Gómez-Urbe, C. A., Mettetal, J. T. & van Oudenaarden, A. A systems-level analysis of perfect adaptation in yeast osmoregulation. *Cell* **138**, 160–171 (2009).
- Falk, T. *et al.* U-Net: Deep learning for cell counting, detection, and morphometry. *Nat. Methods* **16**, 67–70 (2019).
- Koschwanez, H., Foster, K. R. & Murray, A. W. Sucrose utilization in budding yeast as a model for the origin of undifferentiated multicellularity. *PLoS Biol.* **9**, e1001122 (2011).
- Ouyang, W., Mueller, F., Hjelmare, M., Lundberg, E. & Zimmer, C. ImJoy: An open-source computational platform for the deep learning era. *Nat. Methods* **16**, 1199–1200 (2019).
- Sullivan, D. P. & Lundberg, E. Seeing more: A future of augmented microscopy. *Cell* **173**, 546–548 (2018).
- Llamosi, A. *et al.* What population reveals about individual cell identity: Single-cell parameter estimation of models of gene expression in yeast. *PLoS Comput. Biol.* **12**, e1004706 (2016).
- Marinkovic, Z. S. *et al.* A microfluidic device for inferring metabolic landscapes in yeast monolayer colonies. *Elife* **8**, e47951 (2019).

Acknowledgements

The authors would like to thank Pierre Louis Crescitz, Williams Brett and several colleagues and beta testers for their help and critical reading of this manuscript. This work was supported by the European Research Council grant SmartCells (724813) and received supports from grants ANR-11-LABX-0038 and ANR-10-IDEX-0001-02.

Author contributions

Code implementation and automation troubleshooting were performed by L.C., M.L.B. designed, performed and analyzed all experiments. C.C., S.P. and D.M. participated in molecular biology and microfluidic efforts. J.-M.D.M., B.S. and P.H. conceived and designed the study. L.C., M.L.B., A.B., B.S. and P.H. wrote the manuscript.

Competing interests

The authors declare no competing interests.

Additional information

Supplementary Information The online version contains supplementary material available at <https://doi.org/10.1038/s41598-022-15207-5>.

Correspondence and requests for materials should be addressed to P.H.

Reprints and permissions information is available at www.nature.com/reprints.

Publisher's note Springer Nature remains neutral with regard to jurisdictional claims in published maps and institutional affiliations.



Open Access This article is licensed under a Creative Commons Attribution 4.0 International License, which permits use, sharing, adaptation, distribution and reproduction in any medium or format, as long as you give appropriate credit to the original author(s) and the source, provide a link to the Creative Commons licence, and indicate if changes were made. The images or other third party material in this article are included in the article's Creative Commons licence, unless indicated otherwise in a credit line to the material. If material is not included in the article's Creative Commons licence and your intended use is not permitted by statutory regulation or exceeds the permitted use, you will need to obtain permission directly from the copyright holder. To view a copy of this licence, visit <http://creativecommons.org/licenses/by/4.0/>.

© The Author(s) 2022

8.4. Table of strains

parent	YPH	Alias	Opto	Trifusion			Boost		...
				CrtYB	CrtI	CrtE	tHMG		
-	435	CEN.PK2-1C	MATa; his3D1; leu2-3_112; ura3-52; trp1-289; MAL2-8c; SUC2						
435	395	Opto-EXP	EXP-GFP	-	-	-	-	-	-
395	463	EXP-mCh	EXP-mCh	-	-	-	-	-	-
435	394	Opto-INVRT	INVRT-GFP	-	-	-	-	-	-
394	512	INVRT-mCh	INVRT-mCh	-	-	-	-	-	-
435	534	Verwaal's	-	ura3::pTDH3	ura3::pTDH3	ura3::pTDH3	-	ura3::URA3	
534	523	Yvert's	-	ura3::pTDH3(lox)	ura3::pTDH3	ura3::pTDH3	-	ura3::URA3	
435	432	Héry's	-	ho::pGAL1	-	dpp1::pGAL1	dpp1::pGAL10	ΔGAL80	
395	433	Cogex08	EXP-GFP	-	-	dpp1::pTDH3	dpp1::pPGK1	-	
433	434	Cogex09	EXP-GFP	ho::pC120(pb kozak)	-	dpp1::pTDH3	dpp1::pPGK1	-	
434	511/524	Cogex10	EXP-mCh	ho::pC120	-	dpp1::pTDH3	dpp1::pPGK1	-	
529	530	-	INVRT-mCh	ho::pGAL1	-	dpp1::pGAL1	dpp1::pGAL10	-	
435	531	pADH1	-	ho::pADH1	-	dpp1::pTDH3	dpp1::pPGK1	-	
435	532	pTDH3	-	ho::pTDH3	-	dpp1::pTDH3	dpp1::pPGK1	-	
435	533	pPGK1	-	ho::pTEF1	-	dpp1::pTDH3	dpp1::pPGK1	-	
524	551	Cogex11	EXP-mCh	ho::pC120	ho::pTDH3	dpp1::pTDH3	dpp1::pPGK1	-	
530	552	-	INVRT-mCh	ho::pGAL1	ho::pTDH3	dpp1::pGAL1	dpp1::pGAL10	-	
531	553	pADH1	-	ho::pADH1	ho::pTDH3	dpp1::pTDH3	dpp1::pPGK1	-	
532	554	pTDH3	-	ho::pTDH3	ho::pTDH3	dpp1::pTDH3	dpp1::pPGK1	-	
533	555	pPGK1	-	ho::pTEF1	ho::pTDH3	dpp1::pTDH3	dpp1::pPGK1	-	
435	556	556	-	ho::pTDH3	ho::pTDH3	ho::pTDH3	-	-	

8.5. Protocols

Molecular Biology:

- 8.5.1 (8.9.1) Culture media for yeast
- 8.5.2 (8.9.2) MoClo for yeast (YTK)
- 8.5.3 (8.9.3) CRISPR for yeast
- 8.5.4 (8.9.4) Yeast LiAc transformation
- 8.5.6 (8.9.5) Beta-carotene quantification

Illumination devices:

- 8.5.6 (8.9.6) OptoBox
- 8.5.7 (8.9.7) OptoTubes
- 8.5.8 (8.9.8) eVOLVER: list of components
- 8.5.9 (8.9.9) eVOLVER: installing

8.9.1 Culture Media for yeast

CSM

CSM (Complete Supplement Mixture) is one of the most used culture media for *S. cerevisiae*. It is especially useful if you want to select for auxotrophic markers (i.e. remove one or more amino acid).

List of Reagents

Aa Ingredient	# for 1L (gr)	Σ for 200mL (gr)	≡ ref
<u>Yeast Nitrogen Base w/o AA</u>	6.7	1.34	BD ref: 291940
<u>Glucose (Dextrose)</u>	20	4	euromedex ref: UG3050
<u>CSM (Dropout mix)</u>	0.8	0.16	MP Biomedicals™ ref: 114500022 or ForMedium DCS0029
<u>For 2% Agar Plates only : Bacto Agar</u>	20	4	BD Biosciences ref: 214010

Protocol

1. Prepare first a 10x glucose stock solution (200g/L). This can be prepared by dissolving 40g of glucose into 100mL of distilled H₂O, and then complete with distilled water up to 200mL. Autoclave this and keep it sterile (program 4, add tape, unscrew cap).
2. Mix Yeast Nitrogen Base (w/o Amino Acid), CSM dropout mix and if needed agar in a 500mL bottle.
3. Add 180 mL of water (to prepare a 200mL final solution).
4. Autoclave

 [Autoclave](#)

5. Add 20mL of your glucose stock solution working in a sterile environment (under the PSM or near a flame on your bench).

For Auxotrophic marker selection, use a CSM without the desired AA, e.g. CSM-URA. We have several of them in the lab.

Notes

how to autoclave something?

 [Autoclave](#)

It is important to autoclave glucose separately so that the CSM medium remains relatively clear and is not too much autofluorescent for microscopy experiments.



For microfluidics experiments, it is better to mix all the components (glucose powder included), shake until complete dissolution, and filter sterilise the medium to remove dust (that would be a problem in your device during experiments).

CSM 4X for microfluidics

List of Reagents

Aa Ingredient	# for 500 mL (gr)	≡ Ref
<u>Yeast Nitrogen Base w/o AA</u>	13.4	BD ref: 291940
<u>Glucose (Dextrose)</u>	40	euromedex ref: UG3050
<u>CSM (Dropout mix)</u>	1.6	MP Biomedicals™ ref: 114500022

Protocol

Mix the three components in a beaker containing 300 mL of distilled water. Wait for total dissolution under shaking for 30-60 min. Measure the exact volume and adjust to 500 mL with distilled water. Filter sterilise (0.2 um), do not autoclave.

YPD

YPD is a cheap, rich growing media, mainly used for agar petri dishes or for growing to high OD in Li-Ac transformations or before freezing strains.

For agar plates: YPD Agar plate media already prepared (Ref 4001-232 MP Bio) — 67g for 1L — Autoclave and pour

For YPD liquid: YPD powder media already prepared (Ref 4001-032 MP Bio) — 50g for 1L — Autoclave and use

List of Reagents

Aa Ingredient	≡ for 1L	≡ for 200mL	≡ ref
<u>Difco Yeast extract</u>	10g	2g	
<u>Glucose (Dextrose)</u>	20g	4g	
<u>Bacto Peptone</u>	20g	4g	
<u>For 2% Agar Plates only : Bacto Agar</u>	20g	4g	

YPG - Agar plates

YPG means with glycerol as carbon source: eliminates the *petite* phenotype.

List of Reagents

Aa Ingredient	≡ for 1L	≡ for 500mL	≡ ref
<u>Yeast extract</u>	10g	5g	Bacto/BD ref: 212750
<u>Glycerol</u>	50mL	25mL	Sigma Aldrich ref: G2025-1L
<u>Peptone</u>	20g	10g	Bacto/BD ref: 211677
<u>For 2% Agar Plates only : Bacto Agar</u>	20g	10g	Bacto/BD ref 214010


Protocol

For 500mL:

Get the ingredients ready (to be found in chemical shelf)

- 1L/500mL cylinder (glass shelf)
- Spatulas (near the sink)
- 1L Bottle

1. 300 mL of distilled water in the bottle
2. Weigh yeast extract, peptone and agar: put it in the bottle (those take ~30mL volume)
3. Add the Glycerol using the pipetboy and a disposable 25mL pipet
4. Stir using magnetic bar on stirring plate (won't fully dissolve - agar need more heat).
5. Pour in cylinder and top up to 500mL with distilled water
6. Put back in bottle and stir some more
- ▼ 7. Autoclave (stirring bar can stay in)

 [Autoclave](#)

8. Stir while cooling down on stirring plate ~1hour
- ▼ 9. Display in petri dishes (about 13)
 - Prepare petri dishes with appropriate color code
 - Pour medium, close petri dish
 - Leave at RT O/N
 - Flip around and leave at RT for 2 days
 - Keep at 4°C.

SC + 5-FOA plates


5-FOA medium is used to counter-select the URA3 gene.

List of Reagents

Aa Ingredient	≡ for 1L (gr)	≡ for 700mL (gr)	≡ ref
<u>Yeast Nitrogen Base w/o AA</u>	6.7g	4.69g	BD ref: 291940
<u>Glucose (Dextrose)</u>	20g	14g	euromedex ref: UG3050
<u>CSM-URA (Dropout mix)</u>	0.8 g	0,56	MP Bio ref: 4511-212
<u>For 2% Agar Plates only : Bacto Agar</u>	20g	14g	BD Biosciences ref: 214010
<u>Uracil (1g/L in H2O), filtered</u>	50 mL	35 mL	
<u>5-FOA (at the end after autoclave)</u>	0.8 g	0.56 g	Fisher ref: 10619920

Protocol

1. For 700 mL (adjust the volume according to your needs, 5FOA is expensive and plates expires quickly): prepare a bottle filled with 665 mL H2O + 35 mL Uracile solution at 1g/L and add powders (YNB, Glucose, CSM-ura and bacto agar).
2. Autoclave. The bottle should not be filled more than 700mL in 1L bottle. Do not forget to add special autoclave tape and to unscrew the bottle cap.

 Autoclave

3. Cool-down the medium after autoclave. After ~30 min ($T=55^{\circ}\text{C}$, you can hold the bottle bare hand) add the 5-FOA. Let the solution stir for 5 min.

Warning: Wear a mask + goggles while weighing 5-FOA

4. Pour in plate
-

and ligation (42 °C for 2 min, 16 °C for 5 min) followed by a final digestion step (60 °C for 10 min), and a heat inactivation step (80 °C for 10 min).

You can use NEB online tool to design your parts, and they can automatically find you smart overhang to get scareless junction:

<https://goldengate.neb.com/>

Different modules and levels:

⚠️⚠️⚠️ NEVER use a MoClo plasmid lM0 as template for a PCR that will be used for another lM0. The problem is that you will have residual template plasmids during your transformation instead of the new construct. Instead you can use a lM1 for template as it require another antibiotic selection! ⚠️⚠️⚠️

LEVEL 0

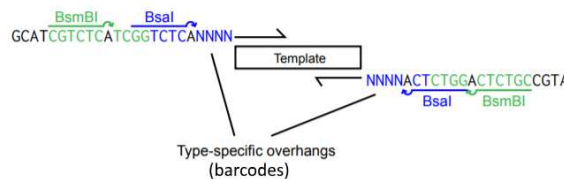
Add a new sequence to the MoClo: Construction of "Part Plasmids" (or "level 0")

The goal is to insert your sequence+overhangs into the "Part Plasmid Entry Vector" (pYTK001)

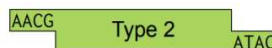
Check if there is BsmBI (CGTCTC) or BsaI (GGTCTC) site in your SOI (see below)

1. Design the primers

- You have to add overhang to your Sequence Of Interest (SOI or template). The overhang should contain: BsmBI site, BsaI site, a barcode and **possibly** start/stop codon or CC linker.

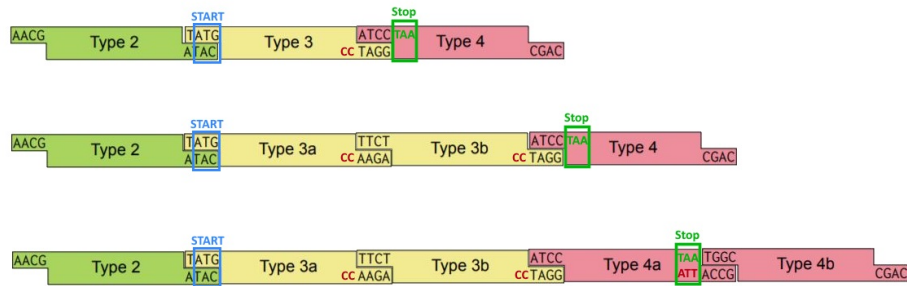


The barcode should correspond to the "Type" of your SOI. For exemple if your SOI is a promoter, you should add AACG and ATAC.



- If your SOI is a coding sequence, you should do type 3, 3a, 3b and 4a !!!
Your SOI should not have neither a Start codon nor a Stop codon; and you should add CC just before the barcode (link for fusion proteins)
Except for the 4a: you have to add a Stop codon at the end: ATT-ACCG
- If your SOI is a terminator, you should do type 4 and 4b !!!
4: You have to add a Stop codon at the beginning: ATCC-TAA
4b: Don't add a stop codon

⚠️ You have to be careful to add or remove start/stop codon and GG linkers for some of them ⚠️



- Do PCR to amplify your fragment (Phusion Master Mix). (don't use template lvl0 !)
Check out PCR protocol "repair fragment" in [CRISPR for Yeast](#)
- Purify PCR product with Wizard kit (not sure if necessary but very probable that it is)
If you are worried that you will have not enough DNA, recover in 30µL H2O instead of 50µL
- Insert your sequence+overhangs into the "Part Plasmid Entry Vector"
Perform a BsmBI Golden Gate reaction with the entry vector and your PCR product (sequence+overhangs)
- Transformation - amplification
This step select only good plasmid and produce a good amount of your "Part Plasmids"
Transform the "Part Plasmid" in bacteria (DH5 or home-made ones works), you can then select for **chloramphenicol** antibiotic and/or **anti-green** expression. Typically I transform 10µL of plasmid (see [Yeast Transformation CRISPR](#))
- [Miniprep \(NucleoSpin\)](#) & sequencing (oPH_331 and oPH_332)

To pick anti-green colonies: use blue led + green filter paper

LEVEL 1

Create an assembly (typically one gene) (or "level 1")

IMPORTANT: there are two ways to get lvl 1: either you use a pre-built vector (eg.pYKT110 or you can make your own with the lvl0 pYTK47) and you will select for anti-GFP; either you build your lvl 1 plasmid using only lvl0 plasmid and will select for anti-RFP.

The goal is to assemble all the part you need to get the synthetic gene.

Typically you will assemble in order: promoter, coding sequence, terminator.

If you have done correctly the first step (Construction of "Part Plasmids"), each "part plasmid" will have the correct barcode.

If you want to use this individual cassette in a multi-gene assembly(lvl2), you as to design first the all multi-gene assembly to choose the right connectors. If not just take **ConLS and ConR1**.

Perform a **Bsal Golden Gate** assembly with the following "part plasmids":

- An assembly connector Left (ConL)
- A promoter
- A coding sequence
- A terminator

- An assembly connector Right (ConR)
- Part type 6 (by default let's say LEU)
- Part type 7 (pYTK082)
- Part type 8 for Bacteria selection (let's say Amp as default: pYTK083 or pYTK089)

Transform the GoldenGate product in bacteria (DH5 or home-made ones works), you can then select for **Ampicilin** antibiotic and/or **anti-red** expression. Typically I transform 10µL of plasmid (see [Yeast Transformation CRISPR](#))

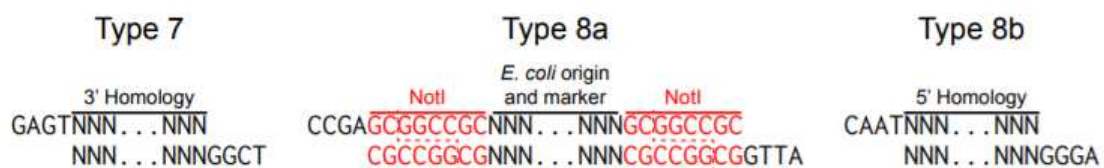
Miniprep&sequencing with oPH_335 and oPH_336

To pick anti-rfp colonies: use green led + red filter paper

- Create a multi-gene assemble (or "level 2")
You should have all your "level 1" assembly, with a good succession of connectors. (The first cassette must contain the ConLS part, and the last cassette must contain the ConRE part)
- Remove a BsmBI (CGTCTC) or Bsal (GGTCTC) site in your SOI
You can remove the restriction site at the same time as inserting your SOI in the lv10 plasmid. To do so, you need to do two different PCR of your SOI, one before the restriction site and one after. The 2 primers used close to the restriction site should be design with only a BsmBI site, with a user-defined barcode which will replace the restriction site to remove (mutate one nucleotide with a silent mutation), so that the two PCR will assemble during the GoldenGate reaction .

Genomic integration:

- Using PCR (best and easiest method for CRISPR)
 - For CRISPR:
Use your plasmid to PCR the fragment of interest + overhangs with homology to the locus to target.
Typically you can use oPH524&525 to PCR anything between **ConLS** and **ConR1** for HO loci integration
In this case, use pML104 plasmide expressing the gRNA targeting HO = pPH_162
 - For Selection marker (homologous recombination)
Use your plasmid to PCR the fragment of interest (including the Type 6 selection marker) + overhangs with homology to the locus to target.
If this PCR is too long or fail (notably for lv12), use the restriction enzyme NotI below
- Using restriction enzyme NotI (not convenient because one plasmid only target one locus)
If you have a NotI restriction site in your construct, you have to do a PCR as repair fragment, otherwise:
You just have to choose 2 part for locus homology, ex:
 - 7 URA3 3' Homology (pYTK086)
 - 8b URA3 5' Homology (pYTK092)
 Between them : 8a AmpR-CoIE1 (pYTK089). This will be use as selection in bacteria AND to cut your plasmide (NotI restriction site) before transformation in yeast



You can do 2 types au genome integration:

- Selection marker (homologous recombination)

You will choose a "classic" type 6, ex:

- 6 URA3 (pYTK074)
- CRISPR

You have to choose a "silent" type 6 (YTK108)

Golden Gate Assembly protocol optimization

NEB conference for SynBioBeta: they tested a lot of conditions and give their results:

- Use these overhangs (if you need to design new ones):

Just tell us what overhangs to use!

30 overhangs for use with T4 DNA Ligase and BsaI or BsmBI
(predicted ~90% fidelity, excludes low-efficiency pairs)

AAAC, AACA, AAGA, AAGT, AATG, ACAC, ACGA, AGAA, AGCC, AGGG,
AGTA, ATAG, ATCA, ATGA, ATTG, CAAA, CACG, CAGA, CCAG, CCTA, CGAA,
CGGC, CTCC, CTTA, GAGC, GATA, GCAA, GGGA, GTAA, TCCA

Any subset of the above should work as well!

BioLabs

You can test overhang crosstalk : <https://ggtools.neb.com/viewset/run.cgi>

You can generate a good set : <https://ggtools.neb.com/getset/run.cgi>


- Use the T4 DNA Ligase, it's much more reliable !!! (the T7 is good for some overhang but not for others)

8.9.3 CRISPR for *S. cerevisiae*

Based on [Laughery et al. 2015](#)

1. In silico design


1.0 Get things ready

- Get onto  [Geneious](#)
- ▼ Get initial genomic state of the region of interest and annotate it.
 - can be raw from yeast database:

Saccharomyces Genome Database | SGD

The Saccharomyces Genome Database (SGD) provides comprehensive integrated biological information for the budding yeast *Saccharomyces cerevisiae*.

 <https://www.yeastgenome.org/>



Find gene/area and generally download "Genomic DNA +/- 1kb".

- can be from previous construction according to the strain and loci.

1.1 CRISPR design

- ▼ Decide where to CUT
 - On geneious, use the "Find CRISPR Sites" in the "Cloning" toggle at the TOP of the window.
 - Choose the best one (best "Doench activity score")
 - Annotate the PAM sequence and the CRISPR site
 - Name the file "myregion_CRISPR"
- ▼ Design Oligos to produce the guideRNA
 - Get to:

CRISPR Toolset

Click here to identify guide RNA target sites in a user specified yeast gene

<http://wyrickbioinfo2.smb.wsu.edu/crispr.html>

Mutation Target

```
Rm1 protein: T T I E L D N L A A E T C A Y M T...
gDNA: 5'...aca aca atc gaa cta gaa aac tta gCG GCT GAA ACA TGC GCT TAT ATG act... 3'
                                     PAM = guide target
                                     (on opposite strand)
rm1 D57N protein: T T I E L N N L A A E T C A Y M T...
Template: 5'...aca aca atc gaa cta Aac aac tta gCG GCT GAA ACA TGC GCT TAT ATG act... 3'
```

Mutations in **Blue**

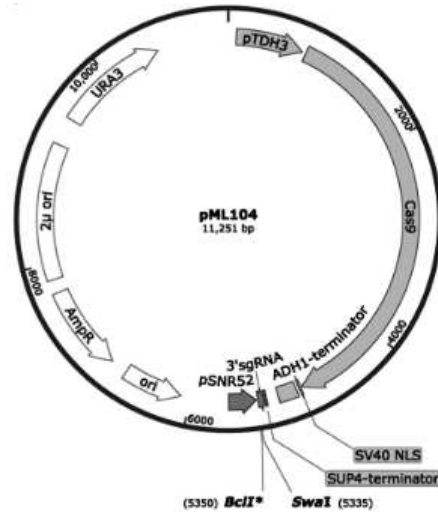
Mutant Oligonucleotide Template:

0AH108
#BfctctgpaaggtgtcacaacatgpaactaAagaaattagCGGCTGAAGATGCCCTTATATGactactgttcacagattagcc

- Chose to design [user-designed guide RNA sequences](#) (3rd choice)
- Enter guide RNA sequences INCLUDING PAM and submit
- /\ If your guide is reverse, still **always give a Forward** sequence to the website : use the revert complement, that is, always give a sequence ending with the NGG PAM.
- You now have the two oligos to build the guideRNA and insert the sequence into the pML104 plasmid. Oligo lengths are 37 and 33 (for oligo 1 and 2 respectively)

▼ *More details*

- The oligos are built in a way such that they overlap to create a double-stranded DNA strand that will insert in the *BclI* and *SwaI* restriction sites upon digestion/ligation etc. into the plasmid below that also contains the Cas9 protein.



1.2 Final sequence

Draw the final sequence expected in the genome.

- Copy the previous "_CRISPR" file and copy/cut/paste various DNA sequences!

▼ **Get rid of the CRISPR PAM site !** (avoiding Cas9 cut in your final construct)

Either:

- Delete the whole sequence
- Turn NGG into NCG or other (if in coding sequence, find a synonym mutation with similar frequency: <https://www.kazusa.or.jp/codon/cgi-bin/showcodon.cgi?species=4932>)

▼ Add **linker** for fusion protein if needed

- remove previous stop codon
- remove subsequent start codon

▼ *More details*

These modifications will be introduced in the repair strand

1.3 Repair strand design

From another plasmid or genomic DNA sequence, oligos need to be designed in such a way that primers overhangs will correspond to genomic regions for homologous recombination (~70bp) while ~20bp correspond to the region to amplify from a plasmid containing the part to insert into the genome (à revoir).

- Copy the _Final file and create the _Repair file

▼ Design the **90bp oligos**

- Start with G for better hybridization
- Make sure the forward and reverse seqs make sense because geneious revcom options can be a bit tricky if not careful.

1.4 Primers for further verification

After transformation etc. we will check if the inserted sequence is correct:

▼ Design 20bp primers

- 150bp away from what we really want
- Expect 800nt sequenced for 1 primer
- Start with G for better hybridization
- Make sure the forward and reverse seqs make sense because geneious revcom options can be a bit tricky if not careful
- Check 9 to 14 CGs out of the 20bp

1.5 Order oligos

▼ Get onto [IDTDNA](https://www.idtdna.com)

Integrated DNA Technologies - Home

Integrated DNA Technologies, Inc. (IDT) is your Advocate for the Genomics Age, providing innovative tools and solutions for genomics applications

 <https://www.idtdna.com/pages>



- paste the info in the table format using an excel sheet as intermediary

2. At the bench

2.0 Get things ready

▼ Prepare oligos

- Generally received 2 days after ordering
- Get ultrapure distilled water stock (15mL)

▼ Dilute to 100uM

[Resuspension of Oligonucleotides](#)

- Spin down (coz some lyophilized DNA might be on the lid)
- Add the right amount of water:
 - If written 29.5 nmol on the tube: add 295 μ L.
 - If written 65 nmol on the tube: add 650 μ L.
- Shake shake shake it up
- Spin down
- Write number on lid
- Stock in the -20 in common oligonucleotides database (red boxes)
- Can make your own 10uM fyawanna

2.1 Build guide-containing plasmid

▼ pML104 Maxiprep - *if needed*

- Grow pML104 (glycerol stock bPH_140) O/N

Note: pML104 must be grown in a dam- cell type for the subsequent steps to work.

▼ pML104 Digestion - *if needed*

Warning: it is recommended to do a big pool of digested pML104 for the common stock. Typically, do 16 individual 1µg in 50 µL reactions in PCR microtubes (2 strips of 8 PCR tubes) and combine them together before PCR cleanup step. Prepare a master mix with 16 µg of pML104 in 800 µL reaction volume and then do 50 µL aliquots in microtubes.

- For a 50 µL reaction volume:
 - 1 µg pML104
 - 1 µL BclI
 - 1 µL SwaI
 - 5 µL Buffer 3.1 (NEB)
 - Top up with dH2O
- Digest at 25C for ~6 hours and then 50C for ~6 hours.
- Add 1 µL rSAP and incubate at 37C for 1 hour.

▼ Use PCR clean-up (Nucleospin).

pool 4 digestion tubes together and put each 200 µL on a purification column. In total: 4 columns with 200 µL/column. For each column, resuspend DNA after purification in 50 µL ultrapure water (expected concentration after elution = 30-60 ng/µL)

- Use Nanodrop to get concentration (optional: check to digestion on a gel, with non digested plasmid as a control)
- !\ Might be already digested plasmid stock somewhere!

▼ gRNA hybridization

- Better start at ~3pm for O/N ligation
- Get the 33 and 37bp oligos designed online (*100µM stock fridge-20 drawer n°2 or make stock from powder*)
- **For a 10µL reaction volume in PCR tubes:**
 - 6.5 µL dH2O (*commercial*)
 - 1.0 µL first oligo (100µM stock)
 - 1.0 µL second oligo (100µM stock)
 - 1.0 µL 10X (NEB) T4 **Ligase** Buffer (*fridge-20 drawer n°3*)
 - 0.5 µL T4 **PNK** (*fridge-20 drawer n°3*)

- Yes this is: Ligase buffer and PNK, this has been optimized
- T4 PNK adds a 5' phosphate to the oligos

▼ Incubate at 37C for 30 minutes, 95C for 5 minutes, then decrease 1C every minute to 25C (~1h45). (*"HYBRIDIZ" program on PCR machine*)

- Use the programme HYBRIDIZ in Fabien's saved programs
- On the PCR machine, make sure 4 empty tubes are at the corners for homogeneous balance thing, with the same caps as your tubes.

▼ Ligation

Here the guide is inserted into the plasmid:

- **For a 25 µL reaction volume in PCR tubes:**
 - 100 ng of digested pML104 vector (*possible stock in fridge-20*)

- 2.0 µL of 1/20 diluted hybridized gRNA (add 190µL H₂O in previous PCR tubes)
- 2.5 µL 10X T4 ligase Buffer (NEB) (*fridge-20 drawer n°3*)
- 1.0 µL T4 ligase (Invitrogen) (*fridge-20 drawer n°3*)
- Top up with dH₂O (*commercial*)
- Incubate overnight at 16C followed by a 10 minutes at 65C. ("*LIGAT-CRISPR*" program on PCR machine ~16h)

▼ Transformation in Bacteria

- First thing in the mornin', - and + controls plz.
- ▼ Get a 50 µL DH5alpha stock (*fridge -80C*) - keep on ice
 - + control: 500pg plasmid pUC (*standard plasmid with high transformation yield, fridge -20C drawer n°3*)
 - - control: no plasmid
 - THEREFORE GET 3 TUBES (if you do more, you can take 5 DH5alpha tubes for 6 transformations because they contain a bit more than 50µL)
- Gently mix cells with pipette tip and aliquot 50µL in 1,7mL tubes **on ice**
- Add 2-10 µL of ligation product - do not pipet up&down but mix with the pipette
- Keep on ice 30 min
- Heat Shock: 20 seconds at 42°C (*bain-marie or hot tube holder*)
- Place back on ice for 2 min
- Under PSM or burner:
- Add 250 µL of SOC (*fridge 4°C*), incubate for 1 hour at 37°C (225 RPM, maybe more ?) - *prepare two LB plate per transformation (at RT)*
- Plate 150 µL on LB+Amp using glass balls
- ▼ Grow O/N at 37°C

Parafilm your plate and put them in the incubator upside down
- The next day: put them in the fridge 4°C
- ▼ Expected results
 - Relatively few transformants (about 10) but no false positives.
 - The negative control is helpful to checking that the Amp plates are still effective. If all is well, there should be ZERO colonies on the negative control.
 - The positive control should produce thousands of transformants if all is well. If fewer than thousands of colonies appear on the pUC plate, the cells may have poor viability.

▼ PCR screen insert - *if needed*

In order to eliminate any transformed uncut WT plasmid from being used.

- Colony PCR: Take only part of colony so that there is more to glycerol stock later (and note which colony you have chosen).
- Screen 2-8 colonies per transformation using primer oPH_0032 (in the backbone of the plasmid) and one of the gRNA primers (check to make sure it's the correct direction, should be the primer with the overhang, total of 37 bp in length). It is an important negative control to also perform a PCR on pML104 (other gRNAs are not adequate controls because all have the primer sequence in common).

▼ Miniprep good colonies

- Grow 2-4 positive colonies for 12-16 hours in 5 ml LB + 5 ul 100mg/ml Ampicillin.

Use  [Miniprep \(NucleoSpin\)](#) kit (elute in ~30 ul).

- ▼ Use  [NANODROP](#) to get concentration.

Should be in the range of ~250 ng/uL. Anything below ~100 ng/ul is likely to fail

▼ Check Plasmid

- Sequence miniprep using primer oPH_0032 to confirm correct gRNA insertion
- After sequences are back confirming correct insertion, prepare a glycerol stock.

2.2 Prepare Repair fragment

▼ PCR protocol

PCR mix (per 50 µL reaction): **on ice**

- 25 µL Phusion 2x Master Mix (*fridge -20°C drawer n°3*) - contains the taq etc.
- 1 µL Primer Fwd 10 µM (*dilute the stock solution by 1/10, you can keep the diluted solution at -20°C*)
- 1 µL Primer Rev 10 µM (*dilute the stock solution by 1/10, you can keep the diluted solution at -20°C*)
- 1.5 µL DMSO (*fridge -20°C drawer n°3*)
- 16.5 µL dH2O (*commercial*)
- 5 µL DNA template (20 ng/µL plasmid or just water if primers are the template)

Thermocycler protocol:

1. 98°C for 2 min
2. 98°C for 20 sec
3. 55°C for 20 sec
4. 72°C for 30 sec (adapt this time depending on your oligo length)
5. Repeat 2-4 34 times
6. 72°C for 10 min
7. 10°C forever

After PCR, run 5 µL of each sample on 1% Agarose gel with SybrSafe and take a picture under UV lamp.

2.3 Transformation in Yeast

[Yeast Transformation CRISPR](#)

You will end up with ~8 yeast patches per transformation.

2.4 Verify colonies by sequencing

[Yeast colony PCR screening](#)

Purify 2-3 successful PCR sample per transformation, send them to sequencing

[How to sequence DNA samples](#)

2.5 Remove pML104

Patch the good clones onto 5FOA plates. 30°C for 2 days.

⚠️ If you intend to keep your clones for more than 1 week, patch them back to YPD (or YPG).

2.6 Add glycerol stock to yeast collection

8.9.4 *S. cerevisiae* LiAc transformation

Materials & Equipment

- ▼ PEG 3350 50% (Sigma Aldrich/ref: 20244-250G)
 - 25g for 50mL
 - 25g + 20 mL distilled water in beaker w/ magnetic bar
 - put on heating plate (50C) for around 45min under agitation
 - measure volume w/ pipet and add water up to 50mL
 - Filter using 0.45um filter (too viscous for 0.2um)
- ▼ LiAc 1M (Sigma Aldrich/ref: L4158-250G)
 - 5.1g in 50mL dH₂O
 - filter 0.2 um
- ▼ LiAc 0.1M
 - 5mL of 1M solution + 45mL dH₂O
- ▼ Salmon Sperm DNA at 2 mg/mL (Sigma Aldrich/ref: D9156-5ML)
 - aliquots stored at -20°C
 - YPD medium (liquid) (MP Biomedicals™ 114001032)
 - sterile distilled water
 - plasmid to be transformed
 - (repair strand)

 - Water bath 42°C
 - Incubator 30°C

Protocol

1. **grow strain o/n** at 30C in at least 2mL YPD
2. **grow for 4 hours** in the morning: 100-200uL of cells in 5mL YPD: (to get $\sim 10^7$ cells/mL)
 - Check water bath at 42°C
 - Check Salmon Sperm DNA was boiled (10 min at 99°C in PCR machine)
 - Check all solutions are at Room Temperature (including water)
 - Check plasmid volume for transformation (for 500 ng to 1 µg)
3. **Clean cells:** water, water, LiAc 0.1 M
 - Big centrifuge in the lab at the entrance for culture tubes:
 - 3 000 rpm x 7min at RT**
 - Empty supernatant
 - Add **950uL dH₂O** (yeasts are strong, they can sustain that)

- resuspend w/ ups and downs w/ the pipette
- transfer in an **ependorf tube**
- centrifuge 11 000 rpm x 1min (smaller centri)
 - remove supernatent w/ pipet
 - wash again with **950uL dH2O** (resuspend)
- centrifuge 11 000 rpm x 1min
 - remove sup
 - wash with **950uL LiAc 0.1M**
- centrifuge 11 000 rpm x 1min
 - remove sup

4. **Add to clean pellet** (watch out for the order:)

- 240 uL PEG 50% (slowly pipet)
- 36 uL LiAc 1M
- 50 uL boiled Salmon Sperm DNA (2mg/mL)
- 32 uL repair fragment
- 2 uL plasmid at ~ 300-500 ng/uL

▼ **Note : no more than 6min for all those steps**

Otherwise PEG is going to damage the cells → Set pipets to rights volumes before

5. **VORTEX** the tubes

6. **Incubate** at **30°C** x 30min

in the classic big incubator

7. **Incubate** at **42°C** x 30min

in the water bath that was preheated at least one hour before)

8. **Clean** with dH2O, resuspend in 110uL dH2O

to remove transformation reactants.

- centrifuge 11 000 rpm x 1min
- discard supernatant **with P1000**
- resuspend pellet with 1mL dH2O: gently pipet up and down, this resuspension will be a bit longer than before (you can do it in 2 steps).
- centrifuge again 11 000 rpm x 1min
- discard supernatent
- resuspend in 110 uL dH2O

9. **Plate on SC-URA** petri dishes and grow for > 2 days

2 petri dishes per transformation :

- 100 uL on the first one
- transfer 10 uL in 90uL dH2O to dilute the cells and plate on the second one.

10. **Streak colonies** on new SC-URA plates (**18 streaks per transformation**), grow for > 2 days

After the transfo, big colonies are typically the good ones to select for streaking

- Under PSM or burner: Patch on YPG (**8 patches per transformation**), grow for > 2 days

11. **PCR and sequence** 2-4 clones

check 🧪 [How to sequence DNA samples](#)

12. **Remove pML104:**

- Replicate YPG patch on 5-FOA
- Freeze positive strains

8.9.5 Beta-carotene quantification

Based on [Reyes Kao 2018 - Growth-Coupled Carotenoids Production Using Adaptive Laboratory Evolution](#):
Dodecane extraction and absorption using plate-reader.

- 3 mL of YPD was inoculated with cells from frozen stocks: incubated at 30 °C for 72 h
- Cell density was determined using spectrophotometry (OD₆₀₀).
- 1 mL of culture were transferred to a 2 mL collection tube: centrifugation at 12,000 rpm for 2 min (remove supernatant)
- Add 250 µL of 425–600 µm acid-washed glass beads (Sigma) and 1 mL of dodecane.
- Lyse cells: Disruptor Genie Cell Disruptor (Scientific Industries) → 5 x 1min
- Cell debris and glass beads were separated from the supernatant by centrifugation at 15,000 rpm for 2 min (If pelleted cells remain pigmented, this indicates that extraction was not complete; therefore, the disruption time should be increased.)
- transfer 200 µL of the supernatant to a Corning 96 well black-wall clear-bottom plate for quantification
- Survey scan from OD₃₅₀ to OD₅₅₀ (TECAN Infinites M200)
- The relative total carotenoids production was determined by calculating the area under the curve of the survey scan, using the parental strain as reference
- β-carotene quantification was determined by the absorption at OD₄₅₄ (Verwaal et al., 2007) → The maximum absorbance of β-carotene occurs at 454 nm
- A **standard curve** for β-carotene quantification was generated using commercially available β-carotene (Enzo Life Sciences) at OD₄₅₄.

8.9.6 OptoBox

The LPA or Optobox is a device that can perform light activation experiments on 24-well plate. You can have maximum 2 different LEDs per well (top and bottom).

You can not go below 1s of time resolution.

Original data:

- Paper: <https://www.nature.com/articles/srep35363>
- Github: <https://github.com/taborlab/LPA-hardware>
- Online software: <http://taborlab.github.io/Iris/>

To convert the input in irradiance (exemple): $4000 \times 0,0007 = 2,8\text{mW/cm}^2$

LAUNCHING AN EXPERIMENT

Go to <http://taborlab.github.io/Iris/>

Iris then generates a zip file containing i) a device-readable binary file (.lpf) used to run the LPA, ii) a session file for reloading a program into Iris at a later time, and iii) a CSV file containing user-readable well randomization information.

The .lpf is then transferred to an SD card, which is inserted into the LPA (Optobox), and the Reset Button is pressed to run the light program.

BUILD AND SETUP THE OPTOBOX

How to build and set up the Optobox (more details are in the original publication)

- 3D printed parts can be found in the original publication.
- Place all the LED sockets in the "LEDSpacer" 3D printed part
- Solder the LED sockets to the board
- 5V should be used every time.

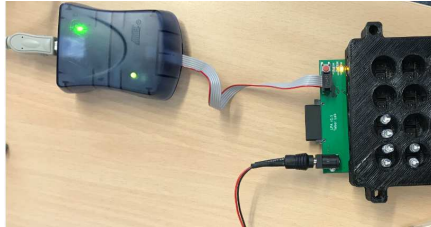
Programming the board:

You need a "AVR microcontroller programmer". We use a "AVRISP mkII programmer"

You have two options to flash the board: use the precompiled file (.elf) or compile your own file (you will have to do it to calibrate the clock of the microcontroller but its optional)

- ▼ Compile your own file (optional, you can use the precompiled version)
 - Use an old Arduino IDE: 1.6.0 works !!!
- ▼ Flash the board

1. Install Atmel Studio (if not already done) (now it's called "**Microchip Studio**")
<https://www.microchip.com/en-us/development-tools-tools-and-software/microchip-studio-for-avr-and-sam-devices#Downloads>
2. Connect your programmer to your computer and the Optobox board. Power the Optobox too.



3. On Atmel Studio, go to Tools -> Device Programming. Select "AVRISP mkII" under "programmer", select "ATmega328" under "Device" and "ISP" under "Interface". Click on the "Apply"
4. Click on the "Read" button, the "Device signature" box should be filled, the "Target voltage" should be 3.3V.
5. If it's the first time the new device is programmed: select "Fuses" from the list. Disable CKDIV8, enable CKOUT, set SUT_CKSEL box to EXTOSC_8MHZ_XX_1KCK_14CK_65MS. Click on the "Program". Fuse warning window is ok, click on "continue"
6. Select "Production file" from the list, click on the "..." button, locate your file "firmware.elf".
7. Activate "Flash", "Erase memory before programming", and "Verify programmed content" checkboxes, and click on the "Program" button.
8. The messages "Erasing device... OK", "Programming Flash...OK", and "Verifying Flash...OK" should appear below.
If not: just try a second time to click on "Program" and/or on "Verify"

We had this error message: "Verifying Flash...Failed! address=0x0000 expected=0x0c actual=0x00" but we just clicked on "Program" a second time and it worked.

Calibrating LEDs

LED compensation is achieved by setting the grayscale and dot correction for each LED. Grayscale and dot correction values are stored on the device's SD card as files "gcal.txt" and "dc.txt", respectively, and must be space delimited integers from 0-255 and 0-63, respectively. Coarse adjustments can be made by setting the LED dot correction (useful during calibration to set ALL LEDs to the range of the spectrometer) , while fine adjustments can be made setting the gray scale value (use to calibrate each LED independently).

There are different methods:

Image analysis method or Probe spectrometer method.

At the end you will need to measure the photon flux with the Probe spectrometer for both.

Or we can use a power meter.

For simplicity we use the ThorLabs power meter + S120C sensor

You should use a 3D printed adaptor to make the sensor alignment more reproducible

The basic idea is to trace irradiance=f(LED input) for each LED and get the rate. Then we will modify the dcal.txt depending on the rate of each LED. The following procedure is semi-automated in order to go faster.

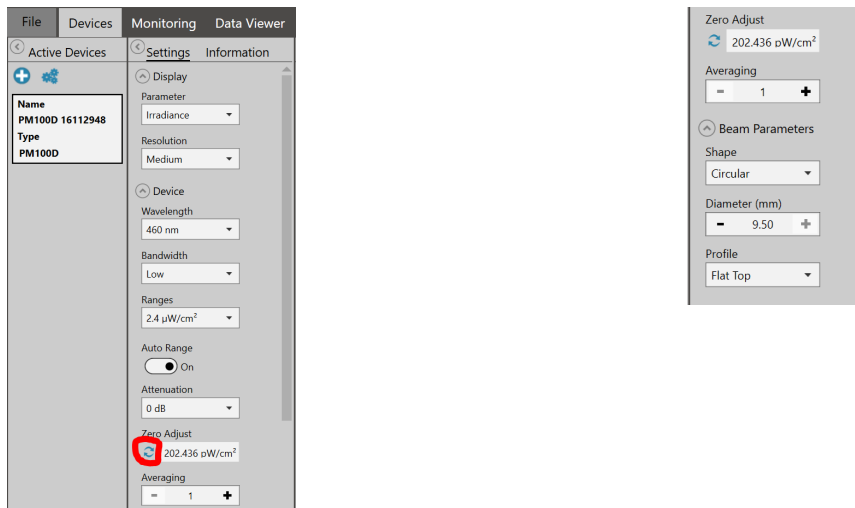
To do so you need to create a protocol in the iris software so all the top LEDs increase in intensity every seconde in the following order: 10,50,100,300,600,1000,2000,3000,4000 (you will do the same for the bottom LEDs independently)

Load your optobox with the file

Power meter parameters:

- Install Thorlabs software : https://www.thorlabs.com/software_pages/ViewSoftwarePage.cfm?Code=OPM
- Plug the S120C sensor in the PM100D, and plug the PM100D to your computer.
- Close the sensor and set the zero, and use the following parameters:

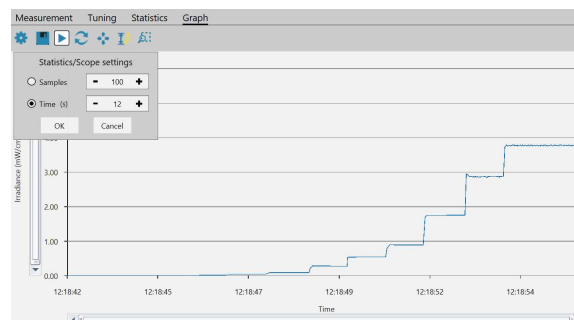
Parameters:



On the software

In Device, go to Graph

set 12s (gear icon):



Put the sensor in the adaptor

Push the reset button on the optobox, 1 sec later reset the Graph measurement

After 12 sec stop the measure (make sure to have a similar profil see above) and save with the name of the LED, ex: "TA5" top A5, "BD6" bottom D6

→ Play with play, pause (when the graph is in the frame), save, reset on optobox, play, pause, save, reset etc.

When you have done every LED (24 top then 24 bottom):

Python script to be downloaded.

If the script does not work, try to modify the range function according to the lowest column number in your excel files. Furthermore, if the matrix does not fit, you should increase the range because you are missing values. Remember to modify it for the bottom analysing code too. CHECK IF YOUR .CSV ARE SAVED IN mW and not in μ W

Run the python script in the same folder as your 48 files, it will automatically create a newgcal.txt file.

In the script, you should typically find a rate (slopes) of ~ 0.0009 . Some LED should be over or under this value. We calibrated each LED to get a final rate of 0.0007. To do so we simply did $(0.0007 \times 255) / (\text{rate calculated by script}) = \text{new value of grayscale}$ entered in the new gcal.txt file.

You should get $\sim 2.1\text{mW}$ at 4000

Detector diameter=0.95cm || Area = 0.71cm²

Figure to help you:

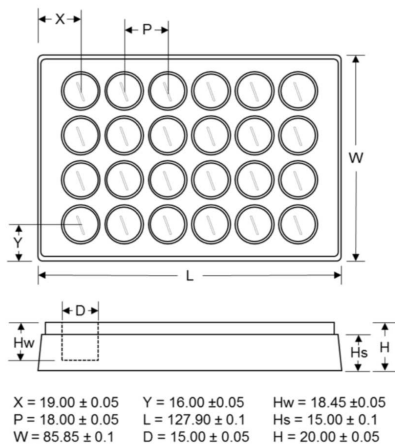
Fichier	Edition	Format	Affichage ?										
255	255	255	255	255	255	255	255	255	255	255	255	255	A
255	255	255	255	255	255	255	255	255	255	255	255	255	B
255	255	255	255	255	255	255	255	255	255	255	255	255	C
255	255	255	255	255	255	255	255	255	255	255	255	255	D
TOP	Bottom	TOP	Bottom	TOP	Bottom	TOP	Bottom	TOP	Bottom	TOP	Bottom	TOP	Bottom
1		2		3		4		5		6			

Time calibration

(We checked two optoboxes for $\sim 20\text{h}$ and the time was already calibrated)

WELL-PLATES

- The sup data of the optobox paper recommends the 24-well culture plate (AWLS-303008, ArcticWhite LLC). But they're shipped from the US, expensive and too much shipping fees.
- We are using eppendorf plates, but they stopped to produce this model. (Plastic film bottom instead of a coverglass bottom)



ORIGINAL PAPER PLATES DIMENSIONS

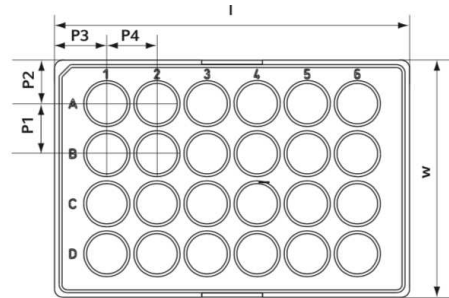


Plate dimensions [mm]							
Length		Width		Height			
i	i1	w	w1	h	h1	fh	
127.8	124.2	85.5	82.0	15.0	0.4	9.3	
Well dimensions [mm]				Positions of well center [mm]			
Diameter		Thickness		Depth			
d	d1	bt	h2	P1	P2	P3	P4
14.5	13.2	Glass: 0.17 Foil: 0.025	14.6	18.0	15.7	18.9	18.0

EPPENDORF DIMINTIONS

8.9.7 OptoTubes

To program the OptoTubes:

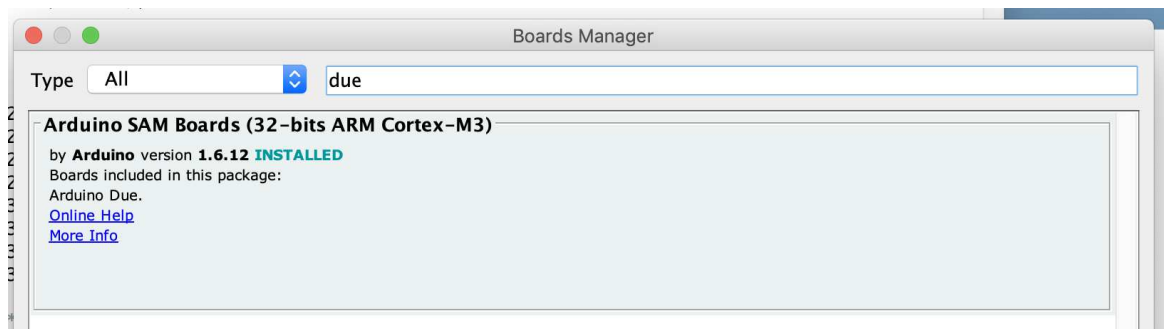
- Install Arduino IDE

On ubuntu: `sudo apt-get install arduino`

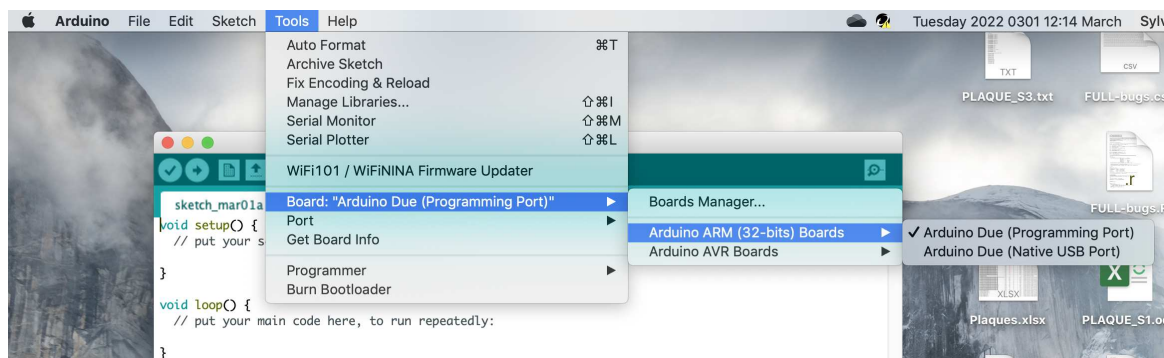
On windows: go online

- Update from Board Manager to have access to the arduino DUE programming

In the Arduino IDE, you need to add the right board from the board settings (search for "due")



- Select the Board



- Select you arduino from the right port COM

Tools > Port > ...

- Write your **PROGRAM**

TO program; upload such a code in the Arduino DUE:

```
void setup() {
  pinMode(LED_BUILTIN, OUTPUT);
}

void loop() {
  analogWrite(2, 255);
  analogWrite(3, 200);
  analogWrite(4, 150);
  analogWrite(5, 100);
  analogWrite(6, 50);
  analogWrite(7, 30);
  analogWrite(8, 20);
  analogWrite(9, 0);
}
```


- Si avec OptoTubes BIS

```

/* Arduino due */

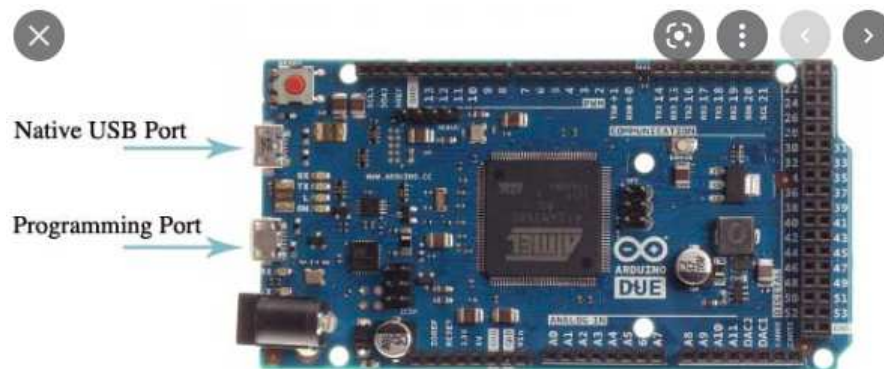
void setup() {
  pinMode(LED_BUILTIN, OUTPUT);
}

void loop() {
  /*OptoTubes*/
  analogWrite(2, 255);
  analogWrite(3, 200);
  analogWrite(4, 150);
  analogWrite(5, 100);
  analogWrite(6, 50);
  analogWrite(7, 30);
  analogWrite(8, 20);
  analogWrite(9, 10);

  /*OptoTubes.BIS*/
  analogWrite(10, 0); /*2*/
  analogWrite(11, 0); /*3*/
  analogWrite(12, 0); /*4*/
  analogWrite(13, 0); /*5*/
}

```

- Connect to the arduino due and televise
 - You might need to choose the right "port" to select your card.
 - Use the programming port if this is what was selected:



- Troubleshoot
 - not the right board selected
 - not the right port selected
 - not the right port connected to (physically)
 - cable problem (that happened to me, I could only do it with the cable de Rémy)

8.9.8 eVOLVER - List of components

Exhaustive list for one eVOLVER unit

Aa Name	Part	Company	Reference	Quantity	Price for one evolver	Available	Order some more	Link
Fan	Bioreactor	Digikey	Q619-ND	1	6.61	0	5	https://www.digikey.com/products/en?keywords=562-FAD1-04020CBHW11
Magnets	Bioreactor	Conrad	-	2	0.948	10 (5)	1	https://www.conrad.fr/p/aimant-permanent-velleman-magnet5-cylindrique-ndfeb-1-pc-081876
0.5 Plexiglas x2	Bioreactor	Lab	-	2	1	10 (5)	-	-
3D printed holder	Bioreactor	Lab	-	1	1	0	9	-
Vial board	Bioreactor	EUROCIRCUITS	-	1	10.332	5	-	https://www.eurocircuits.com
Heaters	Bioreactor	mouser	684-MP915-20	2	7.08	4 (2)	6	https://www.mouser.fr/ProductDetail/Caddock/MP915-200-12?qs=sGAEpiMZZMv61gTfUdNhG5iIVFqxD0i9nuVXsNbiqHw=
Thermistor	Bioreactor	mouser	954-103JT-025	1	1.13	0	10	https://www.mouser.fr/ProductDetail/Semitec/103JT-025?qs=wgQ0AD00p1vsYGIEnr
IR Led	Bioreactor	mouser	720-SFH4845	1	2.71	3	5	https://www.mouser.fr/ProductDetail/OSRAM-Opto-Semiconductors/SFH-4845?qs=sGAEpiMZZMvzy9EAOJZmOwseFBUJQvtn0GHISPBqgZ4%3D
39 Ohm resistor	Bioreactor	Conrad	084518	1	0.017	x	-	https://www.conrad.fr/p/jeu-de-resistances-a-couche-carbone-velleman-kres-e12-ser-axiale-025-w-1-set-084518
IR PhotoDiode	Bioreactor	mouser	859-LTR-323DB	1	0.225	Inf	-	https://www.mouser.fr/ProductDetail/Lite-On/LTR-323DB?qs=%2Fha2pyFaduimxd%252bprCO8JlbfRqCq4z9wFRGxLeyb8Y%3D
Blue Led	Bioreactor						-	
82 Ohm resistor	Bioreactor	Conrad	084518	1	0.017	x	-	https://www.conrad.fr/p/jeu-de-resistances-a-couche-carbone-velleman-kres-e12-ser-axiale-025-w-1-set-084518
Photoresistor	Bioreactor	mouser	485-161	1	0.855	0	10	https://www.mouser.fr/ProductDetail/Adafruit/161?qs=%2Fha2pyFaduimj5aA3JbgCY8jNg1nTA8TP5shFLXnk%2FVxzTHlvQmTPSyZ1
7x2pins socket	Bioreactor	Digikey	S9170-ND	1	0.366	0	10	https://www.digikey.fr/product-detail/fr/sullins-connector-solutions/SBH11-PBPC-D07BK/S9170-ND/1990063
Jumper wires		Digikey	1528-1162-ND	1	1.765	3	2	https://www.digikey.fr/product-detail/fr/826/1528-1162-ND/5353622/?itemSeq=29124
Board (platine)	Controler	RS-online	897-1679	1	2.94	7	-	https://fr.rs-online.com/web/p/platines-dessai/8971679/
15pins fiche	Controler	Digikey	S7013-ND	4	3.52	10	40	https://www.digikey.fr/product-detail/fr/PPTC151LFBN-RC/S7013-ND/810153/?itemSeq=291892181
2pins fiche	Controler	Digikey	S7035-ND	5	1.45	1	50	https://www.digikey.fr/product-detail/fr/PPPC021LFBN-RC/S7035-ND/810174/?itemSeq=291892230
transistor MOSFET	Controler	RS-online	185-580	1	0.696	1	20	https://fr.rs-online.com/web/p/products/0185580/
1K2 Resistor	Controler	Conrad	084518	1	0.017	1	-	https://www.conrad.fr/p/jeu-de-resistances-a-couche-carbone-velleman-kres-e12-ser-axiale-025-w-1-set-084518
1M Resistor	Controler	Conrad	084518	1	0.017	1	-	https://www.conrad.fr/p/jeu-de-resistances-a-couche-carbone-velleman-kres-e12-ser-axiale-025-w-1-set-084518
10M Resistor (2).	Controler	mouser	603-HHV-50FR-52-10M	1	0.432			https://www.mouser.fr/ProductDetail/603-HHV-50FR-52-10M
10K Resistor	Controler	Conrad	084518	1	0.017	1	-	https://www.conrad.fr/p/jeu-de-resistances-a-couche-carbone-velleman-kres-e12-ser-axiale-025-w-1-set-084518
Arduino nano	Controler	Digikey	1050-1001-ND	1	19.64	2	3	https://www.digikey.fr/product-detail/fr/A000005/1050-1001-ND/2638989/?itemSeq=291241201
Arduino cable	Controler	Digikey	Q362-ND	1	1.79	2	4	https://www.digikey.fr/product-detail/fr/3021003-03/Q362-ND/1531289/?itemSeq=291240983
(Green Led + resistor)	Controler	Lab	-	1	0	5	-	-
(Yellow Led + resistor)	Controler	Lab	-	1	0	5	-	-
(Plexiglas plateform)		Lab	-	1	2	0	5	-
Aluminum Tube	Bioreactor	Weber-metaux	-	1	2	3	?	https://www.weber-metaux.com
Vial Glass tube	Bioreactor	Optimus	-	1	1.298	70	-	https://chemglass.com/sample-vials-only-clear-borosilicate
Vial Glass cap	Bioreactor	Optimus	-	1	1.693	70	-	https://chemglass.com/gpi-24-400-screw-thread-closures - pas exactement celui la
Stirring Magnet	Bioreactor	Fisher	11818862	1	1.43	10	-	https://www.fishersci.fr/shop/products/nfe-stir-bars-pivot-ring-16/11818862

Aa Name	Part	Company	Reference	Quantity	Price for one evolver	Available	Order some more	Link
Screws		Lab	-	2	0.02	Inf	-	-
Untitled								

Total cost of one unit: 75€. (17 units: 1275€)

▼ Commande du 201911081659 pour faire du stock pour anticiper des réparations éventuelles et potentiellement remplacer certains composants des eVOLVERS nuls

704	Sylvain	8/11/2019	TA.22	Aimant permanent Velleman MAGNET5 cylindrique NdFeB 1 pc(s)	81876 Conrad	1	4,740 €	4,74 €	
			TA.22	Jeu de résistances à couche carbone Velleman K/RES-E12 sortie axiale 0.25 W	84518 Conrad	1	10,320 €	10,32 €	
			TA.22	Frais de port de sa mère					9,95 €
705	Sylvain	8/11/2019	TA.22	MOSFET, Canal-N, 5 A 80 V PWR moulé 2, 3 broches	185-580	RS components	20	0,696 €	13,92 €
			TA.22	Carte de développement MCU Nemo 3.0	696-1667	RS components	2	18,030 €	36,06 €
706	Sylvain	8/11/2019	TA.22	Résistances à couche épaisse - Trou traversant 20 ohm 15W 1% TC-126 PKG PWR FILM	684-MP915-20	Mouser	10	3,150 €	31,50 €
			TA.22	Thermistances CTN 10kohm 1% Length: 25mm	954-103JT-025	Mouser	10	0,978 €	9,78 €
			TA.22	Émetteurs infrarouges Infrared 950nm	720-SFH4845	Mouser	5	2,710 €	13,55 €
			TA.22	Accessoires Adafruit Photo Cell CDS Photoresistor	485-161	Mouser	10	0,855 €	8,55 €
			TA.22	couche métallique - Trou traversant 1/2W 10M Ohm 1%	603-HHV-50FR-52-10M	Mouser	30	0,262 €	7,86 €
707	Sylvain	8/11/2019	TA.22	FAN AXIAL 40X20MM 12VDC WIRE	Q619-ND	Digikey	5	6,610 €	33,05 €
			TA.22	CONN HEADER VERT 14POS 2.54MM	S9170-ND	Digikey	10	0,378 €	3,78 €
			TA.22	JUMPER WIRE MIF 5.91" 1PC	1528-1162-ND	Digikey	3	3,950 €	11,85 €
			TA.22	CONN HDR 15POS 0.1 TIN PCB	S7013-ND	Digikey	20	0,881 €	17,22 €
			TA.22	CONN HDR 2POS 0.1 GOLD PCB	S7035-ND	Digikey	60	0,315 €	18,90 €
			TA.22	CBL USB A-MINI B CON 3' 28/28 AWG	Q362-ND	Digikey	4	2,000 €	8,00 €
			TA.22	RES 10M OHM 1/4W 1% AXIAL	MOX200F-10ME-ND	Digikey	2	2,640 €	5,28 €

Smart-sleeve components: All material

Aa Name	Part	Company	Reference	details	Quantity	Status	Link
Extra long 200 uL pipette tips	vials	(JUM) Fisher	2681420	There are the colibri ones in the lab and the ones in the blue boxes	1	received	https://www.fishersci.fr/shop/products/art-barri
Magnets	Sleeve	Conrad	081876	8x3mm pack:10	5	received	https://www.conrad.fr/p/aimant-permanent-vel
Stirring magnets	vials	Fisher	11587802	12x4,5mm pack:5 Weight=0.004kg		received	https://www.fishersci.fr/shop/products/ptfe-stir
Stirring magnets again (replacement product)	vials	Fisher	11818862	12x4,5mm pack:10 Weight=0.00752kg			https://www.fishersci.fr/shop/products/ptfe-stir
Laser Cut 1/4" Acrylic Base	Sleeve	CRI Lab	-	Plexiglass is fine	16 (20)	received	Part: made by Guillermo at the CRI
2 pieces of laser cut 1/8" Acrylic Fan Spacers	Sleeve	CRI Lab	-	Plexiglass is fine (Perspex)	16 (20)	received	- Made by Guillermo at the CRI
Heating Resistors	Sleeve	mouser	684-MP915-20		16 (20)	received	https://www.mouser.fr/ProductDetail/Caddock/gqs=sGAEPiMZZMu61gFTUdNhG5tVExqDO9r
5/64" Hex Key	Sleeve	Lab	-		1	-	-
2x Socket head screw	Sleeve	Lab	-		16	-	-
IR LED	Sleeve	mouser	475-2943-ND	digilkey 720-SFH4845 mouser	16 (25)	received	https://www.mouser.fr/ProductDetail/OSRAM-gqs=sGAEPiMZZMvzv9FAQJZmOwseFBUIQv
IR Photodiode	Sleeve	mouser	160-1987-ND		16 (100)	received	https://www.mouser.fr/ProductDetail/Lite-On/LI-gqs=%2fha2pyEaduimhxd%252bprCO8JhRfRq
Blue LED	Sleeve	Lab	-	460nm	16 (xx)	received	-
Photoresistor for blue light	Sleeve	mouser	485-161	455 notsuper 20% activation	16 (20)	received	https://www.mouser.fr/ProductDetail/Adafruit/1-gqs=%2fha2pyEaduimhxd%252bprCO8JhRfRq
Thermistor	Sleeve	mouser	954-103JT-025		16 (20)	received	https://www.mouser.fr/ProductDetail/Semitec/1
DC Computer Fan	Sleeve	mouser	562-FAD1-04020CBHW11	12V, 40x20x40 Original	-	Replaced	https://www.mouser.fr/ProductDetail/Qualtek/E-gqs=%2fha2pyEaduimhxd%252bprCO8JhRfRq
DC Computer Fan	Sleeve	mouser	490-CFM-4020V-180275		-	Replaced	https://www.mouser.fr/ProductDetail/490-CFM
DC Computer Fan	Sleeve	Digikey			16	received	https://www.digikey.com/products/en?keyword
Lab Tape	Sleeve	Lab			-	received	-
3D Printed Part	Sleeve	Lab		Modified OK	16	received	-
Machined Aluminum Tubes	Sleeve	Lab Weber-metaux		Check modifs 32x2.5	16 4 metres	received	-
Cable adaptor	Sleeve	mouser	424-6003-310-001	JTAG 2x7 pin cable	16 (20)	received	https://www.mouser.fr/ProductDetail/?q=s=BZBr
40 mL glass vials	vials	Chemglass	CG-4902-08	x100	-	Replaced	
40 mL glass vials	vials	Fisher	CG-4902-08	x100	-	Replaced	https://www.fishersci.com/shop/products/vial-o

Aa Name	Part	Company	Reference	details	Quantity	Status	Link
40 mL glass vials	vials	Optimus	CG-4902-08	x100	1	received	https://www.optimus-instruments.com/index.ph
vial screw caps	vials	Optimus	CG-4910-04	x100	1	received	https://chemoglass.com/qpi-24-400-screw-threa
Custom polypropylene vial cap inserts	vials			No need so far	-	-	
Resistance for LEDs	Sleeve	Lab			2x16 (xx)	-	
Raspberry PI	Board			Which one???	1	received	
RS458 shield	Board	Conrad	1267832 RB-RS485		1	received	https://www.conrad.fr/p/platine-dextension-ras
SAMD21 Microcontrollers Mini (Arduino)	Board	mouser	474-DEV-13664		4 (5)	received	https://www.mouser.fr/ProductDetail/SparkFunqs=%2fha2pyFaduUjajXN5UxBZ38RMnRldzfv
Socket for the sleeve PCB: CONN HEADER VERT 14POS 2.54MM	Sleeve	Digikey	S9170-ND		20	received	https://www.digikey.fr/product-detail/fr/sullins-cND/1990063
Vial board	Sleeve	EUROCIRCUITS			16 (20)	received	
Motherboard	Board	EUROCIRCUITS		Warnings	1 (1)	Cancelled	
PWM	Board	EUROCIRCUITS			4 (10)	Cancelled	
ADC	Board	EUROCIRCUITS			3 (5)	Cancelled	
RS458 board	Board	EUROCIRCUITS			1 (5)	Cancelled	
Wires for power supply	Board	Lab				-	
Generator	Board	Lab				-	
2x Stainless Steel Screws 2.5" 4-40 threading	Board	Lab				-	
Supports CI et composants SINGLE ROW COLLET SOLDER TAIL 10 PINS	Board	mouser	535-10-0518-10	Send to Eurocircuits	66x10=660 Not compatible FEMALE: socket Received	received	https://eu.mouser.com/ProductDetail/Aries-Fileqs=sGAEmMZMs%2fSh%2fkjph1tjJZcYmfa
Embases et logements de câbles 25 SIL VERTICAL PIN HEADER GOLD HT	Board	mouser	855-M20-9992545	Send to Eurocircuits	35x25=875 Not compatible MALE: pins received	received	https://www.mouser.fr/ProductDetail/Harwin/M:qs=%252bk6%2f5FB6qrmC3qkVOGtZUg%3df
Câbles nappe / Câbles IDC .100" Slim Body Double Row IDC Ribbon Cable Assembly, Socket	Sleeve	mouser	200-IDSD07D1500TG	Nickel	20	received	https://www.mouser.fr/ProductDetail/Samtec/IFqs=sGAEmMZMsqLz308WEU09nkw8SPjPpDF
Supports CI et composants 32P IC SOCKET STRIP 2.54MM PITCH	Board	mouser	855-D01-9973242		25x32=800 Order cancelled	Replaced	https://www.mouser.fr/ProductDetail/Harwin/Dfqs=sGAEmMZMs%2fSh%2fkjph1tjOnk5oEEf
Untitled							
compatible PINS	Board	Digikey	ED10064-64-ND	pfliou	20 20x64=1280	received	https://www.digikey.fr/product-detail/fr/mill-maxND/357033
More SOCKETS	Board	Digikey	A834AR-ND	pfliouuu	20 20x20=400	received	https://www.digikey.fr/product-detail/fr/aries-elf
Arduino NANO	Board	Digikey	A000005	Commande du	15	received	https://www.digikey.fr/product-detail/fr/A000005
Cable pour Arduino nano	Board	Digikey	3021003-03	06 Mai 2019:	20	received	https://www.digikey.fr/product-detail/fr/3021003
JUMPER WIRE M/F 5.91" 1PC	Board	Digikey	1528-1162-ND	more detail on	7	received	https://www.digikey.fr/product-detail/fr/B26/152
Sockets halalala *15	Board	Digikey	S7013-ND	this specific	60 +40	received	https://www.digikey.fr/product-detail/fr/PPTC15
Sockets *2	Board	Digikey	S7035-ND	commande	60 +30	received	https://www.digikey.fr/product-detail/fr/PPPC02
BREADBOARD GENERAL PURPOSE PTH 22*30	Board	Digikey	1738-1000-ND	below (other PCBs)	10	received	https://www.digikey.fr/product-detail/fr/FIT0089
BREADBOARD GENERAL PURPOSE PTH 60*30	Board	Digikey	SBPTH3060-1-ND		5	received	https://www.digikey.fr/product-detail/fr/SBPTH5
Jeu de résistances à couche carbone Velleman K/RES-E12 sonie axiale 0.25 W 1 set	Board	Conrad	084518	...	1	received	https://www.conrad.fr/p/jeu-de-resistances-a-c084518
Set de 6 pinces pour mécanique de précision	Board	Conrad	825199		1	received	https://www.conrad.fr/p/set-de-6-pinces-pour-n
Platine d'essai RS PRO. Dimensions de 80 x 60 x 10mm	Board	RS-online	102-9147		2	received	https://fr.rs-online.com/web/p/products/102914
TRANSISTOR MOSFET Canal-N 5 A 60 V PW moulé 2_3 broches	Board	RS-online	185-580		20	received	https://fr.rs-online.com/web/p/products/018558
More heaters	Board	mouser	684-MP915-20	coz j'avais commandé que la moitié de ce qu'il fallait	25	received	https://www.mouser.fr/ProductDetail/684-MP91

Aa Name	Part	Company	Reference	details	Quantity	Status	Link
<u>Hub USB, NewLink, USB 2.0</u>	Board	RS-online	706-7110	USB 2.0 is fine selon Williams avec	2	received	https://fr.rs-online.com/web/p/hubs-usb/706711
<u>adapteur pour les hubs</u>	Board	RS-online	668-3698	coz UK plug	3	received	https://fr.rs-online.com/web/p/adaptateurs-univ
<u>Untitled</u>							

8.9.9 eVOLVER - Re-install

Re-install everything to new cpu :

Because big bug on the previous cpu, ubuntu wdnt load the desktop after login.

▼ 20200304 BIG FAIL of resetting the cpu and make a new working node-red

Because after a try to update the proxy or whatever, after login, ubuntu wdnt start. Solution: overwrite everything w a brand new UBUNTU 18.04.4 LTS version.

- Install Ubuntu 18.04.4 LTS

▼ other stuff

```
https://s3-us-west-2.amazonaws.com/secure.notion-static.com/3f603743-f28c-4ddf-b53b-684e6da02755/eVOLVER\_scripts.zip
```

```
https://s3-us-west-2.amazonaws.com/secure.notion-static.com/7200a18a-c696-4f12-98aa-f64b28973193/images.zip
```

install tweaks

- appearance > Background > Adjustments > Wallpaper
- Top bar > Clock > Date (ON) & Seconds (ON)
- Windows > Placement (LEFT)

```
sudo apt-get update && sudo apt-get install folder-color
```

- Install node-red

```
sudo apt-get install npm
#Check the version of node and nodeJS w "node -v" and "nodejs -v", should be >= 8
sudo npm install -g --unsafe-perm node-red
```

installing npm installs node v8.10.0 and nodejs v8.10.0

In node-red, in palette, install the modules:

- node-red-contrib-configurable-interval
- node-red-contrib-counter
- node-red-contrib-pid
- node-red-contrib-simpletime
- node-red-dashboard
- node-red-node-arduino
- node-red-node-serialport (?)

```
ls /dev/ttyUSB*
```

Update node?

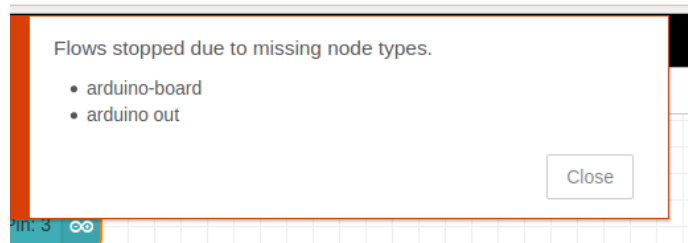
<https://stackoverflow.com/questions/41195952/updating-nodejs-on-ubuntu-16-04>

```
sudo apt-get install curl
curl -sL https://deb.nodesource.com/setup_11.x | sudo -E bash -
sudo apt-get install -y nodejs
```



```
node -v
nodejs -v
```

ca donne du v11.15.0 pr les dx



alors que je les ai installés bordel

```
cd /home/lab513/.node-red
```

```
"PortInfo.comName" has been deprecated. You should now use "PortInfo.path". The property will be removed in the next major release.
5 Mar 18:54:49 - [error] [arduino-board:17abb08b.cdd89f] port not found : /dev/ttyUSB0
```

- Update SYMLINKS

```
lab513@lab513-Precision-Tower-7910:~$ cat /etc/udev/rules.d/99-arduino.rules
SUBSYSTEM=="tty", KERNEL=="ttyUSB*", KERNELS=="3-11.5.4:1.0", SYMLINK+="eVOLVER01"
SUBSYSTEM=="tty", KERNEL=="ttyUSB*", KERNELS=="3-11.5.3:1.0", SYMLINK+="eVOLVER02"
SUBSYSTEM=="tty", KERNEL=="ttyUSB*", KERNELS=="3-11.5.2:1.0", SYMLINK+="eVOLVER03"
SUBSYSTEM=="tty", KERNEL=="ttyUSB*", KERNELS=="3-11.5.1:1.0", SYMLINK+="eVOLVER04"
SUBSYSTEM=="tty", KERNEL=="ttyUSB*", KERNELS=="3-11.2:1.0", SYMLINK+="eVOLVER05"
SUBSYSTEM=="tty", KERNEL=="ttyUSB*", KERNELS=="3-11.3:1.0", SYMLINK+="eVOLVER06"
SUBSYSTEM=="tty", KERNEL=="ttyUSB*", KERNELS=="3-11.4:1.0", SYMLINK+="eVOLVER07"
SUBSYSTEM=="tty", KERNEL=="ttyUSB*", KERNELS=="3-11.7:1.0", SYMLINK+="eVOLVER08"
SUBSYSTEM=="tty", KERNEL=="ttyUSB*", KERNELS=="3-8.5.4:1.0", SYMLINK+="eVOLVER09"
SUBSYSTEM=="tty", KERNEL=="ttyUSB*", KERNELS=="3-8.5.3:1.0", SYMLINK+="eVOLVER10"
SUBSYSTEM=="tty", KERNEL=="ttyUSB*", KERNELS=="3-8.5.2:1.0", SYMLINK+="eVOLVER11"
SUBSYSTEM=="tty", KERNEL=="ttyUSB*", KERNELS=="3-11.5.5:1.0", SYMLINK+="eVOLVER12"
SUBSYSTEM=="tty", KERNEL=="ttyUSB*", KERNELS=="3-8.2:1.0", SYMLINK+="eVOLVER13"
SUBSYSTEM=="tty", KERNEL=="ttyUSB*", KERNELS=="3-8.3:1.0", SYMLINK+="eVOLVER14"
SUBSYSTEM=="tty", KERNEL=="ttyUSB*", KERNELS=="3-8.4:1.0", SYMLINK+="eVOLVER15"
SUBSYSTEM=="tty", KERNEL=="ttyUSB*", KERNELS=="3-8.7:1.0", SYMLINK+="eVOLVER16"
SUBSYSTEM=="tty", KERNEL=="ttyUSB*", KERNELS=="3-8.6:1.0", SYMLINK+="eVOLVER17"
```

→ Solution used on 20200306: Descendre l'ordi que j'avais ds mon bureau et sur lequel node-red/arduino fonctionne et relancer tous les eVOLVERs dessus.

Could that be a problem of versions ? Thats likely according to Williams.

- ▼ Would need to check the versions of...

- node version
- nodejs version
- (npm version?)
- node-red version
- and node-red modules version
- firmata version on arduino, which may conflict with newer version of other softwares / modules?

- ▼ BIG CRASH and subsequent death of HD of the Feb 2022 - INSTRUCTIONS:

for unknown reasons really

Here are the details:

- INSTALL UBUNTU 20.04.4
- Connect to an internet WITHOUT proxy or crapy stuff of any sort (ie: via usb to a phone)
- update

```
sudo apt-get update
sudo apt-get upgrade
sudo apt-get install npm
```

- Check and update node
via <https://askubuntu.com/questions/426750/how-can-i-update-my-nodejs-to-the-latest-version>

```
node -v
nodejs -v
sudo npm cache clean -f
sudo npm install -g n
sudo n stable
sudo n latest
```

- Restart terminal

```
node -v
nodejs -v
```

→ v17.6.0
→ v10.19.0

- Install node-red

```
sudo npm install -g --unsafe-perm node-red
```

- Launch node-red

```
node-red
```

▼ Install packages needed for the code via the palette:

- **node-red-node-arduino** → need updates en tout genre pour marcher
- **node-red-contrib-configurable-interval**
- **node-red-contrib-counter**
- **node-red-contrib-pid**
- **node-red-contrib-simpletime**
- **node-red-dashboard**
- **node-red-node-serialport**

Sur cet ordi (instructions année 2020):

```
spouze@spouze-OptiPlex-9020:~/node_modules$ node -v
v11.12.0
spouze@spouze-OptiPlex-9020:~/node_modules$ nodejs -v
v4.2.6
spouze@spouze-OptiPlex-9020:~/node_modules$ npm -v
6.7.0
spouze@spouze-OptiPlex-9020:~/node_modules$ node-red
6 Mar 10:52:15 - [info]
```

Welcome to Node-RED

=====

```
6 Mar 10:52:15 - [info] Node-RED version: v0.20.3
6 Mar 10:52:15 - [info] Node.js version: v11.12.0
6 Mar 10:52:15 - [info] Linux 4.15.0-88-generic x64 LE
6 Mar 10:52:15 - [info] Loading palette nodes
6 Mar 10:52:15 - [warn] rpi-gpio : Raspberry Pi specific node set inactive
6 Mar 10:52:15 - [warn] rpi-gpio : Cannot find Pi RPi.GPIO python library
6 Mar 10:52:16 - [info] Dashboard version 2.14.0 started at /ui
6 Mar 10:52:16 - [info] Settings file : /home/spouze/.node-red/settings.js
6 Mar 10:52:16 - [info] Context store : 'default' [module=memory]
6 Mar 10:52:16 - [info] User directory : /home/spouze/.node-red
6 Mar 10:52:16 - [warn] Projects disabled : editorTheme.projects.enabled=false
6 Mar 10:52:16 - [info] Flows file : /home/spouze/.node-red/flows_spouze-OptiPlex-9020.json
6 Mar 10:52:16 - [info] Server now running at http://127.0.0.1:1880/
6 Mar 10:52:16 - [warn]
```

Your flow credentials file is encrypted using a system-generated key.

If the system-generated key is lost for any reason, your credentials file will not be recoverable, you will have to delete it and re-enter your credentials.

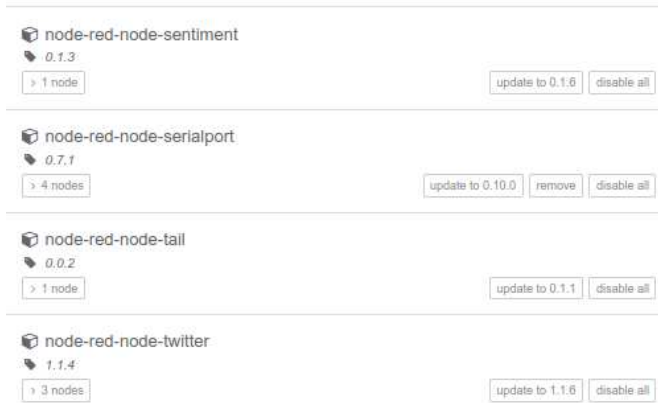
You should set your own key using the 'credentialSecret' option in your settings file. Node-RED will then re-encrypt your credentials file using your chosen key the next time you deploy a change.

```
6 Mar 10:52:16 - [info] Starting flows
6 Mar 10:52:16 - [info] Started flows
6 Mar 10:52:16 - [error] [arduino-board:67f10405.1cfe14] port not found : /dev/ttyACM0
```

▼ Node-red modules sur cet ordi (palette)

The screenshot shows the Node-RED module palette with the following modules listed:

- node-red** (v0.20.3): 49 nodes, [in use]
- node-red-contrib-configurable-interval** (v0.9.1): 1 node, [remove] [disable all]
- node-red-contrib-counter** (v0.1.5): 1 node, [in use]
- node-red-contrib-pid** (v1.1.4): 1 node, [update to 1.1.5] [in use]
- node-red-contrib-simpletime** (v2.4.0): 1 node, [update to 2.8.1] [in use]
- node-red-dashboard** (v2.14.0): 21 nodes, [update to 2.19.4] [in use]
- node-red-node-arduino** (v0.1.0): 3 nodes, [update to 0.3.1] [in use]
- node-red-node-email** (v1.3.0): 2 nodes, [update to 1.7.7] [disable all]
- node-red-node-feedparser** (v0.1.14): 1 node, [update to 0.1.15] [disable all]
- node-red-node-rbe** (v0.2.4): 0 nodes



https://s3-us-west-2.amazonaws.com/secure.notion-static.com/ed976ed8-07a5-45f9-b28b-2ab432416502/Node-red_save.zip

▼ Parameter eVOLVER SYMLINKS on this new computer, based on Serial numbers

New Symlinks based on serial numbers - more robust

```
Future Technology Devices International,
idVendor 0403
idProduct 6001
iSerial for each of the eVOLVER:
ev01 AK05AV97
ev02 AH06EYUK
ev03 AH06F0KD
ev04 A90833DB
ev05 AL03QJX6
ev06 AH06N50M
ev07 A908372V
ev08 AH06AHDU
ev09 AH06AKVA new: AK05ATM4
ev10 AH06F46R
ev11 AH06AKKA
ev12 AH06AHYB
ev13 AH06F0CY
ev14 A90838NY
ev15 AK05ATPR
ev16 AI02PN4P
ev17 AI02PNX9
```

<https://skjoldtech.wordpress.com/2019/04/20/persistent-usb-serial-device-name-in-linux/>

First test avec All arduinos in but targets only unit17:

Operational.

```
spouze@spouze-OptiPlex-9020:~$ cat /etc/udev/rules.d/99-usb-serial.rules
SUBSYSTEM=="tty", ATTRS{idVendor}=="0403", ATTRS{idProduct}=="6001", ATTRS{serial}=="AI02PNX9", SYMLINK+="eVOLVER17"

cat /etc/udev/rules.d/99-arduino.rules
SUBSYSTEM=="tty", ATTRS{idVendor}=="0403", ATTRS{idProduct}=="6001", ATTRS{serial}=="AI02PNX9", SYMLINK+="eVOLVER17"

spouze@spouze-OptiPlex-9020:~$ ls -l /dev/ev*
lrwxrwxrwx 1 root root 8 mars  6 11:16 /dev/eVOLVER17 -> ttyUSB16
```

yen a dx la en fait. Mais le 99-arduino-rules suffit. Et il fonctionne car il devait deja etre present.

Let's add unit01.

```
sudo nano /etc/udev/rules.d/99-arduino.rules

spouze@spouze-OptiPlex-9020:/etc/udev/rules.d$ cat /etc/udev/rules.d/99-arduino.rules
SUBSYSTEM=="tty", ATTRS{idVendor}=="0403", ATTRS{idProduct}=="6001", ATTRS{serial}=="AI02PNX9", SYMLINK+="eVOLVER17"
SUBSYSTEM=="tty", ATTRS{idVendor}=="0403", ATTRS{idProduct}=="6001", ATTRS{serial}=="AK05AV97", SYMLINK+="eVOLVER01"
```

```
sudo /etc/init.d/udev reload
```

udev reload doesnt seem to work.

Let's reboot

```
reboot
spouze@spouze-OptiPlex-9020:~$ ls -l /dev/ev*
lrwxrwxrwx 1 root root 8 mars 6 11:30 /dev/eVOLVER01 -> ttyUSB15
lrwxrwxrwx 1 root root 7 mars 6 11:30 /dev/eVOLVER17 -> ttyUSB0
```

The reboot seems to have worked !

Ca marche on Node-red. C'est parti pr la totale:

```
SUBSYSTEM=="tty", ATTRS{idVendor}=="0403", ATTRS{idProduct}=="6001", ATTRS{serial}=="AI02PNX9", SYMLINK+="eVOLVER17"
SUBSYSTEM=="tty", ATTRS{idVendor}=="0403", ATTRS{idProduct}=="6001", ATTRS{serial}=="AK05AV97", SYMLINK+="eVOLVER01"

SUBSYSTEM=="tty", ATTRS{idVendor}=="0403", ATTRS{idProduct}=="6001", ATTRS{serial}=="AH06EYUK", SYMLINK+="eVOLVER02"
SUBSYSTEM=="tty", ATTRS{idVendor}=="0403", ATTRS{idProduct}=="6001", ATTRS{serial}=="AH06F0KD", SYMLINK+="eVOLVER03"
SUBSYSTEM=="tty", ATTRS{idVendor}=="0403", ATTRS{idProduct}=="6001", ATTRS{serial}=="A90833DB", SYMLINK+="eVOLVER04"
SUBSYSTEM=="tty", ATTRS{idVendor}=="0403", ATTRS{idProduct}=="6001", ATTRS{serial}=="AL03QJX6", SYMLINK+="eVOLVER05"
SUBSYSTEM=="tty", ATTRS{idVendor}=="0403", ATTRS{idProduct}=="6001", ATTRS{serial}=="AH06N50M", SYMLINK+="eVOLVER06"
SUBSYSTEM=="tty", ATTRS{idVendor}=="0403", ATTRS{idProduct}=="6001", ATTRS{serial}=="A908372V", SYMLINK+="eVOLVER07"
SUBSYSTEM=="tty", ATTRS{idVendor}=="0403", ATTRS{idProduct}=="6001", ATTRS{serial}=="AH06AHDU", SYMLINK+="eVOLVER08"
SUBSYSTEM=="tty", ATTRS{idVendor}=="0403", ATTRS{idProduct}=="6001", ATTRS{serial}=="AH06AKVA", SYMLINK+="eVOLVER09"
SUBSYSTEM=="tty", ATTRS{idVendor}=="0403", ATTRS{idProduct}=="6001", ATTRS{serial}=="AH06F46R", SYMLINK+="eVOLVER10"
SUBSYSTEM=="tty", ATTRS{idVendor}=="0403", ATTRS{idProduct}=="6001", ATTRS{serial}=="AH06AKKA", SYMLINK+="eVOLVER11"
SUBSYSTEM=="tty", ATTRS{idVendor}=="0403", ATTRS{idProduct}=="6001", ATTRS{serial}=="AH06AHYB", SYMLINK+="eVOLVER12"
SUBSYSTEM=="tty", ATTRS{idVendor}=="0403", ATTRS{idProduct}=="6001", ATTRS{serial}=="AH06F0CY", SYMLINK+="eVOLVER13"
SUBSYSTEM=="tty", ATTRS{idVendor}=="0403", ATTRS{idProduct}=="6001", ATTRS{serial}=="A90838NY", SYMLINK+="eVOLVER14"
SUBSYSTEM=="tty", ATTRS{idVendor}=="0403", ATTRS{idProduct}=="6001", ATTRS{serial}=="AK05ATPR", SYMLINK+="eVOLVER15"
SUBSYSTEM=="tty", ATTRS{idVendor}=="0403", ATTRS{idProduct}=="6001", ATTRS{serial}=="AI02PN4P", SYMLINK+="eVOLVER16"
```

On a :

```
spouze@spouze-OptiPlex-9020:~$ cat /etc/udev/rules.d/99-arduino.rules
SUBSYSTEM=="tty", ATTRS{idVendor}=="0403", ATTRS{idProduct}=="6001", ATTRS{serial}=="AI02PNX9", SYMLINK+="eVOLVER17"
SUBSYSTEM=="tty", ATTRS{idVendor}=="0403", ATTRS{idProduct}=="6001", ATTRS{serial}=="AK05AV97", SYMLINK+="eVOLVER01"
SUBSYSTEM=="tty", ATTRS{idVendor}=="0403", ATTRS{idProduct}=="6001", ATTRS{serial}=="AH06EYUK", SYMLINK+="eVOLVER02"
SUBSYSTEM=="tty", ATTRS{idVendor}=="0403", ATTRS{idProduct}=="6001", ATTRS{serial}=="AH06F0KD", SYMLINK+="eVOLVER03"
SUBSYSTEM=="tty", ATTRS{idVendor}=="0403", ATTRS{idProduct}=="6001", ATTRS{serial}=="A90833DB", SYMLINK+="eVOLVER04"
SUBSYSTEM=="tty", ATTRS{idVendor}=="0403", ATTRS{idProduct}=="6001", ATTRS{serial}=="AL03QJX6", SYMLINK+="eVOLVER05"
SUBSYSTEM=="tty", ATTRS{idVendor}=="0403", ATTRS{idProduct}=="6001", ATTRS{serial}=="AH06N50M", SYMLINK+="eVOLVER06"
SUBSYSTEM=="tty", ATTRS{idVendor}=="0403", ATTRS{idProduct}=="6001", ATTRS{serial}=="A908372V", SYMLINK+="eVOLVER07"
SUBSYSTEM=="tty", ATTRS{idVendor}=="0403", ATTRS{idProduct}=="6001", ATTRS{serial}=="AH06AHDU", SYMLINK+="eVOLVER08"
SUBSYSTEM=="tty", ATTRS{idVendor}=="0403", ATTRS{idProduct}=="6001", ATTRS{serial}=="AH06AKVA", SYMLINK+="eVOLVER09"
SUBSYSTEM=="tty", ATTRS{idVendor}=="0403", ATTRS{idProduct}=="6001", ATTRS{serial}=="AH06F46R", SYMLINK+="eVOLVER10"
SUBSYSTEM=="tty", ATTRS{idVendor}=="0403", ATTRS{idProduct}=="6001", ATTRS{serial}=="AH06AKKA", SYMLINK+="eVOLVER11"
SUBSYSTEM=="tty", ATTRS{idVendor}=="0403", ATTRS{idProduct}=="6001", ATTRS{serial}=="AH06AHYB", SYMLINK+="eVOLVER12"
SUBSYSTEM=="tty", ATTRS{idVendor}=="0403", ATTRS{idProduct}=="6001", ATTRS{serial}=="AH06F0CY", SYMLINK+="eVOLVER13"
SUBSYSTEM=="tty", ATTRS{idVendor}=="0403", ATTRS{idProduct}=="6001", ATTRS{serial}=="A90838NY", SYMLINK+="eVOLVER14"
SUBSYSTEM=="tty", ATTRS{idVendor}=="0403", ATTRS{idProduct}=="6001", ATTRS{serial}=="AK05ATPR", SYMLINK+="eVOLVER15"
SUBSYSTEM=="tty", ATTRS{idVendor}=="0403", ATTRS{idProduct}=="6001", ATTRS{serial}=="AI02PN4P", SYMLINK+="eVOLVER16"
```

Et on reboot.

```
spouze@spouze-OptiPlex-9020:~$ ls -l /dev/ev*
lrwxrwxrwx 1 root root 8 mars 6 11:46 /dev/eVOLVER01 -> ttyUSB15
lrwxrwxrwx 1 root root 8 mars 6 11:46 /dev/eVOLVER02 -> ttyUSB14
lrwxrwxrwx 1 root root 8 mars 6 11:46 /dev/eVOLVER03 -> ttyUSB12
lrwxrwxrwx 1 root root 8 mars 6 11:46 /dev/eVOLVER04 -> ttyUSB10
lrwxrwxrwx 1 root root 7 mars 6 11:46 /dev/eVOLVER05 -> ttyUSB2
lrwxrwxrwx 1 root root 7 mars 6 11:46 /dev/eVOLVER06 -> ttyUSB4
lrwxrwxrwx 1 root root 7 mars 6 11:46 /dev/eVOLVER07 -> ttyUSB6
lrwxrwxrwx 1 root root 7 mars 6 11:46 /dev/eVOLVER08 -> ttyUSB8
lrwxrwxrwx 1 root root 8 mars 6 11:46 /dev/eVOLVER10 -> ttyUSB11
lrwxrwxrwx 1 root root 7 mars 6 11:46 /dev/eVOLVER11 -> ttyUSB9
lrwxrwxrwx 1 root root 8 mars 6 11:46 /dev/eVOLVER12 -> ttyUSB16
lrwxrwxrwx 1 root root 7 mars 6 11:46 /dev/eVOLVER13 -> ttyUSB1
lrwxrwxrwx 1 root root 7 mars 6 11:46 /dev/eVOLVER14 -> ttyUSB3
lrwxrwxrwx 1 root root 7 mars 6 11:46 /dev/eVOLVER15 -> ttyUSB5
lrwxrwxrwx 1 root root 7 mars 6 11:46 /dev/eVOLVER16 -> ttyUSB7
lrwxrwxrwx 1 root root 7 mars 6 11:46 /dev/eVOLVER17 -> ttyUSB0
```

Looks very fine to me.

Now check one by one arduinos on node-red.

- ERROR WITH UNIT09: indeed the serial number must be different because the arduino was changed to arduino#18.

on corrige le fichier:

```
sudo nano /etc/udev/rules.d/99-arduino.rules

spouze@spouze-OptiPlex-9020:~$ cat /etc/udev/rules.d/99-arduino.rules
SUBSYSTEM=="tty", ATTRS{idVendor}=="0403", ATTRS{idProduct}=="6001", ATTRS{serial}=="AI02PNX9", SYMLINK+="eVOLVER17"
SUBSYSTEM=="tty", ATTRS{idVendor}=="0403", ATTRS{idProduct}=="6001", ATTRS{serial}=="AK05AV97", SYMLINK+="eVOLVER01"
SUBSYSTEM=="tty", ATTRS{idVendor}=="0403", ATTRS{idProduct}=="6001", ATTRS{serial}=="AH06EYUK", SYMLINK+="eVOLVER02"
SUBSYSTEM=="tty", ATTRS{idVendor}=="0403", ATTRS{idProduct}=="6001", ATTRS{serial}=="AH06F0KD", SYMLINK+="eVOLVER03"
SUBSYSTEM=="tty", ATTRS{idVendor}=="0403", ATTRS{idProduct}=="6001", ATTRS{serial}=="A90833DB", SYMLINK+="eVOLVER04"
SUBSYSTEM=="tty", ATTRS{idVendor}=="0403", ATTRS{idProduct}=="6001", ATTRS{serial}=="AL03QJX6", SYMLINK+="eVOLVER05"
SUBSYSTEM=="tty", ATTRS{idVendor}=="0403", ATTRS{idProduct}=="6001", ATTRS{serial}=="AH06N50M", SYMLINK+="eVOLVER06"
SUBSYSTEM=="tty", ATTRS{idVendor}=="0403", ATTRS{idProduct}=="6001", ATTRS{serial}=="A908372V", SYMLINK+="eVOLVER07"
SUBSYSTEM=="tty", ATTRS{idVendor}=="0403", ATTRS{idProduct}=="6001", ATTRS{serial}=="AH06AHDU", SYMLINK+="eVOLVER08"
SUBSYSTEM=="tty", ATTRS{idVendor}=="0403", ATTRS{idProduct}=="6001", ATTRS{serial}=="AK05ATM4", SYMLINK+="eVOLVER09"
SUBSYSTEM=="tty", ATTRS{idVendor}=="0403", ATTRS{idProduct}=="6001", ATTRS{serial}=="AH06F46R", SYMLINK+="eVOLVER10"
SUBSYSTEM=="tty", ATTRS{idVendor}=="0403", ATTRS{idProduct}=="6001", ATTRS{serial}=="AH06AKKA", SYMLINK+="eVOLVER11"
SUBSYSTEM=="tty", ATTRS{idVendor}=="0403", ATTRS{idProduct}=="6001", ATTRS{serial}=="AH06AHYB", SYMLINK+="eVOLVER12"
SUBSYSTEM=="tty", ATTRS{idVendor}=="0403", ATTRS{idProduct}=="6001", ATTRS{serial}=="AH06F0CY", SYMLINK+="eVOLVER13"
SUBSYSTEM=="tty", ATTRS{idVendor}=="0403", ATTRS{idProduct}=="6001", ATTRS{serial}=="A90838NY", SYMLINK+="eVOLVER14"
SUBSYSTEM=="tty", ATTRS{idVendor}=="0403", ATTRS{idProduct}=="6001", ATTRS{serial}=="AK05ATPR", SYMLINK+="eVOLVER15"
SUBSYSTEM=="tty", ATTRS{idVendor}=="0403", ATTRS{idProduct}=="6001", ATTRS{serial}=="AI02PN4P", SYMLINK+="eVOLVER16"
```

And reboot again

SUCCESS

```
cat /etc/udev/rules.d/99-arduino.rules
spouze@spouze-OptiPlex-9020:~$ cat /etc/udev/rules.d/99-arduino.rules
SUBSYSTEM=="tty", ATTRS{idVendor}=="0403", ATTRS{idProduct}=="6001", ATTRS{serial}=="AI02PNX9", SYMLINK+="eVOLVER17"
SUBSYSTEM=="tty", ATTRS{idVendor}=="0403", ATTRS{idProduct}=="6001", ATTRS{serial}=="AK05AV97", SYMLINK+="eVOLVER01"
SUBSYSTEM=="tty", ATTRS{idVendor}=="0403", ATTRS{idProduct}=="6001", ATTRS{serial}=="AH06EYUK", SYMLINK+="eVOLVER02"
SUBSYSTEM=="tty", ATTRS{idVendor}=="0403", ATTRS{idProduct}=="6001", ATTRS{serial}=="AH06F0KD", SYMLINK+="eVOLVER03"
SUBSYSTEM=="tty", ATTRS{idVendor}=="0403", ATTRS{idProduct}=="6001", ATTRS{serial}=="A90833DB", SYMLINK+="eVOLVER04"
SUBSYSTEM=="tty", ATTRS{idVendor}=="0403", ATTRS{idProduct}=="6001", ATTRS{serial}=="AL03QJX6", SYMLINK+="eVOLVER05"
SUBSYSTEM=="tty", ATTRS{idVendor}=="0403", ATTRS{idProduct}=="6001", ATTRS{serial}=="AH06N50M", SYMLINK+="eVOLVER06"
SUBSYSTEM=="tty", ATTRS{idVendor}=="0403", ATTRS{idProduct}=="6001", ATTRS{serial}=="A908372V", SYMLINK+="eVOLVER07"
SUBSYSTEM=="tty", ATTRS{idVendor}=="0403", ATTRS{idProduct}=="6001", ATTRS{serial}=="AH06AHDU", SYMLINK+="eVOLVER08"
SUBSYSTEM=="tty", ATTRS{idVendor}=="0403", ATTRS{idProduct}=="6001", ATTRS{serial}=="AK05ATM4", SYMLINK+="eVOLVER09"
SUBSYSTEM=="tty", ATTRS{idVendor}=="0403", ATTRS{idProduct}=="6001", ATTRS{serial}=="AH06F46R", SYMLINK+="eVOLVER10"
SUBSYSTEM=="tty", ATTRS{idVendor}=="0403", ATTRS{idProduct}=="6001", ATTRS{serial}=="AH06AKKA", SYMLINK+="eVOLVER11"
SUBSYSTEM=="tty", ATTRS{idVendor}=="0403", ATTRS{idProduct}=="6001", ATTRS{serial}=="AH06AHYB", SYMLINK+="eVOLVER12"
SUBSYSTEM=="tty", ATTRS{idVendor}=="0403", ATTRS{idProduct}=="6001", ATTRS{serial}=="AH06F0CY", SYMLINK+="eVOLVER13"
SUBSYSTEM=="tty", ATTRS{idVendor}=="0403", ATTRS{idProduct}=="6001", ATTRS{serial}=="A90838NY", SYMLINK+="eVOLVER14"
SUBSYSTEM=="tty", ATTRS{idVendor}=="0403", ATTRS{idProduct}=="6001", ATTRS{serial}=="AK05ATPR", SYMLINK+="eVOLVER15"
SUBSYSTEM=="tty", ATTRS{idVendor}=="0403", ATTRS{idProduct}=="6001", ATTRS{serial}=="AI02PN4P", SYMLINK+="eVOLVER16"
```

```
spouze@spouze-OptiPlex-9020:~$ ls -l /dev/eV*
lrwxrwxrwx 1 root root 8 mars 6 12:05 /dev/eVOLVER01 -> ttyUSB15
lrwxrwxrwx 1 root root 8 mars 6 12:05 /dev/eVOLVER02 -> ttyUSB14
lrwxrwxrwx 1 root root 8 mars 6 12:05 /dev/eVOLVER03 -> ttyUSB12
lrwxrwxrwx 1 root root 8 mars 6 12:05 /dev/eVOLVER04 -> ttyUSB10
lrwxrwxrwx 1 root root 7 mars 6 12:05 /dev/eVOLVER05 -> ttyUSB2
lrwxrwxrwx 1 root root 7 mars 6 12:05 /dev/eVOLVER06 -> ttyUSB4
lrwxrwxrwx 1 root root 7 mars 6 12:05 /dev/eVOLVER07 -> ttyUSB6
lrwxrwxrwx 1 root root 7 mars 6 12:05 /dev/eVOLVER08 -> ttyUSB8
lrwxrwxrwx 1 root root 8 mars 6 12:05 /dev/eVOLVER09 -> ttyUSB13
lrwxrwxrwx 1 root root 8 mars 6 12:05 /dev/eVOLVER10 -> ttyUSB11
lrwxrwxrwx 1 root root 7 mars 6 12:05 /dev/eVOLVER11 -> ttyUSB9
lrwxrwxrwx 1 root root 8 mars 6 12:05 /dev/eVOLVER12 -> ttyUSB16
lrwxrwxrwx 1 root root 7 mars 6 12:05 /dev/eVOLVER13 -> ttyUSB1
lrwxrwxrwx 1 root root 7 mars 6 12:05 /dev/eVOLVER14 -> ttyUSB3
lrwxrwxrwx 1 root root 7 mars 6 12:05 /dev/eVOLVER15 -> ttyUSB5
lrwxrwxrwx 1 root root 7 mars 6 12:05 /dev/eVOLVER16 -> ttyUSB7
lrwxrwxrwx 1 root root 7 mars 6 12:05 /dev/eVOLVER17 -> ttyUSB0
```

https://s3-us-west-2.amazonaws.com/secure.notion-static.com/2be187c3-3471-4708-b7d8-57547a4d8c95/202003051216_REFERENCE_working_version_for_single.json